The functionality of starch and the related water mobility during wheat bread making

Mieke NIVELLE

SUPERVISOR
Prof. J. A. Delcour, KU Leuven

MEMBERS OF THE EXAMINATION COMMITTEE
Prof. B. Sels, KU Leuven, chairman
Prof. B. Goderis, KU Leuven
Prof. A. Van Loey, KU Leuven
Dr. E. Breynaert, KU Leuven
Mr. Phil Latham, AB Mauri

Dissertation presented in partial
fulfilment of the requirements for the
degree of Doctor of Bioscience Engineering

January 2020

Doctoraatsproefschrift nr. 1620 aan de faculteit Bio-ingenieurswetenschappen van de KU Leuven

Uitgegeven in eigen beheer, Mieke Nivelle, Kasteelpark Arenberg 20 – bus 2463, 3001 Leuven

Voorwoord

Het is zover: Mijn broodje is gebakken! Inderdaad beste lezer, met trots stel ik u voor: mijn doctoraat! Al is het eigenlijk niet alleen “mijn” doctoraat. Want het zou nooit tot stand zijn gekomen zonder een heel aantal begeleiders, ondersteuners en supporters. Ik wend me daarom graag eerst tot deze mensen om hen uitgebreid te bedanken voor ik u met alle plezier de rol van zetmeel en water in brood uit de doeken doe.

Pas tijdens de laatste jaren van mijn studies bio-ingenieurswetenschappen begon ik te denken dat een doctoraat wel eens iets voor mij kon zijn. Voordien ging ik ervan uit dat ik het in Leuven na vijf jaar studeren wel gezien zou hebben. Het is tijdens de boeidende lessen levensmiddelenchemie van Prof. Jan Delcour en het bijhorende practicum dat mijn interesse voor onderzoek naar levensmiddelen en meer bepaald graanproducten aangewakkerd werd. Ik wist dan ook snel aan welk labo ik mijn thesisonderzoek zou starten, in de hoop hier nadien te kunnen doctoreren. Een jaar later mocht ik inderdaad mijn verblijf aan het labo verlengen en begon ik vol overtuiging een doctoraat onder begeleiding van Prof. Delcour. Jan, ik wil u oprecht bedanken voor deze kans, voor de steun en het vertrouwen. Al verbetert u tegenwoordig wel vijf doctoraten tegelijk, toch kon ik steeds rekenen op snelle verbeteringen en kritische input. Bovendien mocht ik ondanks uw drukke agenda altijd binnenwandelen voor eender welke vraag. Jan, heel erg bedankt voor de aangename samenwerking!

I wish to thank all the members of the examination committee for taking the time to read this work and to provide constructive feedback during the preliminary defense. Graag dank ik mijn assessoren, Prof. Ann Van Loey en Bart Goderis, om mijn werk van meet af aan op te volgen. Bart, tot jou richt ik een extra woordje van dank voor de leerrijke en aangename tripjes naar Grenoble, de hulp bij de verwerking van de WAXD-data, en de interessante discussies.

During the first year of my PhD research, I was given the opportunity to cooperate with DSM Food Specialties and Mauri Research. Thank you Phil, Joke, Maarten and Emmie for the pleasant collaboration and the fruitful discussions. I learned a lot from it.
Kristof, Brijs, ik heb toen ook heel fijn met jou samengewerkt. Ik kijk uit naar een verdere samenwerking!

I also want to thank Toshiki Nakamura and Patricia Vrinten for providing the NIL flour samples and for the nice collaboration.

Geertrui, jij mag hier natuurlijk niet ontbreken. Vanaf het begin van mijn doctoraat stond jij met raad en daad voor mij klaar. Ik heb enorm veel van je bijgeleerd. Je leerde me brood bakken, sleutelde aan wetenschappelijke verwoordingen in artikels, toonde me hoe ik een presentatie net dat beetje duidelijker maakte, dacht mee over nieuwe hypotheses en niet te vergeten, je maakte me wegwijs in de wondere wereld van de NMR. Jouw enthousiasme werkte aanstekelijk en motiveerde me extra om verder te werken. Daarnaast kon ik (en kan ik nog) steeds bij je terecht voor een fijne babbel, op het werk of tijdens een gezellig etentje. Want ook na je vertrek aan het labo bleef je geïnteresseerd in mijn onderzoek. Geertrui, voor alles, merci!

Naast de begeleiding die ik kreeg, mocht ik de afgelopen jaren ook zelf enkele thesisstudenten begeleiden. Ze hadden verschillende dingen gemeen. Ofwel waren het blondjes van de KULAK ofwel waren ze jarig op 7 juli. Maar nog belangrijker, het waren stuk voor stuk topstudenten waarmee ik graag samenwerkte en die een belangrijke bijdrage aan dit werk geleverd hebben. Alice, Ella en Marie: een dikke merci! Alice, voor jou nog een extra woordje van dank. Je bent ondertussen namelijk een fijne collega geworden en ik wens je nog … (Ik zal hier al maar stoppen en deze verboden zin niet afmaken). Nu serieus. De combinatie Limburg en West-Vlaanderen bleek een heel goede match, we zijn een topteam sinds 2016! Je zal nooit zomaar mijn bureau passeren zonder even iets te komen zeggen of een knuffel te komen halen/geven en ik weet dat ik steeds bij je terecht kan (ook met geheimpjes 😉). Bedankt he!
Myrthe, jouw werk draagt misschien niet bij tot mijn doctoraat, toch wil ik ook jou graag bedanken voor de fijne samenwerking.

Uiteraard wil ik ook al mijn collega's bedanken. Ik denk dat je dit in het voorwoord van eender welk doctoraat aan ons labo zal terug vinden. Maar het is gewoon zo. De leuke sfeer aan het labo zorgt ervoor dat ik elke dag met plezier kom werken. Buiten de werkuren worden bovendien nog tal van activiteiten georganiseerd die bijdragen aan de groepssfeer: de jaarlijkse kerstfeestjes, laboweekends, -brunches, en -BBQ's zijn hier slechts enkelen van. Ik prijs me gelukkig met zo'n groep toffe collega's en besef dat dit uniek is in het werkend leven. In het bijzonder wil ik hier ook Luc en Christa bedanken. Wat zou het labo zonder jullie moeten doen?! Luc kan werkelijk alles repareren, zet 's ochtends vroeg de fermentatiekast voor je op of zorgt dat er koffie en koekjes klaarstaan bij een vergadering. Dankjewel hiervoor, Luc! Christa leidt alle administratieve zaken in goede banen. Moet je labomateriaal bestellen, lunch voorzien tijdens een vergadering of vluchten en hotels voor een congres boeken? Gewoon even langs Christa passeren, zij brengt dat snel en efficiënt in orde. Bedankt, Christa!

Free, Sarah, Chiara, Elien, Margarita, Niels, Stijn, en Boeve, we started our PhD's together in 2015-2016. We form an excellent team when organizing lab activities, it's always fun! I really appreciate your support and help while going through all different stages of the PhD track. Thank you!

Sarah en Chiara, op regelmatige basis spreken we af om iets te gaan eten of drinken, maar vooral om bij te babbelen. Een welgekomen ontspanning na het werk, merci!

Alle bureaugenoten die deel uitgemaakt hebben van "Office Awesome" (al was dat soms maar voor korte tijd) wil ik extra in de bloemetjes zetten. Free, Sarah, Sara, Lomme, Nand, Geertrui, Alice, Lore, Anneleen, Joke, Nele, Brecht en Julie, ik vond het heel fijn om met jullie een bureau te delen. De occasionele bureaufrietjes, de jaarlijkse Secret Santa en de vele housewarmings waren steeds momenten om naar uit te kijken. Niels, Pieter, Karin, Stijn en Lauren, de bureaugenoten op ons "Schoon verdiep", ook aan jullie een dikke merci voor de goede sfeer, de nodige stilte tijdens het schrijven en de even hard nodige ontspannende babbeltjes tussendoor. Sarah, je bent geen bureaugenoot meer, maar als bureauburen lopen we nog heel vaak bij elkaar binnen. Om een stukje tekst te helpen herformuleren, om een figuur te beoordelen, om nuttige bouwinformatie uit te wisselen of gewoon om ons hart te luchten. Ik heb hier echt heel veel aan. Dankjewel! Arno, ik vind het heel fijn dat je regelmatig de bureau eens binnenwandelt om te peilen naar de gemoedstoestand van de schrijvers. We delen hetzelfde gevoel voor humor. Bedankt voor alle grappige momenten en babbeltjes!

Lotte & Maarten, Hanne & Ward, Sarah & Kevin, Free & Kelly, Michiel & Dorien, lieve "boerenvriendjes". Voor ontspanning kon ik bij de helft van jullie al tijdens onze studententijd terecht. TD's en Gnorgl-avonden (al dan niet voorafgegaan door een kelderfeestje bij Free en Michiel), cantussen, of gewoon samen koken, altijd plezier verzekerd! Ondertussen nemen we ook onze wederhelften mee naar etentjes, housewarmings, trouwfeesten (en de bijhorende cadeauvoorbereidingen) en gaan we jaarlijks op weekend. Dingen die we zeker moeten blijven doen. Bedankt voor alle leuke momenten en om er steeds te zijn!

Leen, wij kennen elkaar al van het eerste middelbaar, toen we samen terecht kwamen in het beruchte 1AL3. Van toen tot nu hebben we al heel wat mooie herinneringen verzameld. We zien elkaar nu niet meer zo heel vaak, maar als we afspreken is het altijd even gezellig. Hoog tijd om nog eens een date vast te leggen dus!

De meisjes van het thuisfront: Alana, An, Anneke, Anouk, Birgit, Brauns, Dorien, Jolien B., Jolien P., Lise, Lore, Rebecca, Roxane, Ruth, Sibylle, Sofie, VDS en Veronique, vrienden voor 't leven. Onze band werd jaren geleden gesmeed als lid en leiding bij de Chiro. Uren en uren hebben we versleten in onze tweede thuis, het lokaal. Dat was een onvergetelijke tijd die ik voor altijd koester. Dat we ondanks ons gebekvecht en lawaai nu nog steeds met z'n allen

afspreken, zegt meer dan genoeg over onze vriendschap. Jullie zorgen na het werk en in het weekend steeds voor de nodige ontspanning bij tal van verjaardagsfeestjes, spelletjesavonden, terrasjes in de zomer en noem maar op. Ons jaarlijks weekend, Nacht der Nachten en kermismaandag worden lang op voorhand met pen in de agenda genoteerd. Tradities om in ere te houden! Naast al het plezier, kan ik bij jullie ook terecht als het eens wat minder gaat. Voor alles, een hele dikke merci!

Mijn schoonfamilie wil ik bedanken om mij ondertussen al meer dan tien jaar geleden met open armen in de familie op te nemen. Brigitte en Herman, heel erg bedankt voor alle hulp en steun waar Andy en ik steeds op kunnen rekenen. Niets is ooit te veel, altijd kunnen we bij jullie terecht. Merci!
Dorien, Niels, Milou en Mats, Jonas en Esmee, met jullie erbij zijn de zondagmiddagen en familiefeestjes steevast van animatie voorzien. Bedankt om er altijd voor ons te zijn!

Ook mijn familie verdient uiteraard een woordje van dank. Ma, tantes en nonkels, bedankt voor de steun en de aanmoedigingen.
Marie, buurmeisje, babysit, maar eigenlijk ook een soort van grote zus. Jij was er altijd op de belangrijke momenten in mijn leven, merci!
Mama en papa, jullie staan zonder uitzondering en onvoorwaardelijk voor Andy en mij, Béke en Brecht, en Mathias klaar. Het kan zijn wat het wil, ik kan echt altijd bij jullie terecht. Ik prijs mezelf gelukkig dat ik in zo'n warm en liefdevol gezin ben opgegroeid. Ik kan jullie niet genoeg bedanken voor alle steun en hulp, alle kansen die jullie mij gegeven hebben. Jullie hebben mij geleerd om door te bijten en volop voor iets te gaan, om met tegenslagen om te gaan en bij succes mooi met de voetjes op de grond te blijven. Zonder jullie zou ik nooit staan waar ik nu sta of zijn wie ik nu ben. Weet dat ik ontzettend dankbaar ben voor wat jullie allemaal voor mij doen. Uit de grond van mijn hart, een hele dikke merci!
Béke, het kon vroeger al eens stevig botsen tussen ons. Maar dat was meestal ook weer snel vergeten. Wanneer mama en papa nog steeds gefrustreerd en opgejaagd waren van ons geruzie, waren wij al lang weer samen aan het spelen. Als Justine Henin en Kim Clijsters maakten we de koer onveilig met spannende tenniswedstrijden en we namen als echte radiosterren onze eigen cassettes op. Onze zussenband is er met de tijd alleen maar beter op geworden. Ik weet dat ik altijd op jou en ook op Brecht kan rekenen en daarvoor ben ik heel dankbaar! Mathias, van de kleine broer die ik vroeger vele koosnaampjes gaf, blijft niet meer veel over. Van jouw (paarden)kracht hebben we al handig gebruik kunnen maken op onze bouw. We delen misschien niet altijd dezelfde mening, maar ik weet dat je er voor mij bent als het nodig is en dat is meer dan genoeg. Merci!

En dan kom ik bij jou, Andy. De laatste, maar zeker niet de minste in dit dankwoord. In tegendeel. Al meer dan tien jaar sta je aan mijn zij. Het begon in de Chiro en ging zoveel verder. Je moest naar Afghanistan, ik ging op kot in Leuven, we woonden samen in ons appartement, we trouwden en kochten een huis. Ondertussen is het zelfs zo ver gekomen dat we midden tussen de verbouwingswerken van dat huis in een caravan wonen. Om maar aan te tonen dat we samen al heel ver gekomen zijn en heel wat aankunnen. Ik ben zo dankbaar dat je er altijd voor mij bent. Ik zou niet weten wat ik zonder jou zou moeten doen.
Ik kan niet wachten om samen met jou verder te bouwen aan onze toekomst en kijk enorm uit naar de komst van ons kindje. Ik weet nu al dat je een fantastische papa gaat worden.
Liefje, ik hou van jou!

Mieke
Januari 2020

Summary

Bread is the main food product prepared from wheat and a staple food in the Western world. It fits well in a balanced diet since it is an excellent source of energy, fiber, vitamins and minerals. Unfortunately, of all bread produced, about 25% is wasted. The loss of bread in a home environment represents the largest share of this waste. Consumers indeed prefer fresh bread with a soft, but sliceable crumb, a crispy crust and a desired flavor. Regrettably, upon storage the crumb firms, the crust loses its crispiness and the flavor characteristics of fresh bread disappear. Storage therefore renders bread unacceptable for consumers. To address the crumb firming component of this problem in an efficient way, a **thorough understanding of bread constituent transitions during baking and cooling and their impact on crumb firming** is required. Although the impact of different bread components on the properties of fresh and stored bread in general is well known, the exact timing and extent of constituent transitions during bread making remain to be elucidated.

For bread making, at least wheat flour, water, yeast and salt are needed. In quantitative terms, starch is the main flour component. It greatly contributes to the properties of fresh and stored bread. Starch is almost exclusively made up of amylopectin (AP) and amylose (AM) molecules which appear in highly ordered, partially crystalline starch granules. Starch crystallinity is mainly attributed to parts of the AP component.

When heating starch in sufficient water (such as during bread baking) the order of starch granules is lost and starch gelatinizes. This phenomenon is accompanied by substantial granule swelling due to water absorption, leaching of AM from the granules and melting of AP crystals. At what point and to what extent these phenomena take place during bread baking depends on the level and the structure of AM and AP. During bread cooling, AM gelation occurs. In the process, (leached) AM crystallizes and forms a network throughout the bread crumb. Together with the gluten network formed during baking, this network provides the crumb of fresh bread with its desired texture. During storage, AP recrystallization reinforces the starch network. In this process, water is withdrawn from the gluten network and immobilized in the starch network. Together with water redistribution between crumb and

crust this results in dehydration and (further) firming of gluten and starch networks and, thus, of crumb.

To provide a proper background for investigating the functionality of starch and its interaction with water during wheat bread making, an overview of the literature on the characteristics of wheat starch and its role during bread making and storage is presented in a first part of this doctoral dissertation. Useful analytical approaches are also described. Starch transformations and water redistribution during bread making and storage can accurately be analyzed with time domain proton nuclear magnetic resonance (TD ^{1}H NMR). This technique can be used in a temperature-controlled fashion to study the starch transitions and water dynamics in bread while it is being baked and subsequently cooled. Although changes in the starch fraction during cooling are of major importance for the quality of fresh bread, this part of the bread making process has not been investigated with temperature-controlled TD ^{1}H NMR. Furthermore, NMR measurements in bread dough have mainly been performed during stepwise heating, which is not representative for how bread is baked. Such NMR measurements yield a complex set of data. To the best of our knowledge, these data have never been interpreted in combination with different techniques that monitor starch crystallinity, swelling and leaching phenomena.

Against this background, the aim of this doctoral dissertation was to **develop an innovative toolbox primarily based on temperature-controlled TD ^{1}H NMR for studying starch transitions and water dynamics in dough and bread during heating and cooling processes relevant for bread making**. In a first part of the experimental section, the combined use of temperature-controlled TD ^{1}H NMR, time-resolved wide angle X-ray diffraction, differential scanning calorimetry (DSC) and colorimetric and gravimetric analyses of starch properties proved to be powerful when investigating changes in the starch fraction and the related water mobility in bread during baking and cooling. This way, an integrated view on gelatinization and gelation phenomena at different length scales during bread making was created.

Temperature-controlled NMR was then used to **specifically look into AM and AP functionality during bread making**. In this context, wheat flours containing unique starches and a successful antifirming amylase, *i.e.* the maltogenic α-amylase from *Bacillus stearothermophilus* (BStA), were excellent research tools.

Some of the flours used were from near-isogenic wheat lines (NILs). NIL 5-5 flour contained less AM and higher levels short AP chains than the control, *i.e.* NIL 1-1 flour. In addition, wheat flour of which the starch has a very low AM level was used. Incorporation of these flours in a bread recipe resulted in altered temperature ranges of gelatinization and gelation. It was

found that the stability of AP crystals was higher when starch contained little AM such that the temperature range over which gelatinization occurred during baking shifted to higher temperatures. In contrast, AP crystal stability was lower when starch contained higher levels of AP branch chains that are too short to form stable crystals such that gelatinization temperatures decreased.

Although starch hydrolysis by BStA also resulted in increased levels of short AP branch chains, no such shift in gelatinization temperature was detected when baking bread prepared with use of BStA. It follows that BStA only significantly hydrolyzes starch after the onset of gelatinization. Later during baking, a slightly weakened starch network with more mobile AM molecules due to hydrolysis of AM by BStA was obtained. This pointed to the structure-building role of AM in bread crumb, as also described in literature, which was further validated. When starch contained less AM, cooling to lower temperatures was required for AM crystallization to start. Eventually, a less extended AM network with less AM crystals was formed. Protons in lower AM starch networks were more mobile, which was indicative for softer fresh bread crumb.

To study **the impact of AM and AP characteristics on fresh and stored bread**, bread was prepared from unique wheat flours or by incorporating BStA in the recipe. The breads were stored at room temperature. Crumb firming was monitored by TD ^{1}H NMR, DSC and texture measurements. When the starch AM content was lower, a less extended AM network was formed during cooling of freshly baked bread. As a result, the crumb in the fresh, cool bread was too soft to be sliceable. However, after 7 days of storage, crumb firmness readings of bread containing little if any AM were more than twice those of control bread. Since very low starch AM levels imply very high AP levels, it is evident that the extent of AP recrystallization during storage substantially increased. In contrast, the amount of recrystallized AP and the crumb firmness after 7 days of storage were half those of control bread when bread was prepared with use of BStA or from NIL 5-5 flour containing starch with a higher level of AP branch chains that are too short to crystallize.

In the last part of this doctoral dissertation, not the bread recipe but its production process was altered. Bread was prepared by first partial and, following intermediate storage, final baking. The **impact of variations in duration of partial baking on fresh and stored bread** was examined. The initial crumb resilience increased with partial baking time as a result of more extended starch and gluten networks. With prolonged partial baking, more AM leached and was available for crystallization during cooling. Gluten protein cross-linking was enhanced as well.

During intermediate storage after the first, partial baking, the extent of crumb firming was higher when bread had been baked for a longer time. It is believed that leaching of AM and also of AP outside the granules continued during prolonged baking. Consequently, a more extended AM network with more AM crystals that serve as nuclei for AP retrogradation was formed during cooling. Moreover, the resultant higher concentration of AP in the outer zones of the gelatinized granule remnants and the presence of leached AP molecules in the extragranular space enhanced both intragranular and intergranular AP retrogradation during intermediate storage. In addition, the crust moisture content (MC) of fresh partially baked bread was lower when baking times had been longer such that moisture redistribution between crumb and crust occurred to greater extent during intermediate storage.

During final baking after intermediate storage, the recrystallized AP melted. The moisture redistribution that had occurred during the preceding intermediate storage phase, however, was not heat-reversible. In bread prepared from 100 g of flour, crumb MC decreased typically by 8% during 7 days of storage due to crumb to crust moisture migration. In bread prepared from 270 g flour, stored for the same time, crumb MC decreased only by 1% because of their high crumb to crust ratio. Since the crumb MC of the latter breads remained high during intermediate storage, melting of the recrystallized AP was sufficient to refresh the crumb and to restore firmness and resilience readings to their initial values in fresh bread. In contrast to what is generally believed, the refreshed bread loaves did not firm faster than those produced by conventional, one-step baking. The size of bread loaves is crucial in this context. Indeed, bread loaves prepared from only 100 g of flour were subject to substantial crumb dehydration during storage. Since the latter was not heat-reversible, we assume that smaller bread loaves, prepared by partial and later final baking after intermediate storage, do firm more rapidly than their conventionally baked counterparts.

In conclusion, starch transitions and water redistribution greatly determine fresh and stored bread properties. AP characteristics mainly determine the timing of gelatinization during baking and the extent to which AP recrystallizes during storage. AM characteristics impact on the timing and extent of AM crystallization and the formation of the AM network during cooling. Redistribution of water is an integral part of crumb firming, especially in the case of partial and later final baking, since moisture redistribution during intermediate storage at room temperature is not heat-reversible. **In-depth understanding of the functionality of AM and AP and the related water mobility allows defining an ideal starch in flour for bread making purposes**. Such starch has an AM to AP ratio and AM chain length distribution corresponding to that of regular wheat starch and a high portion of outer AP branch chains that are too short to crystallize (DP 6-10).

Samenvatting

Brood is het voornaamste product gebaseerd op tarwe en is een basisvoedingsmiddel in de Westerse wereld. Brood past uitstekend in een gezond voedingspatroon aangezien het een goede bron van energie, vezels, vitaminen en mineralen is. Helaas wordt 25% van al het geproduceerde brood verspild, en dit voornamelijk door de consument. Consumenten verkiezen vers brood met een zacht, maar versnijdbaar kruim, een knapperige korst en de gewenste smaak en aroma's. Tijdens bewaring verstevigt het kruim, wordt de korst taai en gaan de gewenste smaak en aroma's verloren zodat het brood niet meer acceptabel is voor de consument. Om de problematiek van kruimverharding op efficiënte wijze aan te pakken, is **grondige kennis van de transformaties van broodconstituenten tijdens de broodbereiding en de impact ervan op het verouderingsmechanisme** vereist. Hoewel de bijdrage van verschillende broodconstituenten aan de eigenschappen van vers en bewaard brood relatief goed gekend is, blijft het inzicht in de exacte 'timing' en mate van structuurwijzigingen tijdens de broodbereiding beperkt.

Essentiële ingrediënten voor de broodbereiding zijn tarwebloem, water, gist en zout. Kwantitatief gezien is zetmeel de belangrijkste bloemcomponent. Het draagt in belangrijke mate bij tot de eigenschappen van vers en bewaard brood. Zetmeel bestaat voornamelijk uit amylopectine (AP)- en amylose (AM)- moleculen die georganiseerd zijn in gedeeltelijk kristallijne granulen. De kristalliniteit van zetmeel wordt voornamelijk aan AP toegeschreven.

Wanneer zetmeel wordt verwarmd in aanwezigheid van voldoende water, zoals tijdens het broodbakproces, treedt verstijfseling op waarbij de orde van zetmeelgranulen verloren gaat. Verstijfseling gaat gepaard met een aanzienlijke wateropname en dus zwelling van de granulen, uitloging van AM buiten de granulen en afsmelting van de AP-kristallen. Wanneer en in welke mate deze fenomenen optreden tijdens bakken, is afhankelijk van de concentratie en de structuur van AM en AP in zetmeel. Wanneer brood kan afkoelen, vindt gelering van AM plaats. (Uitgeloogde) AM-moleculen kristalliseren en vormen een netwerk doorheen broodkruim. Samen met het glutennetwerk dat wordt gevormd tijdens bakken, draagt dit netwerk bij tot de gewenste textuureigenschappen van vers broodkruim. Tijdens bewaring

treed rekristallisatie van AP op zodat het zetmeelnetwerk verstevigt. Water, dat werd onttrokken aan het glutennetwerk, wordt in dit zetmeelnetwerk geïmmobiliseerd. Samen met de herverdeling van water tussen kruim en korst zorgt dit voor uitdroging en (verdere) verharding van gluten- en zetmeelnetwerken, en dus van kruim.

Als vertrekpunt voor het onderzoek naar de functionaliteit van zetmeel en zijn interactie met water tijdens de bereiding van tarwebrood, werd in een eerste deel van dit doctoraatsproefschrift een literatuurstudie over de eigenschappen van tarwezetmeel en de rol ervan tijdens de broodbereiding- en bewaring uitgevoerd. Nuttige analytische benaderingen in deze context werden eveneens vermeld. Wijzigingen van zetmeel en de herverdeling van water tijdens de broodbereiding en -bewaring kunnen nauwkeurig geanalyseerd worden met 'time domain' proton nucleaire magnetische resonantie (TD ^{1}H-NMR). Deze techniek kan op temperatuur-gecontroleerde wijze worden toegepast om wijzigingen in de zetmeel- en waterfractie in brood op te volgen terwijl het bak-, en later het afkoelproces, plaatsvindt. Hoewel veranderingen van zetmeel tijdens de koelfase cruciaal zijn voor de kwaliteit van vers brood, werd dit proces tot dusver niet bestudeerd met temperatuur-gecontroleerde TD ^{1}H-NMR. NMR-metingen op deeg werden overigens meestal uitgevoerd tijdens stapsgewijze opwarming, hetgeen niet representatief is voor het broodbakproces. De experimentele gegevens die met NMR-analyses worden verzameld, zijn complex. Voor zover we weten werden deze gegevens tot nog toe niet geïnterpreteerd in combinatie met andere technieken die de kristalliniteit van zetmeel en zijn zwel- en uitloginsgedrag meten.

In dit kader was het doel van dit doctoraatsonderzoek **een vernieuwende 'toolbox' gebaseerd op temperatuur-gecontroleerde TD ^{1}H-NMR te ontwikkelen zodat zetmeeltransities en de herverdeling van water in deeg en brood bestudeerd kunnen worden tijdens een opwarm- en koelproces dat relevant is voor de broodbereiding**. In een eerste deel van dit proefschrift werd aangetoond dat de combinatie van temperatuur-gecontroleerde TD ^{1}H-NMR met tijdsafhankelijke metingen van X-stralen diffractie bij grote hoeken, differentiële 'scanning' calorimetrie (DSC) en colorimetrische en gravimetrische analyses van zetmeeleigenschappen, krachtige analysemogelijkheden biedt om wijzigingen in de zetmeel- en waterfractie in brood te bestuderen tijdens een bak- en koelproces. Zodoende werd een geïntegreerd beeld van verstijfselings- en geleringsfenomenen op verschillende lengteschalen ontwikkeld.

De temperatuur-gecontroleerde NMR 'toolbox' werd vervolgens gebruikt om **dieper in te gaan op de functionaliteit van AM en AP tijdens de broodbereiding**. Unieke tarwebloemstalen met verschillende AM- en AP-karakteristieken en een efficiënt anti-

broodverouderingsenzym, *i.e.* het maltogeen α-amylase uit *Bacillus stearothermophilus* (BStA) vormen in deze context uitstekende hulpmiddelen.

Bloemstalen afkomstig van 'near-isogenic' tarwecultivars (NILs) verschilden uitsluitend op vlak van AM- en AP-eigenschappen. NIL 5-5 bloem bevatte minder AM en een hogere portie korte AP-ketens dan de controle, *i.e.* NIL 1-1 bloem. Verder werd tarwebloem met een zeer laag AM-gehalte in zetmeel gebruikt. Wanneer deeg bereid werd met deze bloemstalen, trad een verandering van het temperatuurbereik van verstijfseling en gelering op. De stabiliteit van AP-kristallen nam toe wanneer zetmeel minder AM bevatte zodat verstijfseling plaatsvond bij hogere temperaturen. Een grotere hoeveelheid korte AP-zijketens, die te kort zijn om stabiele kristallen te vormen, was daarentegen verantwoordelijk voor de afname van de AP-kristalstabiliteit. Dit uitte zich in lagere verstijfselingstemperaturen.

Hoewel de hydrolyse van zetmeel door BStA eveneens een toename van zulke korte AP-zijketens veroorzaakte, bleef een verschuiving van de verstijfselingstemperatuur tijdens het bakken van brood bereid met BStA uit. Hieruit werd afgeleid dat BStA zetmeel slechts significant hydrolyseert nadat zetmeel begint te verstijfselen. Door inwerking van BStA op AM werd aan het eind van de bakfase een enigszins verzwakt zetmeelnetwerk met mobielere AM-moleculen bekomen. AM wordt dan ook als structuurvormer in broodkruim beschreven. Wanneer AM-concentraties in broodkruim lager waren, startte AM-kristallisatie bij lagere temperaturen, en dus later tijdens de koelfase. Bovendien werd een minder uitgebreid AM-netwerk met minder AM-kristallen gevormd. Dat protonen in dit netwerk mobieler bleven, duidde op een zachter vers broodkruim.

Om **het effect van AM- en AP-karakteristieken op de eigenschappen van vers en bewaard brood** te onderzoeken, werd brood bereid met unieke bloemstalen of met toevoeging van BStA. Deze broden werden vervolgens bewaard bij kamertemperatuur. Het verouderingsmechanisme werd opgevolgd met TD ^{1}H-NMR, DSC en textuurmetingen. Wanneer het AM-gehalte in brood lager was, werd het AM-netwerk slechts in beperkte mate gevormd. Vers, afgekoeld broodkruim was bijgevolg te zacht en niet versnijdbaar. Na 7 dagen bewaring was de kruimhardheid van brood dat weinig of geen AM bevatte bijna dubbel zo hoog als de kruimhardheid van bewaard controlebrood. Dit werd toegeschreven aan de sterk toegenomen mate van AP-rekristallisatie als gevolg van het zeer lage AM- en, dus, zeer hoge AP-gehalte van zetmeel in brood. Aangezien brood bereid met NIL 5-5 bloem of met toevoeging van BStA meer AP-zijketens bevatte die te kort zijn om te rekristalliseren, nam de hoeveelheid gekristalliseerd AP en de kruimhardheid tijdens 7 dagen bewaring maar half zoveel toe als in controlebrood.

In het laatste deel van deze thesis werd niet de broodreceptuur maar het bakproces gewijzigd. Brood werd eerst slechts gedeeltelijk gebakken en pas na een intermediaire bewaarperiode volledig afgebakken. De **impact van een variërende baktijd tijdens de eerste bakfase op de eigenschappen van vers en bewaard brood** werd onderzocht. Met toenemende baktijd nam de veerkracht van kruim in vers, voorgebakken brood toe. Dit was te wijten aan de vorming van een meer uitgestrekt AM- en glutennetwerk. Een langere baktijd werd geassocieerd met een sterkere mate van AM-uitloging zodat meer AM-moleculen konden kristalliseren tijdens de koelfase. De verknoping van glutenproteïnen werd eveneens bevorderd.

Tijdens de intermediaire bewaarfase, nam de mate van kruimverharding toe wanneer het brood gedurende langere tijd voorgebakken werd. Er werd aangenomen dat de uitloging van AM, en ook van AP, voortging wanneer de baktijd toenam. Zodoende werd een sterker ontwikkeld AM netwerk, met meer AM-kristallen die dienst doen als nuclei voor AP-retrogradatie, gevormd tijdens koelen. Bovendien werd zowel intra- als intergranulaire AP-retrogradatie bevorderd door de hogere AP-concentratie in de buitenste zones van de granulerestanten en de aanwezigheid van uitgeloogd AP in de extragranulaire ruimte. Verder werd brood met een lager korstvochtgehalte bekomen wanneer de baktijd toenam. Vervolgens trad vochtmigratie tussen kruim en korst tijdens bewaring in sterkere mate op.

Na de intermediaire bewaarperiode werden de broden afgebakken zodat gekristalliseerd AP terug afsmolt. De herverdeling van water die optrad tijdens intermediaire bewaring kon echter niet ongedaan gemaakt worden tijdens deze finale bakfase. Het kruimvochtgehalte van brood bereid met 100 g bloem nam af met 8% tijdens 7 dagen bewaring ten gevolge van kruim naar korst vochtmigratie. In brood bereid met 270 g bloem en bewaard gedurende dezelfde termijn, nam het kruimvochtgehalte met slechts 1% af door de hoge kruim tot korst verhouding. Het kruimvochtgehalte van deze laatste broden bleef dus hoog tijdens intermediaire bewaring. Zodoende volstond het afsmelten van gerekristalliseerd AP om een vers, afgebakken brood te verkrijgen met een kruimhardheid en –veerkracht die vergelijkbaar was met die van vers, voorgebakken brood. In tegenstelling tot wat algemeen wordt aangenomen, verhardde het kruim van dit afgebakken brood bovendien niet sneller dan dat van brood bereid via een conventioneel, enkelvoudig bakproces. Het broodvolume is zeer belangrijk in deze context. Kruim van brood bereid met 100 g bloem droogde namelijk aanzienlijk uit tijdens intermediaire bewaring. Aangezien dit niet ongedaan gemaakt kan worden tijdens afbakken, gaan we ervan uit dat kleiner brood na afbakken wel sneller zal verouderen dan zijn conventioneel gebakken equivalent.

Wijzigingen in de zetmeelfractie en de herverdeling van water dragen dus in belangrijke mate bij tot de eigenschappen van vers en bewaard brood. De 'timing' van verstijfseling tijdens bakken en de mate van AP-rekristallisatie tijdens bewaring zijn grotendeels afhankelijk van AP-karakteristieken. AM-karakteristieken bepalen het moment waarop en de mate waarin AM-kristallisatie en de ontwikkeling van het AM-netwerk optreden tijdens koelen. Er werd aangetoond dat de herverdeling van water van groot belang is tijdens de broodveroudering, zeker wanneer het om afgebakken brood gaat. De waterherverdeling die plaatsvindt tijdens intermediaire bewaring is namelijk niet omkeerbaar tijdens de finale bakfase. **De verworven inzichten over de rol van AM en AP en de hiermee gerelateerde watermobiliteit laten toe de optimale zetmeeleigenschappen in brood te beschrijven.** In zulk zetmeel komen de verhouding van AM en AP en de ketenlengteverdeling van AM overeen met deze in normaal tarwezetmeel, terwijl de AP-fractie een aanzienlijke hoeveelheid ketens bevat die te kort zijn om te kristalliseren.

List of abbreviations and symbols

SYMBOLS

^1H	proton
B_0	external, static magnetic field
ΔB_0	differences in the static magnetic field due to field inhomogeneities
B_1	oscillating magnetic field
ΔH_{AP}	melting enthalpy of (retrograded) amylopectin crystals
2θ	scattering angle
T_1	longitudinal
T_2	transverse (natural)
T_2^*	transverse (total)

ABBREVIATIONS

AM	amylose
AM-L complex	amylose-lipid complex
AP	amylopectin
au	arbitrary units
BStA	*Bacillus stearothermophilus α-amylase*
BSuA	*Bacillus subtilis α-amylase*

CB	conventionally baked
CHL	carbohydrate leaching
CL	chain length
CO_2	carbon dioxide
CPMG	Carr-Purcell-Meiboom-Gill
dm	dry matter
DMSO	dimethylsulfoxide
DP	degree of polymerization
DSC	differential scanning calorimetry
DTT	dithiothreitol
EP	extractable proteins
FB	fully baked
FID	free induction decay
GBSSI	granule bound starch synthase I
H-AP	high-amylopectin
HPAEC-PAD	high performance anion exchange chromatography with pulsed amperometric detection
MC	moisture content
MW	molecular weight
nc	no crust
n.d.	not determined
NIL	near-isogenic wheat line
NMR	nuclear magnetic resonance
PB	partially baked

SANS	small angle neutron scattering
SAXS	small angle X-ray scattering
SDS	sodium dodecyl sulfate
SE-HPLC	size exclusion high performance liquid chromatography
SH	sulfhydryl
SS	disulfide
SSIIa	starch synthase IIa
SP	swelling power
TD	time domain
WAXD	wide angle X-ray diffraction
WE-AX	water extractable arabinoxylan
WRC	water retention capacity
WU-AX	water unextractable arabinoxylan

Table of contents

Context and aims

Wheat bread is a staple food in the Western world. Essential ingredients for bread making are wheat flour, water, yeast and salt. In Europe, bread is mainly manufactured via the straight-dough process. First, the ingredients are mixed to form viscoelastic dough (a foam) which then is fermented and proofed. Fermentation and proofing result in what is referred to as leavened dough. During subsequent baking, dough is transformed into gas continuous bread (a sponge). After cooling, fresh bread is sliceable and has a desired softness and crumb structure.

During baking, biopolymer transitions such as starch gelatinization and gluten protein cross-linking occur. Together with the redistribution of water, they contribute to the transformation of the foam structure of dough to the sponge structure of bread. During cooling, gelatinized starch regains a certain degree of order and forms a network. Starch and gluten networks in fresh bread codetermine the crumb texture. During storage, starch retrogradation on the one hand and moisture redistribution from crumb to crust and from gluten to starch on the other cause the crumb to firm.

Today, different antifirming strategies such as the use of enzymes or altered bread making processes and storage conditions are in place for enhancing the shelf life of bread. In spite of this, bread still significantly contributes to global food waste since a substantial portion of it is lost in different parts of the supply chain. To improve bread quality and reduce bread waste and the associated economical losses, in-depth understanding of bread constituent transitions during bread making and how they impact on changes during storage is crucial.

Starch is quantitatively the main flour constituent. It greatly determines the properties of fresh and stored bread. It has high affinity for water and neither in dough nor in bread is miscible with the second most abundant flour constituent, *i.e.* gluten. Water is indeed redistributed between gluten and starch during bread making and storage. Starch consists of two biopolymers, *i.e.* the nearly linear amylose (AM) and the highly branched amylopectin (AP). The former is responsible for starch network formation during cooling of baked bread while the latter determines the further development of the starch network during storage.

Time domain proton nuclear magnetic resonance (TD ^{1}H NMR) is a valuable technique to study molecular and mesoscale aspects of the starch network and the mobility of water therein before and after bread baking and during storage. However, **at what point and to what extent starch transitions and water redistribution exactly occur during both baking and cooling and how these transitions relate to changes during subsequent storage** are not entirely understood.

Against this background, in this doctoral dissertation an innovative toolbox based on temperature-controlled TD ^{1}H NMR is optimized and used to *in situ* study changes in the starch fraction and the related water mobility during bread baking and cooling. Unique wheat flours containing atypical starches and a much used antifirming amylase are included in the bread recipe as research tools to specifically figure out AM and AP functionality during bread making and storage. Furthermore, an alternative, interrupted bread making process, *i.e.* parbaking, is used to clarify how changes during baking and cooling relate to the crumb firming mechanism.

The focus of **Chapter 1** of the **literature review** of this thesis is on the structural organization at different length scales and the physicochemical behavior of wheat starch (Figure i.1). Atypical starch characteristics can result from crossing different wheat lines with null mutations in certain genes. Their impact on the physicochemical properties of starch is discussed as well. In **Chapter 2** the current view on the role of starch and other bread constituents during the different stages in the chain from flour to (stored) bread is summarized. Some antifirming strategies and the underlying mechanisms are discussed. Furthermore, techniques for studying biopolymer transitions and water redistribution during bread making and storage are described. Special attention is given to TD ^{1}H NMR as it is the main technique used to monitor starch transitions and water dynamics in this work.

The **experimental work** is subdivided in three parts (Figure i.1). In the first part, the main goal of **Chapter 3** is to optimize a temperature-controlled TD ^{1}H NMR methodology to study changes in the starch fraction and the related water redistribution *in situ* during bread baking and cooling. Wide angle X-ray diffraction (WAXD) is used in an *in situ* fashion to monitor the different crystalline forms of starch during baking and cooling. TD ^{1}H NMR and WAXD measurements are performed while the sample is heated and subsequently cooled with a temperature profile typical for that in the center of bread crumb during conventional baking and cooling. The **toolbox** is complemented with differential scanning calorimetry (DSC), colorimetric and gravimetric analyses that are used for measuring gelatinization associated phenomena. This combination of techniques which allow executing measurements at different length scales, underpins the interpretation of the complex NMR data.

In the second part, the specific functionality of AM and AP in bread making is considered. Hereto, the **bread recipe** is altered (Figure i.1). Flour from wheat containing unusual starches is used for dough preparation and a successful antifirming amylase is included in the recipe. The resulting doughs are analyzed with the temperature-controlled NMR toolbox during bread baking and cooling in **Chapter 4** to elucidate the functionality of AM and AP. The *in situ* approach furthermore allows to examine the impact of the amylase during bread making. A toolbox consisting of *inter alia* TD ^{1}H NMR, DSC and texture analysis is applied in **Chapter 5** to study the crumb firming mechanism of bread loaves with atypical starch characteristics at different length scales. Furthermore, the impact of atypical starch transitions on the texture of fresh and stored bread is assessed.

In the last part of the experimental section, alternative **process conditions** for bread making are dealt with (Figure i.1). In **Chapter 6**, bread is produced by partial and later final baking. The two baking phases are separated by an intermediate storage period at room temperature. The impact of different baking times for the first baking phase on fresh partially and later fully baked bread properties and their crumb firming mechanism is investigated. The firming mechanism of fully baked bread is further compared to that of conventionally baked bread, produced by a single baking step, to verify whether the former firms more rapidly than the latter, as is generally believed.

The final part of this doctoral dissertation contains a general discussion on the functionality of AM and AP and the related water mobility during bread making and storage. The **main conclusions** drawn from the experimental results and some perspectives for future research are presented.

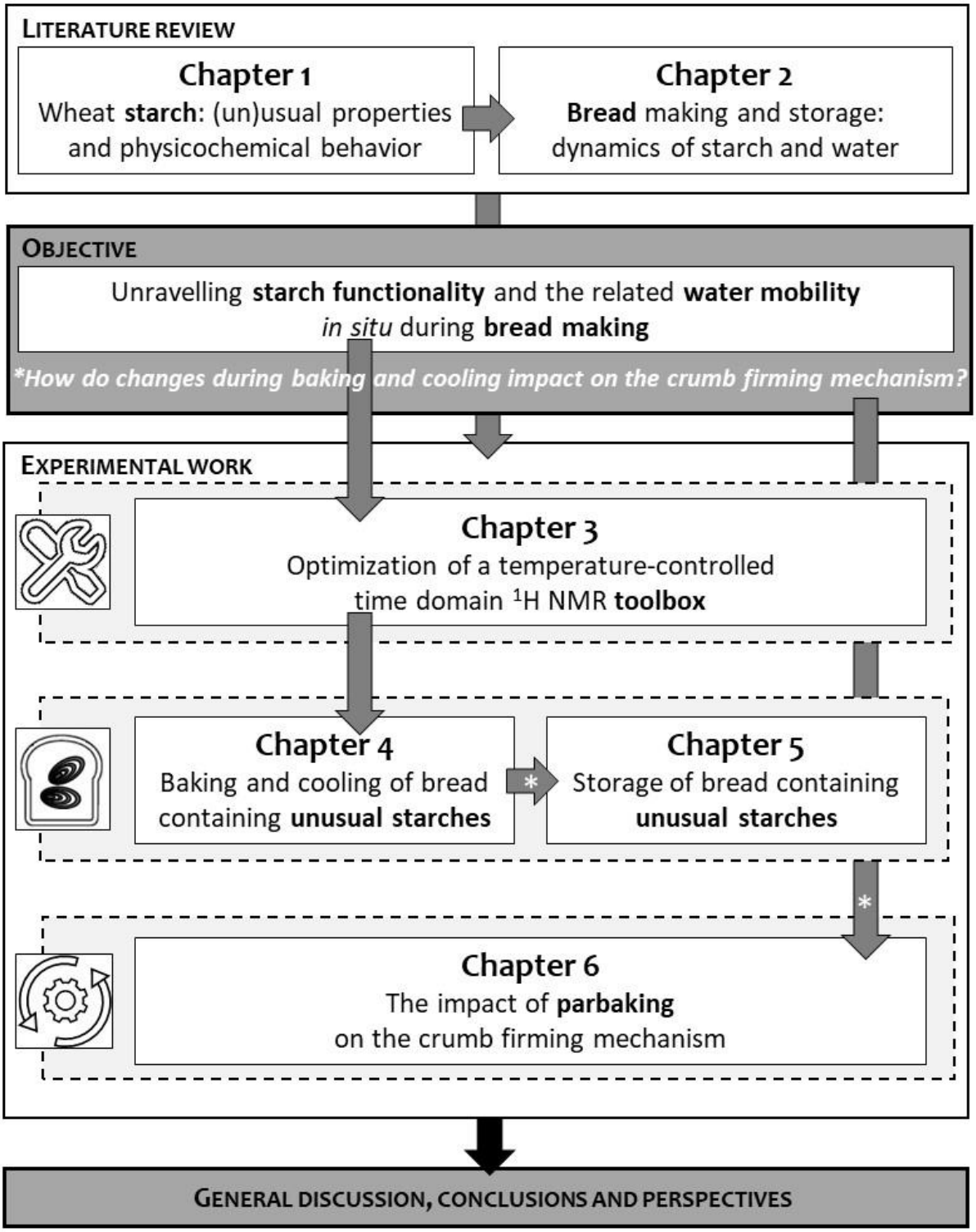

Figure i.1 Schematic overview of the different chapters in this doctoral disstertation and how they are interconnected.

Part one

Literature review

Chapter 1

Wheat starch: (un)usual properties and physicochemical behavior

Chapter 2

Bread making and storage: dynamics of starch and water

Chapter 1
Wheat starch: (un)usual properties and physicochemical behavior

1.1 INTRODUCTION

Starch occurs as storage carbohydrate in the organs of various green plants, *e.g.* in fruits, seeds, roots and tubers (French, 1984; Shannon *et al.*, 2009). It is a major carbohydrate source in the human diet since it is a main constituent of staple foods such as bread, breakfast cereals, pasta, rice and potatoes (Aston *et al.*, 2008; Delcour & Hoseney, 2010).

Regular starch contains two α-glucan biopolymers, amylose (AM) and amylopectin (AP) (Tester *et al.*, 2004). They are organized in highly ordered, semicrystalline granules (Buléon *et al.*, 1998). The texture and appearance of *inter alia* cereal-based foods is brought about by the AM/AP ratio, the granular organization and the physicochemical behavior of starch during heating, cooling and storage and depends on the botanical origin of starch (Mason, 2009; Waterschoot *et al.*, 2015). The focus of this chapter lies on the composition, structure and physicochemical properties of wheat (*Triticum aestivum* L.) starch.

1.2 WHEAT STARCH COMPOSITION

In general, starch biopolymers represent 98-99% of starch granules' dry matter (dm). AM is in essence a linear molecule while AP appears as a large, heavily branched structure (Tester *et al.*, 2004). Regular wheat starch contains 71-75% AP and 25-29% AM (Jane *et al.*, 1999; Sargeant, 1982; Swinkels, 1985; Vansteelandt & Delcour, 1999; Waterschoot *et al.*, 2015; Young, 1984). Minor constituents of wheat starch are lipids (*ca*. 1%) (Buléon *et al.*, 1998) and proteins (*ca.* 0.5%) (Swinkels, 1985).

1.2.1 Amylopectin

AP consists of D-glucospyranosyl units linked by α-1,4 bonds and a substantial portion of α-1,6 bonds (*ca*. 5%). Wheat starch AP has an average degree of polymerization (DP) of 5,000-9,400 (Shibanuma *et al.*, 1994) and an average chain length (CL) of 19-23 (Hizukuri, 1996; Jane *et al.*, 1999; Shibanuma *et al.*, 1994).

The branched structure of AP of starches from different botanical origin is well described by the **cluster model** proposed by French (1972) and Robin *et al*. (1974). In this model, AP branch points are clustered rather than being randomly distributed (Lineback, 1986). One cluster has an average length of 27-28 glucosyl residues (Hizukuri, 1986) and consists of an amorphous branching region and a crystalline region. The latter is composed of closely packed **double helices** of outer AP branch chains with an average CL of 12-16 (Figure 1.1) (Hall & Manners, 1980; Hizukuri, 1986; Robin *et al.*, 1974). A CL of at least 10 is required for double helix formation of pure oligosaccharides (Pfannemüller, 1987). Shorter chains can however cocrystallize with longer chains (CL > 10) (Gidley & Bulpin, 1987).

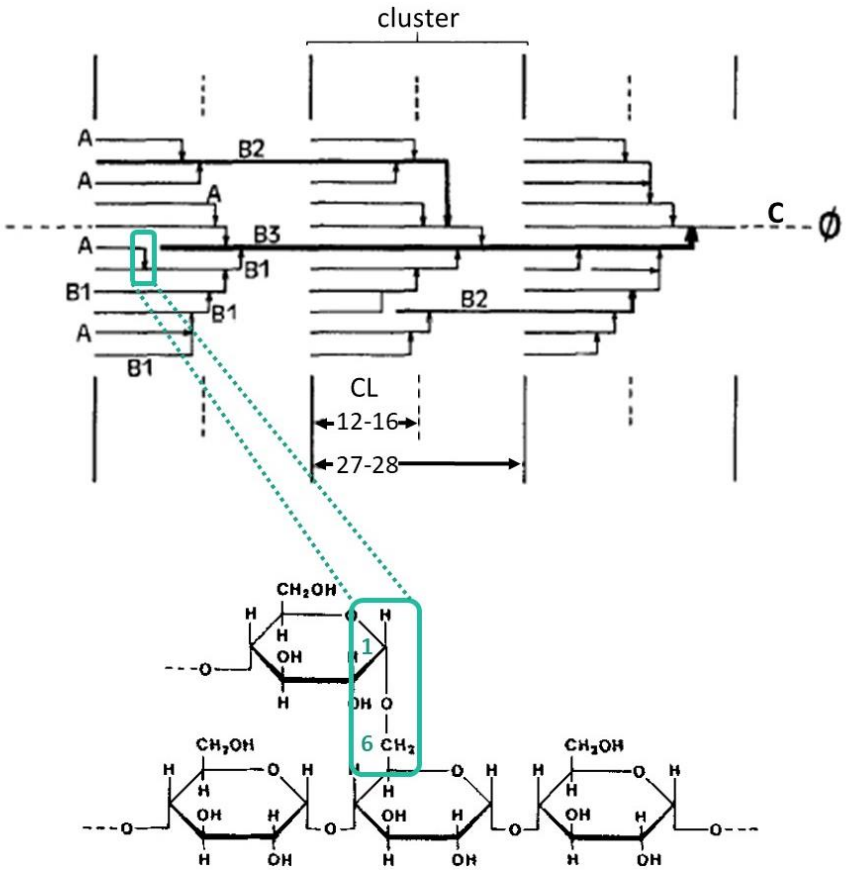

Figure 1.1 The cluster model of amylopectin (AP) from starches of different botanical origin. The chain with the sole reducing end (Ø) is the C-chain. A and B_1-B_3 branch chains are indicated. A- and B-chains are connected to other B-chains or the C-chain through α-1,6 linkages. The average chain length (CL) of one periodic cluster unit consisting of branch chain clusters and the branching region is 27-28. The outer AP branch chains have an average CL of 12-16. Based on Hizukuri (1986) and Zobel (1988).

Three types of AP chains are distinguished, *i.e.* A-, B- and C- chains. The C-chain is the only one which has a reducing end (Peat *et al.*, 1956). It carries B-chains which are connected with their reducing ends through α-1,6 linkages (Figure 1.1). These B-chains in turn carry one or more A- or B-chains. The A-chains are the exterior branches of the AP structure and are unsubstituted. The B-chains are subdivided in B_1-, B_2-, B_3- and B_4-chains depending on the number of clusters they are part of (Figure 1.1). A- and B_1-chains intertwine into double helices (Hizukuri, 1986).

High performance anion exchange chromatography with pulsed amperometric detection (HPAEC-PAD) is currently used to study the chain length distribution following debranching. Chains with DPs up to 50-60 can be separated individually (Koizumi *et al.*, 1991). Longer AP chains can be separated with size exclusion high performance liquid chromatography (SE-HPLC) (Hizukuri, 1985). Using HPAEC-PAD, Nagamine and Komae (1996) separated chain fractions of wheat AP with respectively DPs 6-18, 19-34 and ≥ 35 and assigned them to A-, B_1- and B_2-chains.

1.2.2 Amylose

AM consists mainly of α-1,4 linked D-glucospyranosyl units (Zobel, 1988) with few α-1,6 linkages (Banks & Greenwood, 1966). Wheat starch AM has an average DP range of 800-1,600 (Hanashiro & Takeda, 1998; Shibanuma *et al.*, 1994; Swinkels, 1985) and contains on average five chains per molecule (Takeda *et al.*, 1987). Although regular wheat starch contains more AP than AM on a weight basis, more AM than AP molecules per mass unit of starch are present (Waterschoot *et al.*, 2015).

The α-1,4 bonds of AM chains bring about a **helical structure** (Zobel, 1988). In the presence of a suitable ligand, a single left-handed helix (French & Murphy, 1977) with six glucose units per turn is formed (Figure 1.2) (Rundle & Edwards, 1943). The hydrophobic cavity of this helix can interact with the apolar part of different ligands (Whittam *et al.*, 1989) such as wheat endogenous starch lipids (Morrison *et al.*, 1975). This results in **AM-lipid (AM-L) complex** formation. The level of AM-L complexes in native wheat starch is *ca.* 0.5% (Vansteelandt & Delcour, 1999).

Different methods can be used to determine starch AM content. A first relies on the ability of AM to complex with suitable ligands. With iodine, AM forms complexes that have a typical blue color which can be measured colorimetrically. To avoid underestimations due to interference by AM-L complexes present in native cereal starches, lipids should be extracted prior to analysis (Gérard *et al.*, 2001). Furthermore, AP-iodine complexation can occur to a limited extent and lead to overestimation of AM contents (Vilaplana *et al.*, 2012). AM contents can also be determined by SE-HPLC. Prior to analysis, starch is debranched with isoamylase to

separate AM from AP (Ong *et al.*, 1994). Another method to measure AM content relies on the fact that AP contains many more nonreducing ends than does AM. The lectin concanavalin A interacts with nonreducing ends of α-glucans which lead to formation of insoluble aggregates (Goldstein *et al.*, 1965). Precipitation of AP using concanavalin A allows subsequent determination of the AM content in the supernatant (Gibson *et al.*, 1997).

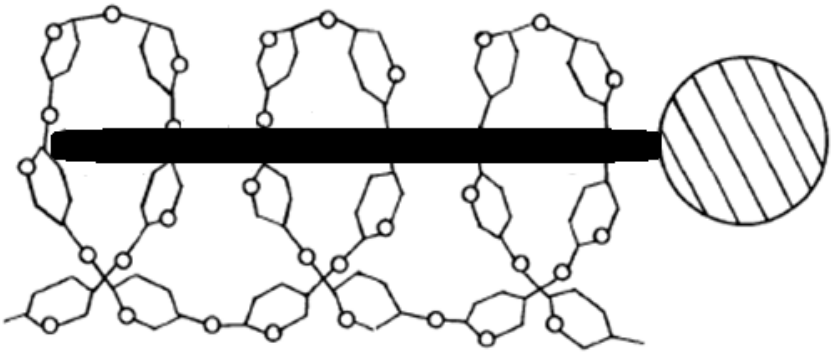

Figure 1.2 Complex formation of amylose (AM) with a ligand of which the aliphatic chain resides in the hydrophobic cavity of a single left-handed AM helix while its polar head group is located outside the helix. Adapted from Carlson *et al*. (1979).

1.2.3 Minor constituents

Wheat starch lipids consisted of nonpolar free fatty acids (6-9%), glycolipids (3-5%) and phospholipids (86-91%) (Morrison *et al.*, 1975). The latter are predominantly lysophospholipids which complex with AM (Hargin & Morrison, 1980). The lipid content of cereal starches is correlated with their AM content (Morrison, 1988). Other minor wheat starch constituents are proteins including puroindolines (Kim *et al.*, 2012), which form the genetic basis of wheat hardness (Morris, 2002), and granule bound starch synthases (GBSS) (Baldwin, 2001). The former can interact with lipids (Kim *et al.*, 2012).

1.3 GRANULAR ORGANIZATION

Wheat starch granules have a bimodal size distribution with both large lenticular and small spherical granules of respectively **22-36 µm** and **2-10 µm** (Evers, 1973; Glaring *et al.*, 2006; Jane *et al.*, 1994). Small granules account for 23-30% by weight and for more than 90% of the total number of granules (Evers, 1973; Morrison & Gadan, 1987).

Starch granules are highly ordered at different **length scales**. At the lowest level of structural organization, they are made up by AM and AP molecules. The outer AP branch chains intertwine into double helices and associate into clusters. The clustered AP structure gives rise

to crystalline and amorphous lamellae that are organized in blocklets which in turn are stacked in growth rings (Buléon *et al.*, 1998).

The long range order of starch polymers in the granules and not crystallinity itself are held responsible for the birefringence of starch granules (Zobel, 1988). Starch birefringence is observed with polarized light microscopy as typical Maltese crosses centered at the hilum (Blanshard, 1987; French, 1984).

1.3.1 Crystalline structure

The crystalline nature of starch was evidenced with X-ray diffraction by Scherrer (1922) and Katz (1928). Starch crystallinity is attributed mainly to AP (French, 1972; Rundle *et al.*, 1944) as it decreases with increasing AM levels (Fujita *et al.*, 1998). Different wide angle X-ray diffraction (WAXD) patterns are distinguished depending on the packing arrangement of AP double helices, which *inter alia* varies with the botanical origin of starches (Figure 1.3) (Hizukuri, 1996).

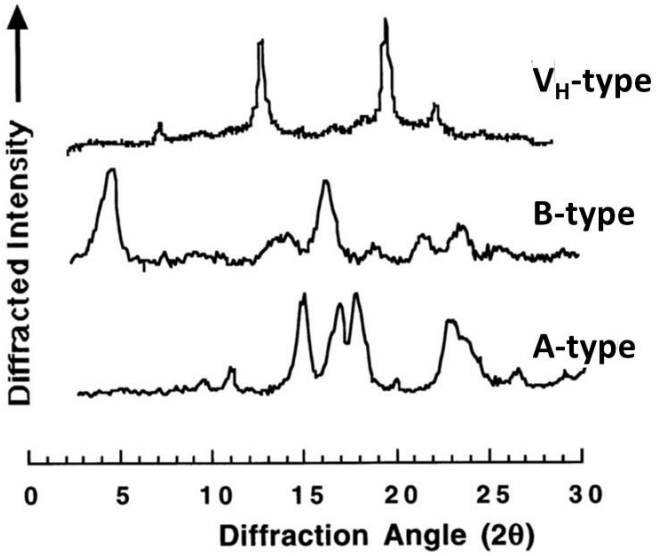

Figure 1.3 Wide angle X-ray diffraction patterns characteristic for A-, B- and V_H-type starch crystals. Diffraction angles (2θ) are displayed as if $Cu_{K\alpha}$ radiation was used (Buléon *et al.*, 1998).

Native cereal starches display an A-type pattern while tuber starches have a B-type pattern (Hizukuri, 1996). The **A-type** WAXD pattern has characteristic reflections at 15.1, 17.2, 18.1 and 23.2 °2θ $Cu_{K\alpha}$ (Figure 1.3) (Vermeylen *et al.*, 2004). Based on the intensity of X-ray diffraction patterns, native wheat starch has been reported to have a crystallinity of 36% (Hizukuri, 1996). Specific reflections of **B-type** patterns occur at 5.6, 15.0, 17.2, 22.4 and 24.1 °2θ $Cu_{K\alpha}$ (Figure 1.3) (Vermeylen *et al.*, 2004). The B-type is also characteristic for retrograded AP and crystallized AM (Miles *et al.*, 1985a; Rundle *et al.*, 1944). However, some AM CLs can

yield the A-type polymorph (Pfannemüller, 1987). The complexed, hydrated form of AM shows a **V_H-type** pattern with intensity maxima at 7.5, 13.0 and 20.0 °2θ $Cu_{K\alpha}$ (Figure 1.3) (Putseys *et al.*, 2010). Although AM-L complexes are present in native cereal starches, no V_H-type pattern has been found. Possibly, they are not crystalline, V_H-type crystals in native cereal starches are too small or their V_H-type pattern is dominated by that of native A-type starch crystals (Gernat *et al.*, 1993; Putseys *et al.*, 2010).

A- and B- type crystals respectively have monoclinic and hexagonal unit cells consisting of 12 glucose units of double, left-handed, parallel stranded helices [Figure 1.4 (a) and (b)] (Imberty *et al.*, 1988; Imberty & Perez, 1988). A-type crystals are more dense than B-type crystals and include eight water molecules in their unit cell (Popov *et al.*, 2009). In the B-type conformation, six double helices are connected through a network of hydrogen bonds such that they surround a central channel. The unit cell contains 36 water molecules in this channel (Imberty *et al.*, 1991).

In V_H-complexes, AM helices stack into antiparallel oriented crystals that are either regularly or randomly organized. This results in respectively an orthorhombic (Rappenecker & Zugenmaier, 1981) or hexagonal crystal unit cell. These unit cells contain six glucose units and eight intrahelical and interstitial water molecules [Figure 1.4 (c)] (Brisson *et al.*, 1991). Based on WAXD patterns of AM-glycerol monostearate complexes, Goderis *et al*. (2014) concluded that V_H-type crystals are stacked in a hexagonal mode.

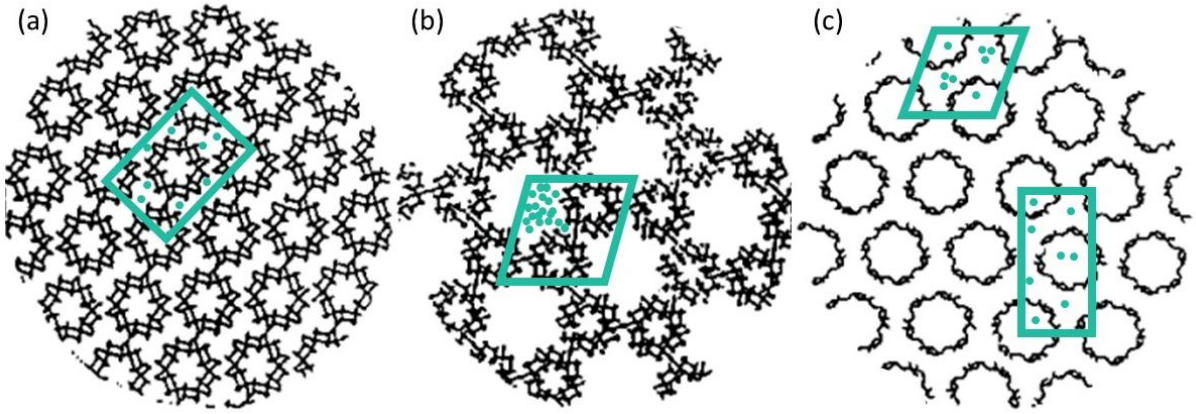

Figure 1.4 Threedimensional projection of starch crystal structures on to the a,b plane. (a) A-type crystals are characterized by monoclinic, (b) B-type crystals by hexagonal and (c) V_H-type crystals by hexagonal (upper) or orthorhombic (lower) unit cells. The unit cells of A-, B- and V_H-type crystals contain respectively 8, 36 and 8 water molecules. Adapted from Gernat *et al*. (1993).

1.3.2 Lamellar structure

Kassenbeck (1975) revealed the presence of periodic lamellar structures in wheat starch granules. AP side chain clusters and branching points are part of respectively crystalline and amorphous lamellae (Lineback, 1986). When using 0.35 nm as the length of one anhydrous glucose unit (Jane *et al.*, 1999), the suggested periodic cluster unit length of 27-28 glucosyl residues (Hizukuri, 1986) corresponds to a repeat distance of **9-10 nm** for alternating crystalline and amorphous lamellae. The former lamellae are **5-7 nm** thick and the latter **2-4 nm** as revealed by electron microscopy and small angle neutron and X-ray scattering (SANS and SAXS) studies (Blanshard *et al.*, 1984; Cameron & Donald, 1992; Kassenbeck, 1975).

It is currently accepted that individual AM polymers are randomly distributed between radially oriented AP polymers in starch granules (Kasemsuwan & Jane, 1994; Pérez & Bertoft, 2010). Kasemsuwan and Jane (1994) suggested, based on gel permeation chromatography and ^{31}P nuclear magnetic resonance (NMR), that maize starch AM molecules are in close proximity of AP molecules but not of other AM molecules. With increasing AM content in native wheat starch the electron density contrast between amorphous and crystalline lamellae decreases (Jenkins & Donald, 1995) while the thickness of crystalline lamellae and overall cluster size remain similar (Yuryev *et al.*, 2004). This has been attributed to accumulation of structural defects (Bocharnikova *et al.*, 2003) resulting from AM chains being arranged between the AP crystals (Matveev *et al.*, 1998). Structural defects impact on the surface entropy in a way that the surface free energy of the crystallites increases (Bocharnikova *et al.*, 2003; Yuryev *et al.*, 2004). The AP crystal stability consequently decreases (Gomand *et al.*, 2012).

1.3.3 Granular structure

AP and AM polymers are ordered radially in starch granules (Blanshard, 1987; Kassenbeck, 1978). The AM concentration increases towards the granule surface (Glaring *et al.*, 2006; Morrison & Gadan, 1987). Starch lipids, which to a degree occur as AM-L complexes, are also assumed to adopt a radial orientation in the starch granule (Blanshard, 1987; Pérez & Bertoft, 2010). The alternating crystalline and amorphous lamellae resulting from clustered AP molecules are ordered in blocklets which are stacked in concentric shells, *i.e.* growth rings (Gallant *et al.*, 1997). The blocklet concept was already introduced by Hanson and Katz (1934) and Badenhuizen (1938) who with light microscopy observed radially and tangentially ordered resistant building blocks in starch degraded by acid hydrolysis. The less dense, amorphous phase of the granule is acted on during acid or enzymatic hydrolysis, while the more resistant, crystalline material remains essentially unattacked (Figure 1.5) (Kainuma & French, 1972; Robin *et al.*, 1974; Saibene & Seetharaman, 2010).

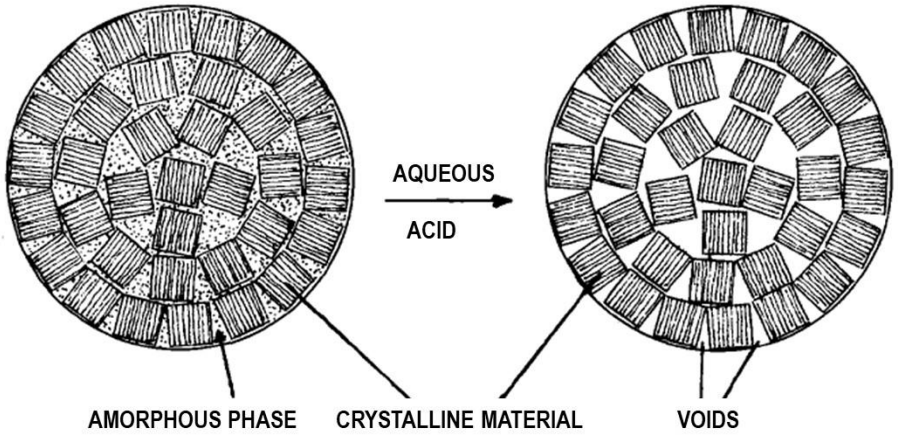

Figure 1.5 Schematic representation of a native starch granule (left) and a granule after acid hydrolysis (right). The amorphous phase is hydrolyzed while the crystalline material remains essentially intact (Kainuma & French, 1972).

In native starch, the resistant blocklets are dispersed in a soft AM matrix throughout the granule (Ridout *et al.*, 2003). 'Regular blocklets' occur in semicrystalline growth rings and contain amorphous and crystalline lamellae that originate from clustered AP molecules (Gallant *et al.*, 1997). In the granule, semicrystalline and amorphous growth rings alternate (French, 1984). AM is mainly deposited in amorphous growth rings (Blennow *et al.*, 2003; Jenkins & Donald, 1995) which are composed of loosely arranged 'defective blocklets' (Ridout *et al.*, 2003). These blocklets contain not only AM but also less ordered AP (Tang *et al.*, 2006) with less chains that are apt to participate in double helix formation (Craig *et al.*, 1998). That amorphous growth rings also contain AP, be it in less ordered form than in semicrystalline growth rings, follows from the observation that chemically degraded and waxy starches, containing no AM, are still organized in growth rings (French, 1984; Pérez & Bertoft, 2010). Electron microscopy images of α-amylase treated wheat starch granules have revealed that 'regular and defective blocklets' have diameters of **80-120** and **25 nm**, respectively (Gallant *et al.*, 1997). Growth rings have a radial thickness of **120-400 nm** (Yamaguchi *et al.*, 1979).

1.3.4 Current view on the granular organization of amylopectin and amylose in cereal starches

In summary, starch crystallinity mainly originates from AP molecules that are radially oriented in granules [Figure 1.6 (a)]. AP molecules have a clustered structure and are ordered in 'regular blocklets' that in turn are stacked in semicrystalline growth rings [Figure 1.6 (b) and (c)]. These blocklets consist of alternating amorphous and crystalline lamellae which result from respectively AP branching points and AP branch chain clusters (*cf.* §1.3.2 and 1.3.3). Only half of the AP fraction is sufficiently ordered to participate in double helix formation (Gérard *et al.*, 2002). The less ordered AP fraction together with AM occurs in 'defective blocklets' which are arranged in amorphous growth rings that alternate with semicrystalline growth rings [Figure 1.6 (b) and (c)]. Individual amorphous AM molecules are radially oriented in starch granules. They are mainly dispersed among AP polymers in amorphous growth rings and appear only to a limited extent between AP clusters in semicrystalline growth rings [Figure 1.6 (a)] (*cf.* §1.3.2) (Saibene & Seetharaman, 2010).

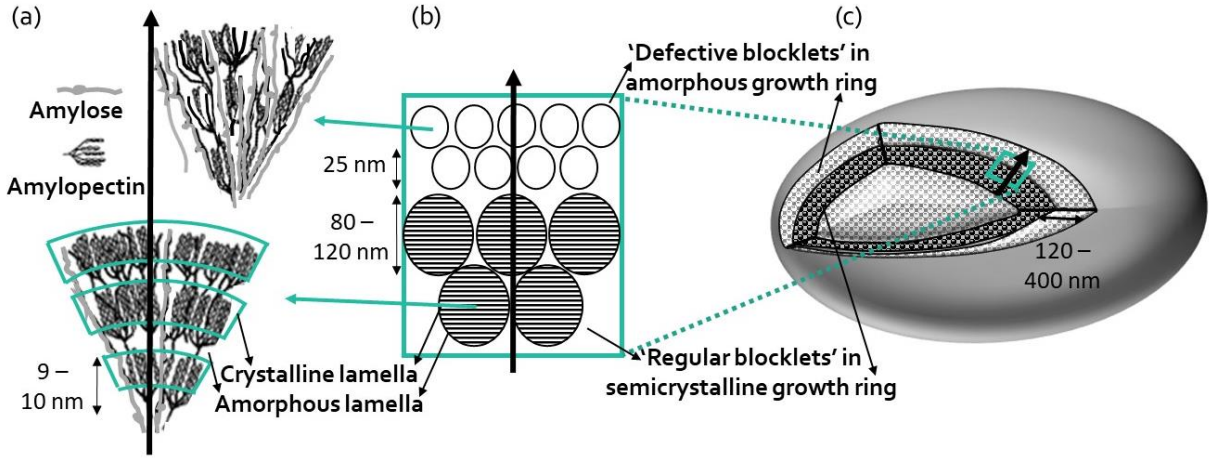

Figure 1.6 Schematic overview of the different levels of granular organization in (wheat) starch. (a) Amylose (AM) and amylopectin (AP) molecules are radially oriented (indicated by thick black arrows) in the starch granule [adapted from Jane (2009)]. Side chain clusters and branching points of AP are responsible for respectively crystalline and amorphous lamellae. The lamellar repeat distance equals 9-10 nm. AM molecules are dispersed among AP molecules and predominantly deposited in (b) amorphous growth rings that are built up of 'defective blocklets' with a diameter of 25 nm. The latter contain AM and less ordered AP. 'Regular blocklets' have a diameter of 80-120 nm and consist of the alternating crystalline and amorphous lamellae. The latter blocklets are stacked in semicrystalline growth rings (c) that alternate with amorphous growth rings. Growth rings appear as concentric shells in the granule and have a radial thickness of 120-400 nm.

1.4 STARCH BIOSYNTHESIS

Starch biosynthesis in the endosperm starts at the hilum of the granule, which is less ordered than the rest of it (French, 1984). During starch growth, successive concentric growth rings are deposited around the hilum (Badenhuizen & Dutton, 1956). Starch biosynthesis requires the coordinated action of different enzymes, *e.g.* starch synthases, starch branching and debranching enzymes (Morell *et al.*, 2001; Nakamura, 2002).

Starch synthases elongate linear AM or AP chains by connecting glucosyl units to the nonreducing end of the chain (Jeon *et al.*, 2010). AM synthesis is governed by GBSS and therefore confined to the granule such that branching of the molecule is hampered. AP is synthesized by soluble starch synthase (Jane, 2009). When outer AP chains are of sufficient length, they are branched by action of an enzyme (French, 1984). Branching enzymes indeed catalyze the cleavage of α-1,4 bonds in separate polymer chains that are randomly reconnected through an α-1,6 bond. The resulting randomly branched molecule requires selective trimming by debranching enzymes to achieve the nonrandomly clustered structure of AP. Debranching enzymes which hydrolyze α-1,6 linkages are involved in removing improperly positioned branch chains (Ball *et al.*, 1996; Jeon *et al.*, 2010).

Wheat is a hexaploid plant that has three copies of each gene (A-, B- and D-genome), which in general are all expressed (Inokuma *et al.*, 2016). Genes that encode for *e.g.* GBSSI, *i.e.* the Waxy protein (Nakamura *et al.*, 1998) or starch synthase IIa (SSIIa), are essential to either AM synthesis or elongation of AP short side chains. Null mutations in some copies of these genes result in **atypical starch characteristics** in terms of reduced wheat AM contents or AP branch chain lengths (Inokuma *et al.*, 2016). The waxy phenotype of wheat does normally not appear since it requires the simultaneous presence of null mutations in all copies of genes encoding the Waxy protein. Crossing of partial waxy wheat lines with one or two null GBSSI genes, however, allows to produce waxy wheat (Fujita *et al.*, 1998; Graybosch, 1998; Nakamura *et al.*, 1995).

1.5 PHYSICOCHEMICAL BEHAVIOR

The chemical composition and the structural organization at different length scales of starch granules determine its physicochemical behavior during processing (Donald *et al.*, 2001). Processing for many cereal-based foods involves heating, cooling and storage. When heating starch in water, the granules lose their molecular order and, thus, birefringence. This phenomenon is termed gelatinization and the temperature at which it takes place is the gelatinization temperature. The solubilization of starch after gelatinization during further heating is defined as pasting (Atwell *et al.*, 1988; Delcour & Hoseney, 2010). During subsequent cooling and storage, the amorphous starch paste reobtains a certain degree of order. During cooling already, gelation takes place. AM polymers crystallize and a starch gel is formed. During subsequent storage, AP retrogradation occurs by which AP polymers reassociate into crystalline structures and further strengthen the formed starch gel (Miles *et al.*, 1985a).

1.5.1 Gelatinization and pasting

The **loss of birefringence** during gelatinization starts at the hilum and is accompanied by granule swelling, partial starch solubilization and AP crystal melting. Wheat starch gelatinization occurs in a **51** to **60 °C** temperature range (Delcour & Hoseney, 2010).

1.5.1.1 *The mechanism of gelatinization*

Starch granules in excess water at room temperature absorb up to 30% of their dry weight in water and thereby swell reversibly with a 5% increase in volume (Delcour & Hoseney, 2010). The amorphous regions in the starch granule are responsible for water absorption and granule swelling (French, 1972). When water is absorbed in a certain region, this region becomes less dense and therefore scatters X-rays less (Zobel, 1988). Differences in the density of growth rings and lamellae observed with SAXS and SANS indicate that wheat starch granules in excess water swell rapidly upon heating. The amorphous growth rings which are less constrained and more apt to absorb water thereby swell to a much larger extent than do the amorphous lamellae (Cameron & Donald, 1993; Jenkins & Donald, 1997). In line with results of Donovan (1979), Jenkins and Donald (1998) stated that gelatinization of starches from different botanical origins is a **swelling driven process** by which swollen amorphous growth rings exert stress on the semicrystalline growth rings and thereby destabilize the AP crystals that as a result dissociate and melt. The melting transition during heating in excess water is detected with differential scanning calorimetry (DSC) as a single, sharp endothermic peak (Figure 1.7). With decreasing water contents, this peak broadens and becomes bimodal. It has been suggested that when the system's water content is limited, swelling is insufficient to

completely disrupt the molecular order of starch and higher temperatures are required to melt the more stabile AP crystals (Donovan, 1979).

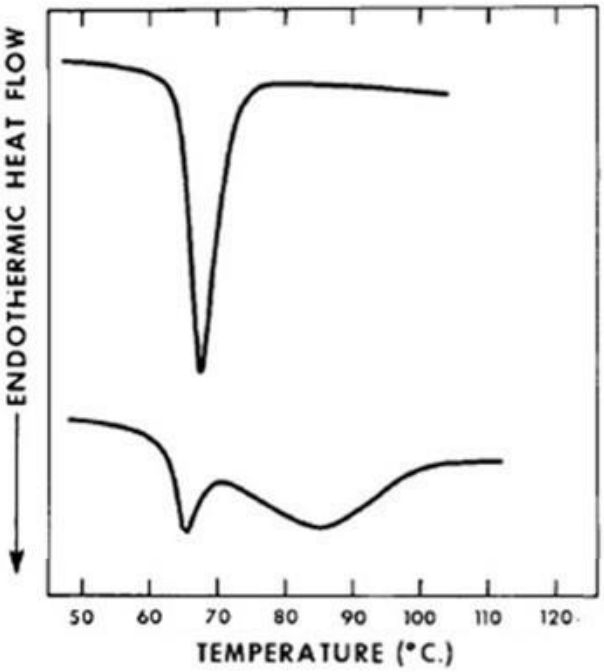

Figure 1.7 DSC thermograms of the endothermic melting transition of potato starch during heating in excess (upper) and limited (lower) water levels. Adapted from Donovan (1979).

In another view on starch gelatinization the hydration and plasticization of the amorphous regions depresses the glass transition temperature and causes the **transition of a glassy to a rubbery amorphous phase**. During heating of cereal starches in water, several authors (Biliaderis *et al.*, 1986; Slade & Levine, 1988) have detected the glass transition of the amorphous regions at the onset of the crystal melting transition with DSC and consequently considered it to be a prerequisite for substantial swelling and AP crystal melting. This, however, is not supported by X-ray measurements of heated aqueous suspensions of cereal starches (Liu *et al.*, 1991). Furthermore, it is unlikely that the glass transition occurs right before gelatinization since wheat AP crystals can be annealed in a temperature range between the glass transition and gelatinization temperature (Yost & Hoseney, 1986). Zelzenak and Hoseney (1987) indeed have shown that the glass transition of wheat starch during heating in water occurs at a significantly lower temperature than the onset temperature of gelatinization.

The currently most accepted model for starch gelatinization is based on the lamellar organization of clustered AP (*cf*. §1.2.1) which is described as a **side-chain liquid-crystalline polymer**. The branch points of AP represent flexible spacers in the liquid phase while the AP double helices are the rigid elements in the crystalline phase. The double helices in the

crystalline lamellae interact side by side. This helix-helix interaction dissociates first during gelatinization. In limited water systems, further heating is required to unwind the double helices. In excess water systems, the second phenomenon immediately follows the first one (Waigh *et al.*, 2000b). This model provides a framework to interpret the abovementioned bimodal DSC endothermic transition in limited water systems. The first endotherm represents the loss of lamellar order and coincides with the loss of the characteristic SAXS peak indicating a 9-10 nm lamellar spacing. The endothermic unwinding of the double helices requires higher temperatures (Waigh *et al.*, 2000a).

1.5.1.2 *Phenomena associated with gelatinization*

Slight granule swelling at temperatures below the gelatinization temperature is reversible. According to Tester and Morrison (1990), the onset of significant and irreversible **granule swelling** coincides with the start of the birefringence loss during heating. In excess thereof, substantial amounts of water are absorbed and granules swell several times in volume. Waxy cereal starches swell substantially more than their regular counterparts. Swelling is thus considered to be a property of AP and to be inhibited by AM (Tester & Morrison, 1990). The swelling power (SP) of starch is related to its ability to hold water by hydrogen bonding. During gelatinization, hydrogen bonds that stabilize AP double helices are broken and replaced by hydrogen bonds between starch and water (Tester & Karkalas, 1996). Due to substantial uptake of water, granules become distorted and release soluble starch polymers into the extragranular space (Figure 1.8) (Goesaert *et al.*, 2005).

The extent of **carbohydrate leaching** (CHL) is positively correlated with the extent of granule swelling (Tester & Morrison, 1990). Both the solubilization of starch polymers and the continued water absorption of distorted granules results in a **viscosity increase** of the system (Delcour & Hoseney, 2010). Starches with lower AM contents swell to a larger extent and the starch suspension reaches a higher viscosity during heating. Furthermore, the granules are fragile and therefore more prone to degradation due to the low content of AM which otherwise would reinforce the molecular network within the granules (Bahnassey & Breene, 1994; Schirmer *et al.*, 2013).

Mainly AM but also some AP at higher temperatures leach from regular wheat starch granules (Doublier, 1981) while understandably only AP leaches from waxy cereal starches (Tester & Morrison, 1990). In wheat starch pastes, phase separation of AM and AP is observed. The center of granule remnants is rich in AM while the outer granule region is enriched in AP because AM preferentially leached to the extragranular space (Langton & Hermansson, 1989). Phase separation of polymers like AM and AP is *inter alia* determined by their shape (*e.g.* linear or branched) and their affinity for the solvent. It occurs more readily when the molecular

weight (MW) of the polymers is higher (Dobry & Boyer-Kawenoki, 1947; Kalichevsky & Ring, 1987).

Mobile, solubilized AM molecules can form complexes with available lipids (Conde-Petit *et al.*, 2006; Evans, 1986; Kugimiya & Donovan, 1981) during further heating after gelatinization (Le Bail *et al.*, 1999). Different types of **AM-L complexes** are distinguished. Type I complexes have been considered to be amorphous and typically formed at or below 60 °C and dissociate at 95-100 °C (Biliaderis & Seneviratne, 1990; Karkalas *et al.*, 1995). Goderis *et al*. (2014), however, observed SAXS and WAXD patterns of Type I AM-L complexes with typical (but broad) reflections for V_H-type crystals. These patterns were clearly distinct from amorphous patterns. Type I complexes are thus suggested to adopt a V_H-type crystal packing, be it that the crystals are less perfect than those of Type II complexes. The latter are typically formed at about 90 °C and melt at 115-120 °C (Biliaderis & Seneviratne, 1990; Karkalas *et al.*, 1995). Type II complexes can recrystallize from molten Type I complexes during further heating or subsequent cooling. The more ordered Type II complexes are characterized by sharp maxima of the typical V_H-type crystal reflections in a WAXD pattern (Goderis *et al.*, 2014).

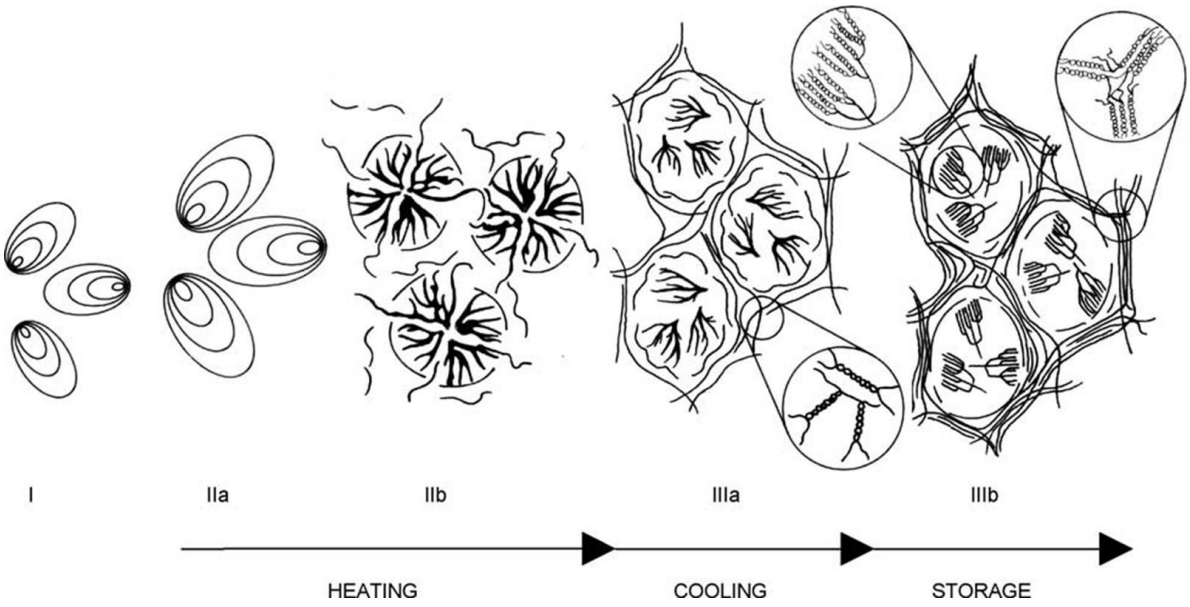

Figure 1.8 Physicochemical changes of starch in excess water during heating, cooling and storage. In the presence of excess water, native starch granules (I) absorb water and swell reversibly during heating (IIa). When the gelatinization temperature is reached, granules swell irreversibly and partially desintegrate, amylopectin (AP) crystals start to melt and amylose (AM) molecules leach to the extragranular space (IIb). During subsequent cooling and storage of the formed paste, crystallizing AM polymers (IIIa) and recrystallizing AP polymers (IIIb), respectively, form a structured starch network (Goesaert *et al.*, 2005).

The loss of birefringence, visualized with polarized light microscopy as the disappearance of the Maltese cross, coincides with the **melting of AP crystals** detected by DSC during heating of starch in water. In excess water, the birefringence loss of wheat starch occurs over a temperature range of 7 to 10 °C. With decreasing water levels the onset temperature of gelatinization remains similar, but the loss of birefringence is delayed and occurs over a range of about 30 °C (Ghiasi *et al.*, 1982). The area of the endothermic transition measured during heating with DSC represents the melting enthalpy of AP crystals (Donovan, 1979) and reflects the starch crystallinity. The gelatinization temperature depends on the water content (Ghiasi *et al.*, 1982) and on the crystal stability (Gomand *et al.*, 2012). The latter is negatively impacted by the crystal surface free energy which increases with AM content (*cf*. §1.3.2) (Bocharnikova *et al.*, 2003; Yuryev *et al.*, 2004). Both higher gelatinization enthalpy and temperature are observed for waxy than for regular wheat starch since the former has a higher crystallinity and a more closely packed crystal structure (Fujita *et al.*, 1998) containing less structural defects (Bocharnikova *et al.*, 2003). The crystal stability is further determined by the AP chain length distribution. Short AP branch chains (DP 6-10) are believed to be uncapable of forming stable double helices (*cf*. §1.2.1) (Gidley & Bulpin, 1987) such that an increased portion of these chains in wheat starch results in a decreased gelatinization temperature (Inokuma *et al.*, 2016; Singh *et al.*, 2010). In addition, the level of short AP branch chains has been negatively correlated with the gelatinization enthalpy (Singh *et al.*, 2010). This negative relation between the level of short AP branch chains and both gelatinization temperature and enthalpy has also been observed for starches from other botanical origins (Noda *et al.*, 1998). Short AP branch chains are related to a defective crystalline structure which requires a lower temperature and less energy to melt (Jane *et al.*, 1992; Singh *et al.*, 2010).

1.5.2 Gelation

AM crystallization during cooling of a starch paste involves the **association of leached AM molecules into double helices** (Figure 1.8) (Goesaert *et al.*, 2005). Such crystalline structures can be formed by cooling the system to between its melting and glass transition temperatures. The latter equals -5°C for gelatinized wheat starch in excess water (Slade *et al.*, 1991). Crystallized AM displays a B-type diffraction pattern (Rundle *et al.*, 1944) and melts at temperatures of 120 to 150 °C (Leloup *et al.*, 1992; Ring *et al.*, 1987).

To form a gel rather than a precipitate during cooling of starch solutions, a concentration of 6% w/w starch (*i.e. ca.* 1.5% w/w AM) is required as it is critical for entanglement of AM polymers (Ellis & Ring, 1985; Miles *et al.*, 1985b). For increasingly concentrated AM solutions, less undercooling is needed such that gelation occurs at a higher temperature (Vallera *et al.*, 1994). Furthermore, a higher storage modulus of the gel (Miles *et al.*, 1985b; Orford *et al.*,

1987), which can be related to gel firmness, is obtained after cooling (Thebaudin *et al.*, 1998). In addition, high levels of short AM chains favor gel formation (Reyniers *et al.*, 2018).

AM double helices aggregate and form a **continuous, intergranular, semicrystalline AM gel network** during further cooling (Goesaert *et al.*, 2009b; Putseys *et al.*, 2011; Tolstoguzov, 2003). The formed AM network is semicrystalline since only certain regions of the AM chains participate in double helix formation. It can be described as a fringed micelle network (Eerlingen *et al.*, 1993) consisting of crystalline junction zones, *i.e.* micelles, connected by the amorphous regions, *i.e.* fringes (Figure 1.9) (Slade & Levine, 1987). The junction zones evidently consist of AM crystals, but also contain AM-L complexes (Goesaert *et al.*, 2009b). The latter enhance AM gelation (Conde-Petit & Escher, 1995). The swollen granule remnants act as fillers in the AM matrix. Since AP only recrystallizes during storage, the AM network is responsible for the initial strength of a starch gel (Miles *et al.*, 1985a).

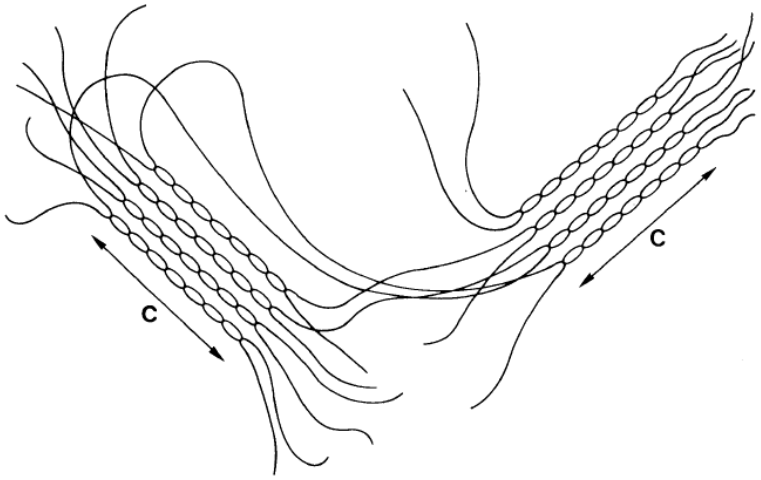

Figure 1.9 A schematic representation of a fringed micelle AM network. Micelles consist of aggregated AM double helices (C: crystalline junction zones) and are linked to each other by fringes that consist of amorphous AM chains. Only certain regions of AM chains participate in double helix formation (Eerlingen *et al.*, 1993).

1.5.3 Retrogradation

As outlined above, the development of a starch gel during cooling is attributed to the crystallization of AM within hours (*cf*. §1.5.2) (Miles *et al.*, 1985b). **Reassociation of outer AP side chains in double helices** occurs in a time frame of days to weeks (McIver *et al.*, 1968; Ward *et al.*, 1994) and reinforces the starch network during storage (Figure 1.8) (Miles *et al.*, 1985a). AP recrystallization is termed retrogradation and results in formation of B-type AP crystals that, in the case of wheat starch, have a melting temperature in the range of 50 to 60 °C (Hug-Iten *et al.*, 2001; Slade & Levine, 1987). In contrast to AM crystallization, AP

recrystallization can thus be undone by heating of the stored starch gel (< 100 °C) (Miles *et al.*, 1985a).

Both AM and AP (re)crystallization occur in a temperature range between that of the glass transition of the gelatinized starch paste and melting of AM and AP crystals (*cf*. §1.5.2). During the first step of the crystallization process, *i.e.* nucleation, crystal nuclei are formed which grow into crystals during the subsequent propagation step. Finally, during maturation, further crystal growth and/or perfection occur (Slade & Levine, 1987). At higher storage temperatures in the above mentioned temperature range, the rates of nucleation and propagation respectively decrease and increase (Slade & Levine, 1987; Vandeputte *et al.*, 2003).

The extent of AP retrogradation depends on the starch concentration. A higher starch gel concentration results in a higher storage modulus, which can be related to the firmness of the starch gel (*cf.* §1.5.2) after storage (Orford *et al.*, 1987). Using DSC, Zeleznak and Hoseney (1986) showed that retrogradation occurred to minor extent in both very concentrated and diluted starch gels. Water is essential during retrogradation since it acts as a plasticizer to mobilize polymer chains and needs to be incorporated in the B-type crystal structure. AP retrogradation is enhanced when the moisture content (MC) of wheat starch gels increases from 27% up to 40%. Further increasing MCs, however, decrease the extent of retrogradation due to dilution of starch polymers (Slade *et al.*, 1991). Furthermore, the chain length distribution of AP codetermines the rate and extent of retrogradation. The AP exterior branches with an average DP of 15 (Ring *et al.*, 1987) and a DP of at least 10 (Gidley & Bulpin, 1987) are responsible for retrogradation. Shi and Seib (1992) showed a positive or negative relation between the extent of retrogradation and the relative amounts of chains with DPs 14-24 or DPs 6-9, respectively. In line with this, several authors observed faster and more retrogradation of pea and tuber AP than of cereal AP (Kalichevsky *et al.*, 1990; Orford *et al.*, 1987). The average branch chain length of the latter is shorter (Kalichevsky *et al.*, 1990).

Leaching of (mainly) AM results in a higher local concentration of AP in the outer parts of gelatinized wheat starch granule remnants (Hug-Iten *et al.*, 2001) such that intragranular AP retrogradation during storage is enhanced (Goesaert *et al.*, 2009b). Furthermore, AM crystals and AM-L complexes in the semicrystalline AM network formed during cooling can serve as nuclei that facilitate AP retrogradation (Van Soest *et al.*, 1994; Vandeputte *et al.*, 2003). At higher temperatures AP also leaches from wheat starch granules (Doublier, 1981) which allows intergranular AP associations (Goesaert *et al.*, 2009b). Both intramolecular and intermolecular AP double helices are formed and pack into crystals that together with AM crystals and AM-L complexes serve as junction zones in the fringed micelle starch network. In

stored starch gels a **continuous, intergranular, semicrystalline AM and AP network** is present (Goesaert *et al.*, 2009b).

During storage, the starch system partially regains its crystallinity. A fully retrograded wheat starch gel only has a crystallinity of about 15%. Concomitant with AP retrogradation, the water in the gel becomes increasingly bound such that its mobility (such as monitored with ^{1}H NMR) decreases. Water molecules are rendered unfreezable in the formed B-type crystals (Wynne-Jones & Blanshard, 1986) which include more water in their crystal structure than do A-type crystals of native wheat starch (Imberty *et al.*, 1991). The reduced proton mobility of wheat starch gels during storage is furthermore attributed to strengthening of the gel network due to AP retrogradation (Bosmans *et al.*, 2013c). Although heating of a stored starch gel to about 100 °C melts AP crystals (Miles *et al.*, 1985a), the proton mobility is not restored to its initial value. The network organization of a stored starch gel is consequently not entirely heat-reversible (Bosmans *et al.*, 2013c).

1.6 STARCH IN BREAD MAKING

In this chapter the structural and physicochemical properties of (un)usual (wheat) starches was described. A thorough understanding of these starch properties is crucial to interpret the behavior of starch and its interaction with other components in a complex food system such as bread. In general, the main ingredient for bread making is wheat flour of which starch is quantitatively the main biopolymer. Starch characteristics therefore largely contribute to the properties of this food system at the different stages in the chain from flour to (stored) bread.

Chapter 2 focuses on wheat bread making and the current knowledge of starch functionality and its interaction with water during baking, cooling and subsequent storage. Some useful techniques to study starch transitions and water dynamics during these processes are described.

Chapter 2
Bread making and storage: dynamics of starch and water

2.1 INTRODUCTION

Bread is the principal food product prepared from wheat and worldwide a staple food (Cauvain, 2015; Maningat *et al.*, 2009). In Europe, bread making is mainly done via the so called straight-dough procedure (Delcour & Hoseney, 2010). Ingredients for bread making are mixed and fermented into a leavened dough that retains gas. The fermented dough is then baked (Bloksma, 1972) and after cooling a fresh bread with a desired soft and fine crumb structure is obtained (Goesaert *et al.*, 2005).

Wheat flour contains mainly starch, water, protein, nonstarch polysaccharides and lipids (Goesaert *et al.*, 2005). During the production of wheat bread, the flour constituents, especially starch and protein, undergo complex transformations. Starch is quantitatively the main flour component of bread dough. It holds a substantial portion of the dough water (Bushuk, 1966). Starch transitions and water dynamics during bread making therefore strongly influence bread crumb structure (Goesaert *et al.*, 2008). In fresh bread, starch and protein networks together determine crumb texture and the desired initial crumb softness and resilience (Goesaert *et al.*, 2009b). Deterioration of bread quality during storage involves crumb firming and loss of the crust's crispiness and the desired flavor and aroma characteristic of fresh bread (Willhoft, 1973). Different bread improving agents (*e.g.* amylases) (Goesaert *et al.*, 2005) or alternative bread making processes (*e.g.* parbaking) have been adopted to overcome the undesired changes during bread storage and, thus, extend the shelf life of bread (Almeida *et al.*, 2016).

2.2 STRAIGHT-DOUGH BREAD MAKING

2.2.1 Dough preparation

The essential ingredients for bread making are wheat flour, water, yeast and salt (Bloksma, 1972). **Wheat flour** for white bread making is obtained by roller milling the cereal and subsequent sieving such that its particle sizes range from less than 1 to about 200 µm (Delcour & Hoseney, 2010). Wheat flour typically has a MC of about 14%. The flour solids consist of starch (*ca.* 80-85%), protein (*ca.* 12-14%), nonstarch polysaccharides [*ca.* 2-3%, mainly arabinoxylans (AX)] and lipids (*ca.* 2%) (Goesaert *et al.*, 2005).

Together with **water**, wheat flour is transformed into a viscoelastic dough when **energy** is applied upon mixing (Bloksma, 1972; Singh & MacRitchie, 2001). Water acts as a plasticizer. It hydrates flour components such that they are in a mobile, rubbery state (Singh & MacRitchie, 2001; Slade *et al.*, 1991). In optimally mixed dough, starch and protein are fully hydrated (Delcour & Hoseney, 2010). Furthermore, mixing results in a homogeneous distribution of ingredients, a protein network and incorporation of air in dough (Bloksma, 1990). The latter is crucial since no new gas cells are formed during fermentation (Gan *et al.*, 1995).

Wheat flour proteins consist of **gluten proteins** (*ca.* 80-85 %), and albumins and globulins (*ca.* 15-20%) (Veraverbeke & Delcour, 2002). The former contain by and large equal levels of polymeric glutenins (made up of glutenin subunits) and monomeric gliadins. Glutenin subunits and gliadins contain cysteine residues that are involved in intramolecular disulfide (SS) bonds. In addition, glutenin subunits contain free cysteine residues which form intermolecular SS bonds that link different subunits (Wieser, 2007). The input of mechanical energy by mixing causes large glutenin polymers to align and polymerize end-by-end through sulfhydryl (SH)-SS exchange reactions (Belton, 1999; Delcour *et al.*, 2012). While the large, extended glutenins confer elasticity to the dough (Singh & MacRitchie, 2001), gliadins interact noncovalently with the glutenin network and weaken the degree of interaction between glutenin chains. At the same time, that makes the gluten network viscous (Khatkar *et al.*, 1995; Shewry *et al.*, 2001).

Dough is considered to be a foam as its gas cells are dispersed in a continuous liquid phase (Eliasson & Larsson, 1993). The gluten network together with liquid lamellae around the gas cells is responsible for **gas retention** during fermentation (Figure 2.1). Surface active proteins and polar lipids contribute to gas cell stability through adsorption at the liquid film (Gan *et al.*, 1995; Sroan *et al.*, 2009; Sroan & MacRitchie, 2009). Also, water extractable AX (WE-AX) account for 25-30% of total AX in wheat flour (Courtin & Delcour, 2002; Koehler & Wieser, 2013; Mares & Stone, 1973) and bestow viscosity upon the liquid phase in dough (Gan *et al.*,

1995). In contrast to water unextractable AX (WU-AX), they positively impact the stability of gas cells (Courtin *et al.*, 1999).

Wheat dough is a **bicontinuous phase** consisting of a gluten phase and a liquid phase (Eliasson & Larsson, 1993) in which native starch granules, nongluten proteins and nonstarch polysaccharides are dispersed. Starch and gluten thus are present in different phases. Moreover, they are immiscible (Larsson & Eliasson, 1996; Tanaka, 2012; Tolstoguzov, 1997). Dough MC is usually about 45% (Bloksma, 1972) of which *ca.* 46% is associated with starch (Bushuk, 1966). Dough components compete for water. Important in this context is that starch has a higher affinity for water than gluten (Tolstoguzov, 1997). That proton distributions in wheat flour dough [detected with time domain (TD) ^{1}H NMR measurements] are comparable to those in starch-containing model systems and differ from those of gluten-water mixtures indicates that proton mobility in wheat dough is dominated by starch and its interaction with water (Doona & Baik, 2007).

Dough leavening results from the production of carbon dioxide (CO_2) by baker's **yeast**, *i.e. Saccharomyces cerevisiae*, as a result of sugar fermentation (Gabriela & Daniela, 2010). CO_2 dissolves in the aqueous dough phase until it is saturated. As soon as the aqueous phase is saturated, CO_2 diffuses to the preexisting gas cells which then expand. During fermentation, the dough is typically punched or remixed to subdivide gas cells in many smaller cells into which CO_2 can diffuse. Furthermore, punching or remixing causes the ingredients to be redistributed and brought again in proximity of immobile yeast cells. Finally, the dough is molded, optionally put in a baking tin and proofed at 30-35 °C and 85% relative humidity. During proofing, gas cells expand strongly and the dough volume increases (Figure 2.1) (Sievert & Hoseney, 2007).

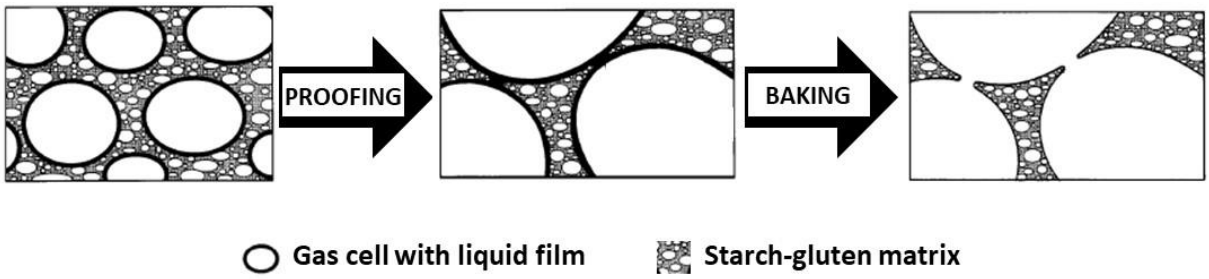

Figure 2.1 Schematic representation of gas cell expansion during proofing and transformation of the foam structure in dough to the gas continuous sponge structure in crumb during baking. Gas cells are lined with a liquid film and dispersed in a starch-gluten matrix. Adapted from Gan *et al.* (1995).

2.2.2 Bread baking

During baking, starch gelatinizes, protein polymerizes, yeast is inactivated and the desired color and flavor of fresh bread is developed (Bushuk, 1966). The rapid dough expansion during the early baking phase is termed **oven spring**. It results from the increased yeast activity and, thus, CO_2 production (up to yeast inactivation at about 55 °C), the decreased solubility of CO_2 in the aqueous phase, the thermal expansion of gases, and the vaporization of water and ethanol induced by temperature (Delcour & Hoseney, 2010).

Heat penetrates rather slowly into bread dough. During early baking, there is a temperature gradient from the surface region (which rapidly reaches 100 °C) to the centre of the sample where a **maximum crumb temperature of 100 °C** is reached after considerable time (Figure 2.2) (Derde *et al.*, 2014; Sievert & Hoseney, 2007; Zanoni *et al.*, 1993). Water is redistributed during baking. The MC of the surface region decreases because of **water evaporation** to *inter alia* the dry oven environment. Water vapor also migrates inwards, to cooler regions of the dough, where it condenses again. Consequently, the MC of the core region slightly increases (Purlis & Salvadori, 2009a; Wagner *et al.*, 2007).

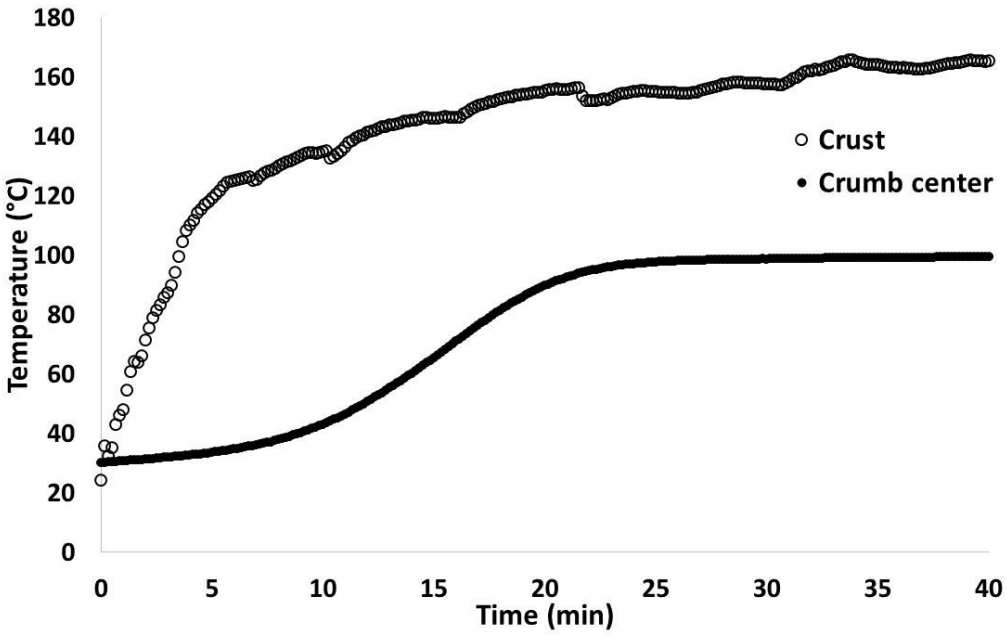

Figure 2.2 In house determined temperature profile in the crust and crumb center during baking of bread for 40 min at 210 °C.

During early baking, considerable quantities of water evaporate at the dough surface. The needed heat of evaporation is withdrawn at this surface which results in it remaining cool. Since both water and elevated temperature are needed for starch to gelatinize, starch in bread crust is still largely not gelatinized (Delcour & Hoseney, 2010). Only when most of the available water has evaporated, does the temperature of the **dehydrated surface region exceed 100 °C**

and further increase towards that in the oven (Figure 2.2) (Zanoni *et al.*, 1993). Both the high temperature and the low water activity of the dehydrated surface region then allow for Maillard reactions between reducing carbohydrates and proteins. These reactions lead to the desired **formation of flavors** characteristic for fresh bread (Belitz *et al.*, 2009) and **crust browning** (Purlis & Salvadori, 2009b; Zanoni *et al.*, 1995).

In the inner dough region, **starch gelatinization** occurs when a sufficiently high temperature is reached. It is accompanied by irreversible granule swelling, AP crystal melting and leaching of starch polymers (Delcour & Hoseney, 2010), *i.e.* mainly AM and also some AP, the latter at higher temperatures (Doublier, 1981) (*cf*. §1.5.1). Since bread dough is a system with only limited water availability, starch swelling occurs without complete disruption of granules. As a result, the granular identity is largely retained (Hug-Iten *et al.*, 1999; Varriano-Marston *et al.*, 1980). Notwithstanding the above, starch gelatinization is complete by the end of baking as evidenced by the disappearance of the Maltese cross (Derde *et al.*, 2014; Hug-Iten *et al.*, 1999; Schoch & French, 1947).

Heating also promotes **unfolding of gluten proteins** such that previously unavailable reactive SS bonds and SH groups are exposed (Li & Lee, 1998) and the surface hydrophobicity increases. The latter has been detected for glutenin at temperatures starting from 45 °C during heating of gluten suspensions. Conformational changes of gliadin require higher temperatures and clearly occur when heating at 90 °C (Guerrieri *et al.*, 1996). The exposure of reactive groups facilitates oxidative cross-linking of SH groups, SH-SS exchange reactions and hydrophobic interactions (Li & Lee, 1998).

The extractability of gluten proteins with sodium dodecyl sulfate (SDS)-containing media decreases during heating. This is indicative for **gluten cross-linking** (Hayta & Schofield, 2004). When heating wet gluten at different temperatures for 10 min, its extractability in such media starts decreasing once the temperatures is 60 to 70 °C. This is attributed to polymerization of glutenin (Figure 2.3) (Schofield *et al.*, 1983). Such onset temperatures of glutenin polymerization can also be observed when heating gluten-water and gluten-starch-water mixtures under shear with a rapid visco analyzer (Lagrain *et al.*, 2008a; Lagrain *et al.*, 2005). For the extractability of gliadin in SDS-containing medium to decrease, temperatures of at least 90 °C are required (Lagrain *et al.*, 2008a; Lagrain *et al.*, 2005; Schofield *et al.*, 1983). Apart from glutenin cross-linking by SH-SS exchange reactions, oxidative cross-linking of glutenin SH groups also occurs since the level of free SH groups decreases during heating up to about 90 °C, when the extractability decrease of glutenin ceases. Incorporation of gliadin into the glutenin network during further heating occurs through SH-SS exchange reactions as the level of free SH groups remains constant (Figure 2.3) (Lagrain *et al.*, 2008a).

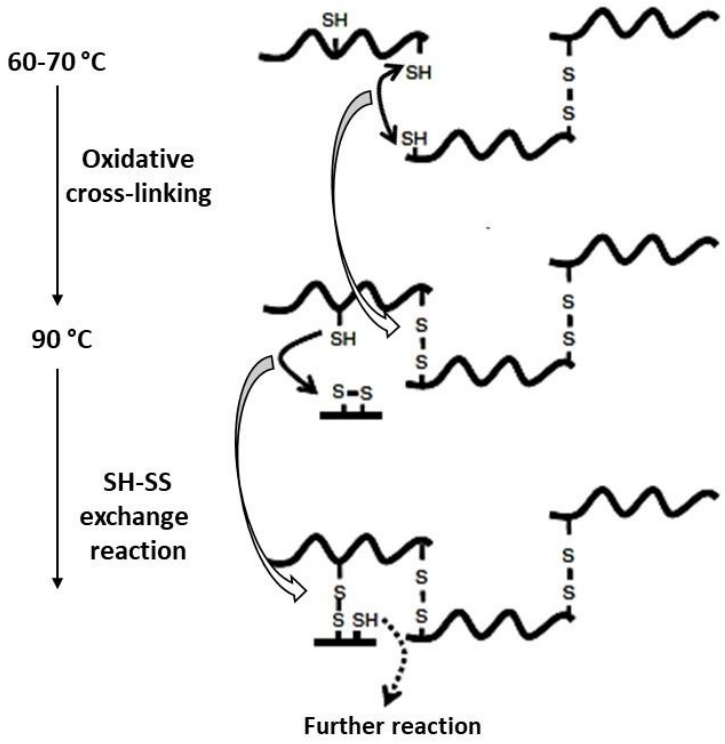

Figure 2.3 Gliadin-glutenin cross-linking during hydrothermal treatment. Heating promotes unfolding of gluten proteins and therewith exposes previously unavailable free sulfhydryl (SH) groups. Heating to 90 °C leads to cross-linking of glutenin through *inter alia* oxidation of free SH groups. At temperatures exceeding 90 °C gliadin is incorporated into the glutenin network through SH-disulfide (SS) exchange reactions. Adapted from Lagrain *et al.* (2008c).

Changes in the starch and gluten fractions during baking result in **redistribution of water** (Tolstoguzov, 1997). Swelling of starch and unfolding and polymerization of gluten proteins increase the water retention capacity of starch and decrease that of gluten proteins, respectively (Bushuk, 1966). Moreover, starch is more hydrophilic than and not compatible with gluten (Tolstoguzov, 1997). Consequently, water is withdrawn from gluten to starch (Tolstoguzov, 1997; Willhoft, 1971a) such that about 80% of the water in fresh bread is associated with starch (Bushuk, 1966; Willhoft, 1971a).

During bread baking, gelatinization starts at temperatures between **60 to 65 °C** (Bloksma, 1972; Delcour & Hoseney, 2010). Moreover, at about such temperatures, oxidative cross-linking of glutenin occurs (Lagrain *et al.*, 2008a; Lagrain *et al.*, 2005; Schofield *et al.*, 1983). In combination with water withdrawal from the gluten network (Tolstoguzov, 1997; Willhoft, 1971a) this stiffens the gluten-starch matrix (Babin *et al.*, 2006). Continuous gas expansion causes the liquid film surrounding gas cells to thin and eventually rupture (Gan *et al.*, 1995). Together with stiffening of the gluten-starch matrix this **sets the crumb structure** (Babin *et al.*, 2006; Gan *et al.*, 1995). The foam structure of dough is thereby transformed into the gas continuous sponge structure of bread (Figure 2.1) (Bloksma, 1990; Gan *et al.*, 1995). When the

inner dough region eventually is transformed into crumb, it can no longer retain CO_2 and the oven spring is finished (Delcour & Hoseney, 2010).

At the end of baking, a **fresh, warm bread**, with a continuous gas phase (Gan *et al.*, 1995) and a gluten network in which swollen granule remnants and entangled leached starch polymers are dispersed, is obtained (Goesaert *et al.*, 2009b).

2.2.3 Bread cooling

In **fresh, cool bread**, the starch fraction is phase separated. As a result of AM leaching during baking, the outer region of starch granule remnants is enriched in AP while AM is accumulated in the extragranular phase. Furthermore, the presence of an AM-rich region in the center of granule remnants (Hug-Iten *et al.*, 1999) has been attributed to the phase separation of AM and AP (*cf*. §1.5.1.2) (Kalichevsky & Ring, 1987). Leached AM is an essential structural element in fresh bread crumb as it is responsible for the **continuous, intergranular, semicrystalline AM network** formed during cooling (Goesaert *et al.*, 2009b). Crystallization of leached AM molecules results in B-type AM crystals (Putseys *et al.*, 2011) which together with V_H-type crystals from AM-L complexes (present in native wheat starch or formed with leached AM molecules) (Putseys *et al.*, 2010) function as junction zones in the fringed micelle network (*cf*. §1.5.2) (Goesaert *et al.*, 2009b). However, immediately after cooling, fresh bread crumb has a V_H-type diffraction pattern and no characteristic B-type reflections (Aguirre *et al.*, 2011; Hug-Iten *et al.*, 2001; Zobel & Kulp, 1996).

Together with the gluten network formed during baking, the semicrystalline AM network determines the **desired crumb texture** of freshly baked bread (Goesaert *et al.*, 2009b), *i.e.* the initial crumb resilience (Bosmans *et al.*, 2013b) and firmness (Schoch & French, 1947). The latter makes it possible to slice fresh bread (Cauvain, 2015). Initial crumb firmness readings are positively related to bread density which in turn depends on gluten properties (Axford *et al.*, 1968; Lagrain *et al.*, 2012) and other dough components involved in gas cell stabilization, *e.g.* WE-AX (Courtin *et al.*, 2001) and certain polar nonstarch lipids (Melis *et al.*, 2019). Starch lipids do not impact loaf density as they only become available during gelatinization (Gerits *et al.*, 2013; Melis *et al.*, 2019; Morrison, 1978) when crumb structure is set and the loaf volume no longer increases (Gan *et al.*, 1995).

2.2.4 Bread storage

Storage of bread results in loss of the desired flavors. Also, the crumb firms and the crust loses its crispiness (Willhoft, 1973). The increase in crumb firmness goes hand in hand with a decrease in crumb resilience (Goesaert *et al.*, 2009b). During the first days of storage, **crumb**

firming is strongly linked to **AP retrogradation** (*cf*. §1.5.3). The formed AP crystals give rise to characteristic B-type reflections in a WAXD pattern (Bosmans *et al.*, 2013c; Hug-Iten *et al.*, 2001) and together with AM crystals and AM-L complexes serve as junction zones in a fringed micelle starch network (Goesaert *et al.*, 2009b; Schoch & French, 1947). Apart from AM molecules, also some AP molecules leach to the intergranular space during baking. The crystalline regions of retrograded AP therefore are present both inside and outside granule remnants (*cf*. §1.5.3) (Goesaert *et al.*, 2009b; Zobel & Kulp, 1996). Consequently, a **continuous, intergranular, semicrystalline AP and AM network** is present in crumb of stored bread (Goesaert *et al.*, 2009b).

Thus, retrogradation substantially contributes to crumb firming. However, while the extent of retrogradation such as measured by DSC levels off after 3 to 5 days of storage, crumb firmness further increases continuously during 7 days of storage. Other phenomena therefore codetermine crumb firming (Bosmans *et al.*, 2013c; Ghiasi *et al.*, 1984). Starch and gluten are immiscible and water is redistributed between both fractions during storage (Bushuk, 1966; Tolstoguzov, 1997; Willhoft, 1971a). Furthermore, B-type AP crystals contain more water in their crystal unit cell than the A-type crystals of native wheat starch (Imberty *et al.*, 1991). AP retrogradation therefore not only increases the strength of the semicrystalline starch network, it also results in **migration of water from the gluten to the starch network** (Bosmans *et al.*, 2013c; Willhoft, 1971b). B-type AP crystals, which have a water content of 27% (Zobel & Kulp, 1996), immobilize water and render it unfreezable (*cf*. §1.5.3). Bosmans *et al.* (2013c) have calculated that the amount of B-type crystals formed during storage immobilizes 2 to 3% of the total crumb water in their structure. However, as 8% of the crumb water becomes unfreezable during storage, it has been suggested that part of the crumb water rendered unfreezable during storage is included in the amorphous regions of the fringed micelle network (Bosmans *et al.*, 2013c).

Water not only migrates from gluten to starch, **it also migrates from the crumb to the crust** (Ruan *et al.*, 1996). This occurs mainly during the first days of storage and levels off by the end of a 7 day storage period. Both crumb to crust and gluten to starch moisture migration result in dehydration of the gluten network (Bosmans *et al.*, 2013c). At a local MC of 35%, the amide groups of gluten are fully hydrated (Almutawah *et al.*, 2007). When fresh bread crumb is dried well below this critical MC, dehydration of the gluten strands stiffens the gluten network and leads to an increased crumb firmness. After prolonged storage, the crumb to crust and gluten to starch moisture migration which has happened results in lower gluten MC so that **gluten is no longer fully hydrated**. The resulting rigidification of gluten contributes to crumb firming (Bosmans *et al.*, 2013c). It is further hypothesized that strong dehydration of the amorphous

starch network, which is fully hydrated at a MC of 27% (Slade & Levine, 1988), can also contribute to crumb firmness (Bosmans *et al.*, 2013c).

Crumb of stored bread can be partially **refreshed** by heating to at least 50 °C (Schoch & French, 1947). This is because the effect of AP retrogradation in bread can be reversed by melting the AP cyrstals as evidenced by WAXD (Pisesookbunterng *et al.*, 1983) and DSC measurements (Bosmans *et al.*, 2013b). However, the moisture redistribution between gluten and starch is not heat-reversible (*cf. infra* §2.4.1.2) (Willhoft, 1971a).

2.3 ALTERNATIVE BREAD MAKING CONDITIONS TO EXTEND BREAD SHELF LIFE

Bread is one of the most wasted foods (FOODWIN, 2018). Current strategies to reduce such wastage include the use of bread improving agents in the recipe or altered bread making processes that target the extent of retrogradation and/or the degree of network hydration.

2.3.1 Bread recipe

Bread recipes often contain nonessential ingredients, *e.g.* sugar, fat, antifungal agents such as calcium propionate and improving agents such as α-amylases and surfactants which decrease crumb firmness. Crumb firmness is further impacted when bread is prepared from flours containing starch with atypical characteristics, *e.g.* flour from waxy wheat (Delcour & Hoseney, 2010). The use of different ingredients that impact on crumb firmness is discussed in what follows.

2.3.1.1 *Bacillus stearothermophilus α-amylase*

The **thermoactive maltogenic α-amylase from *Bacillus stearothermophilus*** (BStA)[1] is a bread crumb antifirming enzyme (Dauter *et al.*, 1999; Spendler *et al.*, 2002). BStA is a mainly exoacting enzyme which releases maltose from the nonreducing ends in AM and AP (Figure 2.4). However, as it does not necessarily require a nonreducing end for starch hydrolysis it also has limited endoactivity (Christophersen *et al.*, 1998). The latter is more pronounced at higher temperatures (Bijttebier *et al.*, 2007). BStA slowly but significantly reduces the MW of AM and AP during bread making and thereby mainly shortens the starch polymer chains. The limited endoaction at higher temperatures possibly results in slight weakening of the entangled starch networks in bread at the end of baking (Goesaert *et al.*, 2009a; Hug-Iten *et al.*, 2001).

[1] The optimal temperature for BStA activity is 60 °C as determined on 1.0% soluble starch in sodium maleate buffer (100 mM, pH 6.0) containing calcium chloride. After preincubation for 30 min at 80 °C without substrate, the thermostable enzyme still retains about 50% of its initial activity (Derde *et al.*, 2012a).

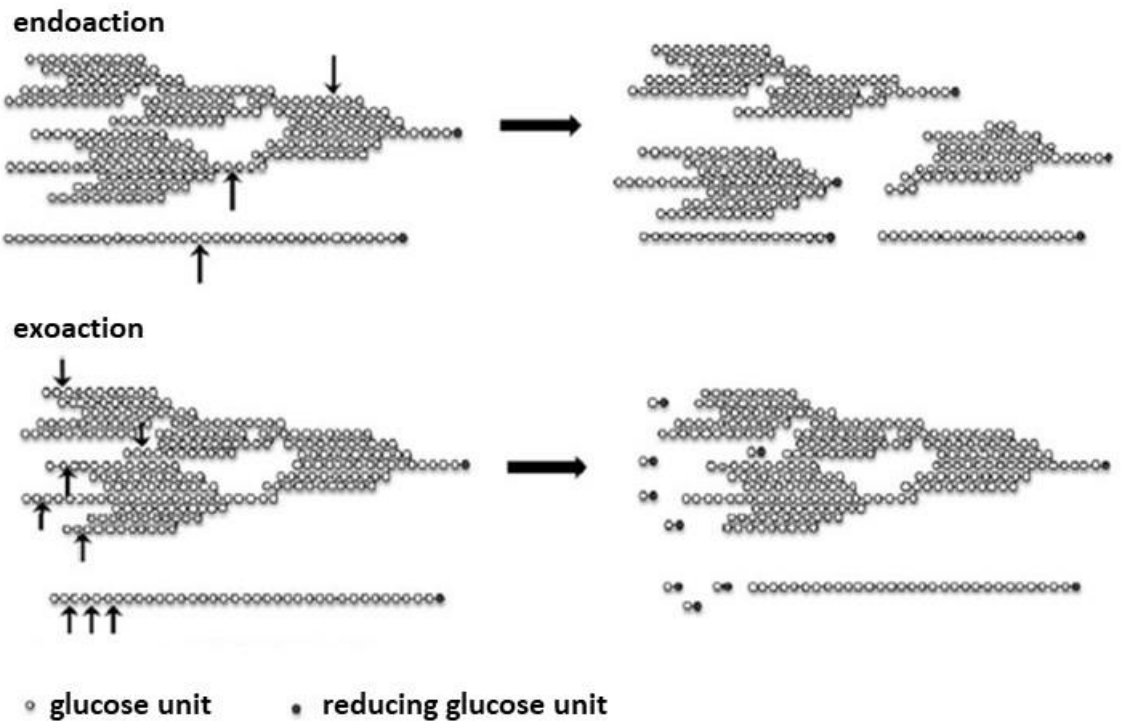

Figure 2.4 Schematic representation of the endoaction and exoaction of amylases on amylose (AM) and amylopectin (AP) (Derde, 2013).

Fresh bread from BStA-containing recipes has a higher crystallinity than does control bread as indicated by ^{13}C NMR (Morgan *et al.*, 1997) and TD ^{1}H NMR measurements (Bosmans *et al.*, 2013a). Indeed, the WAXD pattern of crumb from fresh bread made from BStA-containing recipes not only displays V_H-type reflections, which are the only reflections observed in fresh control bread, but also weak B-type reflections (Hug-Iten *et al.*, 2001). Furthermore, BStA action during bread making results in fresh bread with a decreased initial crumb softness (Goesaert *et al.*, 2009a) and resilience (Bosmans *et al.*, 2013a). The decreased MW of AM molecules, because of the limited endoaction of BStA during baking, is suggested to enhance their mobility such that they tend to crystallize faster. As a result, the formation of the semicrystalline AM network during cooling and, therefore, the **initial crumb firmness is enhanced** (Bosmans *et al.*, 2013a; Goesaert *et al.*, 2009a; Hug-Iten *et al.*, 2001).

The AP molecules which have undergone BStA action during bread making (Goesaert *et al.*, 2009a) are less apt to retrograde during storage. Evidence for this observation is a smaller increase in the amount rigid protons characteristic for AP crystals, the lower AP melting enthalpy and B-type crystallinity as detected with respectively TD ^{1}H NMR, DSC and WAXD (Bosmans *et al.*, 2013a; Goesaert *et al.*, 2009a; Hug-Iten *et al.*, 2001).

A higher level of short AP branch chains (DP 6-9) has been related to a reduced extent of retrogradation (*cf*. §1.5.3). AP hydrolysis by BStA results in an increased level of outer AP

chains that are too short to crystallize (Goesaert *et al.*, 2009a). When the extent of AP retrogradation decreases, a less extended semicrystalline AP network is formed. Consequently, less water is withdrawn from *inter alia* the gluten network and immobilized in the crystalline and amorphous zones of the fringed micelle network. This results in a better hydrated and less firm gluten network as shown with TD ^{1}H NMR (Bosmans *et al.*, 2013a). Combined, the above result in a **decreased rate and extent of crumb firming during storage** of bread the recipe of which which has been supplemented with BStA (Bosmans *et al.*, 2013a; Goesaert *et al.*, 2009a; Hug-Iten *et al.*, 2001; Morgan *et al.*, 1997).

2.3.1.2 *Bacillus subtilis α-amylase*

The endoacting α-amylase of *Bacillus subtilis* (BSuA) is another antifirming amylase (Kulp & Ponte, 1981), be it that it is less effective than BStA. BSuA attacks starch polymers internally such that their MW decreases rapidly. The antifirming action of BSuA is mainly attributed to weakening of the starch network by hydrolysis of the long starch chains that connect the junction zones. The side chain distribution of AP is only slightly changed because of BSuA action such that AP retrogradation and the associated moisture migration from gluten to starch still occur to considerable extent during storage. The BSuA dosage in bread should be limited, especially since the enzyme survives the baking phase. Excessive use of BSuA in bread results in a structural collapsed bread loaf (Goesaert *et al.*, 2009a) with a sticky crumb (Kulp & Ponte, 1981).

2.3.1.3 *Surfactants*

Monoacylglycerols and diacylglycerols can also be included in bread making recipes because they act as crumb softeners (Pareyt *et al.*, 2011). They form complexes with AM (Krog, 1971), which as a result is less available for crystallization. The initial firmness of bread crumb is therefore reduced (Gómez *et al.*, 2004).

2.3.1.4 *Flours with unusual starch characteristics*

Fresh bread crumb with an increased crumb softness is also observed when wheat flour in regular bread (Hayakawa *et al.*, 2004) and wheat starch in starch-gluten bread are (partially) replaced by their waxy counterparts. During storage, retrogradation occurs to a larger extent with increasing portions of waxy wheat starch in the starch-gluten bread (Lee *et al.*, 2001). The crumb firmness of bread prepared from wheat flour with a lower AM content and a higher portion of AP branch chains with DP 6-10 at the expense of those with DP 11-24 has been shown to be lower after both 1 and 3 days of storage. The latter has been attributed to a decreased extent of AP retrogradation (Inokuma *et al.*, 2016).

2.3.2 Process conditions

2.3.2.1 *Parbaking*

Nowadays, **interrupted bread making processes** are widely applied to avoid economic losses that result from the disposal of bread by the consumer. In contrast to the production process of a conventionally baked (CB) bread, which involves only one baking step, an interrupted bread making process consist of both a partial and later a final baking phase (Figure 2.5). The partially baked (PB) bread is intermediately stored. The stored PB bread is later subjected to a second and final baking phase to obtain a fresh, fully baked (FB) bread when desired. The latter, final baking phase is performed by bakers, retailers or consumers themselves (Almeida *et al.*, 2016).

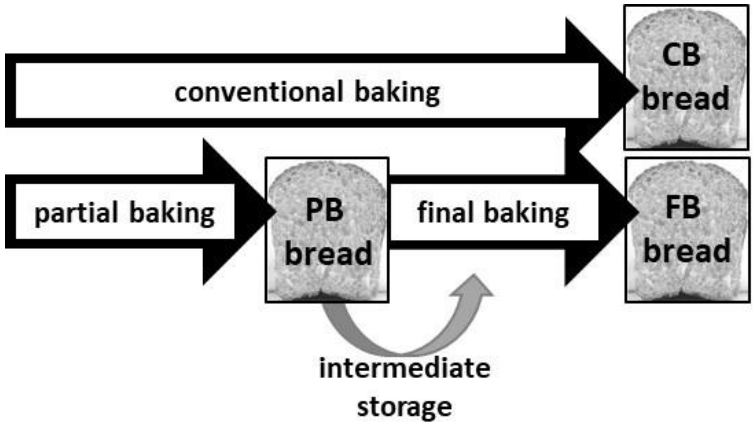

Figure 2.5 Schematic overview of either a conventional or an interrupted bread making process. Conventionally baked (CB) bread is obtained by a single baking step. The interrupted bread making process consists of a partial baking step [resulting in partially baked (PB) bread] and later, after intermediate storage, a final baking step [resulting in fully baked (FB) bread].

The **partial baking phase** is executed in such way that complete crumb setting is realized without significant occurrence of Maillard reactions that would result in crust browning (Almeida *et al.*, 2016; Bárcenas & Rosell, 2006; Leuschner *et al.*, 1997). Furthermore, an adequate crumb center temperature should be reached to prevent microbial spoilage (Bailey & Von Holy, 1993). All moulds and mould spores are killed when a crumb temperature of 85–90 °C is reached during baking (Knight & Menlove, 1961). Bacterial spoilage of bread is mainly due to *Bacillus subtilis* spores, which can survive the baking process. To avoid microbial spoilage, propionates are commonly added in the bread recipe (Cauvain, 2015).

The final baking phase aims at melting the AP crystals formed during intermediate storage (Bosmans *et al.*, 2014). To meet these requirements, a crumb center temperature of respectively 85 to 90 °C in the first and at least 50 to 60 °C in the second baking phase should

be reached (Figure 2.6) (Schoch & French, 1947; Slade & Levine, 1987). Final baking furthermore results in the development of desirable aromas and crust color because of Maillard reactions (Almeida *et al.*, 2016; Leuschner *et al.*, 1997).

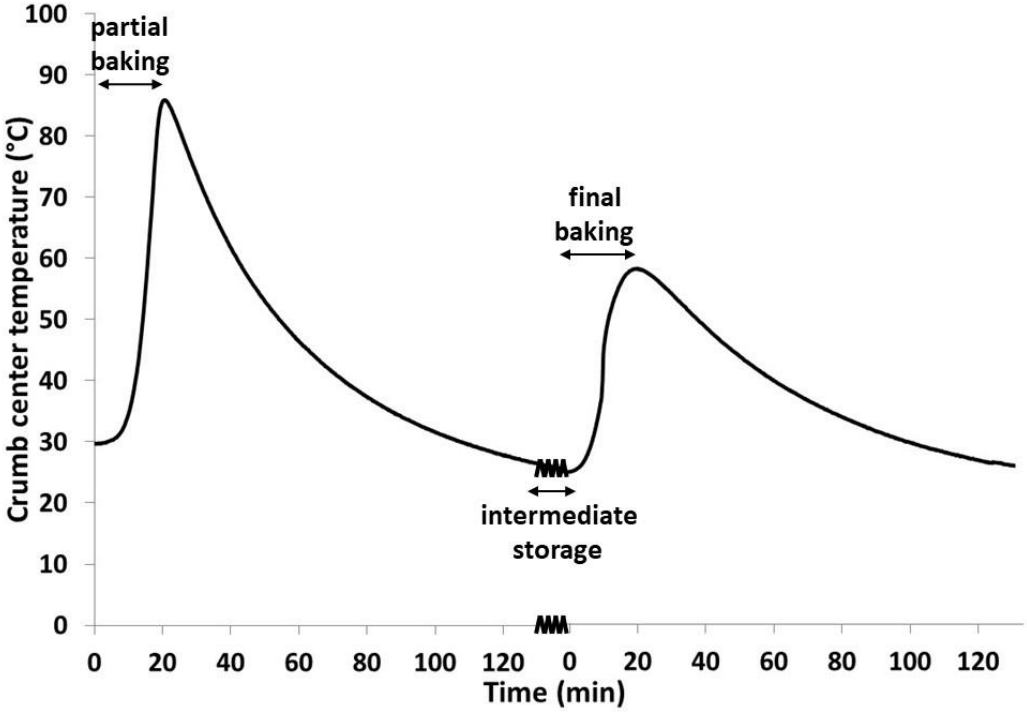

Figure 2.6 In house determined temperature profile in the crumb center of bread during partial and final baking. During partial baking, a center temperature of 85-90 °C should be reached to set the crumb and to restrict microbial spoilage. During final baking, a center temperature of at least 50-60 °C should be reached to melt the retrograded AP crystals that are formed during intermediate storage.

Depending on the temperature-time profile during bread baking, the extents of both AM leaching from the starch granules (Le-Bail *et al.*, 2012) and gluten polymerization vary (Giovanelli *et al.*, 1997; Lagrain *et al.*, 2008a). Differences therein are reflected in differences in crumb texture (Bosmans *et al.*, 2013b; Le-Bail *et al.*, 2012). The initial crumb firmness and resilience are largely determined by the strength of the semicrystalline AM network and that of the gluten network (Goesaert *et al.*, 2009b). Furthermore, AP retrogradation and the related increase in crumb firmness during storage occur to a larger extent with prolonged baking times and higher crumb center temperatures reached during baking (Bosmans *et al.*, 2013b; Giovanelli *et al.*, 1997; Le-Bail *et al.*, 2012).

The quality of FB bread, obtained by final baking of stored PB bread, is often said to be lower than that of CB bread, obtained by a single baking phase (Karaoglu & Kotancilar, 2006; Le-Bail *et al.*, 2005; Ribotta & Le Bail, 2007). FB bread is also believed to firm more rapidly than CB bread (Ghiasi *et al.*, 1984; Rosell & Santos, 2010; Sciarini *et al.*, 2012). The published studies

mostly have involved frozen or refrigerated intermediate storage of labscale or French PB breads.

2.3.2.2 *Storage temperature*

Not only the baking but also the storage conditions impact on crumb firming. As outlined above, crumb firming is strongly related to AP retrogradation (*cf.* §2.2.4) and this process depends on the storage temperature (*cf.* §1.5.3). The rate-limiting step of AP retrogradation is nucleation, which is favored at temperatures near the glass transition temperature (Slade *et al.*, 1991). For a typical bread crumb MC of about 40%, the glass transition temperature is in the subzero range (Cuq *et al.*, 2003; Osella *et al.*, 2005), at -5 °C (Slade *et al.*, 1991). Indeed, the rate of AP retrogradation is maximal at temperatures between 5 and 14 °C, *i.e.* at temperatures close to the glass transition and well below the melting temperature of retrograded wheat starch (*ca.* 60 °C) (Marsh & Blanshard, 1988; Slade *et al.*, 1991).

However, the migration of water from gluten to starch (Willhoft, 1971b) and from crumb to crust (Bosmans *et al.*, 2013b) occurs more slowly at lower temperatures due to the lower rate of water diffusion (Holz *et al.*, 2000). Nevertheless, faster retrogradation results in the formation of a more extended starch network such that the crumb firms to greater extent when stored at 4 °C than when stored at 25 °C (Bosmans *et al.*, 2013b). During storage at temperatures below -18 °C the rate and extent of starch retrogradation is significantly reduced (Aguirre *et al.*, 2011) such that the crumb firmness and resilience remain unchanged during frozen storage for 4 weeks (Bosmans *et al.*, 2014).

2.4 ANALYSIS OF BREAD PROPERTIES AT DIFFERENT LENGTH SCALES

Textural and structural properties of a food system depend on the molecules of which it is made up and how they interact on **molecular (nm), meso- (nm-µm) and macroscale (µm-cm)** (Pascua *et al.*, 2013; Song & Zheng, 2007; Ubbink *et al.*, 2008). In the particular case of bread making, the properties of fresh and stored bread result from complex transformations and interactions of its constituents at different length scales during baking, cooling and storage. To understand the functionality of different biopolymers and their interaction with water in bread, the output of techniques measuring at different length scales can be combined. To learn the exact timing and extent of constituent changes during bread making, these techniques are preferentially used *in situ* during processing. We here elaborate on the use of TD ^{1}H NMR, WAXD, DSC, SE-HPLC and texture analysis to investigate the constituent changes during bread making and storage and/or their impact on fresh and stored bread properties.

2.4.1 Time domain ^{1}H nuclear magnetic resonance

The interaction of water with starch in dough/bread on **molecular and mesoscale** is best studied with TD ^{1}H NMR (Bosmans *et al.*, 2013c; Hills *et al.*, 1991; Tang *et al.*, 2000; van Duynhoven *et al.*, 2010). Using this NMR technique, which operates at relatively low fields, different proton populations are distinguished depending on the environment they are in (Bosmans *et al.*, 2012). NMR active nuclei, *e.*g ^{1}H, have spin values that differ from 0 as a result of their uneven amount of protons and neutrons (Schmidt, 2007).

2.4.1.1 *Principle*

^{1}H nuclei can absorb resonant radiofrequency energy in an external static magnetic field B_0. Outside this magnetic field, the nuclei in a sample are randomly oriented. When the sample is placed in the magnetic field B_0, the nuclei adopt a parallel or antiparallel orientation to B_0 (z-axis) and start to precess randomly about B_0 in the xy-plane such that nuclei lack phase coherence and there is no net magnetization in the xy-plane (M_{xy}=0) (Figure 2.7). The population of parallel nuclei is larger than that of the antiparallel nuclei since the former are of lower energy. Consequently, the magnetization in the z-direction differs from 0 (M_z=M_0). The nuclei in B_0 are said to be in **equilibrium state** (Schmidt, 2007).

During an NMR experiment, a short radiofrequent energy pulse perpendicular to B_0 is applied by an oscillating magnetic field B_1. The pulse frequency equals that by which the nuclei precess about B_0. After the B_1 pulse, equal amounts of nuclei are oriented parallel and antiparallel to B_0 such that no net magnetization is present along the z-axis (M_z=0) (Figure 2.7). Furthermore, the B_1 pulse creates phase coherence amongst the nuclei. As a result, the magnetization in the xy-plane is maximal (M_{xy}). After the B_1 pulse, nuclei return to their equilibrium position through simultaneous **longitudinal** (T_1) and **transverse** (T_2) **relaxation**. The former restores the equilibrium between parallel and antiparallel oriented nuclei while the latter is responsible for the loss of phase coherence (Figure 2.7). The time needed to achieve this is termed the T_1 or the T_2 relaxation time, respectively (Schmidt, 2007).

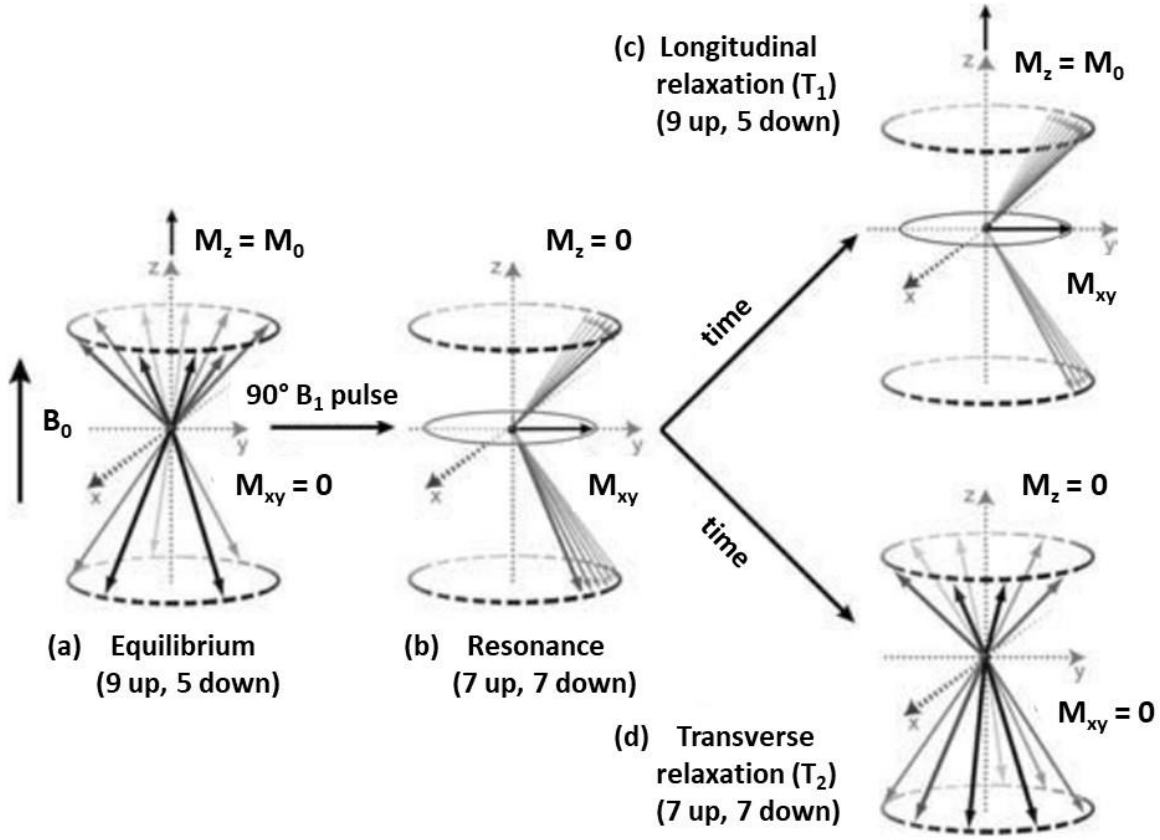

Figure 2.7 Schematic representation of nuclear spins during an ^{1}H NMR experiment. (a) In a static magnetic field B_0, the nuclei align parallel or antiparallel to B_0. More nuclei adopt the lower energetic parallel orientation. This results in a net magnetization (M_z) that equals the equilibrium magnetization (M_0). Nuclei lack phase coherence such that no net magnetization is present in the xy-plane (M_{xy}=0). (b) After a short resonant B_1 pulse perpendicular to B_0 the amount of nuclei with a parallel and antiparallel orientation to B_0 is equalized (M_z=0) and nuclei precess in phase (M_{xy}). (c) After the B_1 pulse nuclei relax back to their equilibrium state. During longitudinal (T_1) relaxation the equilibrium between parallel and antiparallel oriented nuclei is restored (M_z=M_0). (d) During transverse (T_2) relaxation, phase coherence is lost (M_{xy}=0) (Schmidt, 2007).

The **molecular mobility** of protons is positively related to the T_2 relaxation time (Leung *et al.*, 1979). However, T_1 relaxation times can represent both liquid (mobile) and solid (immobile) protons (Schmidt, 2007). T_2 relaxation times are more sensitive than T_1 relaxation times to structural changes such as those during starch gelatinization and gelation (Child & Pryce, 1972; Lelievre & Mitchell, 1975). Therefore, only **T_2 relaxation times** are considered in this doctoral dissertation. The T_2 relaxation time of water is about 2-3 s (Child & Pryce, 1972; Hills *et al.*, 1990; Tang *et al.*, 2000). In a biopolymer-water system, bulk water does not interact with the biopolymer and is therefore very mobile. When water becomes bound with the biopolymer surface or its internal structure, its mobility decreases (Hills *et al.*, 1996).

The **free induction decay** (FID) measurement is the most basic T_2 relaxation experiment and commonly used to study the relaxation of protons in solid crystalline and glassy phases. Such

immobile protons typically relax fast in a submillisecond time frame (van Duynhoven *et al.*, 2010). To investigate phenomena such as gelatinization and gelation of starch suspensions, measurement of longer relaxation times, characteristic for protons in relatively dilute systems, is required (Lelievre & Mitchell, 1975). The relaxation of protons in such mobile systems is substantially influenced by inhomogeneities of B_0. By means of a spin-echo method, this effect can be eliminated. Typically, the **Carr-Purcell-Meiboom-Gill** (CPMG) **pulse sequence**, in which the 90° pulse is followed by several 180° pulses, is used. This way, dephasing due to B_0 inhomogeneities is refocused and the natural signal decay can be monitored in the milliseconds to seconds range (Carr & Purcell, 1954; Meiboom & Gill, 1958; van Duynhoven *et al.*, 2010). T_2 relaxation curves, of which the initial intensity is a measure of the amount of detectable protons in the sample, can be transformed to continuous distributions of T_2 relaxation times with an inverse Laplace transformation. The resulting spectrum shows different proton populations depending on the environment the protons are in (Forshult, 2004).

2.4.1.2 *Nuclear magnetic resonance measurements in bread and model systems*

Molecular and mesoscale aspects of the starch network and the distribution of water therein have been studied with TD ^{1}H NMR in starch-based model systems **before and after heating and cooling** (Bosmans *et al.*, 2012; Ritota *et al.*, 2008; Tananuwong & Reid, 2004; Tang *et al.*, 2001) and in dough (Doona & Baik, 2007) and (stored) bread (Bosmans *et al.*, 2013c; Curti *et al.*, 2011; Wang *et al.*, 2004). Starch-water systems have both **nonexchanging CH protons** and **exchanging protons** of water and *e.g.* hydroxyl groups of starch (Tang *et al.*, 2000). In bread systems, protons of water can further exchange with SH and amino groups of gluten (Wang *et al.*, 2004).

Temperature-controlled TD ^{1}H NMR allows studying starch transitions and water dynamics *in situ* during heating and cooling. This way, starch-based model systems (Kovrlija & Rondeau-Mouro, 2016; Rondeau-Mouro *et al.*, 2015), bread (Engelsen *et al.*, 2001; Kim & Cornillon, 2001; Pojić *et al.*, 2016; Rondeau-Mouro *et al.*, 2015) and biscuit dough (Assifaoui *et al.*, 2006; Serial *et al.*, 2016) have been investigated **during heating**. Changes in areas of specific proton populations in a 20 to 50 °C temperature range presumably result from swelling of starch granules and the concurrent leaching of AM to the extragranular space (Kovrlija & Rondeau-Mouro, 2016; Pojić *et al.*, 2016; Rondeau-Mouro *et al.*, 2015). Further changes in areas and T_2 relaxation times at temperatures between 60 and 90 °C have been related to starch gelatinization (Engelsen *et al.*, 2001; Kovrlija & Rondeau-Mouro, 2016; Pojić *et al.*, 2016; Rondeau-Mouro *et al.*, 2015).

The decreased T_2 relaxation time and thus mobility of exchanging protons of water and extragranular starch during heating has been related to an increased system viscosity resulting from granule swelling and AM leaching (Assifaoui *et al.*, 2006; Kim & Cornillon, 2001). At higher temperatures, the T_2 relaxation time decreases again. It has been hypothesized that this results from granule disintegration (Lelievre & Mitchell, 1975). Proton mobility is also impacted by a thermal activation mechanism obeying Arrhenius' law, in the sense that proton mobility increases with temperature (Kim & Cornillon, 2001; Lucas *et al.*, 2008; Rondeau-Mouro *et al.*, 2015). In contrast, the signal intensities decrease when temperature increases in line with Curie's law (Kim *et al.*, 2004; Lucas *et al.*, 2008; Rondeau-Mouro *et al.*, 2015; Serial *et al.*, 2016).

Dough contains two FID and two or three CPMG populations (Doona & Baik, 2007; Rondeau-Mouro *et al.*, 2015). In fresh bread, two FID and four CPMG populations are detected. Based on the analysis of starch, gluten and flour model systems before and after heating, Bosmans *et al*. (2012) have assigned the least mobile FID protons in **fresh bread** to rigid nonexchanging protons of starch and gluten that are not in contact with water. More mobile FID protons are amorphous nonexchanging protons of starch and gluten only in limited contact with water. CPMG proton populations in fresh bread contain mainly exchanging protons of water, starch and gluten in the gel network containing the granule remnants. In addition, some nonexchanging protons of starch and gluten, and lipid protons are present (Bosmans *et al.*, 2012).

The portion of rigid protons in bread crumb increases **during storage of bread**. This has been attributed to AP retrogradation (Bosmans *et al.*, 2013c) and the loss of water from bread crumb to the crust (Curti *et al.*, 2011). The latter furthermore results in a lower level of rigid protons and a higher proton mobility in crust from bread stored for 7 days than in crust from fresh bread (Bosmans *et al.*, 2013c). A general decrease in mobility of CPMG protons has been related with increasing crumb firmness (Bosmans *et al.*, 2013c; Chen *et al.*, 1997; Engelsen *et al.*, 2001). Both firming of the starch network (due to AP retrogradation) and firming of the gluten network (due to gluten dehydration) (*cf*. §2.2.4), contribute to a decreased proton mobility (Bosmans *et al.*, 2013c).

Reheating of crumb of stored bread causes the amount of rigid protons to decrease again since AP crystals formed as a result of retrogradation have melted (*cf*. §2.2.4). The proton mobility, however, does not increase. Although the impact of AP retrogradation is reversed by heating, it has been suggested that the starch network organization cannot be reversed. The water that has been withdrawn from the gluten network and incorporated in the starch network during storage, presumably remains associated with it (Bosmans *et al.*, 2013b). This

supports earlier findings that moisture migration from gluten to starch during storage is not reversed by heat (Willhoft, 1971a) (*cf*. §2.2.4).

2.4.2 Additional experimental methods

2.4.2.1 *X-ray diffraction measurements*

During X-ray diffraction measurements, an incident X-ray beam is scattered by the electrons in the sample studied. Structural information provided by scattered beams is derived from its electron distribution in the sample (Hukins, 1981). WAXD is used to investigate the structure of crystals at subnanometer scale. Hereto, scattered X-rays are collected at large angles. During SAXS experiments, scattered X-rays are collected at smaller angles and provide structural information at larger length scales, *e.g.* the lamellar structure of starch (Blazek & Gilbert, 2011).

As pointed out in Chapter 1 (*cf.* §1.3.1), different starch crystal types give rise to different WAXD patterns. The diffraction pattern of fresh bread is dominated by a characteristic V_H-type pattern. **As a result of storage of bread**, it acquires a characteristic B-type pattern (Bosmans *et al.*, 2013c; Hug-Iten *et al.*, 2001). By means of **synchrotron radiation**, diffractograms can be measured at short time intervals *in situ* **during heating**. This way, the timing and extent of gelatinization (Jenkins *et al.*, 1994; Vermeylen *et al.*, 2006) and AM complexation can be monitored during heating of starch suspensions (Le Bail *et al.*, 1999).

2.4.2.2 *Differential scanning calorimetry*

Thermal properties of starch in bread can be studied with DSC. Melting of (retrograded) AP crystals and AM-L complexes requires heat. The DSC instrument maintains the temperature balance between a sample and a reference material. Thermal transitions in the sample are monitored as the difference in energy input required to maintain this temperature balance upon heating and cooling. A melting transition results in an endothermic peak of which the area represents the melting enthalpy (Karim *et al.*, 2000). This enthalpy is directly proportional to the crystallinity of the sample. The temperature at which melting occurs is a measure for the stability of the crystals (Gomand *et al.*, 2012). DSC is also used to study the denaturation of proteins such as those of egg white (Donovan *et al.*, 1975). However, during DSC analysis of wheat gluten proteins no endothermic peaks are observed (Hoseney & Rogers, 1990).

2.4.2.3 *Size exclusion high performance liquid chromatography*

SE-HPLC is widely used for *inter alia* MW estimation and separation of molecules such as AM, AP and proteins (Irvine, 1997; Ong *et al.*, 1994; Regnier, 1983). It is also used to evaluate

glutenin and gliadin cross-linking during bread making (Lagrain *et al.*, 2008a) and thus provides information about the **mesoscale** gluten network. Extraction media containing SDS disrupt noncovalent bonds and are used to extract almost all protein from cereals (Lambrecht *et al.*, 2015). Cross-linking of gliadin and glutenin through SS bonds indeed decreases gluten extractability in SDS-containing medium. This is detected as a decreased area of specific chromatogram peaks representing glutenins and gliadins (Lagrain *et al.*, 2008a).

2.4.2.4 *Texture analysis*

The texture of a food system is a combination of its structural, mechanical and surface properties (Szczesniak, 2002). Crumb firmness and resilience are textural parameters and represent the **macroscopic** manifestation of bread constituent changes at different length scales (*cf.* §2.2.3-2.2.4) (Goesaert *et al.*, 2009b; Karim *et al.*, 2000). Crumb firmness can be determined as the force required to compress the sample over a specified percentage (*ca.* 25-40%) of its height (Amigo *et al.*, 2016; Bosmans *et al.*, 2013c; Crowley *et al.*, 2002; Ghiasi *et al.*, 1984; Purhagen *et al.*, 2011). When the applied force is removed, the sample partially recovers and decompresses. Crumb resilience is then the extent to which the latter occurs. In essence, the percentage recoverable work is calculated from the areas under the decompression and compression curves (Amigo *et al.*, 2016; Bosmans *et al.*, 2013a).

2.5 CLOSING THE KNOWLEDGE GAPS

From this literature review (Chapters 1 and 2) it follows that starch characteristics largely determine the properties of fresh and stored bread. The impacts of different AM and AP characteristics on starch transitions in starch-water systems (Fujita *et al.*, 1998; Noda *et al.*, 2001; Singh *et al.*, 2010; Tester & Morrison, 1990) and on the properties of fresh and stored bread (Hayakawa *et al.*, 2004; Inokuma *et al.*, 2016; Lee *et al.*, 2001) have already been investigated. The exact functionality of AM and AP and their interaction with water, however, has never been monitored during the bread baking and cooling process itself. Hereto, methodologies which allow for *in situ* analyses of starch properties and water dynamics, such as temperature-controlled TD ^{1}H NMR, are required.

In spite of the meaningful progress made with temperature-controlled TD ^{1}H NMR in understanding molecular dynamics of starch and water during heating, the NMR data have to the best of our knowledge never been unambiguously interpreted in the light of results obtained by additional techniques that specifically measure gelatinization associated phenomena such as granule swelling and AM leaching (Engelsen *et al.*, 2001; Kim & Cornillon, 2001; Kovrlija & Rondeau-Mouro, 2016; Pojić *et al.*, 2016; Rondeau-Mouro *et al.*, 2015). Moreover, sample temperatures during NMR measurements have mostly been increased stepwise, which is not representative for bread making, and no NMR measurements have been performed during subsequent cooling. Time-resolved X-ray measurements are very suitable to study the evolution of different crystalline forms of starch during bread making. Such measurements have not yet been performed in a bread system during baking and cooling.

In this work, a toolbox based on temperature-controlled TD ^{1}H NMR is developed to monitor starch transitions and water dynamics during bread baking and cooling at different length scales (Chapter 3) (Figure i.1). This toolbox is then applied during baking and cooling of dough prepared from flour with atypical starch characteristics in Chapter 4. Furthermore, BStA is included into the bread recipe to further improve our understanding of the *in situ* AM and AP functionality and the mechanism of the amylase during bread making. In Chapter 5, it is then described how changes in the (atypical) starch fraction and the related water distribution during baking and cooling impact on the properties of fresh and stored tin bread. Finally, the bread making process rather than the bread recipe is altered. Last but not least, in Chapter 6 the impact of an interrupted baking process on the crumb firming mechanism of tin bread with ambient intermediate storage is investigated.

Part two

Experimental work

Chapter 3

Optimization of a temperature-controlled time domain ^{1}H NMR toolbox to monitor molecular dynamics of starch and water during bread making

Chapter 4

Amylose and amylopectin functionality during baking and cooling of bread prepared from flour of wheat containing unusual starches

Chapter 5

Amylose and amylopectin functionality during storage of bread prepared from flour of wheat containing unusual starches

Chapter 6

The impact of parbaking on the crumb firming mechanism of tin wheat bread

Chapter 3

Optimization of a temperature-controlled time domain ^{1}H NMR toolbox to monitor molecular dynamics of starch and water during bread making[2]

3.1 INTRODUCTION

Starch is the most abundant biopolymer in bread dough. As pointed out in Chapter 2, starch transitions during bread baking and cooling together with gluten polymerization during baking bring about the crumb structure of fresh bread. During gelatinization, starch absorbs a substantial amount of water such that water in the dough system is redistributed. TD ^{1}H NMR has proven to be a useful technique to study molecular and mesoscale aspects of the starch network and the distribution of water therein in starch-based model systems (Bosmans *et al.*, 2012; Ritota *et al.*, 2008; Tananuwong & Reid, 2004; Tang *et al.*, 2001) and bread (Bosmans *et al.*, 2013c; Curti *et al.*, 2011; Wang *et al.*, 2004). However, most studies have focused on the proton mobility of biopolymers and water before or after heating or during product storage.

Techniques such as temperature-controlled TD ^{1}H NMR can be used to study the exact timing and extent of starch transitions and/or water dynamics *in situ* during bread baking. Temperature-controlled TD ^{1}H NMR has been used to investigate proton dynamics in starch-based model systems (Kovrlija & Rondeau-Mouro, 2016; Rondeau-Mouro *et al.*, 2015), bread (Engelsen *et al.*, 2001; Kim & Cornillon, 2001; Pojić *et al.*, 2016; Rondeau-Mouro *et al.*, 2015) and biscuit dough (Assifaoui *et al.*, 2006; Serial *et al.*, 2016) during heating. Despite the progress made with the technique for understanding starch transitions and water dynamics during heating, the NMR data have, to the best of our knowledge, never been interpreted in

[2] This Chapter is based on the following reference: Nivelle, M.A., Beghin, A.S., Bosmans, G.M. and Delcour, J.A. (2019) Molecular dynamics of starch and water during bread making monitored with temperature-controlled time domain ^{1}H NMR. Food Research International, 119, 675-682.

combination with results from additional techniques that measure gelatinization associated phenomena such as granule swelling and AM leaching. Moreover, sample temperatures during NMR measurements have mostly been increased stepwise, which is not representative for bread making. Although starch transitions during cooling are crucial for the crumb texture of fresh bread, proton dynamics during cooling of bread have not yet been investigated.

Against this background, a toolbox based on temperature-controlled ^{1}H NMR was optimized here to study starch transitions and water dynamics during simulated bread baking and cooling on molecular and mesoscopic scale. Complementary techniques were applied to underpin the interpretation of the complex NMR data. Time-resolved WAXD was used to monitor the different crystalline forms of starch *in situ* during bread making. Analyses measuring at respectively molecular and mesoscopic scale, *i.e.* DSC and gravimetric and colorimetric analyses, were performed at different temperatures to study AP crystal melting, starch swelling and CHL. This chapter reports on the outcome of the toolbox when analyzing bread dough from regular wheat flour.

3.2 MATERIALS & METHODS

3.2.1 Materials

Wheat flour [Crousti: 79.6% dm starch and 12.7% dm protein] and compressed yeast were obtained from Dossche Mills (Deinze, Belgium) and AB Mauri (Merelbeke, Belgium), respectively. Extra virgin olive oil, sugar and salt were from a local supermarket. Reagents and solvents for starch content analysis were from Acros Organics (Geel, Belgium) and VWR International (Oud-Heverlee, Belgium), respectively. All other chemicals were from Sigma-Aldrich (Bornem, Belgium).

3.2.2 Methods

3.2.2.1 *Experimental approach*

A toolbox consisting of different techniques that analyze starch and its interaction with water during bread baking and cooling at different length scales was developed. During conventional baking, there is a temperature gradient in dough/bread (*cf.* §2.2.2). Evidently, the maximum temperature is reached last in the center, and the accompanying temperature-dependent changes during baking start later. Here, the temperature profile inside the sample during *in situ* analyses was simulated to imitate that in the dough/crumb center during conventional baking. Since dough samples baked in the NMR device were only small, it can be assumed that

only limited temperature gradients were present (if any) and that they were heated uniformly. Using temperature-controlled TD ^{1}H NMR as the main technique, starch and water proton dynamics could be observed *in situ* at molecular and mesoscopic scale during simulated baking and subsequent cooling. As outlined above, additional techniques were applied to underpin the interpretation of the complex NMR data.

3.2.2.2 *Composition of wheat flour*

Starch content was calculated as 0.9 times the total glucose content, measured with gas-liquid chromatography, using a method based on Englyst and Cummings (1984). Protein content was determined using an adaptation of the AOAC Official Method 990.03 (AOAC, 1995) to an automated Dumas protein analysis system (EAS vario Max C/N, Elt, Gouda, The Netherlands) with 5.7 as nitrogen to protein conversion factor. MC of wheat flour was determined according to AACC method 44-15.02 (AACC, 1999a).

3.2.2.3 *Dough and bread making*

Bread was prepared according to a straight-dough method (Finney, 1984). Dough consisted of wheat flour (10.0 or 270 g of flour, *i.e.* 100 parts; 14.0 % MC), deionized water (59 parts), sucrose (6 parts), yeast (5.3 parts), sodium chloride (1.5 parts) and calcium propionate (0.25 parts). When preparing dough from 270 g flour, ingredients were mixed for 330 s in a slightly greased spiral mixer (De Danieli, Legnaro, Italy) at 23 °C. The obtained dough was divided into 450 g pieces. To prepare dough from 10.0 g of flour, ingredients were mixed at 23 °C for 240 s in a slightly greased 10 g pin mixer (National Manufacturing, Lincoln, NE, USA). All doughs were transferred to slightly greased bowls and put in a fermentation cabinet (National Manufacturing) at 30 °C and 90% relative humidity. Fermentation lasted 90 min with intermediate punching at 52, 77 and 90 min using a dough sheeter (National Manufacturing). Final proofing (36 min at 30 °C and 90% relative humidity) was done in a slightly greased baking tin [internal dimensions (width x length x height): 2.5 cm x 5.0 cm x 2.5 cm or 10.0 cm x 16.0 cm x 6.5 cm for dough from 10.0 or 270 g of flour, respectively]. Fermented dough from 10.0 g of flour was further analyzed (*cf.* §3.2.2.5 – 3.2.2.8). Fermented dough based on 270 g of flour was baked in a rotary hearth oven (National Manufacturing) at 210 °C for 24 min, a typical baking time for bread of that size in industrial practice (Nivelle *et al.*, 2017). After baking, bread loaves were cooled for 120 min at 23 °C.

3.2.2.4 *Monitoring dough and crumb temperature*

The temperature profile in the center of the large size dough/bread during conventional baking and subsequent cooling (*cf.* §3.2.2.3) was monitored using Datapaq (Cambridge, UK) equipment which included a Multipaq 21 temperature logger, Type T thermocouples and a

stainless steel thermal barrier used to protect the data logger during baking. The temperature profile during cooling was monitored after removing the baking tin. Both temperature profiles were then used to simulate bread baking and subsequent cooling while performing *in situ* measurements with temperature-controlled ^{1}H NMR and time-resolved WAXD. To verify that the NMR temperature profile sufficiently matched that during conventional baking and cooling, the NMR sample temperature in the probe head was monitored with Datapaq equipment and further adjusted to obtain a satisfying profile.

3.2.2.5 *Temperature-controlled proton nuclear magnetic resonance*

Measurements of proton distributions in dough during simulated bread baking and cooling were performed with a Minispec mq 20 TD NMR spectrometer (Bruker, Rheinstetten, Germany) at an operating resonance frequency of 20 MHz for ^{1}H (magnetic field strength of 0.47 T). The device has a BVT3000 tempering unit (Bruker) to control the temperature of the probe head. Nitrogen gas serves as the tempering medium of which the desired temperature is adjusted by a heating coil inserted in the probe head. Only T_2 relaxation times were investigated.

T_2 relaxation is the loss of phase coherence of nuclei (dephasing). The relaxation of immobile, fast relaxing protons was studied by performing a single 90° pulse, *i.e.* the FID measurement. The relaxation of more mobile protons is substantially influenced by inhomogeneities of B_0 (*cf.* §2.4.1.1). The total T_2 (T_2*) relaxation is then a combination of dephasing spins due to differences in B_0 (ΔB_0) and natural T_2 relaxation:

$$\frac{1}{T_2^*} = \frac{1}{T_2} + \frac{1}{T_{2(\Delta B_0)}}$$ (Schmidt, 2007).

True T_2 relaxation curves for more mobile protons were obtained by performing a CPMG pulse sequence which consisted of an initial 90° pulse along the x-axis followed by a train of 180° pulses along the y-axis. After the applying the 90° pulse, phase coherence was lost due to inhomogeneities of B_0 and true T_2 relaxation. Application of the 180° pulse after time τ refocused the spins that were dephasing due to field inhomogeneities such that an echo was created at time 2τ [Figure 3.1 (a)]. Continuous refocusing of these dephasing spins resulted in a series of echoes of which the intensity died away through natural T_2 relaxation [Figure 3.1 (b)] (Schmidt, 2007).

The lengths of the 90° and 180° pulses were respectively 3.29 and 6.67 µs. The FID was sampled for 0.5 ms and 1,250 data points were acquired. For the CPMG sequence, the pulse separation between the 90° and 180° pulses was 0.1 ms and 3,200 data points were collected. The recycle delay was either 4 or 3 s for respectively FID or CPMG measurements and for both

measurements 16 scans were accumulated to increase the signal to noise ratio. Accurately weighed fermented dough samples (approximately 170 mg) were inserted in different Bruker NMR tubes (10 mm external diameter) and tightly compressed to 5-6 mm height. The exact sample weights were used in further calculations. To avoid excessive moisture loss, a glass rod was introduced into the tube before it was sealed. However, water evaporation from the dough during heating, which also takes place during conventional baking, could still occur. Each tube was subjected to a simulated baking and cooling process (*cf.* §3.2.2.4) while either FID or CPMG measurements were performed at 30, 40, 50, 55, 60, 65, 70, 75, 80, 85, 90 and 98 (both at the start and the end of the isothermal phase) °C during heating and at 85, 75, 65, 55, 45, 35 and 25 °C during cooling. Per fermented dough, two samples were taken to prepare one NMR tube for FID analysis and one for CPMG analysis. In total, six FID and six CPMG analyses during simulated baking and cooling were performed.

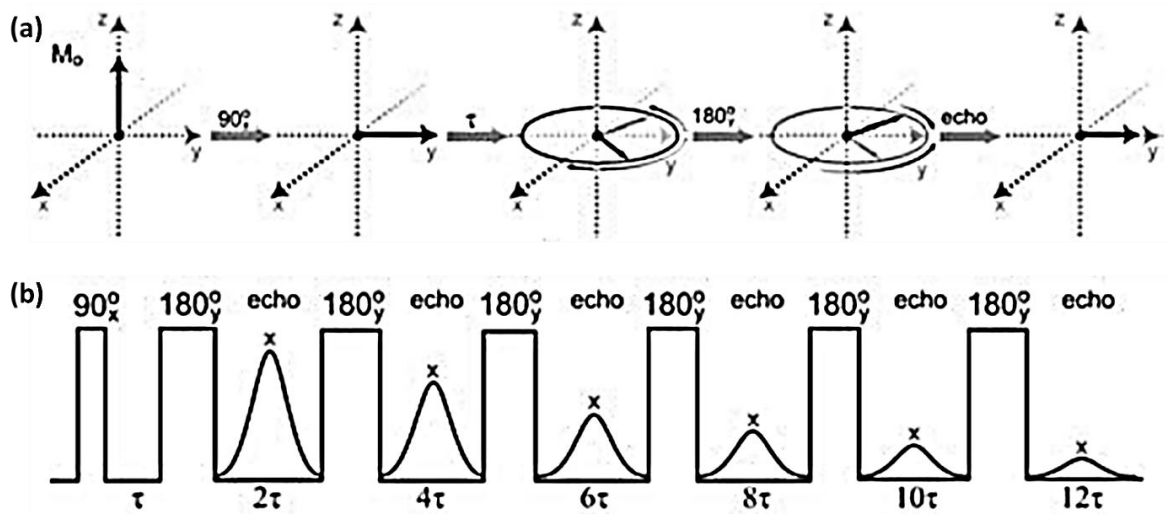

Figure 3.1 The Carr-Purcell-Meiboom-Gill (CPMG) spin-echo pulse sequence. (a) The vector model. In the presence of a static magnetic field (B_0), the net magnetization along the z-axis is maximal (M_0) while there is no net magnetization in the xy-plane because nuclei lack phase coherence. Application of the initial 90° pulse along the x-axis results in loss of net magnetization along the z-axis while nuclei now precess in phase such that magnetization in the xy-plane is maximal. Immediately after the 90° pulse, inhomogeneities of the static magnetic field result in dephasing of the spins. After time τ, the 180° pulse along the y-axis inverts the dephasing spins which refocus and form an echo at time 2τ. (b) Schematic representation of the CPMG spin-echo pulse sequence. The train of 180° pulses gives rise to a series of echoes at times 2τ, 4τ, 6τ, … of which the intensity dies away via natural transverse (T_2) relaxation (Schmidt, 2007).

T_2 relaxation curves, of which the initial intensity is a measure of the amount of detectable protons in the sample [Figure 3.2 (a) and (b)], were transformed to continuous distributions of T_2 relaxation times [Figure 3.2 (c) and (d)] using the CONTIN algorithm of Provencher (Provencher, 1982) (Bruker software). The CONTIN software solves equations like:

$$S(t) = S_0 \int_0^{\infty} P(T_2) \exp\left(-\frac{t}{T_2}\right) d(T_2)$$

With S(t) the nuclear magnetization as a function of time, S_0 the initial magnetization and $P(T_2)$ the fraction of protons with relaxation time T_2. A continuous distribution of T_2 relaxation times is then obtained with an inverse Laplace transformation of $S(t)/S_0$ (Bosmans, 2013; Forshult, 2004).

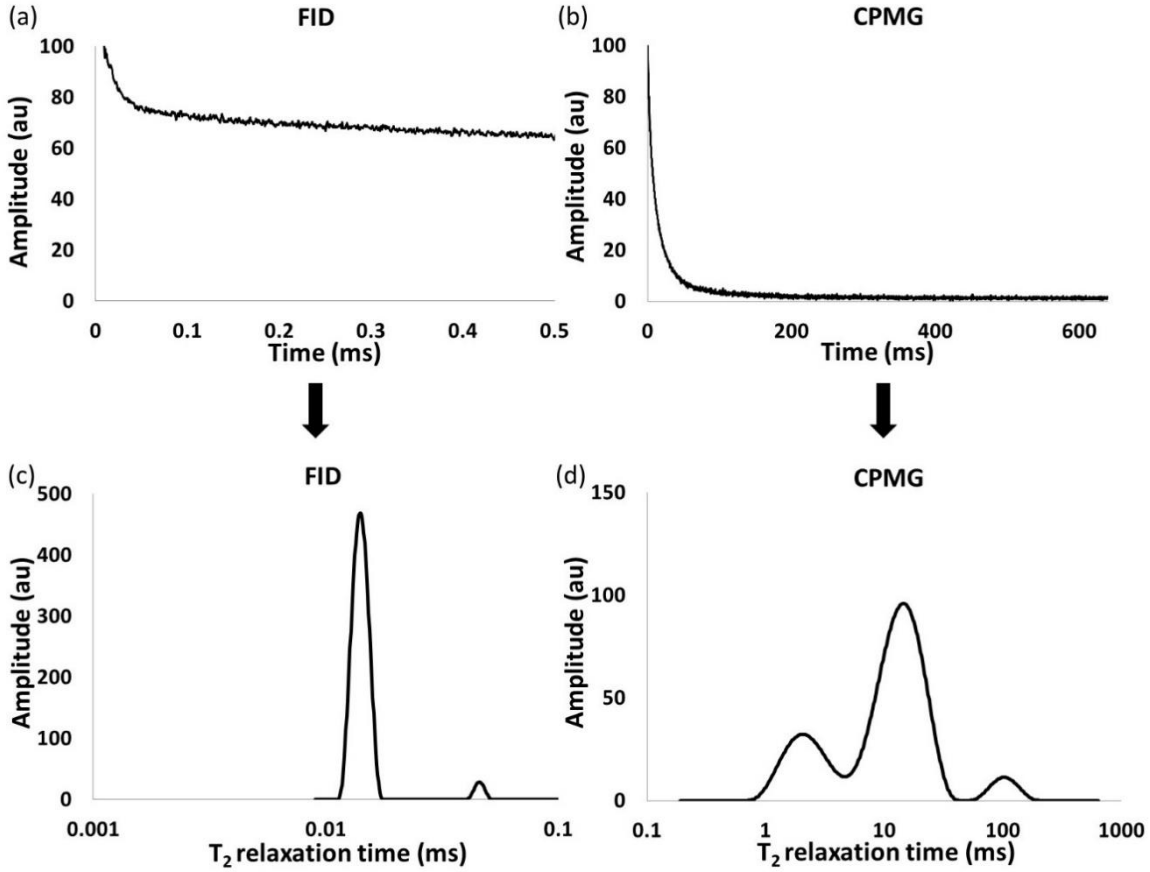

Figure 3.2 Transformation of relaxation curves obtained from free induction decay (FID) (a) and Carr-Purcell-Meiboom-Gill (CPMG) (b) measurements into a continuous distribution of T_2 relaxation times (c,d). Measurements were performed with fermented dough at 30 °C. Amplitudes are given in arbitrary units (au).

The calculations were performed on 500 data points, logarithmically spread between T_2 relaxation times of 0.009 and 0.5 ms and 0.2 and 640 ms for FID and CPMG measurements, respectively. Proton populations in these distributions have an area (which is proportional to the number of protons in a given population) and a mean T_2 relaxation time (which reflects the mobility of the environment the protons are in). Intensities of both FID and CPMG relaxation curves were corrected for temperature effects described by Curie's law using a correction factor based on the intensity of the FID signal of a sample of olive oil when exposed

to the same hydrothermal process. In olive oil, component transitions such as those during baking and cooling of dough/bread do not occur. Changes in its FID signal intensity with temperature therefore obey Curie's law. This approach to correct NMR data for temperature effects has also been adopted by Serial *et al.* (2016). Because the inhomogeneity of the static magnetic field affects the output of the most mobile FID population (around 0.5 ms), this population was not taken into account in the following analyses.

3.2.2.6 *Time-resolved wide angle X-ray diffraction*

Measurements were performed at the Dutch-Belgian beamline (DUBBLE, BM26B) of the European Synchrotron Radiation Facility (Grenoble, France). Fermented dough samples (20.0-30.0 mg) were accurately weighed in aluminum pans (TA Instruments, New Castle, DE, USA) and placed in front of the X-ray beam in a sample holder containing a Linkam Scientific Instruments (Surrey, UK) heating stage. Samples were irradiated at a λ of 1.033 Å (12 keV) while being subjected to a temperature profile simulating a conventional baking process (*cf*. §3.2.2.4). WAXD signals were captured on a two-dimensional Pilatus 300K-W (Dectris, Baden, Switzerland) detector close to the sample. The data were collected in successive time frames which resulted in at least one scattering pattern per °C during baking and subsequent cooling. WAXD scattering angles (2θ) were calibrated with high-density polyethylene of which the reflections are known. WAXD scattering angles were represented as if $Cu_{K\alpha}$ radiation, with a λ of 1.54 Å, was used.

The data were azimuthally averaged using ConeX2_beta software (Gommes & Goderis, 2010). Scattering intensities were normalized to the primary beam intensity measured by a photodiode downstream from the sample and corrected for scattering due to the dark current and empty set-up. For each frame, corrected WAXD scattering intensities were normalized to the corresponding total WAXD intensity. A- and V_H-type crystallinity indices were extracted from the areas of specific WAXD reflections that were separated from the background using straight sectors. V_H-type crystallinity indices of the sample at different time points during baking and cooling were calculated between 18.82-20.72 °2θ $Cu_{K\alpha}$. A-type crystallinity indices, at different time points during baking, and B- crystallinity indices at different time points during cooling were calculated in 16.19-18.82 and 16.26-17.61 °2θ $Cu_{K\alpha}$ ranges, respectively. A- and V_H-type indices were normalized to their maximum value at respectively the start of baking and the end of cooling. The B-type index was normalized to its value after storage of the baked crumb in an above mentioned aluminum pan for 3 days.

3.2.2.7 *Carbohydrate leaching and swelling power*

Dough samples (0.5 g) in Eppendorf tubes were heated in water baths held at 30, 40, 50, 55, 60, 65, 70, 75, 80, 85, 90 or 100 °C for 30 min. Immediately after heating, samples were frozen in liquid nitrogen. Next, heated dough samples were freeze-dried, gently ground and suspended in deionized water [1.11% (w/v)]. The suspensions were centrifuged (1,000 g, 30 min), the sediments weighed and the supernatants transferred to small test tubes to analyze the level of CHL with the phenol-sulfuric acid method of Dubois *et al.* (1956) using glucose as standard. The percentage of CHL on dm flour was expressed as starch (0.9 × glucose). The percentage of CHL included endogenous low MW saccharides as well as starch molecules and sugar which was added during dough preparation.

The SP was calculated as follows:

$$SP = \frac{sediment\ weight * 100}{dm\ sample\ weight * (100 - CHL)}$$

and is a measure of water uptake by starch corrected for CHL (Leach *et al.*, 1959).

3.2.2.8 *Differential scanning calorimetry*

The extent of starch gelatinization as a function of temperature was determined by heating dough samples in Eppendorf tubes in water baths at different temperatures (*cf.* §3.2.2.7). Heated dough samples were freeze-dried and gently ground to measure the portion of AP crystals still present. DSC was performed with a Q2000 DSC (TA Instruments, New Castle, DE, USA). The freeze-dried samples were each accurately weighed (2.5 – 4.0 mg) in at least three aluminum pans (Perkin-Elmer, Waltham, MA, USA) and deionized water was added [1:3 (w/w) sample dm:water]. Pans were hermetically sealed and equilibrated at 0 °C before being heated from 0 to 130 °C at 4 °C/min. The temperatures and enthalpies associated with AP crystal melting (ΔH_{AP}, J/g sample dm) were determined with TA Universal Analysis software.

3.2.2.9 *Statistical analysis*

Statistical analyses were performed with JMP Pro 14 (SAS Inst., Cary, NC, USA). One-way Analysis of Variance was combined with Tukey's honest significant difference test to identify significant differences ($\alpha < 0.05$) for several variables, based on at least three measurements. In case the homogeneity of variance assumption was not met, the Games-Howell test [posthocTGH function, userfriendlypackage (Peters, 2018)] was performed using R software (R Core Team, 2019).

3.3 RESULTS AND DISCUSSION

3.3.1 Assignment of proton populations

Using temperature-controlled TD ^{1}H NMR, five proton populations in fermented dough (Figure 3.3) were assigned based on Bosmans *et al.* (2012). The least mobile protons were present in FID populations A and B. They are respectively CH protons of crystalline starch and amorphous starch and gluten not in contact with water and CH protons of amorphous starch and gluten in little contact with water. Some CH protons of amorphous starch and gluten, protons of gluten in exchange with confined water and intragranular exchanging protons of starch and water are present in the least mobile CPMG population CD. Population E contains exchanging protons of bulk water, gluten and starch on the granule surface, *i.e.* extragranular starch. The most mobile CPMG population F consists of protons of native flour lipids and shortening (Bosmans *et al.*, 2012). Populations A and E dominated the NMR profiles (Figure 3.3). The molecular dynamics of starch and water during baking and subsequent cooling are therefore largely explained by changes in their area and mobility (T_2 relaxation time).

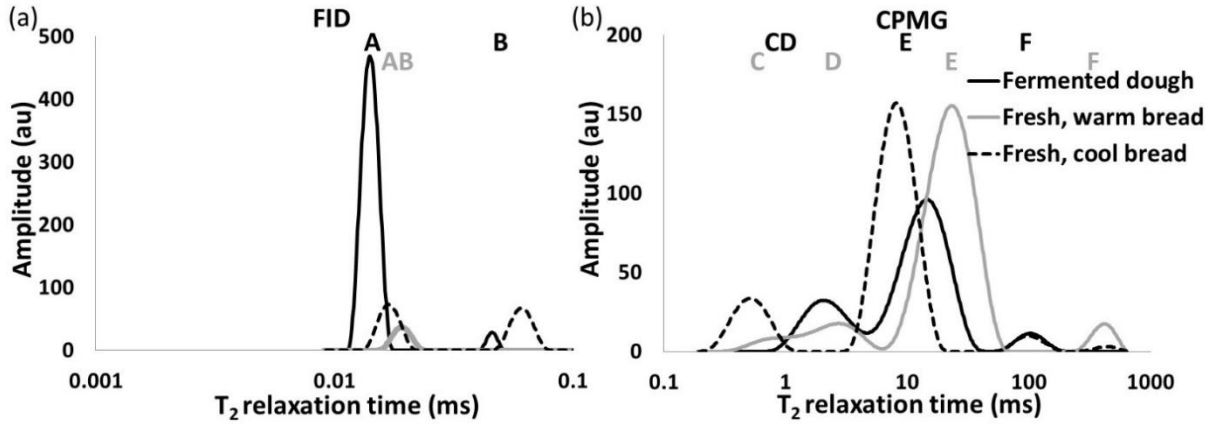

Figure 3.3 Free induction decay (FID) (a) and Carr-Purcell-Meiboom-Gill (CPMG) (b) proton distributions of fermented dough before baking and of fresh bread before and after cooling. Amplitudes are given in arbitrary units (au).

3.3.2 Baking

Fermented dough from 270 g of flour was conventionally baked for 24 min at 210 °C. After baking, the fresh, warm bread was allowed to cool at room temperature for 120 min, resulting in fresh, cooled bread. The temperature profile in its center was monitored and then applied during *in situ* analysis with temperature-controlled TD ^{1}H NMR and time-resolved WAXD. The temperature profile in the sample during NMR experiments was in turn monitored and further adjusted to imitate the baking and cooling process in the center of dough/bread crumb during conventional baking and cooling. Fermented dough samples were analyzed with NMR using

this temperature profile and an alternative profile of which the baking phase was identical but cooling occurred faster (Figure 3.4). The resulting proton distributions evolved similarly with temperature (results not shown). In the interest of time, the temperature profile with fast cooling was thus used for temperature-controlled TD ^{1}H NMR and time-resovled WAXD analyses. This temperature profile consisted of a heating phase from 30 °C to 98 °C at 3.0 °C/min, followed by a 90 s holding phase at 98 °C and a cooling phase from 98 °C to 25 °C at 2.0 °C/min (Figure 3.4).

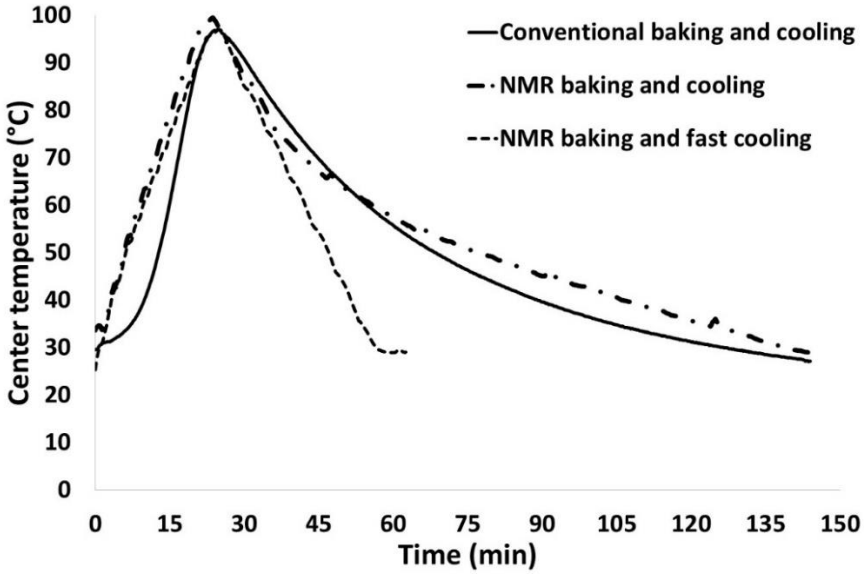

Figure 3.4 Temperature profile in the center of dough/bread crumb during either conventional baking and cooling or during simulated [in the nuclear magnetic resonance (NMR) device] baking and cooling (the latter at two different rates), monitored with Datapaq equipment.

The portion of starch protons in contact with water increased during initial baking (≤ 60 °C), since protons shifted from population A, containing *inter alia* rigid CH protons not in contact with water, to population B, containing amorphous CH protons in little contact with water [Table 3.1 (a), Figure 3.5]. When starch granules absorb water, they swell (Delcour & Hoseney, 2010; Yeh & Li, 1996). Changes in the area and mobility of different populations during the initial baking phase could thus be attributed to water uptake by the starch granules and the related starch granule swelling. In the present case, the SP of dough increased slightly during heating up to 60 °C (Table 3.2). The increase in area of population B because of water uptake by starch did not compensate for the decrease in area of population A [Table 3.1 (a), Figure 3.5]. Furthermore, the area of population E, containing *inter alia* exchanging protons of extragranular starch, increased [Table 3.1 (a), Figure 3.6]. A similar shift of protons from population A to populations B and E during heating of dough to 50 °C has been observed by

Rondeau-Mouro *et al.* (2015) and Pojić *et al.* (2016) and was attributed to water absorption and, thus, swelling of granules and AM leaching. When confronting the above mentioned literature findings with the present results, it seems plausible that AM protons in little contact with water of population B were transferred to the extragranular space and, thus, to population E because of AM leaching. As a result, the increase in area of population B at the expense of that of population A, resulting from water absorption by starch, was partially counteracted.

To confirm this, CHL was determined following heating to different temperatures. It was indeed found that it increased with temperature up to 60 °C (Table 3.2). However, care is to be taken when interpreting these results as the analytical method also analyzed the sugar in the recipe which had not been fermented at the point of sampling. Whatever be the case, that CHL numbers increased compared to the unheated dough sample can be attributed to AM leaching. The mobility of population E decreased during initial baking [Table 3.1 (a), Figure 3.6]. Assifaoui *et al.* (2006) showed that the reduced mobility of extragranular protons during biscuit dough heating coincides with a viscosity increase. Furthermore, Bosmans *et al.* (2012) reported for a flour-water model system that heating and subsequent cooling decreases the mobility of *inter alia* exchanging protons of water and extragranular starch. They attributed this to the increased viscosity as a result of gelatinization and gelation during heating and cooling, respectively. It is therefore postulated that the decreased mobility of population E during the initial bread baking phase results from the increased viscosity because intact granules swell and AM leaches to the extragranular space.

Table 3.1 Transverse (T_2) relaxaxtion times and areas of free induction decay (FID) and Carr-Purcell-Meiboom-Gill (CPMG) proton populations A (rigid CH protons of starch and gluten not in contact with water), AB and B (amorphous CH protons of starch and gluten in little contact with water), C, CD and D [amorphous CH protons of starch and gluten and exchanging protons of (intragranular) starch, gluten and water], E [exchanging protons of (extragranular) starch, gluten and water (in the gel network)] and F (lipid protons) during simulated (a) baking and (b) cooling of fermented dough/bread in the NMR device.

(a)

T (°C)	T_2 A (ms)	Area A (au)	T_2 AB (ms)	Area AB (au)	T_2 B (ms)	Area B (au)	T_2 C (ms)	Area C (au)	T_2 CD (ms)	Area CD (au)	T_2 D (ms)	Area D (au)	T_2 E (ms)	Area E (au)	T_2 F (ms)	Area F (au)
30	0.0119	13838			0.056	1031			1.9	1947			12.5	6821	100 (7)	376
	(0.0005)	(411)			(0.009)	(283)			(0.2)	(250)			(1.0)	(310)		(81)
40	0.0129	10972			0.047	1677			1.6	1780			11.0	7208	117 (8)	426
	(0.0005)	(590)			(0.015)	(413)			(0.2)	(95)			(0.5)	(179)		(48)
50	0.0137	9150			0.045	1701			1.3	1748			10.2	7531	130 (7)	485
	(0.0018)	(310)			(0.006)	(790)			(0.2)	(134)			(0.4)	(268)		(69)
55	0.0125	8568			0.050	2097			0.8	1374			8.6	8190	159 (7)	509
	(0.0010)	(694)			(0.006)	(436)			(0.1)	(90)			(0.3)	(154)		(26)
60	0.0117	7004			0.045	2116			0.9	1115			8.0	8705	148	536
	(0.0014)	(503)			(0.009)	(527)			(0.2)	(125)			(0.5)	(222)	(15)	(52)
65	0.0128	5697			0.050	1384			0.7	859			7.8	9215	106	683
	(0.0005)	(679)			(0.000)	(239)			(0.3)	(300)			(0.4)	(366)	(40)	(141)
70	0.0124	4020			0.040	1327			0.7	898			7.9	9950	146	628
	(0.0017)	(587)			(0.000)	(336)			(0.2)	(94)			(0.4)	(200)	(22)	(46)
75	0.0137	3238			0.027	692			0.7	921			8.8	10253	145	735
	(0.0006)	(976)			(0.023)	(537)			(0.1)	(51)			(0.5)	(245)	(42)	(194)
80	0.0135	1376			0.035	1086			0.9	936			10.4	10592	172	631
	(0.0047)	(808)			(0.010)	(644)			(0.3)	(143)			(0.5)	(284)	(70)	(121)
85			0.021	1713					1.0	1023			12.5	10798	253	567
			(0.003)	(291)					(0.1)	(236)			(1.4)	(202)	(22)	(47)
90			0.025	1273			0.5	500			2.8	1112	16.4	10568	305	536
			(0.004)	(208)			(0.1)	(279)			(0.9)	(182)	(1.4)	(192)	(37)	(47)
98			0.025	786			0.4	422			3.2	1278	19.6	10612	356	530
			(0.010)	(133)			(0.3)	(303)			(0.8)	(128)	(1.1)	(287)	(34)	(38)
98			0.026	854			0.6	511			3.8	1356	22.0	10482	378	510
			(0.004)	(109)			(0.1)	(63)			(0.8)	(187)	(1.4)	(218)	(22)	(52)

(b)

T (°C)	T_2 A (ms)	Area A (au)	T_2 AB (ms)	Area AB (au)	T_2 B (ms)	Area B (au)	T_2 C (ms)	Area C (au)	T_2 CD (ms)	Area CD (au)	T_2 D (ms)	Area D (au)	T_2 E (ms)	Area E (au)	T_2 F (ms)	Area F (au)
85			0.027	1219			0.6	531			2.5	1164	16.3	10173	276	550
			(0.004)	(76)			(0.2)	(228)			(0.3)	(135)	(0.8)	(159)	(17)	(27)
75			0.021	1561			0.6	820			2.7	1044	13.7	9944	213	535
			(0.005)	(154)			(0.1)	(161)			(0.6)	(331)	(0.8)	(534)	(45)	(56)
65	0.0117	1867			0.040	844			1.2	1686			11.9	9681	180	515
	(0.0006)	(47)			(0.010)	(116)			(0.1)	(57)			(0.5)	(330)	(15)	(68)
55	0.0100	1491			0.037	1206			1.0	1798			10.8	9351	153	516
	(0.0000)	(746)			(0.006)	(360)			(0.1)	(109)			(0.6)	(72)	(23)	(59)
45	0.0158	1960			0.043	907			0.8	1957			9.3	8871	117	519
	(0.0025)	(421)			(0.012)	(286)			(0.1)	(121)			(0.4)	(54)	(10)	(94)
35	0.0113	2055			0.049	2006			0.6	1927			8.5	8705	102	470
	(0.0010)	(689)			(0.006)	(424)			(0.0)	(78)			(0.4)	(219)	(8)	(61)
25	0.0127	2399			0.058	2456			0.6	1817			8.2	8629	95	402
	(0.0024)	(209)			(0.005)	(165)			(0.1)	(108)			(0.6)	(134)	(10)	(64)

Areas are given in arbitrary units (au).

Standard deviations are indicated between brackets.

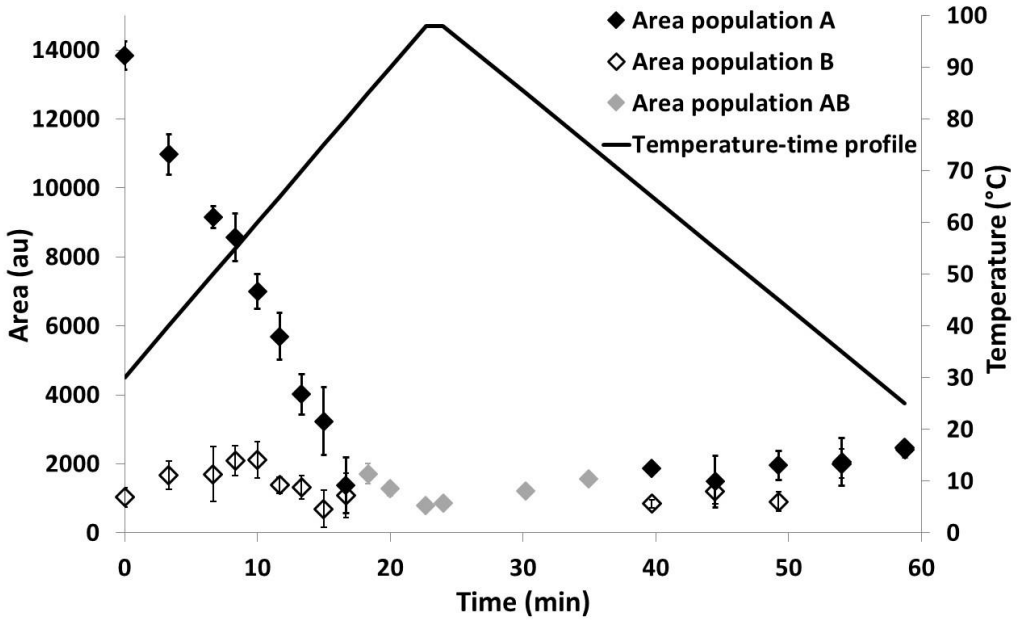

Figure 3.5 Areas of free induction decay (FID) populations A (containing rigid CH protons of starch and gluten not in contact with water), B and AB (containing amorphous CH protons of starch and gluten in little contact with water) as a function of time and temperature during simulated bread baking and cooling. Areas are given in arbitrary units (au).

At temperatures exceeding 60 °C, the area of respectively population A or B continued to decrease or started to do so [Table 3.1 (a), Figure 3.5]. Simultaneously, the amount of crystalline material in dough, analyzed with DSC, began to decrease (Table 3.2) and, thus, the loss of starch molecular order had started (Biliaderis *et al.*, 1980). The further decrease in area of population A, containing *inter alia* protons of AP crystals, was attributed to melting of AP crystals during gelatinization. Together with the onset of gelatinization in a 60 to 65 °C temperature range, the SP started to increase significantly (Table 3.2). This was because of irreversible and substantial swelling of starch granules and is in line with literature data (Tester & Morrison, 1990; Yeh & Li, 1996). The concomitant decrease and increase in respectively the areas of populations B and E at temperatures exceeding 60 °C [Table 3.1 (a), Figures. 3.5 and 3.6] were explained by AM leaching [and some AP leaching at higher temperatures (Doublier, 1981)] as described above. However, the extent of CHL was lower when heating to temperatures exceeding 60 °C (Table 3.2). At 100 °C, the extent of CHL increased again and was comparable to that at 60 °C. It is suggested that this apparent lower extent of CHL in dough heated to temperatures between 60 and 100 °C (Table 3.2) resulted from interference of AM-L complexation with the determination of CHL. In addition to those present in native starch, AM-L complexes typically form after the onset of gelatinization (Delcour & Hoseney, 2010; Kugimiya *et al.*, 1980) since AM needs to be sufficiently solubilized to acquire enough mobility to interact with lipids (Evans, 1986). The melting temperature of Type I complexes is *ca.* 95 °C (Goderis *et al.*, 2014; Karkalas *et al.*, 1995). Complexes formed during heating may

precipitate during cooling provided sufficient lipid is included in the AM helix (Putseys *et al.*, 2009). AM associated with such complexes is therefore not present in the supernatant such that the extent of AM leaching is underestimated. Furthermore, the AM-L complexes formed may sterically prevent the non-complexed AM from moving to the aqueous phase and thereby contribute to underestimation of the extent of AM leached.

Table 3.2 Swelling power (SP) of starch, the portion of carbohydrates leached (CHL) and the (residual) melting enthalpy of amylopectin crystals (ΔH_{AP}) in fermented wheat flour dough heated to different temperatures.

Temperature (°C)	SP (g/g)	CHL (% of dm flour)	ΔH_{AP} [J/g (dm)]
30	3.3 (0.2)^{f}	3.3 (0.1)^{e}	7.1 (0.6)^{a}
40	3.2 (0.2)^{f}	3.0 (0.0)^{f}	7.2 (0.2)^{a}
50	3.7 (0.6)^{def}	3.6 (0.1)^{cde}	7.1 (0.7)^{a}
55	3.7 (0.2)^{ef}	4.2 (0.1)^{b}	7.5 (0.8)^{a}
60	3.9 (0.3)^{def}	4.6 (0.0)^{a}	7.7 (0.2)^{a}
65	4.5 (0.2)^{cde}	3.7 (0.0)^{cd}	5.2 (0.3)^{b}
70	4.6 (0.3)^{cd}	3.8 (0.2)^{c}	3.2 (0.2)^{c}
75	5.2 (0.2)^{c}	3.4 (0.0)^{de}	1.6 (0.1)^{d}
80	n.d.	n.d.	0.8 (0.2)^{de}
85	6.8 (0.4)^{b}	2.7 (0.0)^{g}	0.2 (0.0)^{e}
90	7.4 (0.1)^{b}	3.5 (0.2)^{cde}	/
100	9.6 (0.2)^{a}	4.7 (0.2)^{a}	/

dm: dry matter.
Standard deviations are indicated between brackets.
n.d.: not determined.
Within one column, values with a different letter at various temperatures are significantly different from each other ($P<0.05$).

Goderis *et al*. (2014) showed that Type I AM-L complexes are not amorphous and give rise to a V_H-type WAXD pattern. In this work, AM-L complex formation after the onset of gelatinization was confirmed with time-resolved WAXD measurements during simulated bread baking and cooling (Figure 3.7). To study the evolution of starch polymers' crystallinity in more detail, crystallinity indices for the different crystal types were calculated from the areas of specific WAXD reflections [Figure 3.8 (a)]. During initial baking, the amount of A- and V_H-type crystals remained quite constant [Figure 3.8 (b)]. During later baking, AP crystals started to melt such that A-type crystallinity decreased [Figures 3.7 and 3.8 (b)]. AM polymer leaching during gelatinization made them available for AM-L complex formation. Indeed, additional AM-L complexes were formed after the onset of gelatinization as evidenced by the increasing V_H-type crystallinity index [Figure 3.8 (b)]. The amount of AM-L complexes had almost doubled when a crumb temperature of 90 °C was reached during baking. As expected for Type I complexes (Karkalas *et al.*, 1995), they melted at temperatures exceeding 90 °C

during further baking. At the end of baking, however, more Type I AM-L complexes were present in fresh, warm crumb than in fermented dough before baking [Figure 3.8 (b)].

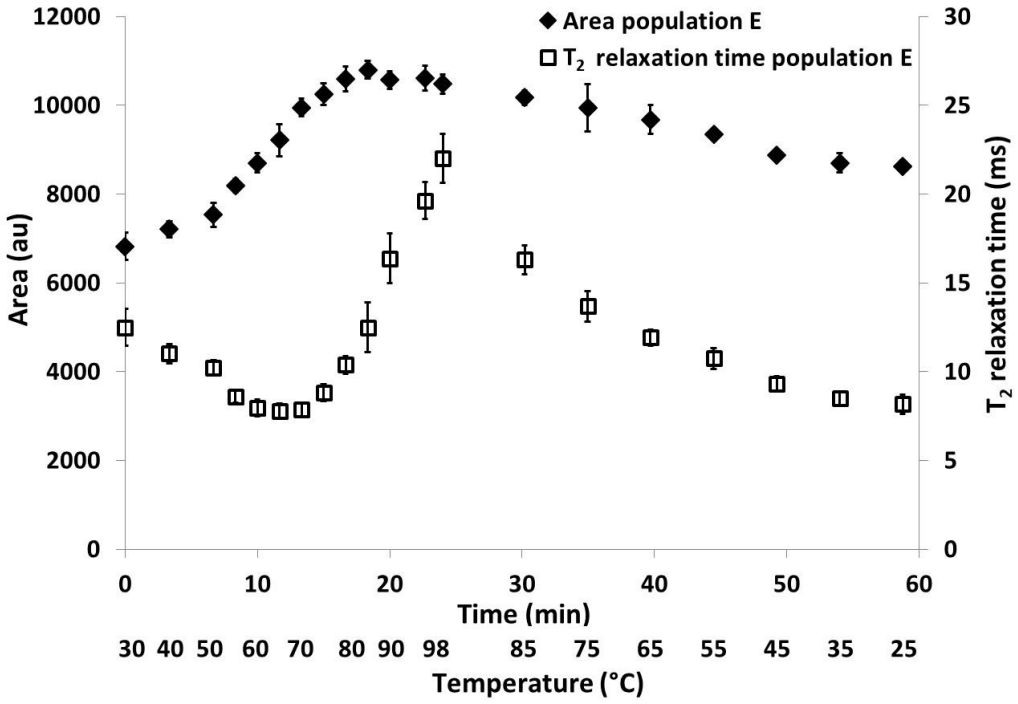

Figure 3.6 Areas and transverse (T_2) relaxation times of Carr-Purcell-Meiboom-Gill (CPMG) population E [containing exchanging protons of (exgtragranular) starch, gluten and water (in the formed gel network)] as a function of time and temperature during stimulated bread baking and cooling. Areas are given in arbitrary units (au).

During gelatinization, the mobility of population E no longer decreased but started to increase when the dough temperature reached 70 °C [Table 3.1 (a), Figure 3.6]. Similar results have already been reported (Kim & Cornillon, 2001; Pojić *et al.*, 2016; Rondeau-Mouro *et al.*, 2015). The increase in molecular mobility with temperature has been attributed to a thermal activation mechanism obeying Arrhenius' law (Lucas *et al.*, 2008; Rondeau-Mouro *et al.*, 2015). When heating olive oil with the temperature profile used for bread dough, evidence for this thermal activation mechanism was provided by the continuous increase in proton mobility with temperature (results not shown). Evidently, component transitions such as those during baking and cooling of dough/bread do not occur in olive oil. In contrast to what was observed for mobile dough protons, the mobility of mobile oil protons thus increased immediately with temperature. Therefore, it is hypothesized that the Arrhenius effect during baking of dough up to 65 °C is overruled by a viscosity increase because of starch swelling and AM leaching. This then resulted in a net decrease in the mobility of the protons in population E. At higher dough temperatures, gelatinization [Table 3.2, Figures 3.7 and 3.8 (b)] and protein cross-linking (Lagrain *et al.*, 2005) caused stiffening of the gluten-starch matrix and the

transition of dough to crumb (Babin *et al.*, 2006; Bloksma, 1972). It seems reasonable that once crumb setting had occurred the dough viscosity no longer increased and, thus, no longer overruled the Arrhenius effect. As a result, the mobility of population E now increased with temperature during further baking [Table 3.1 (a), Figure 3.6].

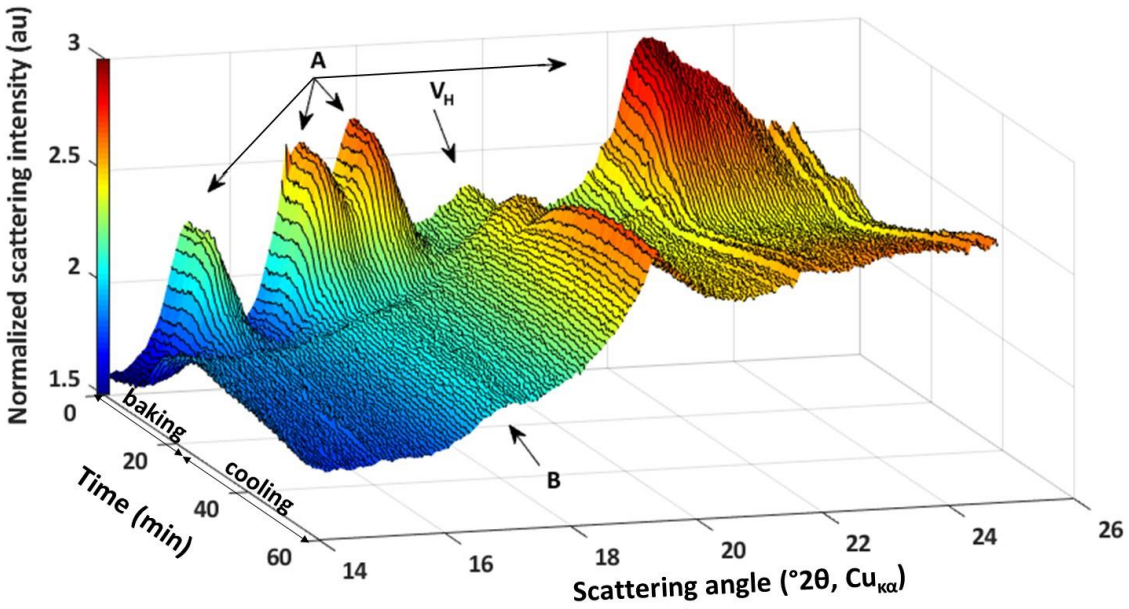

Figure 3.7 3D plot of WAXD patterns during simulated bread baking (from 0 to 22 min) and cooling (from 22 to 56 min). Specific A-, V_H- and B-type reflections are indicated. Normalized scattering intensities are given in arbitrary units (au).

At about 85 °C, only one FID population, population AB, was detected [Figures. 3.3 and 3.5, Table 3.1 (a)] and gelatinization associated changes in the area of population E levelled off (Figure 3.6). Since no melting enthalpy was measured with DSC in dough heated to temperatures exceeding 85 °C (Table 3.2) and A-type crystallinity disappeared at the end of baking [Figures 3.7, 3.8 (a) and (b)], all AP crystals had melted and protons in population AB were assigned to amorphous CH protons of starch and gluten. The areas of populations AB and E remained constant during further heating to the maximum temperature [Table 3.1 (a), Figures 3.5 and 3.6]. It therefore seems plausible that AM leaching under conditions of bread making was complete at a temperature of 85 to 90 °C. The continued increase in mobility of population E at temperatures exceeding 90 °C where starch transitions were complete can again be explained by the temperature effect described by Arrhenius' law [Table 3.1 (a), Figure 3.6] (Lucas *et al.*, 2006; Rondeau-Mouro *et al.*, 2015). At the end of gelatinization, this temperature effect was also reflected in an increased mobility of the more mobile protons in population CD, causing this population to split in populations C and D [Figure 3.3, Table 3.1 (a)]. The latter populations contained respectively less mobile CH protons of amorphous

starch and gluten and more mobile, exchanging protons of starch in granule remnants, gluten and water.

It is of note that water evaporated from the dough/bread sample during baking. As a result, the total amount of protons in the sample decreased. While the area of population E has been related to the sample's MC (Bosmans *et al.*, 2013c), in the present case, its area increased as a result of baking [Table 3.1 (a) and Figure 3.6]. Furthermore, it was expected that the amount of population A protons would have increased as a result of baking induced water loss. Population A contained rigid protons not in contact with water. A decreased amount of water in the system would therefore result in a larger portion protons not in contact with water. Nevertheless, the opposite was observed and the area of population A decreased during baking (Figure 3.5). The net change of the areas of populations A and E during baking was therefore attributed to starch transitions. The area of population A decreased because of AP crystal melting while the area of population E increased because of AM leaching to the extragranular space.

3.3.3 Cooling

Upon cooling, leached AM organizes in double helices which aggregate in polymer rich regions (Putseys *et al.*, 2011), resulting in a continuous semicrystalline AM gel network (Goesaert *et al.*, 2009b). AM crystallization caused a portion of amorphous protons in population AB to become more rigid and, thus, to shift to lower T_2 relaxation times, thereby splitting population AB in populations A and B [Figures 3.3 and 3.5, Table 3.1(b)]. As a result, population A *inter alia* contained protons of AM crystals and amorphous starch not in contact with water and population B *inter alia* contained protons of amorphous starch in little contact with water. Subsequently, the areas of populations A and B increased during further cooling which was attributed to respectively (i) ongoing AM crystallization and (ii) an increased portion of AM polymers only in little contact with water as AM rich regions were formed [Table 3.1 (b), Figure 3.5].

According to literature, crystalline AM is characterized by a B-type X-ray diffraction pattern (Miles *et al.*, 1985a; Rundle *et al.*, 1944). Nevertheless, fresh bread crumb has been shown to be characterized by a V-type diffraction pattern (Aguirre *et al.*, 2011; Hug-Iten *et al.*, 2001; Zobel & Kulp, 1996). In this work, WAXD patterns measured during cooling were indeed dominated by a V_H-type pattern [Figures 3.7 and 3.8 (a)]. However, weak B-type reflections were observed as well. The B-type index extracted from these reflections of a sample analyzed at different time points during cooling increased as time progressed [Figure 3.8 (b)] because of AM crystallization as AP only retrogrades over longer term during storage (Miles *et al.*,

1985a). In addition, the V_H-type index of a sample analyzed at different time points during cooling also increased as time progressed until a plateau was reached [Figures 3.7 and 3.8 (b)]. At the same time, the associated V_H-type reflection sharpened [Figure 3.8 (a)]. Based on Goderis *et al*. (2014), it is hypothesized that more ordered and stable Type II AM-L complexes were formed during cooling. AM crystals (Eerlingen *et al.*, 1993) and AM-L complexes (Conde-Petit & Escher, 1995) act as junction zones in the fringed micelle AM network formed during cooling (Bosmans *et al.*, 2013c; Goesaert *et al.*, 2009b).

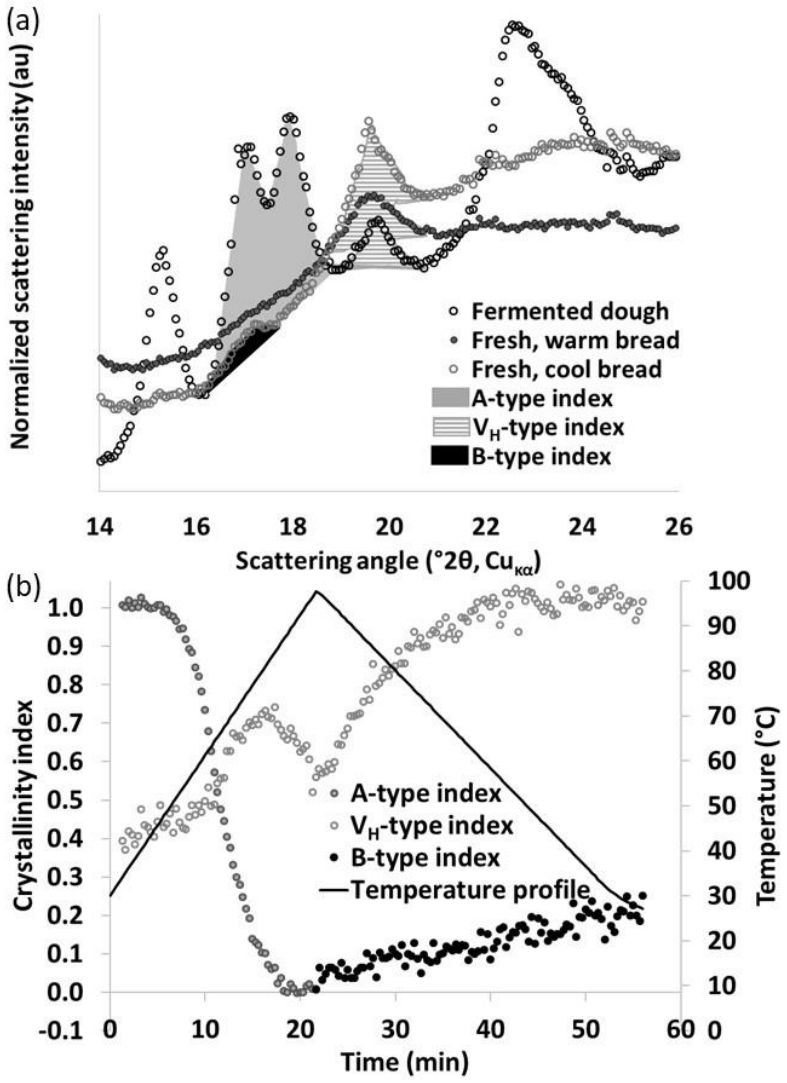

Figure 3.8 (a) Wide angle X-ray diffraction patterns of fermented dough before baking and of fresh bread before and after cooling. Specific A-, V_H- and B-type reflections were separated from the background using straight sectors and integrated into crystallinity indices. Scattering intensities are given in arbitrary units (au). (b) Normalized A-, V_H- and B-type crystallinity indices during simulated bread baking and cooling.

The mobility of population E decreased during cooling (Figure 3.6) and population D merged again with population C [Figure 3.3 and Table 3.1(b)]. As described above, a temperature effect described by Arrhenius' law could explain the decrease in proton mobility when temperature decreased. Moreover, the continuous semicrystalline AM network formed during cooling contributes to the desired initial crumb firmness of fresh, cool bread (Goesaert *et al.*, 2009b). It is postulated that the formation of such network additionally contributed to the reduced mobility of population E which contains exchanging protons of water, starch and gluten in the formed gel network. This is in line with results obtained by Bosmans *et al.* (2012; 2013c). They found a negative relation between crumb firmness and the mobility of exchanging protons of water, starch and gluten in the formed gel network (Bosmans *et al.*, 2013c).

3.4 CONCLUSIONS

Proton distributions in bread dough/crumb were monitored during a simulated bread baking and subsequent cooling process. As dough was heated to 60 °C, the absorption of water by starch granules was visible as an increase in CH protons in little contact with water at the expense of CH protons not in contact with water. At the same time, part of the former protons were transferred to the extragranular space because of initial AM leaching. Up to this point, starch granules swelled only slightly. Both granule swelling and AM leaching were responsible for the increased viscosity of the extragranular space and, thus, the decreased mobility of protons therein. At a temperature of 60 to 65 °C, the onset of gelatinization was detected as a sudden decrease of the level of amorphous CH protons in little contact with water. This coincided with the onset of AP crystal melting, substantial granule swelling and further AM leaching. After the onset of gelatinization, leached AM formed additional Type I complexes with lipids. The system's viscosity increase because of granule swelling and AM leaching remained visible as a decreased mobility of exchanging protons in the extragranular space up to 65 °C when the crumb structure was set. During further heating, the viscosity effect no longer greatly impacted the mobility of these exchanging protons, which now increased with temperature according to Arrhenius' law. Between 85 and 90 °C, gelatinization associated changes in NMR proton distributions levelled off and rigid CH protons were no longer detected because all AP crystals had melted, as confirmed by DSC and time-resolved WAXD data. Type I AM-L complexes melted during further heating. As a result of cooling, rigid CH protons could again be detected since B-type AM crystals were formed during gelation. Also, Type II AM-L complexes were formed. The formation of a continuous, semicrystalline AM gel network together with the Arrhenius temperature effect were responsible for a decreased mobility of exchanging protons.

In conclusion, temperature-controlled ^{1}H NMR in combination with other techniques that measure at different length scales proved powerful for studying the timing and extent of changes in the starch fraction and water (re)distribution *in situ* during simulated bread baking and cooling. The here optimized temperature-controlled NMR toolbox is used to unravel AM and AP functionality and their interaction with water *in situ* during bread baking and cooling. In Chapter 4, bread dough was therefore prepared from a unique set of wheat flours with atypical starch properties. Furthermore, the exact mechanism of a successful bread making amylase was investigated.

Chapter 4

Amylose and amylopectin functionality during baking and cooling of bread prepared from flour of wheat containing unusual starches[3]

4.1 INTRODUCTION

The optimized temperature-controlled ^{1}H NMR toolbox (Chapter 3) proved to be a powerful method to study starch transitions and water dynamics during baking and cooling prepared from regular wheat flour. Regular wheat starches contain two biopolymers, *i.e.* essentially linear AM and highly branched AP. In this chapter, unique wheat flours with atypical AM and AP characteristics or BStA were included in the bread recipe as a tool to specifically study the functionality of AM and AP during bread making with the optimized NMR toolbox. BStA is used since it is a most effective antifirming amylase which is frequently used in bread making.

As outlined in Chapters 1 and 2, several researchers investigated the impact of atypical starch properties on starch transitions in model systems (Fujita *et al.*, 1998; Noda *et al.*, 2001; Singh *et al.*, 2010; Tester & Morrison, 1990) or on fresh and stored bread (Hayakawa *et al.*, 2004; Inokuma *et al.*, 2016; Lee *et al.*, 2001). Also, the action pattern of BStA in starch-containing systems (Bijttebier *et al.*, 2007; Bijttebier *et al.*, 2010; Christophersen *et al.*, 1998; Derde *et al.*, 2012a, 2012b) and its impact on fresh and stored bread (Bosmans *et al.*, 2013a; Goesaert *et al.*, 2009a; Hug-Iten *et al.*, 2001) is well studied. Literature, however, is scarce about the *in situ* timing and extent of changes in the starch fraction and water distribution during baking and cooling of bread containing unusual starches. Moreover, the exact mechanism of BStA *in situ* during bread making is, to the best of our knowledge, not known.

[3] This Chapter is based on the following reference: Nivelle, M.A., Remmerie, E., Bosmans, G.M., Vrinten, P., Nakamura T., and Delcour, J.A. (2019) Amylose and amylopectin functionality during baking and cooling of bread prepared from flour of wheat containing unusual starches: A temperature-controlled time domain ^{1}H NMR study. Food Chemistry, 295, 110-119.

Temperature-controlled NMR measurements allowed for *in situ* monitoring of proton redistributions which related to changes in the starch fraction and its interaction with water on molecular and mesoscale. To focus on the effect of AM and AP properties on proton redistributions, wheat flours used for dough preparation were *inter alia* from unique near-isogenic lines (NILs; NIL 1-1 and NIL 5-5 wheat) with different AM contents and AP chain length distributions but with otherwise uniform genetic backgrounds.

4.2 MATERIALS AND METHODS

4.2.1 Materials

NIL 1-1 and NIL 5-5 wheat seeds generated by crossing lines with null and wild-type Waxy protein and SSIIa genes (*cf.* §1.4) were milled to obtain flour as described in Inokuma *et al.* (2016). Wheat with a very low AM and, therefore a very high AP content (H-AP wheat) was also used. H-AP wheat, developed from matings between different lines containing the Waxy protein null genes (Graybosch *et al.*, 2004), was obtained from Robert Graybosch (University of Nebraska, Lincoln, USA). H-AP kernels were conditioned to 16.0% moisture over a 24 h period and milled to flour with a Bühler MLU-202 laboratory scale mill (Uzwil, Switzerland) using a milling scheme as in Delcour *et al.* (1989). Compressed yeast, sugar, salt and extra virgin olive oil were as in Chapter 3 (*cf.* §3.2.1). Reagents for determining starch and AM contents were from VWR International and Sigma Aldrich. Solvents for this analysis were from Acros Organics. Soluble starch was from Merck (Overijse, Belgium). Other reagents and solvents for determining amylase activity were from VWR International and Sigma Aldrich. Reagents for AP chain length distribution analysis were from VWR International and Thermo Fisher Scientific (Waltham, MA, USA). Isoamylase from *Pseudomonas* sp., the internal (rhamnose) and malto-oligosaccharide (glucose to maltoheptaose) standards used for AP chain length distribution determination, BStA preparation and all other chemicals were from Sigma-Aldrich, unless indicated otherwise.

4.2.2 Methods

4.2.2.1 *Composition of wheat flour*

Starch and protein content and MC of wheat flour were determined as in §3.2.2.2. The AM content of wheat flour was determined using an AM/AP content assay kit (Megazyme, Wicklow, Ireland), which itself is based on Gibson *et al*.(1997). Triplicate flour samples for either total starch or AM determination were completely dispersed in 90% (v/v) dimethyl sulfoxide (DMSO). To avoid underestimation of starch and AM contents due to the presence

of AM-L inclusion complexes, lipid was removed by precipitating the starch by addition of ethanol. After centrifugation (2,000 g, 5 min) the precipitated starch was again dispersed in 90% (v/v) DMSO. AP was removed by precipitation with concanavalin A and centrifugation (14,000 g, 10 min). AM in the supernatant was subsequently hydrolyzed (α-amylase/amyloglucosidase) to glucose. After incubation with glucose oxidase/peroxidase the glucose level was determined colorimetrically (absorbance at 510 nm). In a separate aliquot, the total starch content was determined similarly, but the AP precipitation step was omitted. AM and AP (100% - AM) contents were expressed as a percentage of total starch. The damaged starch content of wheat flour was determined according to AACC method 76-31.01 (AACC, 1999b) using a starch damage assay kit (Megazyme).

4.2.2.2 *Water retention capacity*

The water retention capacity (WRC) was measured as the ability of flour to retain water after application of an external force using an adaptation of AACC International Method 56-11-02 (AACCI, 2009). Flour samples (1.0 g, in triplicate) were suspended in 30.0 ml deionized water and the suspensions were shaken (150 rpm) during 30 min at room temperature. They were then rested during 30 min and centrifuged (4,000 g, 10 min). Supernatants were discarded and the tubes were drained at an angle of 90° (10 min). The WRC was calculated by subtracting the initial sample mass from the weight of the hydrated sample and expressed as a percentage of flour weight on a 14.0% moisture basis.

4.2.2.3 *Amylopectin chain length distribution*

The DPs of AP branch chains were analyzed after enzymatic debranching by HPAEC-PAD on a Dionex ICS 5000 chromatography system (Thermo Fisher Scientific). Flour samples (5.0 mg, in triplicate) were suspended in a test tube in 0.25 mL 90% (v/v) DMSO. The tubes were kept in a bath with boiling water for 30 min before being placed in a water bath at 40 °C. Next, 0.75 mL 40mM sodium acetate buffer (pH 4.0) was added. Starches were then debranched with isoamylase from *Pseudomonas* sp. at 40 °C for 16-24 h (Dries *et al.*, 2016). After enzyme inactivation by boiling (10 min), this incubation step with the same isoamylase was repeated to ensure complete debranching. After enzyme inactivation by boiling (10 min), rhamnose was added as internal standard (such that 10 µg rhamnose/ml solution was present) and samples were filtered (Millex-HP, 0.22 µm, polyethersulfone; Millipore, Carrigtwohill, Ireland) and injected (12.5 µL) on Carbopac PA-100 guard and PA-100 anion exchange (250 × 4 mm) columns (Thermo Fisher Scientific). Elution was with a linear gradient of 0-250 mM sodium acetate in 100 mM sodium hydroxide during 90 min (1.0 mL/min). Malto-oligosaccharide standards (glucose to maltoheptaose, in a concentration of 10 µg standard/ml solution) were used to analyze the debranched AP chains.

4.2.2.4 *Amylase activity assay based on soluble starch*

Amylase activity was determined at 40 °C by quantifying the reducing sugars released from 1.0% soluble starch in 100.0 mM sodium maleate buffer (pH 6.0) containing 5.0 mM calcium chloride. In addition, amylase activity was determined in 23.0 mM calcium propionate solution. The calcium propionate solution is based on the amount of calcium propionate and water added in the bread recipe (*cf.* §3.2.2.3). The amylase activity readings determined in calcium propionate solution were used to determine an appropriate BStA dosage for bread making (*cf. infra* §4.2.2.5).

BStA preparation (5.0 mg) was suspended in 1.0 mL sodium maleate buffer or calcium propionate solution. The suspension was shaken (15 min, 4 °C) and after centrifugation (9,280 g, 10 min, 4 °C) the amylase solution in the supernatant was separated from the carrier. The BStA preparation was appropriately diluted in the sodium maleate buffer or calcium propionate solution and preincubated (5 min, 40 °C). Subsequently, 500 µL of 1.0% soluble starch was added to 200 µL of the diluted enzyme solutions. After different times (0-15 min), the reaction was stopped with 500 µL of an alkaline cupric sulfate solution (Nelson, 1944). The liberated reducing end groups were quantified colorimetrically at 520 nm by making use of a standard curve of maltose (0-1.0 mM). Measurements were performed in duplicate.

4.2.2.5 *Dough making*

Dough was prepared from 10.0 g wheat flour as in §3.2.2.3 (Table 4.1). Dough prepared from respectively NIL 1-1, NIL 5-5 and H-AP flour is referred to as NIL 1-1, NIL 5-5 and H-AP dough. When BStA was included in the recipe, an amylase extract was prepared. 5.0 mg BStA preparation and 1.0 mL deionized water were shaken and the amylase was separated from the carrier as in §4.2.2.4. The BStA solution was diluted with deionized water until the desired concentration. Dough was prepared with this amylase-containing solution (59 parts). The BStA dosage used corresponded to 290 mg BStA granulates/kg dm flour (*i.e.* ppm). This dosage has a similar effect on the peak viscosity during measurements with a rapid visco analyzer of flour suspensions (12% dm w/v) in calcium propionate solution (23.0 mM) as does a BStA dosage recommended in bread making (Spendler *et al.*, 2002) on starch suspensions (11% dm w/v) (Leman *et al.*, 2005). Fermented doughs were prepared at least in triplicate and further analyzed (§4.2.2.6 – 4.2.2.7).

4.2.2.6 *Temperature-controlled proton nuclear magnetic resonance*

Proton distributions in bread dough during baking and cooling were obtained as in §3.2.2.5.

4.2.2.7 *Differential scanning calorimetry and swelling power*

The residual amount of crystalline AP and the SP of fermented dough samples that were heated to different temperatures and subsequently freeze-dried were determined with DSC and gravimetric analysis as outlined in respectively §3.2.2.8 and §3.2.2.7.

4.2.2.8 *Statistical analysis*

Statistical analyses were carried out as described in §3.2.2.9.

Table 4.1 Recipe of NIL 1-1 [with *Bacillus stearothermophilus* (BStA)], NIL 5-5 and H-AP dough based on 10.0 g NIL 1-1, NIL 5-5 or H-AP flour, respectively. Also given are starch, damaged starch, amylose (AM) and protein contents of different flour types.

Dough recipe		Dough type			
		NIL 1-1	NIL 1-1 + BStA	NIL 5-5	H-AP
Flour (14.0% MC) (g)	10.0	x	x	x	x
Water (mL)	5.9	x	x	x	x
Sugar (g)	0.6	x	x	x	x
Yeast (g)	0.53	x	x	x	x
Salt (g)	0.15	x	x	x	x
Calcium propionate (g)	0.025	x	x	x	x
BStA (ppm on dm flour)	290		x		

Flour properties	Flour type		
	NIL 1-1	NIL 5-5	H-AP
Starch (% dm)	80.4 (5.3)[a]	81.4 (3.0)[a]	81.4 (2.2)[a]
Damaged starch (%)	4.1 (0.2)[b]	5.7 (0.2)[a]	5.3 (0.3)[a]
AM (% of starch)	27.0 (1.2)[a]	23.0 (1.3)[b]	2.8 (0.7)[c]
Protein (% dm)	13.3 (0.9)[a]	13.4 (1.1)[a]	13.9 (0.2)[a]

MC: moisture content.
dm: dry matter.
Standard deviations are indicated between brackets.
Within one row, values with a different letter are significantly different from each other ($P<0.05$).

4.3 RESULTS AND DISCUSSION

4.3.1 Doughs prepared from flour containing atypical starches

Because of their uniform genetic backgrounds, the flour from the unique NIL 1-1 and NIL 5-5 wheats had similar characteristics except for their AM to AP ratios (Table 4.1) and AP chain length distributions. NIL 5-5 flour contained less AM and thus more AP than the reference sample, *i.e.* NIL 1-1 flour (Table 4.1). Consequently, more AP branch chains, in particular those with DPs 6-10 were present in NIL 5-5 flour than in NIL 1-1 flour (Figure 4.1). Starch in H-AP flour had a very low AM (Table 4.1) and thus high AP content, of which mainly the portion of longer AP branch chains (DP ≥ 10) was higher than in NIL 1-1 and NIL 5-5 flour (Figure 4.1). The WRC of H-AP flour was only slightly or significantly higher than that of respectively NIL 5-5 or NIL 1-1 flour (Table 4.2). These differences in WRC are consistent with findings of Lee *et al.* (2001) and Hayakawa *et al*. (2004). They observed that the mixograph water absorption was higher in a dough system with a higher portion of waxy wheat starch and thus lower AM content.

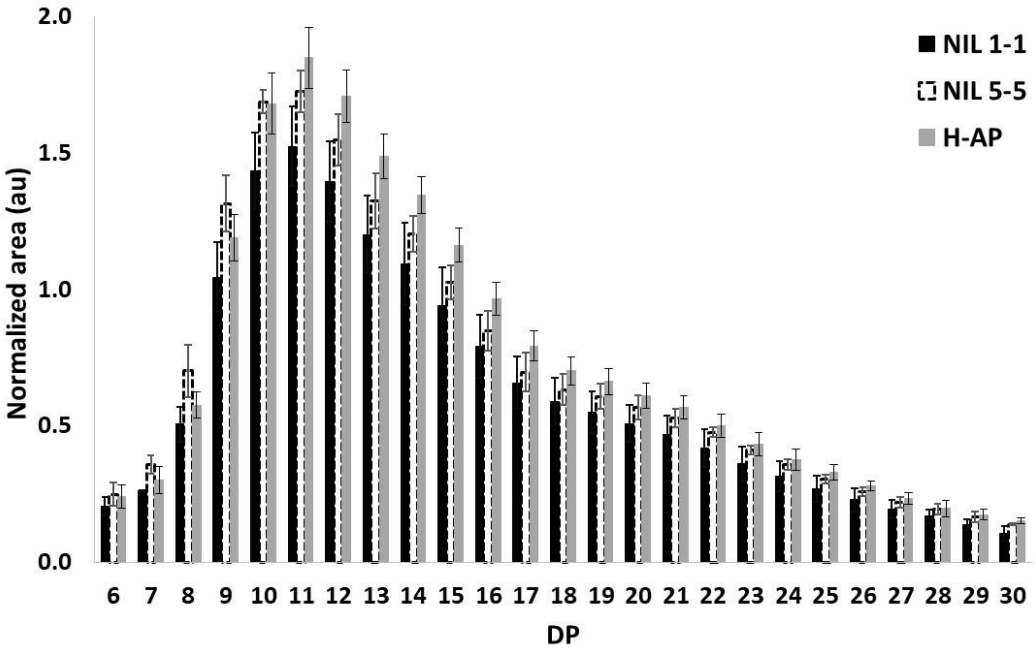

Figure 4.1 Levels of chains with degree of polymerization (DP) 6-30 (normalized to the internal standard, rhamnose) after debranching the starch fraction in NIL 1-1, NIL 5-5 and H-AP flour as measured with high performance anion exchange chromatography and pulsed amperometric detection. Levels are given in arbitrary units (au).

Table 4.2 Water retention capacity (WRC) of NIL 1-1, NIL 5-5 and H-AP wheat flour. Also given are the areas of nuclear magnetic resonance (NMR) populations A, B and E, and the transverse (T_2) relaxation time of population E in NIL 1-1, NIL 5-5 and H-AP fermented dough and fresh, cooled bread.

Sample	Flour	Fermented dough (30 °C)			Fresh cooled bread (25 °C)		
	WRC (%)	Area A (au)	Area E (au)	T_2 relaxation time E (ms)	Area A (au)	Area B (au)	T_2 relaxation time E (ms)
NIL 1-1 (control)	64.8 (2.4)^{b}	14232 (1038)^{a}	6272 (214)^{b}	13.7 (1.0)^{a}	3587 (692)^{a}	2754 (202)^{a}	7.1 (0.3)^{c}
NIL 5-5	72.5 (1.6)^{a}	13099 (716)^{ab}	6618 (224)^{b}	12.3 (1.1)^{a}	2115 (523)^{b}	2674 (344)^{ab}	8.3 (0.2)^{b}
H-AP	75.2 (1.3)^{a}	12407 (944)^{b}	7890 (759)^{a}	7.7 (1.2)^{b}	1484 (141)^{b}	2217 (318)^{b}	10.0 (0.0)^{a}

Areas are given in arbitrary units (au).
Standard deviations are indicated between brackets.
Within one column, values with a different letter at various temperatures are significantly different from each other ($P<0.05$).

In spite of the differences in flour WRC, all doughs were prepared with the same amount of water so that differences in gelatinization behavior and NMR proton distributions would not result from differences in dough MC. Presumably, this explains why dough prepared from H-AP flour was very stiff, that from NIL 5-5 flour was normal and that from NIL 1-1 flour was rather sticky. The stronger interaction with water of H-AP and, to a lesser extent, NIL 5-5 flour components compared to NIL 1-1 flour components in dough was also reflected in the areas of the NMR proton populations of fermented dough (30 °C). When there was more interaction with water, the portion of rigid CH protons of starch and gluten not in contact with water [present in population A (Bosmans *et al.*, 2012)] was lower (Table 4.2, Figure 4.2), and the portion of mobile protons from gluten and extragranular starch in exchange with bulk water [present in population E (Bosmans *et al.*, 2012)] was higher (Table 4.2, Figure 4.3). Moreover, the either slightly or significantly lower T_2 relaxation time and, therefore, mobility of the latter protons in respectively NIL 5-5 or H-AP than in NIL 1-1 dough confirmed an increasingly stronger interaction with water in the order NIL 1-1, NIL 5-5 and H-AP dough (Table 4.2, Figure 4.3).

4.3.1.1 *Baking*

During initial baking (≤ 60 °C) of NIL 1-1 (control) dough, proton distributions changed because of initial starch granule swelling and AM leaching (Rondeau-Mouro *et al.*, 2015). As previously described (*cf.* §3.3.2), these phenomena resulted in respectively

(i) an increased interaction of protons with water as evidenced by a shift of protons from population A [containing CH protons not in contact with water (Bosmans *et al*., 2012)] to population B [containing CH protons in limited contact with water (Bosmans *et al*., 2012)] [Figure 4.2 (a)], and
(ii) a shift of protons from population B to population E and, thus, the extragranular space (Figure 4.3).

The increase in the area of population B because of water uptake by starch granules was thus in part neutralized by a proton shift from population B to population E because of initial AM leaching. Initial starch swelling and AM leaching caused the system's viscosity to increase. This was reflected in a decreased mobility of protons in population E (Figure 4.3).

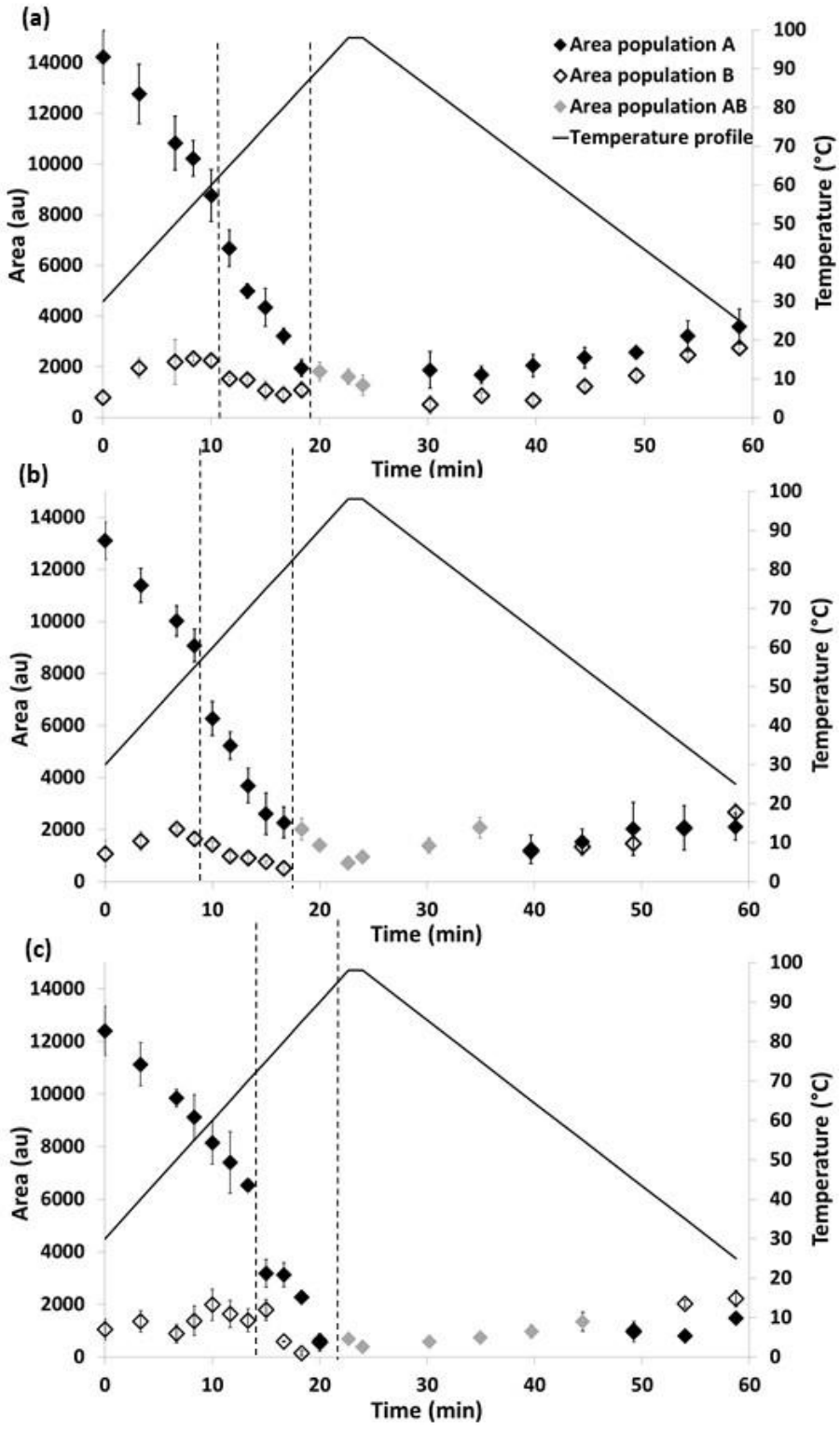

Figure 4.2 Areas of free induction decay (FID) populations A (containing rigid CH protons of starch and gluten not in contact with water), B (containing amorphous CH protons of starch and gluten in little contact with water) and AB (containing amorphous CH protons of starch and gluten in little contact with water) as a function of time and temperature during simulated baking and cooling of (a) NIL 1-1, (b) NIL 5-5 and (c) H-AP bread dough/crumb. The gelatinization (AP crystal melting) temperature range in the different bread types is indicated (dashed lines). Areas are given in arbitrary units (au).

Proton redistributions of NIL 5-5 dough during initial baking occurred in a similar way and were therefore also attributed to initial swelling and AM leaching [Figures 4.2 (b) and 4.3]. During the early simulated baking phase of H-AP dough, the area of population A decreased as well. However, the shift of protons to populations B and E was less pronounced as their areas remained rather constant during initial baking [Figures 4.2 (c) and 4.3]. Moreover, the increased system's viscosity and, thus, decreased mobility of protons in population E because of initial granule swelling and CHL was not observed (Figure 4.3). As pointed out above, the area of population E was already higher and its proton mobility lower in H-AP than in NIL 1-1 and NIL 5-5 fermented dough (30 °C) (Table 4.2 and Figure 4.3). This was attributed to an increased absorption and retention of water by H-AP flour components. It is postulated that flour components interact more strongly with water in fermented H-AP dough when prepared with the amount of water used for NIL 1-1 and NIL 5-5 dough making. The further increased interaction between flour protons and water because of water absorption, initial granule swelling and CHL during initial baking was therefore less marked in this case.

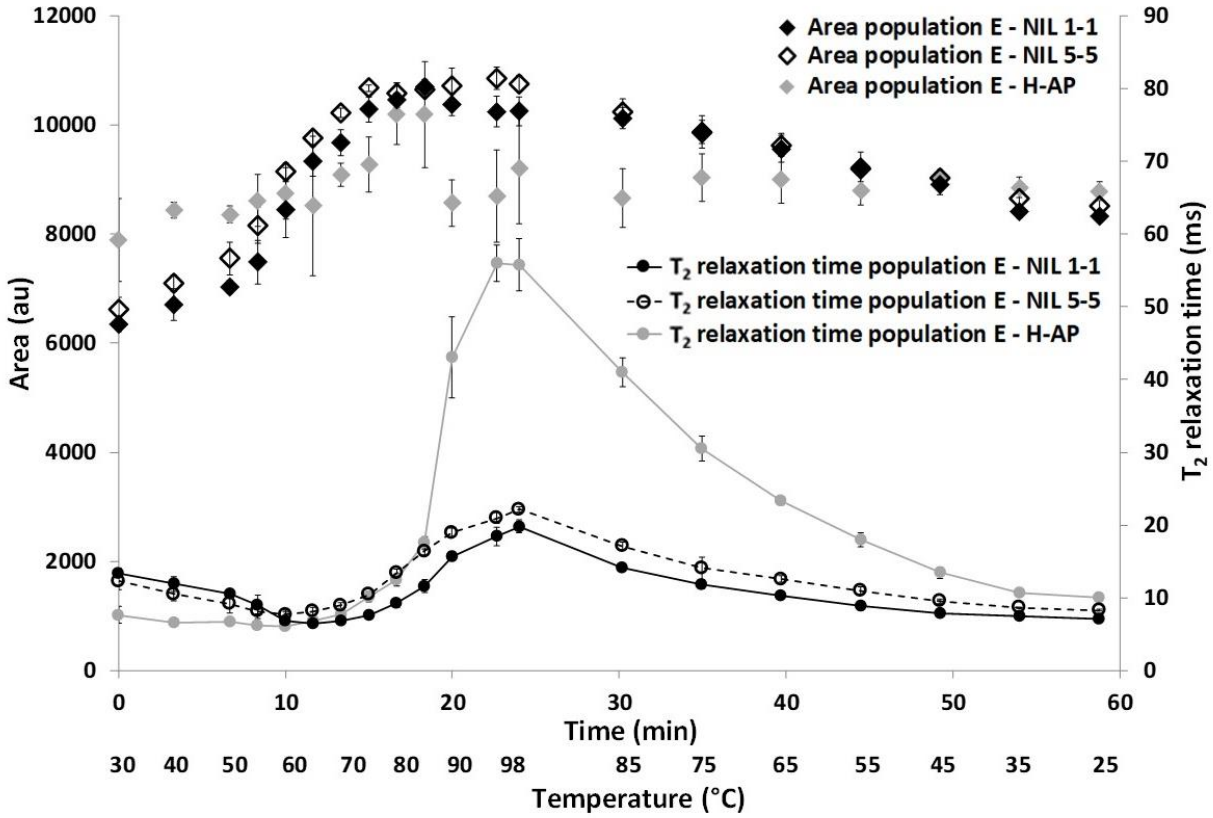

Figure 4.3 Areas and transverse (T_2) relaxation times of Carr-Purcell-Meiboom-Gill (CPMG) population E [containing exchanging protons of (extragranular) starch, gluten and water (in the formed gel network)] as a function of time and temperature during simulated bread baking and cooling. Areas are given in arbitrary units (au).

Further baking caused the starch to gelatinize. Earlier, the onset of gelatinization in dough prepared from wheat flour with regular starch characteristics has been detected in a 60 to 65 °C temperature range using NMR and DSC (*cf.* §3.3.2). This onset temperature was defined as the start of the decrease in respectively the area of population B and the melting enthalpy of AP. In the present case, the melting enthalpies of AP in NIL 1-1 and NIL 5-5 dough heated for 30 min at different temperatures (*cf.* §4.2.2.7) initially increased to values higher than that of fermented dough (30 °C) (Table 4.3). In H-AP fermented dough (30 °C), melting of AP crystals during DSC analysis in excess water involved a higher enthalpy than in NIL 1-1 fermented dough (30 °C) (Table 4.3). Although NIL 5-5 flour also contained more AP than NIL 1-1 flour (Table 4.1), the AP melting enthalpy was lower in NIL 5-5 than in NIL 1-1 fermented dough (30 °C). When heating NIL 1-1, NIL 5-5 or H-AP doughs to 65 °C, 60°C and 70°C, their melting enthalpies started to decrease to readings lower than that of fermented dough (30 °C), indicating the onset of gelatinization (Table 4.3). Simultaneously, the areas of NMR populations B started to decrease during baking of NIL 1-1 and NIL 5-5 dough (Figure 4.2). Moreover, the area of population A was reduced strongly between 55 to 60 °C in NIL 5-5 and between 70 to 75 °C in H-AP dough [Figure 4.2 (b and c)]. This strong decrease at the onset of gelatinization was less clear in NIL 1-1 dough [Figure 4.2 (a)]. Higher AP levels evidently resulted in a higher portion of protons from AP crystals in population A. It follows that the onset of gelatinization in terms of AP crystal melting is more clearly noticeable as a decrease in the area of population A when the portion of AP in starch was higher. From the onset of gelatinization onwards, the decrease in the area of population A has been attributed to melting of AP crystals and no longer solely to a proton shift to population B because of water absorption by starch granules (*cf.* §3.3.2).

Apart from the onset temperature of gelatinization, also that at which gelatinization is complete was different in the different samples. At that temperature, one FID population AB, containing amorphous CH protons of starch and gluten in little contact with water, and no residual melting enthalpy of AP were detected with respectively NMR and DSC measurements [Figures 4.2 and 4.4 (a, c, e), Table 4.3]. Furthermore, the increase in the area of population E because of CHL ceased around that temperature (Figure 4.3) (*cf.* §3.3.2). As was the case for the temperatures of the onset of gelatinization, those at which gelatinization was complete also increased in the order NIL 5-5 (80-85 °C), NIL 1-1 (85-90 °C), and H-AP (90-98 °C) crumb. Gelatinization, in terms of AP crystal melting, thus occurred between 55 to 85 °C in NIL 5-5 bread, between 60 to 90 °C in NIL 1-1 bread and between 70 to 98 °C in H-AP bread (Figure 4.2).

Table 4.3 The (residual) melting enthalpy of amylopectin crystals (ΔH_{AP}) and the swelling power (SP) of starch in fermented wheat flour dough prepared from NIL 1-1, NIL 5-5 or H-AP flour and heated to different temperatures.

Temperature (°C)	ΔH_{AP} [J/g (dm)]			SP (g/g)		
	NIL 1-1	NIL 5-5	H-AP	NIL 1-1	NIL 5-5	H-AP
30	8.1 (0.2)^{cB}	6.3 (0.5)^{abC}	10.3 (0.9)^{aA}	3.4 (0.1)^{eA}	3.4 (0.2)^{gA}	3.4 (0.3)^{gA}
40	7.5 (0.2)^{cB}	6.7 (0.5)^{abB}	11.7 (0.9)^{aA}	3.1 (0.0)^{eB}	3.2 (0.1)^{gAB}	3.5 (0.1)^{gA}
50	8.4 (0.3)^{cB}	8.2 (1.0)^{abcAB}	10.2 (0.7)^{aA}	3.3 (0.0)^{eA}	3.6 (0.1)^{gA}	3.6 (0.1)^{gA}
55	10.4 (0.4)^{aA}	8.2 (0.2)^{aB}	11.3 (0.8)^{aA}	3.5 (0.1)^{eA}	3.8 (0.1)^{fgA}	3.7 (0.3)^{gA}
60	9.2 (0.0)^{abA}	5.7 (0.3)^{bB}	10.8 (0.7)^{aA}	4.1 (0.1)^{dAB}	4.4 (0.2)^{efA}	3.8 (0.2)^{fgB}
65	6.4 (0.1)^{dB}	3.1 (0.1)^{cdC}	10.9 (0.5)^{aA}	4.2 (0.0)^{dB}	4.9 (0.2)^{deA}	4.1 (0.1)^{fgB}
70	4.0 (0.3)^{eB}	2.0 (0.5)^{deC}	9.0 (0.1)^{aA}	4.8 (0.2)^{cAB}	5.2 (0.3)^{dA}	4.5 (0.1)^{efB}
75	1.9 (0.1)^{fB}	0.7 (0.1)^{eC}	6.8 (0.6)^{bA}	5.1 (0.0)^{cB}	6.4 (0.1)^{cA}	5.4 (0.0)^{eB}
80	0.9 (0.2)^{fgB}	0.2 (0.1)^{fC}	3.7 (0.3)^{cA}	5.2 (0.2)^{cB}	6.4 (0.3)^{cA}	6.5 (0.4)^{dA}
85	0.2 (0.1)^{gB}	/	2.3 (0.8)^{cdA}	6.4 (0.3)^{bB}	6.9 (0.1)^{bcB}	10.0 (0.2)^{cA}
90	/	/	0.6 (0.1)^{d}	6.5 (0.1)^{bC}	7.3 (0.2)^{bB}	11.9 (0.2)^{bA}
100	/	/	/	8.6 (0.1)^{aC}	9.3 (0.2)^{aB}	17.4 (0.2)^{aA}

dm: dry matter.

Standard deviations are indicated between brackets.

Within one column, values with a different small letter at different temperatures for the same dough type differ significantly from each other ($P<0.05$). Values of either SP or ΔH_{AP} with a different capital letter at the same temperature for different dough types differ significantly from each other ($P<0.05$).

The enthalpy involved in AP crystal melting was lower in NIL 5-5 and higher in H-AP than in NIL 1-1 samples (Table 4.3). Higher AP melting enthalpies and temperatures with higher AP levels in wheat starch, as was the case for H-AP samples, have been noted before (Bocharnikova *et al.*, 2003; Fujita *et al.*, 1998; Lee *et al.*, 2001; Morita *et al.*, 2002). Fujita *et al.* (1998) attributed this to the positive relationship between crystallinity of wheat starch granules and their AP content. However, while AP melting enthalpy is determined by its crystallinity, the temperature at which melting occurs is determined by crystal stability. The latter is *inter alia* governed by the crystal surface energy (Gomand *et al.*, 2012). According to Bocharnikova *et al.* (2003) and Yuryev *et al.* (2004), the crystal surface free energy is inversely related to the melting temperature and depends on the crystal surface entropy. The surface entropy, in turn, is related to defects in the granular structure which increase in number with AM content. The higher gelatinization temperature of starch during baking of H-AP than of NIL 1-1 dough is hence attributed to a decreased crystal surface energy as less AM and, therefore, less structural defects are present. Furthermore, the AP crystal stability is positively related to the thickness of crystalline lamellae (Gomand *et al.*, 2012), which increases with the portion of longer AP branch chains (DP > 10) (Genkina *et al.*, 2003; Salman *et al.*, 2009). Compared to NIL 1-1 flour, H-AP flour indeed contained mainly more AP branch chains with a DP of at least 10 (Figure 4.1). Although NIL 5-5 flour also contained more AP and, thus, less AM than NIL 1-1 flour (Table 4.1), the AP melting enthalpy and the gelatinization temperatures during baking were lower in NIL 5-5 than in NIL 1-1 samples (Table 4.3). This was attributed to the higher portion of short AP branch chains with DPs 6-10 in NIL 5-5 flour (Figure 4.1). These results are in line with literature data concerning the gelatinization temperature and melting enthalpy of wheat starches (Noda *et al.*, 2001; Singh *et al.*, 2010) and indicate that both gelatinization temperature and enthalpy are negatively related to the portion of short AP branch chains (Cooke & Gidley, 1992). Based on research of Gidley and Bulpin (1987), Singh *et al.* (2010) suggested that double helices formed from short AP branch chains (DP ≤ 10) are unstable and, therefore, require less energy for gelatinization.

It is of note that the temperature and enthalpy of starch gelatinization during baking of the different dough types may have been impacted by the flour damaged starch contents. The gelatinization enthalpy and temperature of wheat starch and flour samples are lower when their damaged starch contents are higher (León *et al.*, 2006; Morrison *et al.*, 1994). The lower gelatinization enthalpy and temperature during baking of NIL 5-5 dough than during baking of NIL 1-1 dough may therefore partly have been related to the higher damaged starch content of NIL 5-5 than of NIL 1-1 flour (Table 4.1). However, gelatinization characteristics during baking of NIL 5-5 dough were also very different from those of H-AP dough while NIL 5-5 and H-AP flour contained similar damaged starch contents. Differences in enthalpy and

temperature of AP crystal melting were therefore mainly attributed to differences in AP content and AP chain length distribution in the flour samples used.

Gelatinization involves irreversible granule swelling (Tester & Morrison, 1990). This was here reflected in the significant increase of the SP of the different dough types at their corresponding onset temperature range of gelatinization (Table 4.3). Once gelatinization had started, SP was higher when the AP content was higher because swelling is a characteristic of AP while AM restricts starch granule swelling (Tester & Morrison, 1990). Furthermore, the exchanging protons in population E gained mobility after the onset of gelatinization (Figure 4.3). This was attributed to the positive effect of temperature on proton mobility according to Arrhenius' law (Rondeau-Mouro *et al.*, 2015). Up to this moment, however, the proton mobility of population E decreased (or remained rather constant in H-AP dough) as this Arrhenius effect was overruled by the dough system's viscosity increase because of granule swelling and CHL (*cf.* §3.3.2). Based on X-ray computed microtomography experiments in a 50 to 70 °C temperature range, Babin *et al.* (2006) postulated that stiffening of the dough matrix *inter alia* because of gelatinization contributes to the transition of dough to crumb. It has further been suggested that the system's viscosity no longer increased when the crumb is set after the onset of gelatinization (*cf.* §3.3.2). Indeed, in the present case, the increase in mobility of population E protons with temperature was noticed after the onset of gelatinization and therefore at a lower temperature in NIL 5-5 than in NIL 1-1 and H-AP crumb (Figure 4.3). During further baking, the increase in mobility of population E protons was more pronounced when the level of AM decreased in the order NIL 1-1, NIL 5-5 and H-AP crumb. The present results are in line with Bosmans *et al.* (2012). They already pointed to a key role of AM as a structural element that reduces the mobility in a gelatinized starch system.

At the end of gelatinization, the Arrhenius effect also caused the mobility of the more mobile protons in population CD to increase, thereby splitting this population in populations C and D [Figure 4.4 (b, d, f)] (*cf*. §3.3.2). Population C consisted of the less mobile protons of population CD, *i.e.* CH protons from amorphous starch and gluten. Population D contained the more mobile protons of population CD, *i.e.* exchanging protons of water, gluten and starch in granule remnants (Bosmans et al., 2012). The strongly increased mobility of exchanging protons in population E of H-AP crumb at the end of gelatinization was accompanied by a reduced area of this population (Figure 4.3). Presumably, only the most mobile protons of population E, *i.e.* those of bulk water in limited interaction with biopolymer protons were much affected by the Arrhenius effect. The somewhat less mobile, more strongly interacting protons were now present in population D [Figure 4.4 (f)].

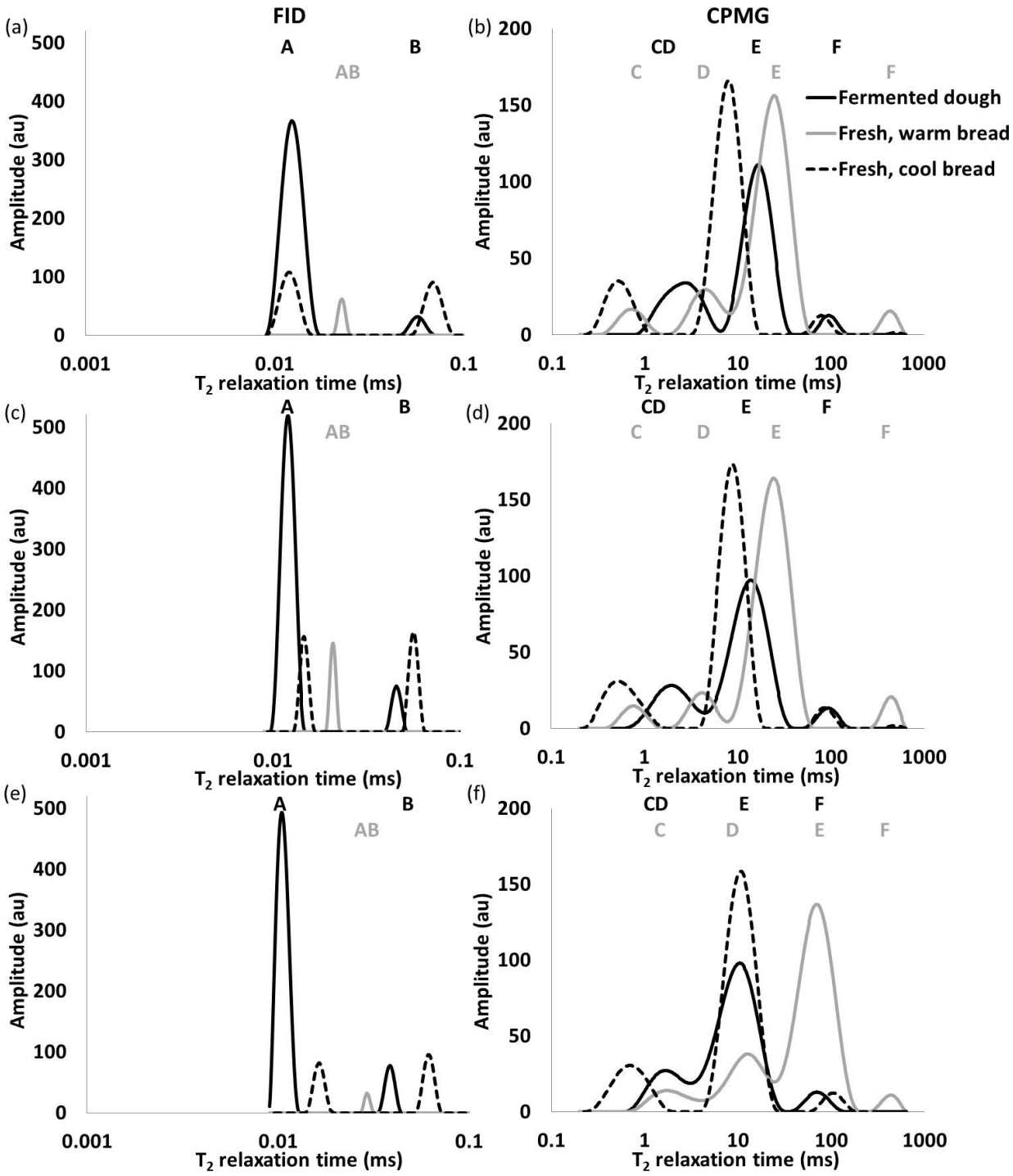

Figure 4.4 Free induction decay (FID) and Carr-Purcell-Meiboom-Gill (CPMG) proton distributions of NIL 1-1 (a,b), NIL 5-5 (c,d), H-AP (e,f) fermented dough before baking and of fresh bread before and after cooling. Amplitudes are given in arbitrary units (au).

4.3.1.2 *Cooling*

As AM crystallized during cooling, part of the protons in population AB became more rigid, causing it to split up in populations A and B, containing *inter alia* protons of AM crystals and amorphous starch not in contact with water and protons of amorphous starch in little contact with water [Figures 4.2 and 4.4 (a, c, e)] (*cf.* §3.3.3). When the AM content was lower, the split of population AB occurred at lower temperatures and, more in particular, at about 85, 65 and 45 °C in respectively NIL 1-1, NIL 5-5 and H-AP bread (Figure 4.2). Such relation between AM concentration and gel formation temperature was already reported by Vallera *et al*. (1994) (*cf.* §1.5.2). The concentration-dependent timing of gelation can be interpreted based on state/phase diagrams which display a component's state in function of both temperature and the component's concentration. Such diagram of starch-water mixtures as in van der Sman & Meinders (2011) allows deducing that the temperature required for the system to enter the gel state depends on its starch content. In the present case, not the starch level but its AM content differs in the studied samples. Since AM is responsible for starch gel network formation during cooling (Miles *et al.*, 1985a), it is plausible that its concentration determines the temperature at which gelation and crystallization starts.

Further cooling caused the areas of populations A and B to increase as AM gelation progressed (Figure 4.2) (*cf.* §3.3.3). As the AM content was lower in NIL 5-5 and H-AP crumb than in NIL 1-1 crumb after cooling, so were the areas of populations A and B (Figure 4.2, Table 4.2). During cooling, the mobility of the protons in population E decreased as a result of both the formation of a semicrystalline AM gel network and the temperature effect described by Arrhenius' law as outlined before (*cf.* §3.3.3). From the start of cooling onwards, these exchanging protons from starch, gluten and water in the developing gel network remained more mobile with decreasing AM content in the order NIL 1-1, NIL 5-5 and H-AP crumb (Figure 4.3, Table 4.2). This was in line with the delayed timing and decreased extent of AM crystallization detected with FID measurements when crumb contained less AM (Figure 4.2, Table 4.2). Understandably, in dough containing lower AM levels, less of it could leach to the extragranular space during baking and be available for crystallization during cooling. Moreover, additional AM-L complexes were formed from leached AM molecules during baking and cooling as described in Chapter 3 (*cf.* §3.3.2 and §3.3.3). Both AM crystals and AM-L complexes served as junction zones in the fringed micelle AM network. As a result, a less rigid and less extended semicrystalline AM network in which protons remain more mobile was formed during cooling of crumb containing less AM. These results confirm that AM fulfils a structure-building role in bread crumb as stated earlier by Bosmans *et al.* (2012).

4.3.2 Doughs prepared with use of maltogenic α-amylase

The higher portion of short AP branch chains in NIL 5-5 flour caused gelatinization to occur at lower temperatures. Hydrolysis of starch by the mainly exoacting BStA *inter alia* increases the portion of short AP branch chains (*cf*. §2.3.1.1) (Goesaert *et al.*, 2009). However, inclusion of BStA in the NIL 1-1 (control) dough recipe significantly altered neither starch AP crystal melting characteristics of samples heated up to 100°C (*cf*. §4.2.2.7) nor their swelling characteristics (data not shown). This was rather surprising as in control dough starch gelatinization started in a 60 to 65 °C temperature range, the temperature for optimal BStA activity is about 60 °C (Christophersen *et al.*, 1998) and BStA is much more active on gelatinized than on ungelatinized starch (Leman *et al.*, 2005). Indeed, higher CHL readings (because of maltose release by BStA) were obtained at temperatures exceeding 60 °C in NIL 1-1 dough samples with than in those without BStA (data not shown). In summary, BStA clearly hydrolyzes starch after the onset of gelatinization. However, because of its mainly exoaction, the MW of starch polymers decreases slowly (Bijttebier *et al.*, 2007) and BStA had little if any impact on the timing and extent of gelatinization during baking.

In line with the above, the (re)distribution of protons in the main NMR populations during baking of dough with BStA remained unchanged (Figure 4.5). During cooling, however, the mobility of population E protons in BStA supplemented samples was higher [Figure 4.5 (b)]. As already pointed out here (*cf*. §3.3.3 and §4.3.1.2) and elsewhere (Bosmans *et al.*, 2013c), the mobility of population E protons is negatively related to the extent of starch network formation and the network's strength. The present results thus indicate that a weaker starch network containing more mobile protons is present in cooling bread samples produced from a recipe containing BStA than in those from a control recipe. These data support the hypotheses and/or findings by several research teams that

(i) the increased endoaction of BStA when temperature rises (Bijttebier et al., 2007) causes slight weakening of the starch network by the end of baking and during cooling (Goesaert *et al.*, 2009b), and that
(ii) the MW reduction of AM chains increases their mobility (Hug-Iten et al., 2001).

The latter has been suggested to enhance AM crystallization during further cooling, thereby strengthening the semicrystalline AM network in fresh bread produced from BStA-containing recipes (Hug-Iten *et al.*, 2001). Enhanced AM crystallization was not reflected in proton (re)distributions during the NMR cooling phase of NIL 1-1 crumb containing BStA (Figure 4.5). After all, that would result in a higher area of population A and a lower mobility of population E protons in cooled bread crumb.

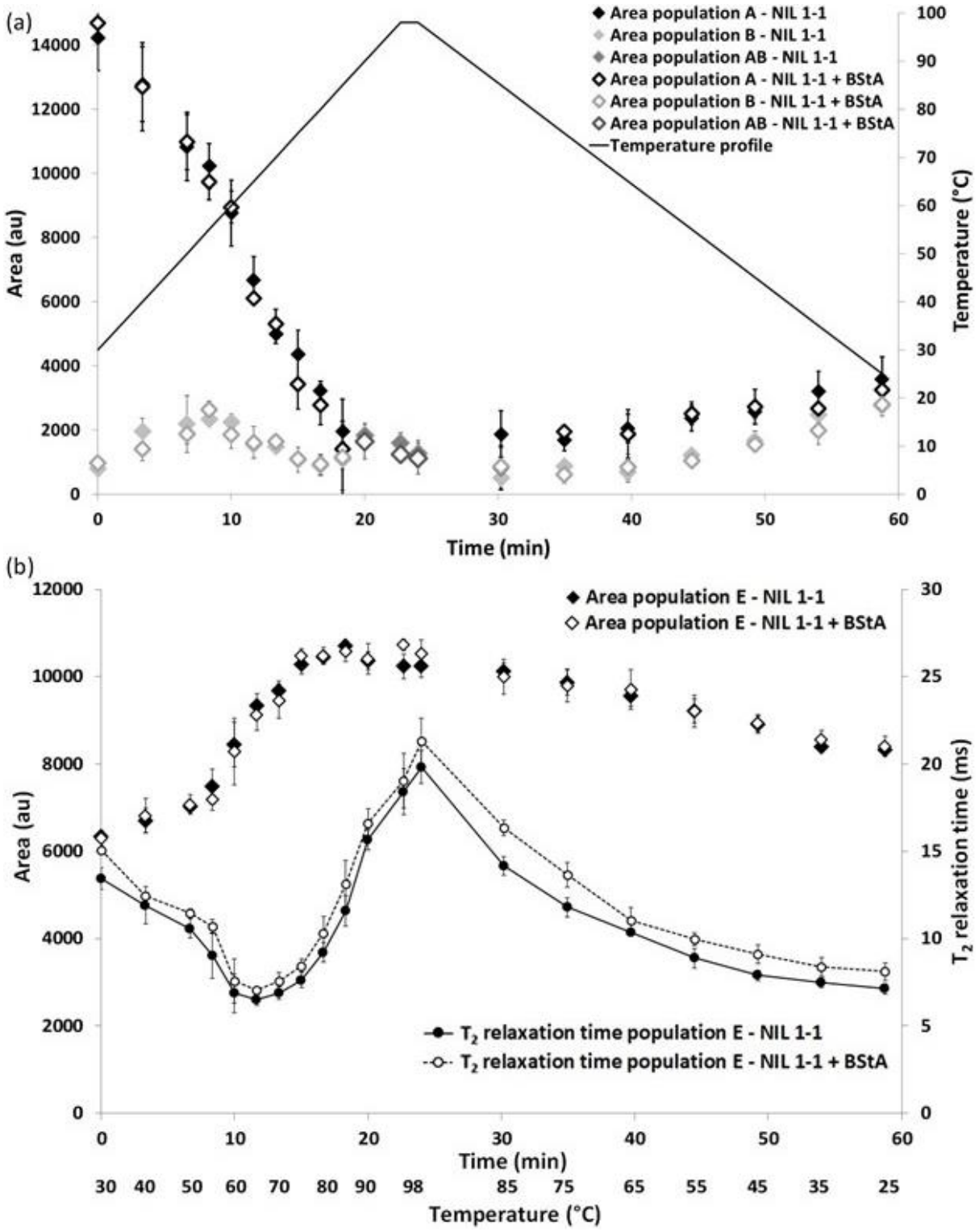

Figure 4.5 (a) Areas of free induction decay (FID) populations A (containing rigid CH protons of starch and gluten not in contact with water), B (containing amorphous CH protons of starch and gluten in little contact with water) and AB (containing amorphous CH protons of starch and gluten in little contact with water) and (b) areas and transverse (T_2) relaxation times of Carr-Purcell-Meiboom-Gill (CPMG) population E [containing exchanging protons of (extragranular) starch, gluten and water (in the formed gel network)] as a function of time and temperature during simulated bread baking and cooling of NIL 1-1 bread dough/crumb with and without inclusion of *Bacillus stearothermophilus* α-amylase (BStA) in the recipes. Areas are given in arbitrary units (au).

4.4 CONCLUSIONS

Starch gelatinization and gelation are in essence determined by respectively AP and AM. AP crystal stability determines the timing of gelatinization and associated phenomena. The gelatinization onset temperature during baking was lower when starch in dough contained (i) more AM and, thus, less AP and (ii) a larger portion of short AP branch chains.

Ad (i): AM content of starch has been associated with defects that increase the crystal surface energy and hence destabilize the AP crystal structure, while

Ad (ii): AP branch chains with DP 6-10 are too short to from stable double helices.

Gelatinization was complete in all bread crumb samples. The extent of the associated swelling, however, increased with AP content as starch granule swelling is due to AP and is restricted by AM. The higher mobility of mobile, exchanging protons at the end of baking and during cooling of bread crumb with a lower AM content points to the key structural role of AM in bread crumb. Indeed, a semicrystalline AM network is formed as AM crystallizes during cooling. The timing and extent of AM crystallization and gelation evidently depends on the AM concentration in starch. When AM contents were lower, cooling to lower temperatures is required for AM crystallization to start. Eventually, less rigid protons and a less extended semicrystalline AM network in which exchanging protons remain more mobile are present in crumb with less AM. The mobility of exchanging protons in the formed gel network was further impacted when BStA was included in the dough recipe. Significant hydrolysis of starch by the mainly exoacting enzyme occurred after the onset of gelatinization. The increased endoaction of BStA with temperature resulted in a slightly weaker starch network at the end of baking. During cooling of crumb produced from BStA-containing recipes, exchanging protons in the gel network therefore remained more mobile.

These results underpin the relevance of the here used NMR toolbox to monitor the timing and extent of transitions in the starch fraction and its interaction with water during baking and cooling. That proton distributions were altered in line with starch AP and AM characteristics, supports the interpretation of NMR profiles suggested in Chapter 3.

While in the present chapter AM and AP functionality during baking and cooling were investigated, Chapter 5 deals with the functionality of these biopolymers during the subsequent storage phase.

Chapter 5

Amylose and amylopectin functionality during storage of bread prepared from flour of wheat containing unusual starches[4]

5.1 INTRODUCTION

From the literature review in Chapter 2 it follows that thorough understanding of crumb firming is essential to further improve the shelf life of bread. After all, bread is worldwide one of the most common but unfortunately also one of the most wasted foods (FOODWIN, 2018). The two most prominent components in wheat flour relevant in this context are starch and gluten.

Thermoset gluten and semicrystalline AM networks formed during bread baking and cooling determine initial crumb resilience (Bosmans *et al.*, 2013b), initial firmness (Schoch & French, 1947), and thus sliceability of fresh bread (Cauvain, 2015). During storage, crumb firmness increases and crumb resilience decreases (Bosmans *et al.*, 2013c). Crumb firming during storage at room temperature is largely associated with AP retrogradation (Schoch & French, 1947; Willhoft, 1973) and crumb networks' hydration (Bosmans *et al.*, 2013c). During storage at lower temperatures (but above the glass transition temperature), crumb firming is dominated by the extent of AP retrogradation. Indeed, the rate of moisture redistribution from crumb to crust and from gluten to starch decreases while that of retrogradation increases when temperature decreases (*cf.* §2.3.2.2) (Bosmans *et al.*, 2013b).

[4] This Chapter is based on the following reference: Nivelle, M.A., Beghin, A.S., Vrinten, P., Nakamura T., and Delcour, J.A. Amylose and amylopectin functionality during storage of bread prepared from flour of wheat containing unique starches. (Submitted for publication).

In this chapter, a toolbox based on TD ^{1}H NMR (Bosmans *et al.*, 2013c) was used to investigate AM and AP functionality in fresh and stored bread at different length scales. This way it was tried to answer the following research questions:

(i) How do atypical starch transitions and water dynamics during baking and cooling of bread from flour containing atypical starches (Chapter 4) impact on biopolymer networks and water (re)distribution in fresh bread and during storage?
(ii) Does inclusion of BStA in the recipe of bread from control flour imitate the effect of a larger portion of short AP branch chains in bread from flour with atypical properties during storage?
(iii) Does hydrolysis by BStA of the already shorter AP branch chains in bread from flour with atypical properties occur and, if so, does it further alter fresh and stored bread quality?

5.2 MATERIALS AND METHODS

5.2.1 Materials

Flour from NIL 1-1 (wild type), NIL 5-5 and H-AP wheat, and other bread making ingredients were obtained as described in Chapters 3 and 4 (*cf*. §3.2.1 and §4.2.1). Reagents, enzymes, solvents and standards for determining starch and AM contents, amylase activity and AP chain length distribution were those described above (*cf*. §4.2.1). Chemicals for extracting protein under nonreducing conditions were from VWR International. Dithiothreitol (DTT) from Acros Organics was used to extract protein under reducing conditions.

5.2.2 Methods

5.2.2.1 *Composition of wheat flour and bread*

Starch and protein contents of wheat flour and MCs of wheat flour, bread crumb and crust were determined as in §3.2.2.2. The AM (and AP) and damaged starch contents of wheat flour were analyzed as described in §4.2.2.1. AP chain length distributions were determined for fresh and stored bread crumb rather than for wheat flour which allowed characterizing the changes in AP chain lengths because of BStA action. Hereto, triplicate freeze-dried and ground crumb samples (5.0 mg) suspended in 0.25 mL 90% (v/v) DMSO were boiled (30 min). The remainder of the procedure was that outlined in §4.2.2.3.

5.2.2.2 *Farinograph analysis*

Water absorption of wheat flour was determined using a Brabender Farinograph (Duisburg, Germany) with a 10 g mixing bowl according to AACC International Method 54-21.02 (AACCI, 2011). Farinograph water absorption is expressed on a 14.0% flour MC basis. Optimal flour water absorption is defined as the amount of water needed to obtain a maximum consistency of 500 Brabender Units.

5.2.2.3 *Amylase activity assay*

Amylase activity was determined as in §4.2.2.4.

5.2.2.4 *Bread making and storage*

Bread was prepared according to a straight-dough method (Finney, 1984) from 100.0 g wheat flour (100 parts). All other ingredients were in appropriate amounts to respect the abovementioned ratios (*cf*. §3.2.2.3) (Table 5.1). For comparison reasons, all doughs were prepared with 59 parts of deionized water. However, according to Farinograph analysis, dough from H-AP flour (H-AP dough) required more water. Therefore, H-AP dough was also prepared with a higher level of water, *i.e.* 70 parts (H-AP 70 dough) (Table 5.1). The amylase extract used for BStA-containing (290 ppm) recipes was prepared as in §4.2.2.5. Ingredients were mixed and dough was fermented as outlined for dough prepared from 10.0 g wheat flour in §3.2.2.3. Final proofing (36 min at 30 °C and 90% relative humidity) was done in a slightly greased baking tin [internal dimensions (width x length x height): 8.0 cm x 14.5 cm x 5.5 cm]. The fermented dough was baked in a rotary hearth oven for 24 min at 215 °C. Bread loaves were cooled for 120 min at 23 °C. Dough/bread prepared from respectively NIL 1-1, NIL 5-5 and H-AP flour is further referred to as NIL 1-1, NIL 5-5 and H-AP dough/bread. Fresh, cooled bread loaves were enfolded with plastic foil and stored at 23 °C in plastic bags which were sealed to avoid moisture loss. After different storage times [0 (*i.e.* fresh bread after 120 min cooling), 2 and 7 days], the loaf volume was determined with a Volscan Profiler (Stable Micro Systems, Godalming, Surrey, UK). During baking, the maximum temperature is reached last in the center and the accompanying changes start later (*cf*. §3.2.2.1). Analyses (*cf*. *infra* §5.2.2.5-5.2.2.8.) were therefore performed on samples from the crumb center of at least two bread loaves.

5.2.2.5 *Proton nuclear magnetic resonance*

Measurements of proton distributions in fresh and stored bread crumb were performed with a Minispec mq 20 TD NMR spectrometer (Bruker) at an operating resonance frequency of 20 MHz for ^{1}H (magnetic field strength of 0.47 T). The probe head was kept at 25 ± 1 °C using an external water bath. The T_2 relaxation curve for less mobile protons was obtained by

performing a single 90° pulse (pulse length of 2.70 µs). The FID, *i.e.* the magnitude of the T_2 relaxation signal in function of time, obtained after this pulse was sampled for 0.5 ms and 500 data points were acquired. A CPMG pulse sequence, consisting of a 90° pulse followed by 180° pulses (pulse length of 5.62 µs) after 0.1 ms, was used to obtain T_2 relaxation signals of more mobile protons (c*f.* §3.2.2.5). 2,500 data points were collected. For both FID and CPMG measurements, the recycle delay was 3.0 s and 32 scans were accumulated to increase the signal to noise ratio.

Per bread loaf, three crumb center samples (*ca.* 0.3 g) were placed in separate NMR tubes and compressed to remove air bubbles (*ca.* 8 mm height). Crumb samples were from fresh and stored (for 2 or 7 days) bread loaves. The tubes were sealed te prevent moisture loss. After FID and CPMG measurements, fresh crumb samples in NMR tubes were also stored (*i.e.* without interference of crumb to crust water migration) and analyzed again after 2 and 7 days of storage.

T_2 relaxation curves were converted to continuous distributions of T_2 relaxation times using CONTIN software (*cf.* §3.2.2.5). The calculations were performed on 500 data points, logarithmically spread between T_2 relaxation times of 0.007 and 0.5 ms and of 0.208 and 500 ms for FID and CPMG measurements, respectively. Proton populations are characterized by their area and mean T_2 relaxation time which respectively relate to the amount of protons in the population and their mobility. The latter depends on the environment the protons are in. Because of static magnetic field inhomogeneity, the most mobile FID population was not taken into account. Changes in the area and mobility of different proton populations during storage were indicative for AP retrogradation, moisture redistribution and crumb firming (Bosmans *et al.*, 2013c).

5.2.2.6 *Crumb texture analysis*

Crumb firmness and resilience were determined with an Instron 3342 (Norwood, MA, USA). From the center of each bread loaf, at least three cylindrical crumb samples (height 25 mm, diameter 30 mm) were removed. Samples were compressed at 100 mm/min by a cylindrical probe (diameter 75 mm). The force-time curve was monitored during 30% compression and decompression. The crumb firmness is the maximal force (N) required to compress the sample. It was corrected for variations in crumb density resulting in intrinsic crumb firmness ($N.cm^3/g$). The crumb resilience was measured as the strain energy recovered and calculated as the ratio of the areas under the decompression and compression curves as in Liu & Scanlon (2004).

5.2.2.7 *Size exclusion high performance liquid chromatography*

Freeze-dried samples from the center of fresh bread loaves were extracted and analyzed in triplicate with SE-HPLC. Under nonreducing conditions, samples were extracted with 0.05 M sodium phosphate buffer (pH 6.8) containing 2.0% (w/v) SDS (medium A). Under reducing conditions, extraction was carried out under nitrogen atmosphere using medium A containing 1.0% DTT (medium B). Samples (1.0 mg protein/mL extraction medium) were shaken (60 min, room temperature) and centrifuged (10,000 g, 10 min). Supernatants were filtered (Millex-HP, 0.45 µm, polyethersulfone; Millipore, Carrigtwohill, Ireland) and injected (20 µL) on a LC-2010 system (Shimadzu, Kyoto, Japan) with a Biosep-SEC-S4000 column (pore size 500 Å, Phenomenex, Torrance, CA, USA). Elution was with medium A (1.0 mL/min, 30 °C) and eluted proteins were detected at 214 nm. The protein extractability in SDS-containing medium (SDS-EP) was expressed as the ratio of the areas under the chromatograms of the sample extracted with medium A to those of the samples extracted with medium B.

5.2.2.8 *Differential scanning calorimetry*

The extent of AP retrogradation was also studied by DSC with a Q2000 DSC. Freeze-dried and gently ground samples from the center of a bread loaf were analyzed as described in Chapter 3 (§3.2.2.8). TA Universal Analysis software was used to determine temperatures and enthalpies [ΔH_{AP} (J/g sample dm)] of retrograded AP crystal melting.

5.2.2.9 *Statistical analysis*

Statistical analyses were carried out as described in §3.2.2.9.

5.3 RESULTS AND DISCUSSION

5.3.1 Breads prepared from flour containing atypical starches

Bread was prepared from the above mentioned unique flour samples containing unusual starches. Since NIL 5-5 bread contained less AM, more AP and thus also AP branch chains were present (Table 5.1). In particular, NIL 5-5 bread contained more such chains of DPs 6-10 than NIL 1-1 bread (Figure 5.1). H-AP flour, with a very low AM (Table 5.1) and therefore very high AP content, was also used for bread making. Mainly the portion of longer AP branch chains (DP ≥ 10) was higher in H-AP than in NIL 1-1 and NIL 5-5 breads (Figure 5.1).

Table 5.1 Recipe of NIL 1-1 [with *Bacillus stearothermophilus* (BStA)], NIL 5-5 (with BStA), H-AP [with addition of a regular and a higher amount of water (H-AP 70)] bread based on 100.0 g NIL 1-1, NIL 5-5 and H-AP flour, respectively. Also given are starch, amylose (AM) and protein contents of different flour types.

Bread recipe		Bread type					
		NIL 1-1	NIL 1-1 + BStA	NIL 5-5	NIL 5-5 + BStA	H-AP	H-AP 70
Flour (14.0% MC) (g)	100.0	x	x	x	x	x	x
Water (mL)	59.0	x	x	x	x	x	
	70.0						x
Sugar (g)	6.0	x	x	x	x	x	x
Yeast (g)	5.3	x	x	x	x	x	x
Salt (g)	1.5	x	x	x	x	x	x
Calcium propionate (g)	0.25	x	x	x	x	x	x
BStA (ppm on dm flour)	290		x		x		

Flour properties	Flour type		
	NIL 1-1	NIL 5-5	H-AP
Starch (% dm)	80.4 (5.3)[a]	81.4 (3.0)[a]	81.4 (2.2)[a]
Damaged starch (%)	4.1 (0.2)[b]	5.7 (0.2)[a]	5.3 (0.3)[a]
AM (% of starch)	27.0 (1.2)[a]	23.0 (1.3)[b]	2.8 (0.7)[c]
Protein (% dm)	13.3 (0.9)[a]	13.4 (1.1)[a]	13.9 (0.2)[a]

MC: moisture content.
dm: dry matter.
Standard deviations are indicated between brackets.
Within one row, values with a different letter are significantly different from each other ($P<0.05$).

Atypical starch transitions during baking, cooling (Chapter 4) and storage impacted on *inter alia* proton distributions in fresh and stored bread as detected with TD ^{1}H NMR (Table 5.2 and Figure 5.2). Based on previous work (Bosmans *et al.*, 2012), these populations were assigned as follows: population A contains rigid nonexchanging CH protons of AM crystals formed during cooling, AP crystals formed during storage and also protons of amorphous starch and gluten not in contact with water. Populations B and C both contain amorphous CH protons of gluten and starch in little contact with water. Protons in population D are CH protons of gluten and exchanging protons of confined water, starch, and gluten. Population E represents mobile exchanging protons of starch, gluten and water in the formed gel network. Population F consists of protons from lipids present in flour and shortening used to grease baking tins. Populations A and E predominated NMR profiles. Changes in their areas and mobility, therefore, are focused on to study the impact of unusual starches on fresh and stored bread loaves.

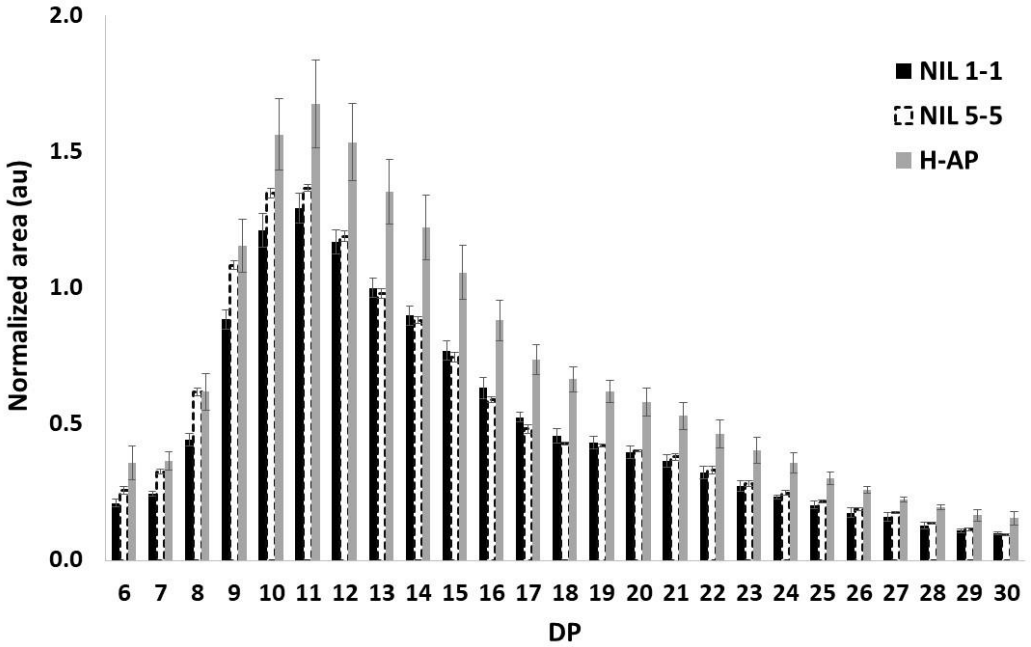

Figure 5.1 Levels of chains with degree of polymerization (DP) 6-30 (normalized to the internal standard, rhamnose) after debranching the starch fraction in fresh crumb from NIL 1-1, NIL 5-5 and H-AP bread as measured with high performance anion exchange chromatography and pulsed amperometric detection. Levels are given in arbitrary units (au).

In Chapter 4, it was shown *inter alia* with TD ^{1}H NMR that primarily H-AP and to a limited extent also NIL 5-5 dough retains water better than NIL 1-1 dough (*cf.* §4.3.1). Earlier, other research teams also noted a higher water absorption with a larger portion waxy wheat, which contains no AM, in a dough system (Hayakawa *et al.*, 2004; Lee *et al.*, 2001). Here, NIL 1-1, NIL 5-5 and H-AP bread loaves were prepared with the same amount of water to study the impact of different AM to AP ratios and/or AP chain length distributions on fresh bread properties and on starch transitions during storage. This resulted in bread loaves with similar crumb MCs (Table 5.3) and, thus, comparable NMR population E areas of their fresh crumbs (Table 5.2). Population E contains mobile exchanging protons of water, starch and gluten in the gel network (Bosmans *et al.*, 2012). Its area has been related to crumb MC (Bosmans *et al.*, 2013c). The crust MC of H-AP bread was (slightly) higher than that of NIL 1-1 and NIL 5-5 bread (Table 5.3).

With AM contents which decreased in the order NIL 1-1, NIL 5-5 and H-AP fresh bread, the area of NMR population A in their crumb, containing rigid CH protons of starch (*e.g.* AM crystals) and gluten not in contact with water (Bosmans *et al.*, 2012), decreased (Table 5.2). The mobility of population E protons in their crumb increased in that order and is inversely related to the strength and rigidity of the gel network (Bosmans *et al.*, 2013c). As pointed out in Chapter 4 (*cf.* §4.3.1.2), these observations thus indicated that in crumb containing less AM, a less rigid and less extended semicrystalline AM network is present. Indeed, the structure of

fresh NIL 5-5 and H-AP bread was such that the bread loaves were not sliceable and that texture parameters could thus not be determined (Table 5.3). In line with observations for bread made from waxy wheat flour (Hayakawa *et al.*, 2004), crumb of H-AP bread loaves was sticky and the bread volumes were significantly lower than those of NIL 1-1 and NIL 5-5 breads (results not shown). It is suggested that the absence of a continuous semicrystalline AM network resulted in collapse of the structure at the end of baking and during cooling. Since the mobility of population E protons is inversely related to the extent to which crumb networks developed, its higher value in fresh H-AP bread crumb than in fresh NIL 1-1 and NIL 5-5 bread crumb (Table 5.2) could also result from the presence of a less extended gluten network in the former. This was evidenced by a higher SDS-EP value of H-AP bread crumb (Table 5.3). Protein polymerization through SS bond formation therefore had occurred to lower extent during H-AP bread baking.

Table 5.2 Transverse (T_2) relaxation times and areas of free induction decay (FID) population A (containing rigid CH protons of starch and gluten not in contact with water) and Carr-Purcell-Meiboom-Gill (CPMG) population E (containing exchanging protons of water, starch and gluten in the gel network) of crumb from NIL 1-1, NIL 5-5, H-AP and H-AP 70 bread stored with crust for 0, 2 or 7 days at 23 °C.

Bread type	Storage time (days)	Population A (FID)		Population E (CPMG)	
		T_2 relaxation time (ms)	Area (au)	T_2 relaxation time (ms)	Area (au)
NIL 1-1	0	0.0131 (0.0004)^{bB}	4632 (171)^{cA}	9.61 (0.62)^{aD}	8731 (205)^{aB}
	2	0.0132 (0.0003)^{bB}	7148 (271)^{bA}	7.69 (0.76)^{bC}	8314 (275)^{bB}
	7	0.0135 (0.0002)^{aA}	9850 (186)^{aA}	5.25 (0.21)^{cC}	7297 (95)^{cC}
NIL 5-5	0	0.0136 (0.0020)^{aA}	4056 (167)^{cB}	10.07 (0.19)^{aC}	8809 (85)^{aB}
	2	0.0136 (0.0005)^{aA}	4945 (316)^{bD}	8.29 (1.00)^{bBC}	8389 (310)^{bB}
	7	0.0135 (0.0002)^{aA}	7943 (215)^{aC}	5.72 (0.25)^{cB}	7781 (171)^{cB}
H-AP	0	0.0144 (0.0021)^{aA}	2656 (208)^{cC}	10.70 (0.93)^{aB}	8735 (194)^{aB}
	2	0.0139 (0.0008)^{aA}	6256 (450)^{bB}	8.30 (0.70)^{bB}	8510 (211)^{bB}
	7	0.0138 (0.0007)^{aA}	9282 (406)^{aB}	5.82 (0.28)^{cB}	7892 (114)^{cB}
H-AP 70	0	0.0095 (0.0012)^{cC}	2870 (531)^{cC}	15.84 (0.77)^{aA}	9516 (160)^{aA}
	2	0.0124 (0.0007)^{bC}	5383 (418)^{bC}	10.53 (1.52)^{bA}	8988 (239)^{bA}
	7	0.0134 (0.0007)^{cA}	8202 (531)^{aC}	7.14 (0.82)^{cA}	8438 (233)^{cA}

Areas are given in arbitrary units (au).
Standard deviations are indicated between brackets.
Within one column, values with a different small letter at different storage times for the same bread type and values with a different capital letter at the same storage time for different bread types differ significantly from each other ($P<0.05$).

During storage at room temperature, both AP retrogradation and moisture redistribution contributed to crumb firming (Bosmans *et al.*, 2013c). Crumb to crust moisture migration in NIL 1-1 and NIL 5-5 bread loaves occurred to similar extents (Table 5.3). However, H-AP crumb moisture was better retained than that of crumb of NIL 1-1 and NIL 5-5 breads. This was

attributed to the higher crust MC of fresh H-AP bread loaves (Table 5.3) which resulted in a lower driving force for crumb to crust moisture migration. That crumb moisture was better retained in H-AP than in NIL 1-1 bread loaves during storage for 7 days went hand in hand with the higher area of NMR population E in crumb of stored H-AP bread than in that of NIL 1-1 bread (Table 5.2). However, the area of population E in crumb of stored NIL 5-5 bread was similar to that in crumb of stored H-AP bread and, thus, higher than that in crumb of stored NIL 1-1 bread. These results indicated that crumb MC during storage decreased less when AP content in bread was higher. Lee *et al*. (2001) also observed higher crumb MCs after storage for 7 days of bread loaves baked from starch-gluten blends with up to 50% waxy wheat starch in the blend.

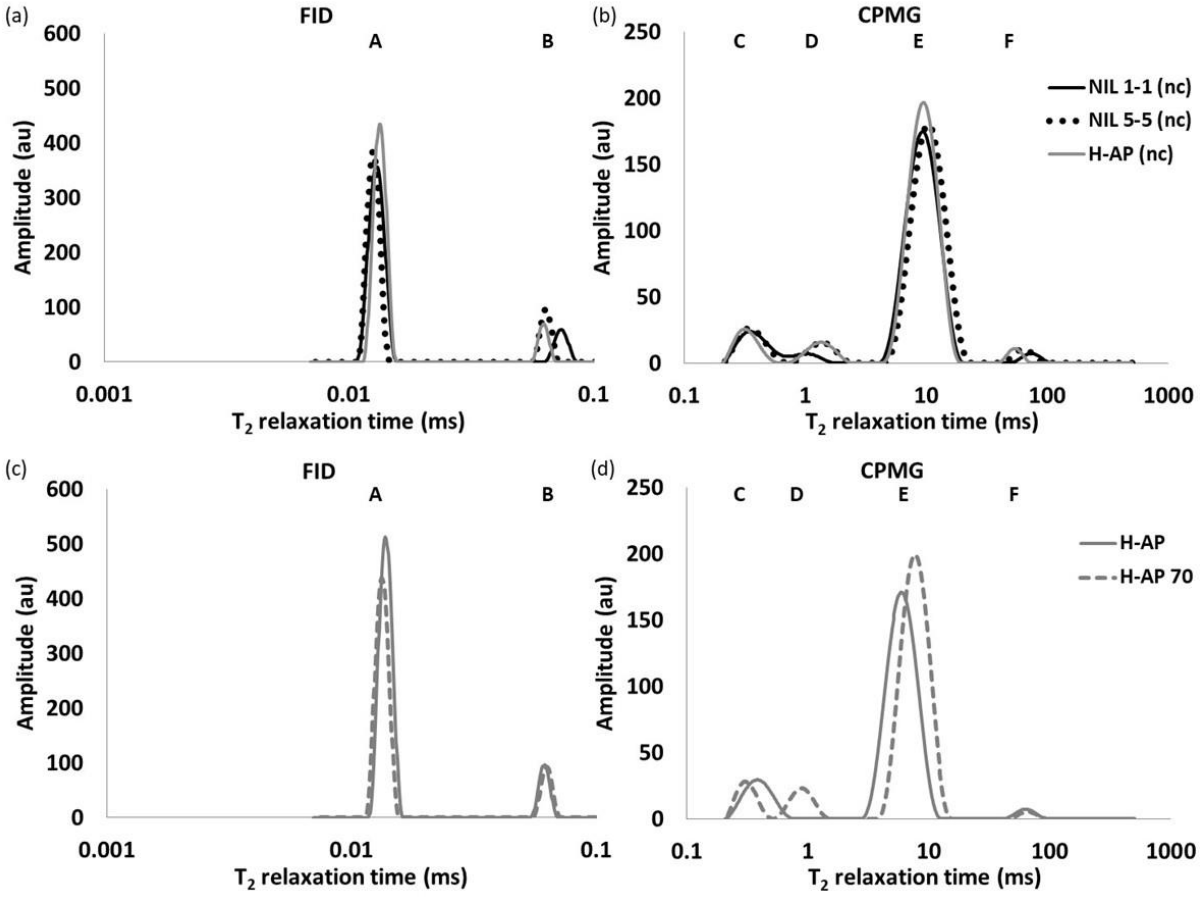

Figure 5.2 (a, c) Free induction decay (FID) and (b, d) Carr-Purcell-Meiboom-Gill (CPMG) proton distributions of crumb from NIL 1-1, NIL 5-5 and H-AP bread stored for 7 days without crust (no crust, nc) and from H-AP and H-AP 70 bread stored for 7 days with crust. Amplitudes are given in arbitrary units (au).

Retrograded AP was quantified over time by measuring the area of population A, containing rigid CH protons of *inter alia* AP crystals not in contact with water, (Table 5.2) and its melting enthalpy (Table 5.3) with respectively ^{1}H NMR and DSC. During storage for 7 days, the increase in the area of population A and the melting enthalpy of retrograded AP occurred to lesser and greater extent in respectively NIL 5-5 and H-AP bread than in NIL 1-1 bread. According to Tolstoguzov (2003), an increased starch content favors retrogradation. Earlier, Zeleznak and Hoseney (1986) found the extent of starch retrogradation to increase with its concentration (up to 60% starch) in starch gels or bread. While the different bread crumbs contained very comparable starch levels, the portion of AP, which is responsible for retrogradation, increased in the order NIL 1-1, NIL 5-5 and H-AP bread. This clearly resulted in an increased extent of retrogradation in H-AP bread during storage. That H-AP crumb retained moisture better than NIL 1-1 crumb may also have contributed to the greater extent of AP retrogradation during storage of H-AP bread. After 7 days of storage, the crumb MC of H-AP bread was 38.2% while that of NIL 1-1 bread was 35.7% (Table 5.3). Maximal starch retrogradation has been observed when the crumb MC was about 40% (Zeleznak & Hoseney, 1986). Furthermore, crumb from H-AP bread contained mainly more longer branch chains (DP ≥ 10) (Figure 5.1). As outlined above, according to Shi and Seib (1992) the extent of retrogradation is positively or negatively related to the portion of AP branch chains with respectively DPs 14-24 or 6-9. That crumb of NIL 5-5 bread contained more short AP branch chains (DPs 6-10) than that of NIL 1-1 bread (Figure 5.1) may explain the lower extent of retrogradation during storage of NIL 5-5 bread despite its higher AP level.

The extent of AP retrogradation during storage of the different bread types was possibly also related to the damaged starch content of the respective flour samples. It has been shown that the melting enthalpy of retrograded AP crystals in pastry crumb stored for 2 days (Ooms *et al.*, 2018) or bread crumb stored for 1 or 3 days (León *et al.*, 2006) is higher when the samples were prepared from flour containing more damaged starch. The greater extent of retrogradation during storage of H-AP bread than during storage of NIL 1-1 bread could thus partly be due to the higher damaged starch content of H-AP flour than of NIL 1-1 flour (Table 5.1). NIL 5-5 flour also contained more damaged starch than NIL 1-1 flour. Nevertheless, retrogradation occurred to lesser extent during storage of NIL 5-5 bread than during storage of NIL 1-1 bread. As was the case for the gelatinization behavior during baking of NIL 1-1, NIL 5-5 and H-AP bread, it is assumed that the extent of retrogradation during bread storage is mainly determined by the AP content and AP chain length distribution of the flour samples used.

Table 5.3. Crumb and crust moisture content (MC), crumb firmness and resilience and crumb melting enthalpy of retrograded amylopectin (ΔH_{AP}) from NIL 1-1 and NIL 5-5 bread produced with and without use of *Bacillus stearothermophilus* α-amylase (BStA), H-AP and H-AP 70 bread stored for 0, 2 or 7 days at 23 °C. Protein extractability in sodium dodecyl sulfate-containing medium (SDS-EP). All breads but H-AP 70 were produced with 59.0% of water, the latter with 70.0% water.

Bread type	Storage time (days)	MC (%)		Intrinsic crumb firmness (N.cm³/g)	Crumb resilience (%)	ΔH_{AP} [J/g crumb (dm)]	SDS-EP (%)
		Crumb	Crust				
NIL 1-1	0	43.7 (0.7)^{aBC}	13.3 (1.9)^{cBC}	2.8 (0.1)^{cB}	54.6 (1.7)^{aA}	0.3 (0.1)^{cA}	18.0 (1.1)^{C}
	2	42.5 (0.4)^{bB}	18.7 (1.0)^{bB}	8.3 (0.5)^{bB}	48.6 (1.2)^{bA}	2.5 (0.4)^{bAB}	
	7	35.7 (1.0)^{cC}	22.6 (1.3)^{aBC}	23.6 (0.8)^{aB}	36.5 (1.2)^{cA}	3.8 (0.3)^{aB}	
NIL 5-5	0	44.4 (0.4)^{aB}	11.9 (0.7)^{cC}	n.d.	n.d.	0.2 (0.1)^{cA}	17.1 (0.7)^{C}
	2	41.3 (0.4)^{bC}	20.3 (2.0)^{bB}	3.5 (0.6)^{bC}	48.2 (2.5)^{aAB}	0.5 (0.1)^{bD}	
	7	35.7 (0.8)^{cC}	23.0 (0.8)^{aB}	11.3 (0.8)^{aC}	37.9 (1.7)^{bA}	1.9 (0.1)^{aC}	
H-AP	0	42.4 (1.1)^{aCD}	16.9 (2.2)^{cAB}	n.d.	n.d.	0.3 (0.1)^{cA}	23.4 (0.9)^{A}
	2	41.0 (1.5)^{aBCD}	24.2 (0.7)^{bA}	14.4 (2.8)^{bA}	41.4 (1.4)^{aCD}	3.0 (0.3)^{bA}	
	7	38.2 (1.0)^{bB}	26.4 (0.9)^{aA}	56.1 (5.2)^{aA}	28.0 (2.8)^{bC}	4.7 (0.5)^{aA}	
NIL 1-1 + BStA	0	42.0 (0.9)^{aD}	13.2 (1.2)^{bC}	3.8 (0.3)^{cA}	44.1 (2.0)^{aB}	0.2 (0.0)^{bA}	n.d.
	2	40.2 (0.7)^{bCD}	19.6 (1.4)^{aB}	7.0 (0.9)^{bB}	44.2 (1.5)^{aBC}	1.1 (0.1)^{aC}	
	7	33.4 (1.0)^{cD}	21.1 (0.6)^{aC}	13.0 (0.6)^{aC}	32.6 (0.9)^{bB}	1.4 (0.4)^{aC}	
NIL 5-5 + BStA	0	42.4 (1.0)^{aCD}	11.5 (1.4)^{bC}	2.2 (0.3)^{bB}	36.8 (0.6)^{bC}	0.1 (0.0)^{cA}	n.d.
	2	38.6 (0.8)^{bD}	20.1 (2.1)^{aB}	5.5 (0.9)^{aBC}	45.1 (0.8)^{aB}	0.2 (0.0)^{bE}	
	7	33.6 (1.3)^{cCD}	21.9 (0.5)^{aBC}	5.4 (0.4)^{aD}	33.8 (1.1)^{cB}	0.6 (0.1)^{aD}	
H-AP 70	0	47.1 (0.4)^{aA}	17.5 (0.9)^{cA}	n.d.	n.d.	0.2 (0.1)^{cA}	20.2 (0.3)^{B}
	2	45.1 (0.7)^{bA}	23.7 (0.8)^{bA}	3.4 (0.9)^{bC}	41.0 (1.2)^{aD}	2.0 (0.4)^{bB}	
	7	41.3 (0.4)^{cA}	26.2 (0.6)^{aA}	20.7 (4.8)^{aBC}	32.9 (1.1)^{bB}	4.8 (0.6)^{aA}	

dm: dry matter.

Standard deviations are indicated between brackets.

n.d.: not determined.

Within one column, values with a different small letter at different storage times for the same bread type and values with a different capital letter at the same storage time for different flour or bread types differ significantly from each other ($P<0.05$).

The firming of bread crumb due to AP retrogradation can be studied without interference from crumb to crust moisture migration (Bosmans *et al.*, 2013c). During storage of NIL 1-1 crumb without crust, the mobility of some CH protons of gluten and exchanging protons of confined water, starch and gluten in population D (Bosmans *et al.*, 2012) decreased such that these protons ended up in population C [Figure 5.2 (b)]. According to Bosmans *et al.* (2013c), this partial merger of populations C and D in crumb stored without crust can be attributed to dehydration of the gluten network when water is withdrawn from gluten and *inter alia* incorporated in the formed B-type AP crystals (*cf.* §2.2.4). In stored NIL 5-5 crumb, populations C and D appeared well separated [Figure 5.2 (b)]. This indicated that a less prominent starch network with less water inclusion was formed during storage such that crumb networks remained better hydrated (Bosmans *et al.*, 2013a). This was in line with the limited extent of AP retrogradation during storage of NIL 5-5 bread as evidenced by ^{1}H NMR and DSC data (Tables 5.2 and 5.3). In H-AP crumb, populations C and D also remained well separated after storage without crust [Figure 5.2 (b)]. Although the extent of retrogradation was higher in H-AP than in NIL 1-1 bread loaves, H-AP crumb networks apparently remained better hydrated. It is postulated that the greater ability of H-AP flour components to bind and retain water (*cf.* §4.3.1) is responsible for better hydrated and plasticized networks in stored bread crumb in spite of the increased extent of AP retrogradation and the related moisture migration from gluten to starch.

During storage of whole bread loaves, both AP retrogradation (and the related moisture migration from gluten to starch) and crumb to crust moisture migration contributed to the increased crumb firmness and decreased resilience (Table 5.3). Firming of crumb networks caused the mobility of population E protons to decrease (Table 5.2). After 7 days of storage of bread loaves, the most firm and less resilient crumbs were those of bread containing little if any AM (Table 5.3). Although NIL 5-5 bread contained less AM than NIL 1-1 bread, its crumb remained softer during storage (Table 5.3). It follows that the extent of crumb firming reflects the degree of AP retrogradation during storage of the different bread types studied. H-AP crumb MC and crumb networks' hydration was better retained during storage. However, the increased degree of retrogradation (and related gluten to starch moisture redistribution) due to H-AP flour's high AP content caused the crumb to firm more than that of NIL 1-1 bread. The higher portion of short AP chains (DPs 6-10) in NIL 5-5 crumb resulted in a limited extent of AP retrogradation and, therefore, crumb firmed less than NIL 1-1 crumb during storage of bread.

5.3.2 Breads prepared with different water contents

As already pointed out in Chapter 4, H-AP flour strongly retains water. For this reason, and to study the impact of different water contents on starch transitions and water redistribution during storage, H-AP dough was also prepared with a higher amount of water (*i.e.* H-AP 70 dough) which was determined with Farinograph analysis. Evidently, the crumb MC and related NMR population E area of crumb from the resulting fresh H-AP 70 bread loaves were higher than those of regular H-AP bread loaves (Tables 5.3 and 5.2). Crust MCs of both bread types were similar (Table 5.3). Because of the increased availability of water, H-AP 70 bread loaves were bigger (results not shown) and their crumbs more sticky than those of the H-AP bread loaves produced at lower moisture levels. Loaf volume and, thus, bread density is strongly related to gluten properties (Lagrain *et al.*, 2012). Since higher loaf volumes result when flour can be developed into dough of higher water levels (Roels *et al.*, 1993) and water is essential for interaction between flour proteins (Huschka *et al.*, 2012), it is postulated that the increased loaf volume of H-AP bread with higher water content *inter alia* resulted from improved interaction between gluten proteins. The lower SDS-EP value of fresh H-AP 70 bread crumb than of fresh H-AP bread crumb (Table 5.3) showed indeed that a more extended protein network was formed in H-AP 70 bread. It is suggested that suboptimal water contents in H-AP dough/bread restrict interaction between flour proteins. Consequently, protein polymerization during baking is limited. When dough was prepared with a higher amount of water, protein network formation during baking was enhanced.

As for fresh H-AP bread, the lack of sliceability of fresh H-AP 70 bread and its lower NMR population A area and higher population E proton mobility than in NIL 1-1 bread (Table 5.2) resulted primarily from the absence of a structure forming semicrystalline AM network. Although the gluten network in fresh H-AP 70 bread was more extended than that of H-AP bread (Table 5.3), the mobility of population E protons in H-AP 70 bread was even higher than in H-AP bread. Evidently, this was the result of the higher crumb MC of H-AP 70 than of H-AP bread.

During storage of H-AP 70 whole bread loaves, crumb MC decreased due to crumb to crust moisture migration. The crumb MC of stored H-AP 70 bread remained higher than that of the other stored bread loaves (Table 5.3). Higher areas of NMR population E in stored H-AP 70 bread crumb than in that of other bread types confirmed these findings (Table 5.2). DSC results demonstrated that during 7 days of storage AP retrogradation occurred to similar extents in H-AP 70 and H-AP bread crumb (Table 5.3). That the area of NMR population A after storage was lower in crumb from H-AP 70 than in that of H-AP bread [Table 5.2, Figure 5.2 (c)] was attributed to its higher MC. The latter understandably increased the contact of protons with

water. Since population A contained rigid protons not in contact with water, the portion of these protons was lower when the crumb MC was higher. Although the extent of retrogradation eventually was similar, it seemed that the rate of retrogradation was lower in crumb of H-AP 70 bread than in that of H-AP bread. In particular, the enthalpy of retrograded AP crystals after 2 days of storage was lower than that in crumb of H-AP bread (Table 5.3). Based on DSC results, several authors earlier concluded that increasing MCs of starch gels and bread increases the extent of AP retrogradation until a maximum is reached. Further increasing MCs causes the extent of retrogradation to decrease again (Zeleznak & Hoseney, 1986) due to dilution of the crystallizing polymer (Slade *et al.*, 1991). Zeleznak and Hoseney (1986) observed maximal starch retrogradation when the crumb MC was about 40%. Crumb MCs of H-AP bread loaves were around such value (Table 5.3). Higher crumb MCs from H-AP 70 bread loaves are thus suggested to slow down AP retrogradation during storage.

During storage of whole bread loaves for 7 days, NMR populations C and D over time merged in H-AP crumb while they remained clearly separated in crumb of stored H-AP 70 bread [Figure 5.2 (d)]. This was attributed to the higher crumb MC of the latter since retrogradation eventually occurred to the same extent in both bread types. From earlier work it follows that a better retained crumb MC during storage relates to better hydration of biopolymer networks (Bosmans *et al.*, 2013b). The higher crumb MC and better plasticized crumb networks resulted in a higher mobility of gel network protons in crumb from stored H-AP 70 bread than in other bread crumb samples (Table 5.2). A higher NMR population E proton mobility reflects a softer crumb (Bosmans *et al.*, 2013c). In the present case, when H-AP bread contained more water, its extent of crumb firming was indeed strongly reduced. In spite of the higher extent of retrogradation in H-AP 70 than in NIL 1-1 bread during 7 days of storage, crumb firmness readings of stored H-AP 70 bread were comparable to those of stored NIL 1-1 bread (Table 5.3). This illustrates the importance of both AP retrogradation and crumb networks' hydration to the firmness of crumb from stored bread.

The decreased extent of crumb firming because of improved plasticization of crumb networks furthermore resulted in a higher final crumb resilience of stored H-AP 70 bread than that of stored H-AP bread. Higher crumb resilience readings presumably also resulted from the presence of a more extended gluten network in H-AP 70 bread (Table 5.3). The resilience of stored H-AP 70 crumb, however, was still lower than that of stored NIL 1-1 crumb due to the absence of an initial structure forming AM network. Also, the gluten network in H-AP 70 bread was less extended than that in NIL 1-1 bread, as evidenced by SDS-EP readings (Table 5.3). Previous work already indicated that less extended AM and gluten networks in fresh bread result in lower crumb resilience (Bosmans *et al.*, 2013b).

5.3.3 Breads prepared with use of maltogenic α-amylase

The NIL 1-1 bread recipe was supplemented with BStA to investigate whether its crumb firming mechanism resembled that of NIL 5-5 bread, which contained more short AP branch chains (DPs 6-10) than NIL 1-1 bread (Figure 5.1). BStA mainly hydrolyzed the exterior AP branch chains such that the resultant NIL 1-1 bread contained more short (DPs 6-8) and less longer (DPs 10-12) AP branch chains [Figure 5.3 (a)]. When BStA was included in the NIL 5-5 bread recipe, the portion of short branch chains with DPs 6-8 increased at the expense of those with a higher DP [Figure 5.3 (a)].

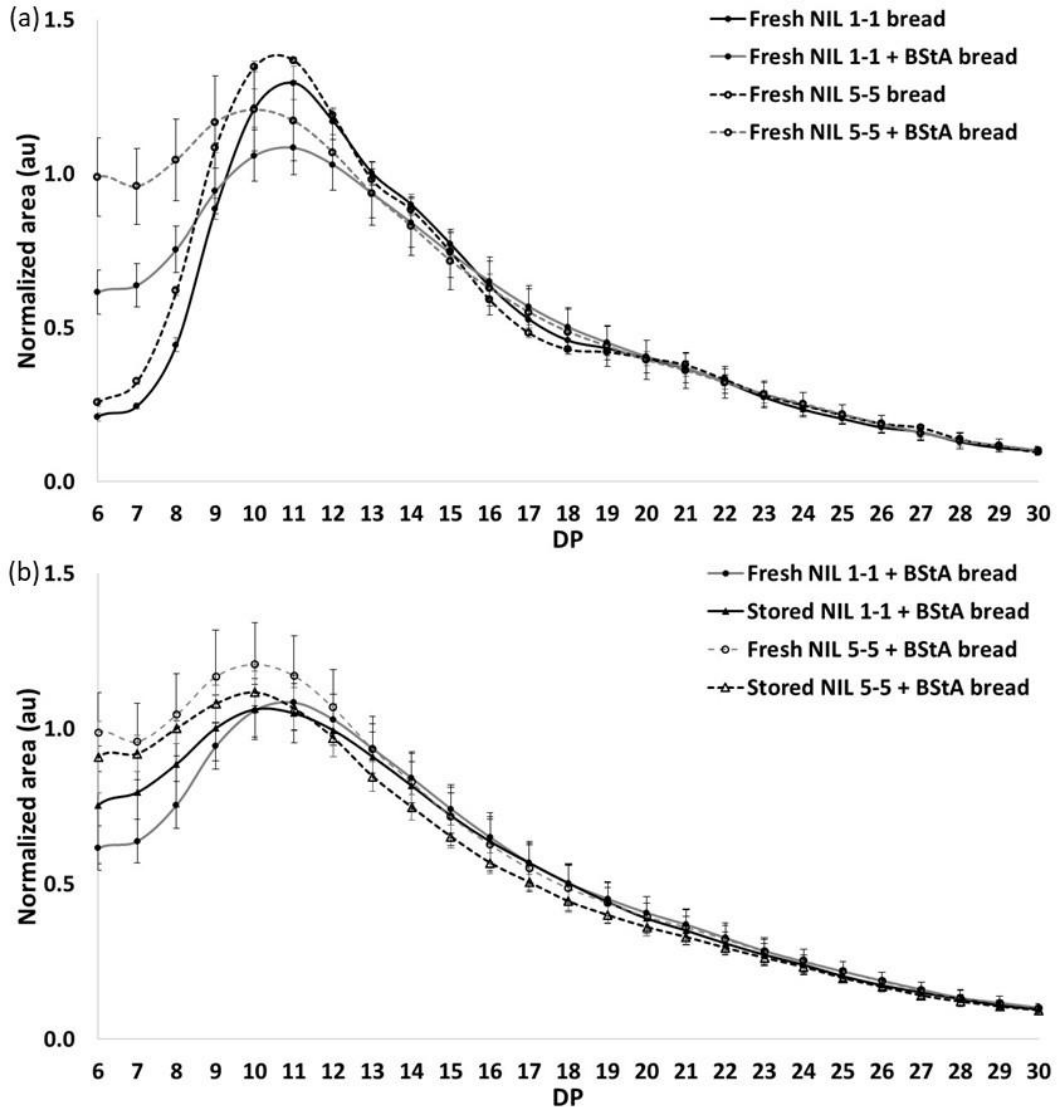

Figure 5.3 Levels of chains with degree of polymerization (DP) 6-30 (normalized to the internal standard, rhamnose) after debranching the starch fraction in (a) fresh crumb from NIL 1-1 and NIL 5-5 bread with and without *Bacillus stearothermophilus* amylase (BStA), and (b) fresh crumb and crumb stored for 7 days from NIL 1-1 and NIL 5-5 bread with BStA as measured with high performance anion exchange chromatography and pulsed amperometric detection. Levels are given in arbitrary units (au).

During storage, AP branch chains of bread loaves produced from BStA-containing recipes were further hydrolyzed [Figure 5.3 (b)] since this enzyme remains active after baking (Bosmans *et al.*, 2013a; Lagrain *et al.*, 2008b). It thereby releases mainly maltose (results not shown) and as a result slightly increases the level of short AP branch chains (DPs 6-10) in crumb of NIL 1-1 bread made from a recipe containing BStA. During storage of NIL 5-5 bread produced with a BStA-containing recipe, branch chain length in general decreased slightly due to release of maltose (results not shown) [Figure 5.3 (b)].

Apart from the MW of AP, also that of AM decreases because of hydrolysis by BStA during baking (Goesaert *et al.*, 2009a). As a result, the AM chains in bread crumb at the end of baking and during cooling have increased mobility (*cf.* §4.3.2). More mobile AM chains have been suggested to enhance AM crystallization and, thus, the formation of a semicrystalline AM network during cooling (Hug-Iten *et al.*, 2001). In line with results of Bosmans *et al*. (2013a), this effect was reflected in an increased area of NMR population A [Figure 5.4 (a)] and a decreased mobility of NMR population E protons [Figure 5.4 (b)] when NIL 1-1 bread was prepared with use of BStA. Fresh crumb of NIL 1-1 bread produced from a BStA-containing recipe was consequently more firm and less resilient than that of fresh control bread (Table 5.3). BStA action during NIL 5-5 bread making also resulted in an increased area of population A in fresh crumb [Figure 5.4 (c)]. However, the population E protons did not become less mobile [Figure 5.4 (d)]. Nevertheless, BStA inclusion in the NIL 5-5 bread recipe resulted in crumb with a desirable initial firmness since fresh bread loaves were sliceable. It is postulated that enhanced AM crystallization increased the rigidity of the AM network and, therefore, the initial crumb firmness and sliceability. The reduced AM content in NIL 5-5 crumb samples, however, was still responsible for a less extended AM network than in NIL 1-1 crumb. The very low initial crumb resilience in NIL 5-5 bread produced with BStA use supports this hypothesis (Table 5.3). From these results, it follows that initial crumb resilience is negatively impacted by either an AM network which is

(i) less extended when crumb contains less AM (*e.g.* NIL 5-5 bread), or
(ii) too rigid due to enhanced AM crystallization (*e.g.* because of BStA action) in crumb with apparently an already optimal resilience (*e.g.* control NIL 1-1 crumb).

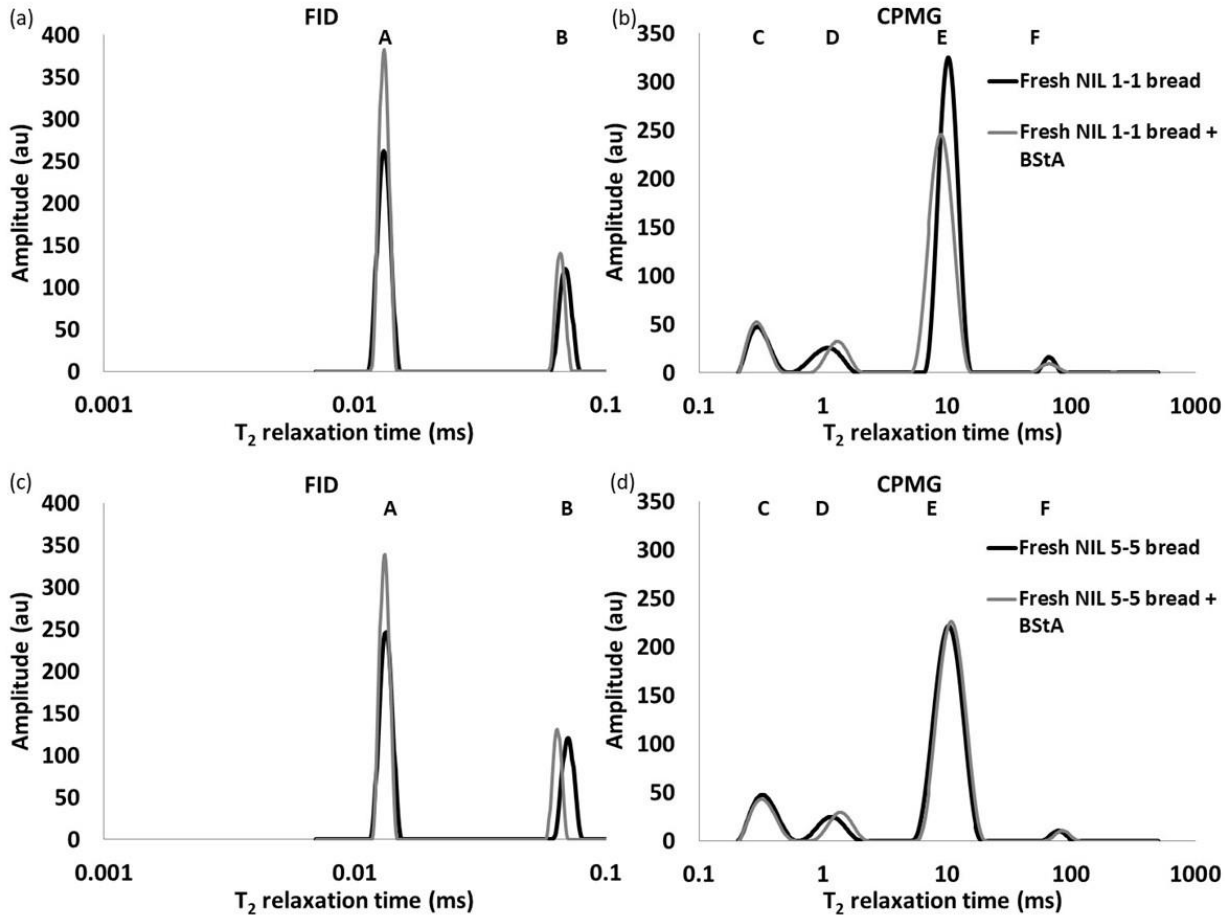

Figure 5.4 (a, c) Free induction decay (FID) and (b, d) Carr-Purcell-Meiboom-Gill (CPMG) proton distributions of crumb from fresh NIL 1-1 and NIL 5-5 bread made with and without use of *Bacillus stearothermophilus* amylase (BStA). Amplitudes are given in arbitrary units (au).

The decrease and increase of respectively crumb and crust MC because of moisture migration during storage occurred to similar extents in NIL 1-1 and NIL 5-5 breads irrespective of whether their recipes contained BStA (Table 5.3). The extent of retrogradation and the related moisture redistribution from gluten to starch thus determined the extent of crumb firming. As a result of BStA action, the portion of short AP branch chains (DPs 6-8) increased. This limited the degree to which retrogradation occurred in crumb from NIL 1-1 bread produced with use of BStA. The final level of retrograded AP crystals formed now resembled that in crumb of NIL 5-5 bread stored for 7 days (Table 5.3). Stored crumb of NIL 1-1 bread produced from a BStA-containing recipe thus contained a less prominent starch network in which less water was included such that the gluten network remained better hydrated. As expected, this resulted in a better conservation of crumb softness than during storage of control NIL 1-1 crumb (Table 5.3). Final firmness readings in crumb of stored NIL 1-1 bread produced with BStA use were similar to those of crumb of stored NIL 5-5 bread. Final crumb resilience values of stored NIL 1-1 bread produced with BStA use were lower than those of stored NIL 1-1 crumb (Table 5.3).

This was related to the lower initial crumb resilience of crumb of NIL 1-1 bread prepared with BStA use which itself was related to a too rigid AM network.

The already limited degree of retrogradation in NIL 5-5 crumb was lower when the outer AP branch chains were further trimmed by BStA [Table 5.3, Figure 5.3 (a)]. As a consequence, crumb softness was even better retained during bread storage. The enzyme thus increased both the quality of fresh and stored NIL 5-5 bread (in terms of crumb texture properties) since the resultant fresh bread loaves were sliceable and crumb firming during 7 days of storage was almost fully prevented (Table 5.3). Limited strengthening of the less extended starch network (due to the lower AM content) initially increased crumb resilience after 2 days of storage (Table 5.3). During further storage, crumb resilience decreased again. The strengthening of crumb networks will mainly result from crumb to crust moisture migration since AP retrogradation was almost prevented in NIL 5-5 bread prepared with BStA use (Table 5.3). These findings support the above mentioned hypothesis that a standard fresh bread loaf with extended, hydrated biopolymer networks has an optimal crumb resilience. When biopolymer networks are less extended, too rigid or become dehydrated, crumb resilience decreases.

5.4 CONCLUSIONS

Starch transitions together with water (re)distribution in bread significantly determine fresh and stored bread quality. The continuous semicrystalline AM network formed during cooling is an essential structuring entity in fresh bread. When AM levels are too low, bread loaves with too soft crumb and, therefore, inferior sliceability are obtained. Inclusion of BStA in the bread recipe results in more mobile AM molecules with a decreased MW that are more apt to crystallize and consequently lead to increased initial crumb firmness. The semicrystalline AM network and thermoset gluten network in fresh bread impact the crumb resilience. Both a less extended AM and gluten network and a too rigid extended AM network decreases initial crumb resilience.

During storage, both AP retrogradation (and the associated moisture migration from gluten to starch) and crumb to crust moisture migration define the extent of crumb firming. In systems with similar starch contents, low AM levels imply high AP levels. Since AP is responsible for retrogradation, higher AP levels evidently increase the extent of AP retrogradation. The latter is codetermined by the AP chain length distribution. Short exterior branch chains (DPs 6-10) restrict and longer exterior branch chains (DPs > 10) enhance the extent of retrogradation. The high water absorption of flour containing little if any AM is

related to a better preservation of crumb MC and crumb networks' hydration. When different bread types were prepared with the same amount of water, the extent of crumb firming was dominated by the degree of AP retrogradation during storage. When bread from flour with a high AP content and high water absorption was prepared with a higher amount of water, the extent of crumb firming was reduced. Since retrogradation eventually occurred to similar extent, the increased crumb networks' hydration because of the increased crumb water content restricted crumb firming.

Finally, the unique NIL 5-5 wheat flour proved to be very interesting for bread making. Its higher level of short AP branch chains (DPs 6-10) restricted the extent of crumb firming. For the same reason, crumb firming was reduced when BStA was used in NIL 1-1 bread making so that it occurred to a similar extent as that in NIL 5-5 bread. Fresh NIL 5-5 bread loaves, however, were too soft and not sliceable due to their low AM content. Inclusion of BStA in this bread recipe increased both fresh and stored bread quality (in terms of crumb texture). Hydrolysis by BStA reduced the MW of both AM and AP. The resultant more mobile AM chains were more apt to cyrstallize during cooling. The improved rigidity of the semicrystalline AM network resulted in a sliceable bread with a desired initial firmness. The further increased portion of short AP branch chains almost prevented crumb firming during storage for 7 days.

In this chapter, the exact role of AM and AP during crumb firming was studied using unique wheat flours with unusual starches for bread making. In Chapter 6, the bread making process rather than the bread recipe was altered to further improve understanding of the crumb firming mechanism and how this mechanism is impacted by the changes during bread baking and cooling.

Chapter 6
The impact of parbaking on the crumb firming mechanism of tin wheat bread[5]

6.1 INTRODUCTION

For a number of years already, partial baking, *i.e.* parbaking, has been applied in the bread making industry. The partial baking phase is executed in such way that complete crumb setting is realized, but without significant occurrence of Maillard reactions that would result in crust browning. After intermediate storage of the PB bread, the final baking step is performed to melt the AP crystals formed during storage and to obtain a refreshed FB bread with a typical brown crust and aroma (Almeida *et al.*, 2016; Bárcenas & Rosell, 2006; Leuschner *et al.*, 1997).

The quality of FB bread is often said to be lower than that of CB bread baked in a single step (Karaoglu & Kotancilar, 2006; Le-Bail *et al.*, 2005; Ribotta & Le Bail, 2007). FB bread is also believed to firm more rapidly than CB bread (Ghiasi *et al.*, 1984; Rosell & Santos, 2010; Sciarini *et al.*, 2012). However, the published studies have involved PB bread prepared from only 100 g of flour or PB French bread with mostly a frozen or refrigerated intermediate storage phase. The former results in bread loaves with a lower crumb to crust ratio than that of larger tin breads (Baardseth *et al.*, 2000; Rouillé *et al.*, 2010) and therefore are subject to pronounced crumb dehydration due to crumb to crust moisture migration during storage. To the best of our knowledge, the firming mechanisms of both PB and the resultant FB tin bread of a size relevant for households and stored at ambient temperature remain to be elucidated. During storage at room temperature, both AP retrogradation and moisture redistribution contribute to crumb firming (Bosmans *et al.*, 2013c) (c*f*. §5.1).

[5] This Chapter is based on the following reference: Nivelle, M.A., Bosmans, G.M. and Delcour, J.A. (2017) The impact of parbaking on the crumb firming mechanism of fully baked tin wheat bread. Journal of Agricultural and Food Chemistry, 65(46), 10074-10083.

Against this background, the aim of this chapter is to investigate for large tin bread loaves whether

(i) different (partial) baking times impact on fresh bread quality and changes thereof during subsequent ambient storage, whether
(ii) PB and later FB bread firms more rapidly than CB bread, and whether
(iii) the crumb firming mechanism differs when the bread loaf volume decreases.

The toolbox based on TD ^{1}H NMR (Bosmans *et al.*, 2013c) used to study AM and AP functionality during storage in Chapter 5 presents an integrated approach at different length scales to study the water distribution and the properties of starch and gluten networks in crumb and how changes thereof impact crumb texture. This toolbox was also used here to study the crumb firming mechanism of large CB, PB and FB breads.

6.2 MATERIALS AND METHODS

6.2.1 Materials

Crousti flour, compressed yeast, sugar and salt were as in Chapter 3 (*cf.* §3.2.1). Reagents and solvents for determining the starch content and protein extractability under reducing and nonreducing conditions were as in §3.2.1 and §5.2.1, respectively. All other chemicals were from Sigma-Aldrich.

6.2.2 Methods

6.2.2.1 *Composition of wheat flour and bread*

Starch and protein content of wheat flour and MCs of wheat flour, bread crumb and crust were determined as in §3.2.2.2.

6.2.2.2 *Bread making and storage*

To obtain bread loaves with different crumb to crust ratios, dough was prepared from either 100.0 (*cf.* §5.2.2.4), 10.0 or 270 g (*cf.* §3.2.2.3) of flour (100 parts) and deionized water (59 parts). All other ingredients were in appropriate amounts to respect the abovementioned ratios (*cf*. §3.2.2.3). Fermented doughs were conventionally baked in a rotary hearth oven for 13 min at 232 °C, 24 min at 215 °C or 40 min at 210 °C depending on flour weight (10.0, 100.0 or 270 g of flour, respectively). Bread loaves prepared from 270 g flour and baked for 100% of total baking time, *i.e.* 40 min, are further referred to as CB_{100} bread. These bread loaves were also baked for 42.5 and 60% of total baking time (Figure 6.1). The former corresponds to the

minimum baking time required for complete gelatinization and crumb setting and is referred to as $PB_{42.5}$ bread. The latter corresponds to the typical baking time of conventionally baked bread from 270 g flour in industrial practice (*cf.* §3.2.2.3) and is referred to as CB_{60} bread.

After intermediate storage for 6 days, final baking of stored $PB_{42.5}$ and CB_{60} bread loaves was done for respectively 30 and 40% of total baking time at 210 °C, resulting in $FB_{42.5\text{-}30}$ and $FB_{60\text{-}40}$ breads (Figure 6.1). After each baking phase, bread loaves were cooled for 120 min at 23 °C. The crumb center temperature during conventional, partial and final baking and subsequent cooling was monitored as described in §3.2.2.4. Fresh, cooled bread loaves were stored as in §5.2.2.4. The loaf volume was determined with a Volscan Profiler and crumb center samples from at least two bread loaves were further analyzed (*cf*. §6.2.2.3-6.2.2.5). Samples were collected after 0 (*i.e.* after cooling), 3 and 6 days storage of CB and PB bread loaves and after 0, 2, 6 and 7 days storage of FB bread loaves. For comparison reasons, CB_{60} bread loaves were analyzed after both 0, 3 and 6 days of storage and 0, 2, 6 and 7 days of storage.

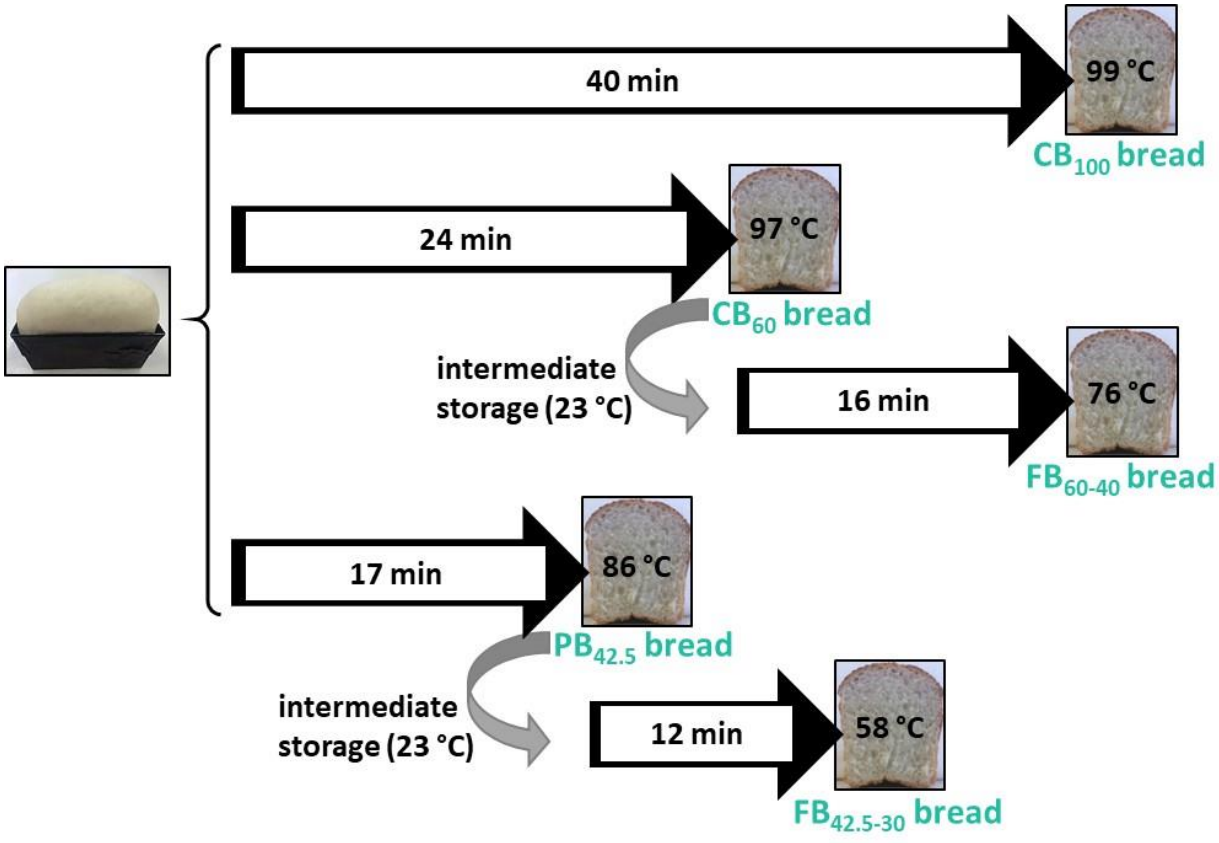

Figure 6.1 Overview of the different baking procedures used. Fermented doughs prepared from 270 g of flour were conventionally baked (CB) or partially baked (PB) for 40, 24 and 17 min, resulting in CB_{100}, CB_{60} and $PB_{42.5}$ bread. The maximum crumb center temperatures reached during these processes were 99, 97 and 86 °C, respectively. After intermediate storage for 6 days at 23 °C, CB_{60} and $PB_{42.5}$ breads were subjected to a second baking step of respectively 16 and 12 min, resulting in fully baked (FB) bread, *i.e.* $FB_{60\text{-}40}$ and $FB_{42.5\text{-}30}$. The maximum crumb center temperatures reached during these processes were 76 and 58 °C, respectively.

6.2.2.3 *Differential scanning calorimetry and proton nuclear magnetic resonance*

The extent of amylopectin retrogradation was studied by DSC as described in §5.2.2.8. Measurements of proton distributions in fresh and stored bread crumb were performed as in §5.2.2.5. Changes in the area and mobility of different proton populations during storage were indicative for AP retrogradation, moisture redistribution and crumb firming.

6.2.2.4 *Size exclusion high performance liquid chromatography*

Freeze-dried samples from fermented dough and from the center of the different bread loaves were extracted under nonreducing and reducing conditions and analyzed as described in §5.2.2.7.

6.2.2.5 *Crumb texture analysis*

Crumb firmness and resilience were measured as described in §5.2.2.6. Crumb firmness was expressed as the maximal force (N) required to compress the sample.

6.2.2.6 *Statistical analysis*

Statistical analyses were carried out as described in §3.2.2.9.

6.3 RESULTS AND DISCUSSION

6.3.1 Breads prepared by different (partial) baking times

After baking for either 42.5, 60 or 100% of the total baking time, a temperature of respectively 86, 97 and 99 °C was reached in the crumb center of the bread loaves prepared from 270 g of flour (Figure 6.1). Apart from its shorter baking time, the crumb center temperature of $PB_{42.5}$ bread was thus lower than that of CB_{60} bread, while the crumb center temperature of the longer baked CB_{100} bread was rather similar to that of CB_{60} bread. Complete crumb setting was attained in all three cases (results not shown). Starch gelatinization was considered to be complete as DSC showed little if any residual melting enthalpy in fresh bread crumb (Table 6.1). Despite differences in maximal crumb temperature, the initial crumb MCs in fresh bread loaves were similar (Table 6.1). Crumb MCs can be related to the areas of NMR population E, containing exchanging protons of water, starch and gluten in the gel network (Bosmans *et al.*, 2012; Bosmans *et al.*, 2013c), which were also similar for all fresh bread loaves (Table 6.2). The initial crust MC, however, decreased with longer baking times (Table 6.1). In fresh $PB_{42.5}$ and CB_{60} bread the areas of NMR population A were similar and significantly lower than that of fresh CB_{100} bread (Table 6.2). The latter population contains rigid CH protons of AM crystals, formed during cooling (*cf.* §3.3.3), and amorphous protons of starch and gluten not in contact with water. Possibly, more AM could crystallize during cooling when the extent of AM leaching during baking increased with increasing baking time and, thus, crumb temperature as reported by Giovanelli *et al*. (1997) and Le-Bail *et al*. (2012). However, using temperature-controlled TD ^{1}H NMR, it was shown for bread prepared from regular wheat flour that AM leaching was complete once the temperature during baking was in a 85 to 90 °C temperature range (*cf.* §3.3.2). The amount of protons in the extragranular space no longer increases because of AM leaching when the crumb temperature further increases until its maximum of about 98 °C after baking for 24 min. This is reflected in similar population A areas in fresh PB_{45} and CB_{60} breads (Table 6.2). Prolonged baking after reaching the maximum crumb temperature might slightly increase the degree to which starch polymers are solubilized in bread crumb. As a result, probably more AM could crystallize during cooling, resulting in an increased area of population A in fresh CB_{100} bread (Table 6.2).

Table 6.1 Moisture content (MC) of crumb and crust, firmness, resilience, melting enthalpy of (retrograded) amylopectin (ΔH_{AP}) and protein extractability in sodium dodecyl sulfate containing medium (SDS-EP) of crumb from bread baked for 42.5 ($PB_{42.5}$), 60 (CB_{60}), or 100% (CB_{100}) of total baking time and stored for 0, 3 or 6 days at 23 °C.

Baking process	Storage time (days)	MC (%)		Crumb firmness (N)	Crumb resilience (%)	ΔH_{AP} [J/g crumb (dm)]	SDS-EP (%)
		Crumb	Crust				
$PB_{42.5}$	0	44.9 (0.5)^{aA}	22.3 (0.4)^{bA}	0.8 (0.1)^{cA}	47.7 (1.9)^{aB}	0.29 (0.22)^{bA}	36.3 (1.1)^{A}
	3	45.2 (0.1)^{aA}	29.0 (0.3)^{aA}	2.2 (0.1)^{bB}	34.0 (0.1)^{bA}	2.29 (0.18)^{aA}	
	6	44.9 (0.1)^{aA}	29.0 (0.4)^{aA}	2.7 (0.2)^{aB}	28.6 (3.0)^{bB}	2.62 (0.18)^{aB}	
CB_{60}	0	45.1 (0.3)^{aA}	20.9 (0.6)^{bA}	1.0 (0.2)^{cA}	54.1 (3.2)^{aA}	0.19 (0.06)^{cA}	22.9 (0.7)^{B}
	3	44.7 (0.1)^{aB}	27.8 (1.9)^{aAB}	2.4 (0.2)^{bB}	36.9 (1.8)^{bA}	2.41 (0.07)^{bA}	
	6	44.2 (0.7)^{aAB}	28.2 (1.2)^{aAB}	3.1 (0.3)^{aB}	33.6 (2.6)^{bAB}	3.14 (0.28)^{aA}	
CB_{100}	0	44.6 (0.9)^{abA}	17.7 (0.4)^{cB}	0.9 (0.2)^{cA}	54.8 (1.0)^{aA}	0.21 (0.09)^{cA}	15.9 (0.4)^{C}
	3	44.5 (0.1)^{aB}	23.8 (0.2)^{bB}	2.9 (0.2)^{bA}	34.2 (3.6)^{bA}	2.26 (0.22)^{bA}	
	6	43.2 (0.3)^{bB}	26.4 (0.6)^{aB}	4.3 (0.4)^{aA}	36.2 (3.2)^{bA}	3.25 (0.33)^{aA}	

Standard deviations are indicated between brackets.

Within one column, values with the same small letter at different storage times of one bread baking process and with the same capital letter at the same storage time for different bread baking processes are not significantly different from each other ($P<0.05$).

In line with previous results (*cf.* §5.3.1), higher population A areas corresponded to lower population E proton mobilities in fresh bread crumb (Table 6.2). A decreased mobility of population E protons was related to the presence of both a more prominent AM network because of more AM crystallization during cooling and a more prominent gluten network. Indeed, SDS-EP values decreased and, therefore, the extent of protein polymerization through SS bond formation increased with increasing baking time and crumb center temperature (Table 6.1). At temperatures lower than 90 °C, mostly glutenin polymerizes (Lagrain *et al.*, 2008a) through both SH-SS exchange reactions (Lavelli *et al.*, 1996; Schofield *et al.*, 1983) and oxidative cross-linking (Veraverbeke *et al.*, 1999). At temperatures exceeding 90 °C, also gliadin becomes covalently incorporated into the gluten network through SH-SS exchange reactions (Lagrain *et al.*, 2008a). Such high temperatures allow for conformational changes which expose regions that are initially unavailable for polymerization reactions (*cf*. §2.2.2) (Guerrieri *et al.*, 1996). In PB_{45} bread, the level of extractable glutenin (eluting between 5 min and 7 min 45 s) and extractable albumin and globulin (eluting between 9 min 30 s and 11 min) had almost decreased to the plateau level of protein extractability observed for CB_{100} bread (Figure 6.2). In $PB_{42.5}$ bread, the center temperature reached was 86 °C. As also noted by Lagrain *et al.* (2008a) some gliadin (eluting between 7 min 45 s and 9 min 30 s) was already incorporated into the gluten network at this temperature. Further incorporation of gliadin required prolonged baking, and its extractability decreased with baking time until a plateau level was reached (Figure 6.2 – CB_{100} bread). Apart from the increased extent of AM crystallization, this increased extent of protein polymerization may contribute to a higher area of population A in CB_{100} bread since the latter would result in an increased portion of gluten polymers interacting with each other instead of with water. Both a more extended AM network and a more extended gluten network in terms of gliadin cross-linking could contribute to a decrease in mobility of population E protons with baking time and temperature. As pointed out above (*cf.* §5.3.3), the presence of more extended biopolymer networks was also reflected in the initial crumb resilience, which was higher for CB_{100} and CB_{60} than for $PB_{42.5}$ bread loaves (Table 6.1). Firmness readings, however, were similar for all fresh bread loaves.

Table 6.2 Transverse (T_2) relaxation times and areas of nuclear magnetic resonance (NMR) free induction decay (FID) population A (containing rigid CH protons of starch and gluten not in contact with water) and Carr-Purcell-Meiboom-Gill (CPMG) population E (containing exchanging protons of water, starch and gluten in the formed gel network) of crumb from bread baked for 42.5 ($PB_{42.5}$), 60 (CB_{60}), or 100% (CB_{100}) of total baking time and stored with crust for 0, 3 or 6 days at 23 °C.

Baking process	Storage time (days)	Population A (FID)		Population E (CPMG)	
		T_2 relaxation time (ms)	Area (au)	T_2 relaxation time (ms)	Area (au)
$PB_{42.5}$	0	0.0129 (0.0004)^{aB}	4601 (87)^{cB}	10.59 (0.32)^{aA}	8958 (123)^{aA}
	3	0.0128 (0.0002)^{aA}	6820 (81)^{bB}	9.67 (0.16)^{bA}	8924 (83)^{aA}
	6	0.0128 (0.0002)^{aA}	7619 (140)^{aA}	8.98 (0.13)^{cA}	8896 (100)^{aAB}
CB_{60}	0	0.0132 (0.0004)^{aA}	4609 (107)^{cB}	10.40 (0.34)^{aA}	8991 (107)^{aA}
	3	0.0129 (0.0003)^{bA}	6857 (166)^{bAB}	9.37 (0.14)^{bB}	9037 (115)^{aA}
	6	0.0129 (0.0002)^{bA}	7607 (341)^{aA}	8.67 (0.23)^{cB}	8944 (82)^{aA}
CB_{100}	0	0.0130 (0.0003)^{aAB}	4803 (129)^{cA}	9.77 (0.19)^{aB}	8893 (130)^{aA}
	3	0.0130 (0.0002)^{aA}	6961 (70)^{bA}	8.88 (0.15)^{bC}	8949 (131)^{aA}
	6	0.0129 (0.0003)^{aA}	7766 (203)^{aA}	8.17 (0.25)^{cC}	8817 (138)^{aB}

Areas are given in arbitrary units (au).

Standard deviations are indicated between brackets.

Within one column, values with a different small letter at different storage times of one bread baking process and with a different capital letter at the same storage time for different bread baking processes are significantly different from each other ($P<0.05$).

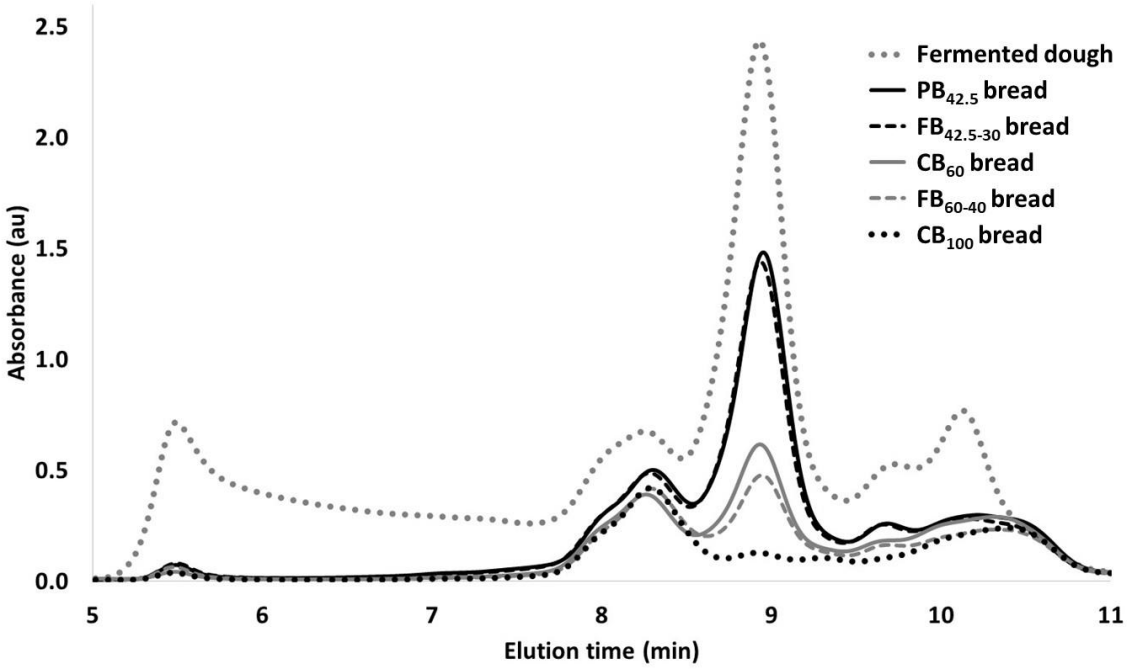

Figure 6.2 Size exclusion high-performance liquid chromatography (SE-HPLC) profiles of protein extracts in sodium dodecyl sulfate (SDS) containing medium of fermented dough, of crumb from fresh bread partially baked for 42.5 ($PB_{42.5}$), 60 (CB_{60}) or 100% (CB_{100}) of total baking time and of crumb from fresh bread fully baked for 42.5 or 60 and 30 or 40% ($FB_{42.5\text{-}30}$ and $FB_{60\text{-}40}$) of total baking time during respectively partial and final baking. Absorbance is given in arbitrary units (au).

Storage impacted crumb MC of all bread loaves to a minor extent. Only that of CB_{100} bread decreased significantly in time (Table 6.1). Accordingly, the area of population E decreased little if any during storage of bread for 6 days, but was the lowest in crumb from stored CB_{100} bread (Table 6.2). However, the crust MC of all bread loaves significantly increased during storage because of crumb to crust moisture migration (Table 6.1). Since the crust MC of fresh CB_{100} bread was lower, a higher moisture gradient between its crumb and crust existed and crumb to crust moisture migration occurred to a larger extent in CB_{100} than in $PB_{42.5}$ and CB_{60} bread loaves. That only a minor portion of crumb water was required to significantly increase crust MC during storage was related to the high crumb to crust ratio of large bread loaves prepared from 270 g of flour. Since crumb MC changed only little during storage, changes in proton distributions observed in crumb samples stored with crust could mainly be attributed to changes in starch and protein networks (Bosmans *et al.*, 2013b). AP retrogradation, measured as an increase in the melting enthalpy of retrograded AP with DSC during storage (Table 6.1), was also detected with ^{1}H NMR as an increase in area of population A (Table 6.2) and a decrease in the areas of populations B and C (Figure 6.3). AP retrogradation causes amorphous CH protons of starch in populations B and C to become more rigid and, thus, to shift to population A (Bosmans *et al.*, 2013c). With higher crumb temperatures reached during baking, a stronger increase in melting enthalpy of retrograded AP as a result of storage was

observed (Table 6.1). This is in line with literature stating that longer baking times and higher crumb temperatures during baking are associated with higher degrees of AP retrogradation (Bosmans *et al.*, 2013b; Giovanelli *et al.*, 1997; Le-Bail *et al.*, 2012). A possible explanation for this is that a lower crumb MC promotes AP retrogradation. Bosmans *et al.*(2014) suggested this based on the relation between crumb MC and the extent of retrogradation described by Zeleznak and Hoseney (1986) (*cf.* §5.3.2). After storage, crumb MC was indeed lower in CB_{100} than in $PB_{42.5}$ bread, although the differences were small (Table 6.1). Zhou *et al.*(2011) further reported that AP retrogradation is affected by AM, provided the water content of starch gels is sufficiently high (70-80%). These authors hypothesized that the AM network, which in our study presumably was more developed in CB_{100} than in $PB_{42.5}$ and CB_{60} bread, immobilizes a considerable amount of water, thereby reduces the local MC, and in this way facilitates AP retrogradation.

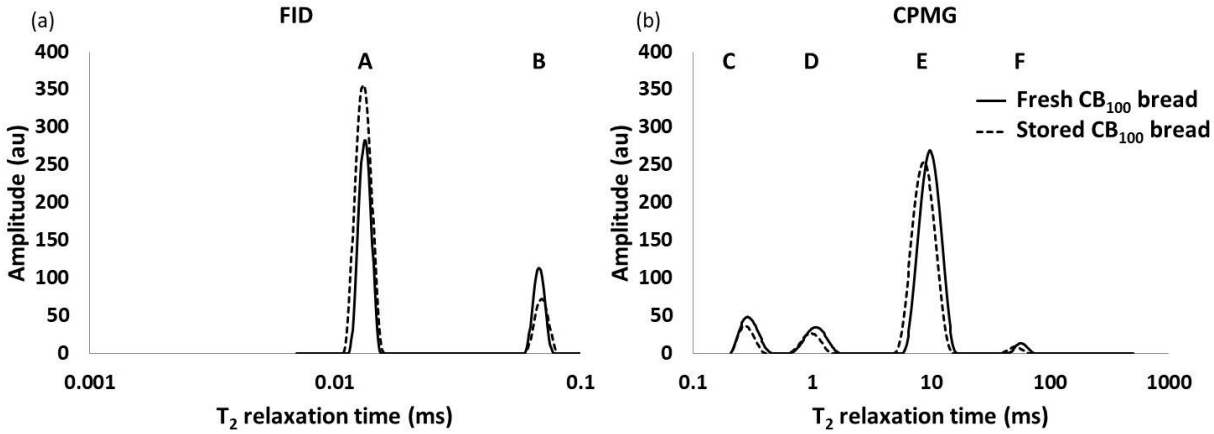

Figure 6.3 Free induction decay (FID) (a) and Carr-Purcell-Meiboom-Gill (CPMG) (b) proton distributions of crumb withdrawn from fresh and stored (6 days at 23 °C) conventionally baked (CB) bread (100% of total baking time). Amplitude is given in arbitrary units (au).

However, it would seem more plausible that the larger extent of AM leaching during prolonged baking results in a higher concentration of AP in the outer zones of the gelatinized granule remnants such that intragranular AP retrogradation during storage can proceed to a larger extent. Several authors have suggested that AM crystals and AM-L complexes in the semicrystalline AM network can serve as nuclei that facilitate AP retrogradation (Van Soest *et al.*, 1994; Vandeputte *et al.*, 2003). The formation of a more extended AM network with more such nuclei because of more AM leaching during prolonged baking may also enhance AP retrogradation. At higher temperatures not only AM but also AP leaches to the extragranular space during baking (Doublier, 1981). Based on research of Ooms *et al*. (2018), it is additionaly hypothesized that when baking continues after reaching the maximum crumb temperature, also more AP is present in the extragranular space. These solubilized AP polymers may be

more apt to recrystallize because they are closer to the extragranular AM network containing crystal nuclei that facilitate AP retrogradation and to other leached AP molecules such that intergranular AP retrogradation is promoted. In contrast to what was detected with DSC, an increased degree of AP retrogradation with increasing baking time could not be detected with NMR (Tables 6.1 and 6.2).

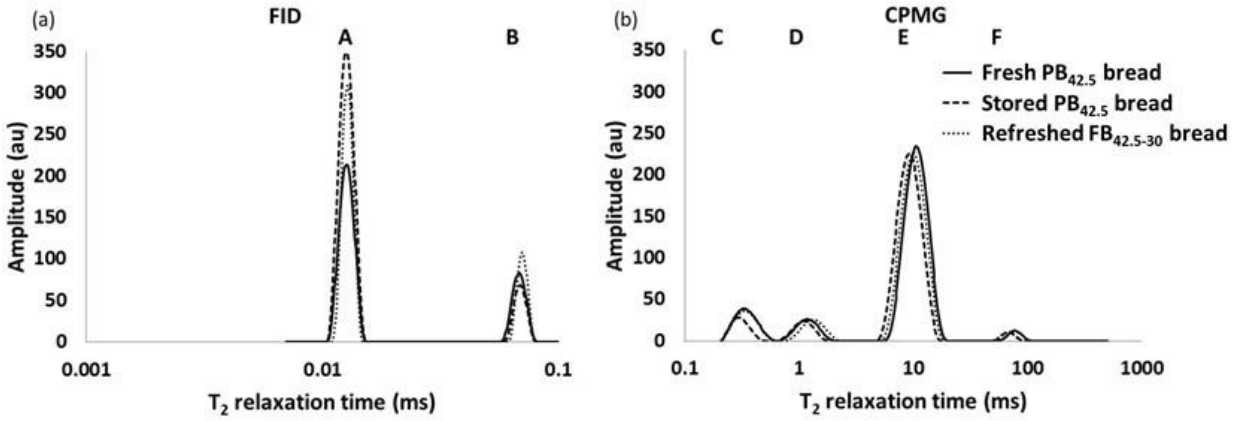

Figure 6.4 Free induction decay (FID) (a) and Carr-Purcell-Meiboom-Gill (CPMG) (b) proton distributions of crumb withdrawn from fresh and stored (6 days at 23 °C) partially baked (PB) bread (42.5% of total baking time) and of refreshed fully baked (FB) bread (42.5 and 30% of total baking time during respectively partial and final baking with an intermediate storage time of 6 days). Amplitude is given in arbitrary units (au).

Independent of baking time, population D shifted to slightly lower T_2 relaxation times during storage [Figures 6.3 (b) and 6.4 (b)]. During storage of bread loaves prepared from 100 g of regular wheat flour, a similar decrease in mobility of population D eventually resulted in it merging with population C (*cf.* §5.3.1) (Bosmans *et al.*, 2013c). This has been attributed to dehydration of the gluten network due to water immobilization in *inter alia* the formed AP B-type crystals and water migration from crumb to crust. In the larger bread loaves described here, populations C and D did not merge as a result of storage [Figures 6.3 (b) and 6.4 (b)]. Possibly, the crumb MC, which remained high during storage of all bread loaves (Table 6.1), compensated for the migration of water from gluten to starch that otherwise would lead to gluten network dehydration. While the area of population E, which is positively related to crumb MC, remained similar, the T_2 relaxation time of this population decreased significantly during storage of all bread types [Table 6.2, Figures 6.3 (b) and 6.4 (b)]. The reduced mobility of population E can be attributed to strengthening of the starch and (to a lesser extent) protein networks during storage due to respectively AP retrogradation and (slight) gluten dehydration. These T_2 relaxation time readings, which are negatively related to crumb firmness, were lower in crumb from stored bread loaves that had been baked for longer times (Table 6.2). Prolonged baking times may well induce more pronounced AP retrogradation and

crumb to crust moisture migration during storage. In any case, crumb firmness of bread loaves baked for longer times increased more during storage (Table 6.1). With shorter baking times, the crumb density (g/cm³) tended to be slightly higher (results not shown) and therefore may enhance crumb firmness (Lagrain *et al.*, 2012). Nevertheless, crumb firmness of stored bread loaves was lower when baking times were shorter. Therefore the impact of crumb density is further not taken into account. Crumb resilience was higher in fresh CB_{100} than in $PB_{42.5}$ bread because of the more extended gluten and starch networks present, but also remained higher during storage (Table 6.1). These and previous results (*cf*. Chapter 5) allow putting forward the hypothesis that the properties of starch and protein networks largely determine the desired crumb texture of fresh and stored bread. In our view,

(i) a flexible and extended semicrystalline starch network because of sufficient hydration and AM crystallization, and
(ii) a flexible and extended gluten network because of sufficient hydration and gliadin incorporation, contribute to the desired initial crumb resilience, while
(iii) starch recrystallization together with water redistribution (from gluten to starch and from crumb to crust), which result in partial gluten dehydration, dominate the undesired changes in crumb softness and resilience during storage as also postulated by Bosmans *et al*. (2013c).

As will be discussed below, the changes in starch network organization and moisture distribution during this storage phase are not fully reversed during the final baking step. In view of the shelf life of refreshed, FB bread, the duration of the first baking phase should therefore be well considered.

6.3.2 Breads prepared by final baking of stored partially baked breads

To meet the requirements that (i) complete gelatinization and crumb setting must be reached during the first baking phase (Leuschner *et al.*, 1997), and (ii) AP crystals formed during the intermediate storage period melt during the second baking phase, a crumb temperature of respectively 85 to 90 °C in the first and 60 °C in the second baking phase should be reached (Slade *et al.*, 1991). In tin bread loaves prepared from 270 g of flour, this corresponded to respectively 42.5 and 30% of the total baking time, *i.e.* 40 min (Figure 6.1). During final baking of stored $PB_{42.5}$ bread (Table 6.1 – day 6) to obtain fresh $FB_{42.5\text{-}30}$ bread (Table 6.3 – day 0), the crust MC decreased while the crumb MC remained rather constant. Similar observations were made by Leuschner, O'Callaghan and Arendt (1997; 1999). Final baking caused all AP crystals formed during intermediate storage of $PB_{42.5}$ to melt, since little if any residual melting enthalpy of AP was detected in fresh $FB_{42.5\text{-}30}$ bread loaves (Table 6.3). This melting of AP

crystals and the related increased starch network mobility was reflected in a decreased area of population A, containing *inter alia* rigid CH protons of starch, and an increased mobility of population E, containing exchanging protons in the gel network, compared to what was observed for stored $PB_{42.5}$ bread (Figure 6.4, Table 6.2 – day 6 and Table 6.4 – day 0). However, neither the area of population A nor the mobility of population E were restored to their initial values in fresh $PB_{42.5}$ bread (Figure 6.4, Table 6.2 – day 0 and Table 6.4 – day 0). These results indicate that heating reversed neither the moisture redistribution between gluten and starch nor that between crust and crumb which occurred during intermediate storage. The former has also been observed by Willhoft (1971a) (*cf.* §2.2.4) and the latter can be explained by the absence of a driving force. Similar results were obtained by Bosmans *et al.* (2013b) when reheating stored bread crumb. They postulated that despite melting of retrograded AP crystals, the starch network organization could not be fully reversed and that water, incorporated in the starch network during storage, remained associated with it.

Moreover, further protein polymerization, resulting in a more extended protein network, could additionally prevent the mobility of population E from being restored to its initial value in $PB_{42.5}$ bread. The latter was investigated in more detail by studying the impact of the final baking time and the corresponding crumb temperature on protein extractability. To that end, CB_{60} bread was also subjected to a second baking phase to obtain $FB_{60\text{-}40}$ bread (Figure 6.2). The time of this baking phase was chosen such that the sum of the partial and the final baking times corresponds to the total baking time of CB_{100} bread (*i.e.* 40 min). During this baking phase, the area of the peak corresponding to gliadins in the HPLC profiles (eluting between 7 min 45 s and 9 min 30 s) was further reduced (Figure 6.2). However, the maximal crumb temperature reached during final baking was 76 °C and, thus, well below the temperature required for gliadin cross-linking (90 °C) (Lagrain *et al.*, 2008a). It has been suggested that when a sufficiently high crumb temperature is reached during partial baking, reactive groups are exposed (Guerrieri *et al.*, 1996) and remain available for polymerization reactions in the subsequent final baking phase. Additional cross-linking of gliadin was not observed during final baking of $PB_{42.5}$ bread for 30% of total baking time, showing that a certain minimal temperature should still be exceeded in this baking phase (Figure 6.2). Nevertheless, the protein network may have further developed through noncovalent interactions during the final baking phase.

Table 6.3 Moisture content (MC) of crumb and crust, firmness, resilience and melting enthalpy of (retrograded) amylopectin (ΔH_{AP}) of crumb from standard fully baked ($FB_{42.5\text{-}30}$: 42.5 and 30% of total baking time during respectively partial and final baking) and standard conventionally baked (CB_{60}: 60% of total baking time) bread stored for 0, 2, 6 or 7 days at 23 °C.

Baking process	Storage time (days)	MC (%)		Crumb firmness (N)	Crumb resilience (%)	ΔH_{AP} [J/g crumb (dm)]
		Crumb	Crust			
$FB_{42.5\text{-}30}$	0	45.3 (0.2)^{aA}	19.6 (0.1)^{cB}	1.1 (0.2)^{cA}	45.4 (2.9)^{aB}	0.26 (0.13)^{cA}
	2	45.3 (0.2)^{aA}	24.0 (0.3)^{bB}	2.3 (0.6)^{bA}	36.6 (2.1)^{bB}	1.90 (0.25)^{bA}
	6	44.2 (0.3)^{bA}	27.6 (0.2)^{aB}	n.d.	31.4 (2.6)^{cA}	2.74 (0.09)^{aB}
	7	43.5 (0.3)^{bA}	27.7 (0.5)^{aB}	3.7 (0.2)^{aA}	29.4 (2.4)^{cA}	2.74 (0.11)^{aB}
CB_{60}	0	45.1 (0.1)^{aA}	20.2(0.1)^{dA}	1.0 (0.2)^{dA}	54.1 (3.2)^{aA}	0.19 (0.06)^{cA}
	2	44.9 (0.1)^{aA}	25.4 (0.4)^{cA}	2.5 (0.2)^{cA}	44.2 (3.0)^{bA}	1.82 (0.31)^{bA}
	6	44.4 (0.1)^{bA}	28.2 (0.2)^{bA}	3.1 (0.3)^{b}	33.6 (2.6)^{cA}	3.14 (0.28)^{aA}
	7	43.6 (0.4)^{bA}	29.1 (0.3)^{aA}	3.8 (0.2)^{aA}	31.6 (1.5)^{cA}	3.42 (0.05)^{aA}

Standard deviations are indicated between brackets.

n.d.: not determined.

Within one column, values with the same small letter at different storage times of one bread baking process and with the same capital letter at the same storage time for different bread baking processes are not significantly different from each other ($P<0.05$).

Although the moisture distribution was not reversed and the protein network may have further developed during final baking, AP crystal metling restored the crumb firmness and resilience of fresh $FB_{42.5\text{-}30}$ bread loaves (Table 6.3 – day 0) to the initial values observed for $PB_{42.5}$ bread (Table 6.1 – day 0). These results further support the above formulated hypothesis that a recrystallizing starch network together with water redistribution dominate the undesired changes in crumb softness and resilience during storage, while extended and flexible starch and gluten networks contribute to the desired initial crumb resilience. The fact that melting of AP crystals formed during intermediate storage without complete reversion of water redistribution was sufficient to obtain similar values than those of initial crumb firmness and resilience, shows that crumb MC of the bread loaves used in this study was still high enough to keep the crumb networks hydrated and flexible. The latter can be explained by their high crumb to crust ratio.

We next compared the properties of FB with those of CB bread. $FB_{42.5\text{-}30}$ bread and its production process meet the above requirements for a standard parbaking and later final baking process. As mentioned before (*cf.* §3.2.2.3), a CB bread based on 270 g of flour is typically baked for about 25 min, which corresponds to CB_{60} bread. Although all AP crystals were melted during final baking (Table 6.3), a higher area of population A and a lower mobility of population E were detected for $FB_{42.5\text{-}30}$ than for CB_{60} bread (Table 6.4). As pointed out above, these findings indicated the presence of an amorphous cross-linked starch network that holds water after final baking, since the moisture redistribution during intermediate storage is not heat-reversible. Nevertheless, crumb firmness was restored to its initial value before intermediate storage (Table 6.1 – day 0 and Table 6.3 – day 0), resulting in similar values of crumb firmness in refreshed $FB_{42.5\text{-}30}$ bread and fresh CB_{60} bread. However, a lower initial crumb resilience was detected for $FB_{42.5\text{-}30}$ than for CB_{60} bread (Table 6.3). This was attributed to a less extended gluten network due to less covalent gliadin incorporation into the gluten network in $FB_{42.5\text{-}30}$ bread, as can be observed in Figure 6.2.

Table 6.4 Transverse (T_2) relaxation times and areas of nuclear magnetic resonance (NMR) free induction decay (FID) population A (containing rigid CH protons of starch and gluten not in contact with water) and Carr-Purcell-Meiboom-Gill (CPMG) population E (containing exchanging protons of water, starch and gluten in the formed gel network) of crumb from standard fully baked ($FB_{42.5\text{-}30}$: 42.5 and 30% of total baking time during respectively partial and final baking) and standard conventionally baked (CB_{60}: 60% of total baking time) bread stored with crust for 0, 2, 6 or 7 days at 23 °C.

Baking process	Storage time (days)	Population A (FID)		Population E (CPMG)	
		T_2 relaxation time (ms)	Area (au)	T_2 relaxation time (ms)	Area (au)
$FB_{42.5\text{-}30}$	0	0.0131 (0.0004)^{aA}	5370 (202)^{cA}	9.43 (0.41)^{aB}	8896 (123)^{abB}
	2	0.0129 (0.0003)^{abB}	6869 (153)^{bA}	8.93 (0.19)^{bB}	8971 (105)^{aA}
	6	0.0127 (0.0003)^{bB}	7979 (114)^{aA}	7.70 (0.13)^{cB}	8787 (132)^{bcB}
	7	0.0128 (0.0002)^{bA}	8082 (199)^{aA}	7.62 (0.16)^{cB}	8678 (209)^{cB}
CB_{60}	0	0.0132 (0.0004)^{aA}	4609 (107)^{cB}	10.40 (0.34)^{aA}	8991 (107)^{aA}
	2	0.0132 (0.0003)^{abA}	6438 (199)^{bB}	10.10 (0.30)^{bA}	8898 (151)^{aA}
	6	0.0129 (0.0002)^{bA}	7607 (341)^{aB}	8.67 (0.23)^{dA}	8944 (82)^{aA}
	7	0.0129 (0.0002)^{abA}	7711 (150)^{aB}	9.12 (0.19)^{cA}	8917 (92)^{aA}

Areas are given in arbitrary units (au).

Standard deviations are indicated between brackets.

Within one column, values with the same small letter at different storage times of one bread baking process and with the same capital letter at the same storage time for different bread baking processes are not significantly different from each other ($P<0.05$).

During storage, AP retrogradation occurred to a larger extent in CB_{60} than in $FB_{42.5\text{-}30}$ bread as detected with DSC (Table 6.3). In this case, this was also measured as a stronger increase in area of NMR population A in CB_{60} bread (Table 6.4). Moreover, the degree of AP retrogradation determined with DSC during storage of $FB_{42.5\text{-}30}$ bread (Table 6.3) was comparable to that during the preceding intermediate storage phase of $PB_{42.5}$ bread (Table 6.1). Ghiasi *et al.*(1984) also reported a similar rate of AP retrogradation in bread before and after refreshing. It is therefore postulated that the rate and extent of retrogradation not only during intermediate storage of PB bread, but also during final storage of FB bread are impacted by the partial baking time and, thus, the reached crumb center temperature. Obviously, this statement is only valid when all AP crystals are melted during final baking. If not, retrogradation slowly progresses from an already advanced state of recrystallization (results not shown). In the present case, crumb to crust moisture migration during storage was more pronounced in $FB_{42.5\text{-}30}$ than in CB_{60} bread, since the area of population E, which *inter alia* is related to crumb MC, decreased to a larger extent in $FB_{42.5\text{-}30}$ than in CB_{60} bread (Table 6.4). Nevertheless, crumb MC of both bread types changed only to minor extent because of their high crumb to crust ratio (Table 6.3). The degree of crumb to crust moisture migration seemed to be counterbalanced by the degree of AP retrogradation, since crumb firmness after 7 days of storage was similar for $FB_{42.5\text{-}30}$ and CB_{60} bread (Table 6.3). Furthermore, despite differences in fresh $FB_{42.5\text{-}30}$ and CB_{60} bread loaves, their resilience was comparable after storage. These observations stress that crumb firmness and resilience in stored bread are dominated by starch recrystallization and water redistribution.

Crumb firming thus did not occur more rapidly in FB than in CB bread, in contrast to what was reported for bread prepared from (only) 100 g of wheat flour with ambient intermediate storage (Ghiasi *et al.*, 1984) and for bread prepared from 100 g of gluten-free flour (Sciarini *et al.*, 2012) or wheat flour (Rosell & Santos, 2010) with refrigerated intermediate storage. It is therefore further investigated if the impact of parbaking on stored bread quality, evaluated as crumb texture, could depend on bread loaf size.

6.3.3 Breads with different crumb to crust ratio

As pointed out above, the minor changes in crumb MC during storage of tin bread based on 270 g of wheat flour (Tables 6.1 and 6.3) were due to its high crumb to crust ratio. It is suggested that when the crumb to crust ratio is low, as is the case for small bread loaves (Rouillé *et al.*, 2010) or French bread (Baardseth *et al.*, 2000), crumb MC decreases and crumb firming rate increases significantly. Since moisture redistribution during intermediate storage is not heat-reversible (*cf.* §6.3.2), it would seem plausible that parbaking of such bread types does result in a higher firming rate of FB than of CB bread. To confirm this hypothesis, changes in water mobility during storage of bread loaves with different crumb to crust ratio were investigated. Figure 6.5 shows the CPMG proton distributions of fresh and stored (either with or without crust) CB bread crumb prepared from different amounts of flour (*i.e.* 10.0, 100.0 or 270 g). As the loaf volume increased, so did the crumb to crust ratio. The decrease in area of population E during storage of bread with crust was more pronounced when the crumb to crust ratio was lower (Figure 6.5). Indeed, during storage of respectively the largest bread loaves and bread loaves prepared from 100.0 g of flour, crumb MC decreased by approximately 1% and 8% (Table 6.5). Furthermore, a larger decrease in crumb MC resulted in a stronger dehydration of the gluten network, since merging of populations C and D was more pronounced in smaller bread loaves stored either with or without crust (Figure 6.5). Moreover, the average mobility of this merged population was lower when the loaf volume was smaller [Figure 6.5 (b) and (c)]. When the loaf volume and, thus, crumb to crust ratio was small, the mobility of population E decreased to a larger extent when crumb was stored with crust (Figure 6.5). Because this mobility is negatively correlated with crumb firmness during storage (Bosmans *et al.*, 2013c) it is assumed that the extent of crumb firming increased with decreasing crumb to crust ratio. Crumb firming is dominated by both AP retrogradation and water redistribution. Since AP retrogradation occurred to a similar extent during storage of bread loaves with different volumes (Table 6.5), differences in the extent of water redistribution are largely responsible for changes in the extent of crumb firming when the bread loaf size was altered.

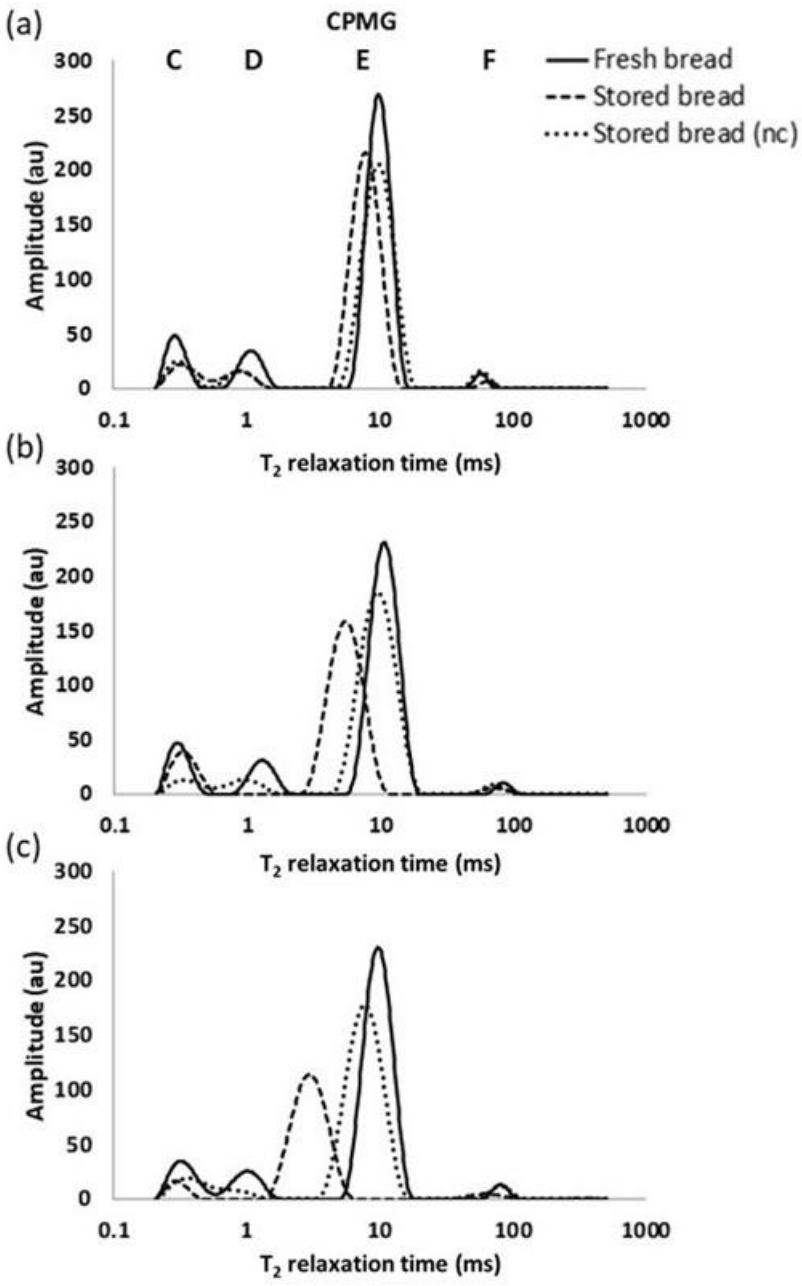

Figure 6.5 Carr-Purcell-Meiboom-Gill (CPMG) proton distributions of crumb withdrawn from fresh and stored (7 days at 23 °C) bread and of crumb from bread stored (7 days at 23 °C) without crust (nc, no crumb to crust moisture migration) prepared from 270 (a), 100 (b), or 10 (c) g of wheat flour.

It can therefore be concluded that a low crumb to crust ratio causes a pronounced decrease in crumb MC during storage, resulting in strong dehydration of crumb biopolymer networks and, hence, a large increase in crumb firmness. Since this moisture redistribution is not heat-reversible as mentioned above, it is thus very well possible that PB small or French bread loaves, which have a low crumb to crust ratio, firm more rapidly after final baking than CB bread as described in literature (Ghiasi *et al.*, 1984; Rosell & Santos, 2010; Sciarini *et al.*, 2012).

Table 6.5 Moisture content (MC) of crumb and crust and melting enthalpy of (retrograded) amylopectin (AP, ΔH_{AP}) of crumb from bread prepared from 10, 100 or 270 g of wheat flour and stored for 0 or 7 days at 23 °C.

Amount of wheat flour used for bread making (g)	Storage time (days)	MC (%)		ΔH_{AP} [J/g crumb (dm)]
		Crumb	Crust	
10	0	n.d.	n.d.	0.44 (0.11)^{A}
	7	n.d.	n.d.	3.39 (0.13)^{A}
100	0	44.7 (0.2)^{A}	14.6 (0.3)^{A}	0.32 (0.18)^{A}
	7	36.6 (0.5)^{B}	24.7 (0.6)^{A}	3.53 (0.33)^{A}
270	0	44.8 (0.1)^{A}	13.8 (0.5)^{A}	0.21 (0.09)^{A}
	7	43.2 (0.6)^{A}	24.6 (0.6)^{A}	3.62 (0.35)^{A}

Standard deviations are indicated between brackets.
n.d.: not determined.
Within one column, values with the same capital letter at the same storage time for bread prepared from different amounts of flour are not significantly different from each other ($P<0.05$).

6.4 CONCLUSIONS

In conclusion, different temperature-time baking profiles impacted the extent of CHL and protein polymerization. With increasing baking time and the corresponding crumb temperature, a more extended starch network and a more extended gluten network in terms of gliadin cross-linking were formed. As a result, the proton mobility in the gel network decreased and the initial crumb resilience increased. During storage of PB and CB bread, the extent of crumb firming increased with longer baking times of the previous baking phase due to (i) more pronounced AP retrogradation (and related moisture redistribution from gluten to starch) and (ii) more pronounced moisture redistribution from crumb to crust.

Ad (i): An increased degree of (a) AM and also (b) AP leaching, which has been shown to occur at higher baking temperatures and longer baking times, is associated with respectively (a) a higher intragranular concentration of AP and the presence of a more extended AM network in bread crumb with more AM crystals that serve as nuclei for AP retrogradation, and (b) the presence of solubilized AP polymers in the extragranular space that retrograde more easily because they are closer to the AM network containing crystal nuclei and to other leached AP molecules.

Ad (ii): A lower fresh crust MC results in a higher driving force for crumb to crust moisture migration.

However, despite the occurrence of crumb to crust moisture migration, crumb MC remained high in all bread types as a consequence of the high crumb to crust ratio.

During final baking, all retrograded AP crystals melted, resulting in refreshed FB bread. However, moisture redistribution from crumb to crust and from gluten to starch during intermediate storage of PB bread loaves could not be reversed. Moreover, additional gluten network organization may occur. As a result, biopolymer organization and water distribution differed between fresh PB and refreshed FB bread. Because of the high crumb MC, however, these differences were not reflected in crumb texture, since softness and resilience of refreshed FB bread were restored to their initial values in fresh PB bread. It can therefore be concluded that starch recrystallization together with water redistribution dominate changes in crumb softness and resilience during storage, while extended and flexible starch and gluten networks dominate initial crumb resilience.

During storage of refreshed FB bread, the extent of AP retrogradation is determined by the partial baking time and occurs to a similar extent as during intermediate storage of PB bread. The degree to which crumb MC is impacted is largely determined by the crumb to crust ratio of the bread. When this ratio is high, such as for tin bread with a large loaf volume, the decrease in crumb MC due to crumb to crust moisture migration during both intermediate and final storage is limited, resulting in biopolymer networks in bread crumb which remain well hydrated. Consequently, parbaking of large tin bread loaves does not result in higher crumb firming rates after final baking than those of CB bread. However, when the crumb to crust ratio is low, such as for small bread loaves or French bread, the decrease in crumb MC during storage becomes more pronounced and results in an increased rate and extent of crumb firming. These results stress the contribution of moisture (re)distribution to the crumb firming mechanism and, thus, the shelf life of bread. This is especially important in the case of parbaking, since moisture redistribution is not heat-reversible during final baking.

General discussion, conclusions and perspectives

GENERAL DISCUSSION

During bread making and storage, wheat flour biopolymers undergo complex transformations. The most abundant flour biopolymers are starch and gluten. Native starch is present as semicrystalline granules. It consists in essence of two biopolymers, *i.e.* the nearly linear amylose (AM) and the highly branched amylopectin (AP). Gluten proteins consist of glutenin and gliadin. Starch is quantitatively the main flour constituent and its structural transformations and interaction with water greatly contribute to the properties of fresh and stored bread. **At what point and to what extent these changes exactly occur during bread making and how they impact on the crumb firming mechanism is still poorly understood.**

To study AM and AP transitions and water dynamics *in situ* during bread baking and cooling, a **temperature-controlled** time domain proton nuclear magnetic resonance (**TD ^{1}H NMR**) method was optimized in this doctoral dissertation. With this method, proton distributions in bread dough/crumb were monitored during a heating and subsequent cooling process representative for that in the dough/crumb center during bread baking and cooling (Figure i.2). To correctly interpret the complex NMR data and to obtain insights in changes at different length scales, additional techniques were used. Time-resolved wide angle X-ray diffraction was also performed *in situ* during bread baking and cooling, and together with differential scanning calorimetry (DSC) provided information about *inter alia* AP crystal melting during gelatinization. Granule swelling and carbohydrate leaching were analyzed with gravimetric and colorimetric analyses, respectively. To the best of our knowledge, such **multiscale analytical approach** to study starch and water dynamics during both bread baking and cooling has never been adopted before.

Subsequently, the impact of these changes during bread making on the properties of fresh bread and the mechanism whereby its crumb firms during storage at room temperature was examined by combining TD ^{1}H NMR, DSC and texture analyses.

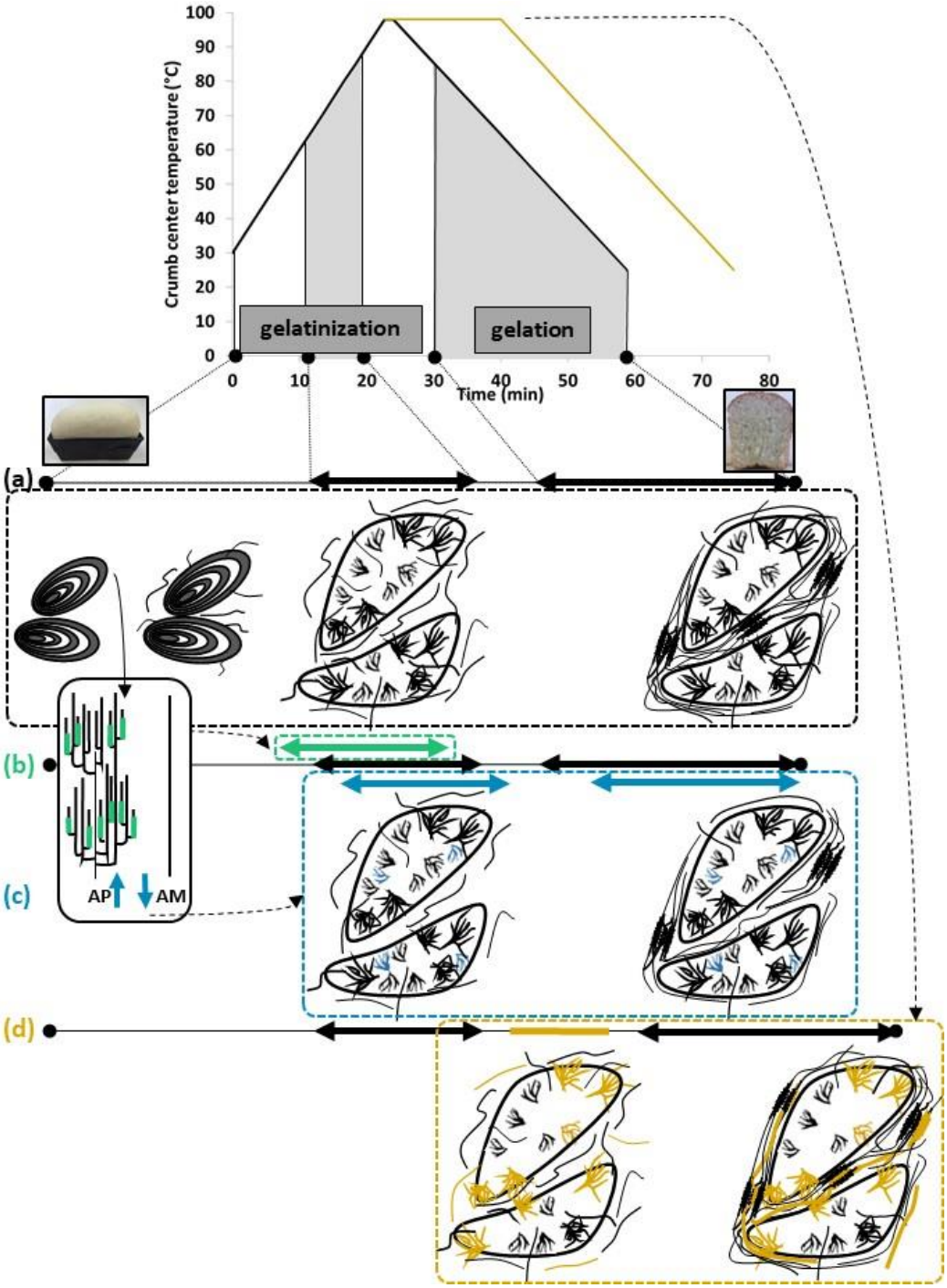

Figure i.2 Schematic representation of starch transitions in the chain from fermented dough to fresh, cool bread. The temperature profile during baking and cooling is that in the dough/crumb center. (a) During initial baking of dough prepared from regular wheat flour, slight granule swelling and amylose (AM) leaching occur. Later in the process, starch gelatinizes, amylopectin (AP) crystals melt, granules swell irreversibly and AM is further solubilized. Upon cooling, leached AM molecules crystallize and form crystalline junction zones in the fringed micelle AM network that is formed during gelation. Swollen granule remnants are dispersed in this network. (b) During baking of bread prepared from flour containing starch of which AP has a higher portion of short outer branches than regular wheat starch, gelatinization occurs at lower temperatures. (c) When bread is prepared from flour containing starch with lower AM and, thus, higher AP levels, gelatinization shifts to higher temperatures. Less AM is solubilized and available for crystallization during cooling such that a less extended AM network with less AM crystals is formed. (d) Prolonged baking results in continued leaching of AM and some AP molecules. During cooling, a more extended AM network with more AM crystals is formed.

The optimized **temperature controlled TD ^{1}H NMR toolbox** was first applied to dough prepared from regular wheat flour. Changes in the area of different proton populations during initial baking were attributed to the absorption of water by slightly swelling starch granules and the concomitant release of carbohydrates (mainly AM) to the extragranular environment [Figure i.2 (a)]. As a result, the viscosity of the extragranular phase increased and the mobility of the protons in it simultaneously decreased until a temperature of 65 °C was reached. Indeed, in a 60 to 65 °C temperature range, starch gelatinization (detected as AP crystal melting) started after which the crumb structure was set and the viscosity of the extragranular phase no longer increased. Gelatinization was also associated with significant granule swelling and further AM leaching [Figure i.2 (a)]. Leached AM complexed with lipids after the onset of gelatinization. Between 85 and 90 °C, gelatinization was complete. The Type I AM-lipid complexes formed during gelatinization melted upon further heating and recrystallized into Type II complexes during cooling. B-type crystals formed from (leached) AM molecules during the gelation process together with Type II complexes made up the crystalline junction zones in the fringed micelle AM network. The formation of such semicrystalline AM network (containing the granule remnants) throughout the bread crumb during cooling [Figure i.2 (a)] was related to decreasing proton mobility. From the above it follows that starch gelatinization and gelation resulted in a starch network in fresh, cool bread which is known to contribute to the crumb texture of fresh bread. The formation, melting and recrystallization of AM-lipid complexes during baking and cooling and the appearance of B-type crystals already during cooling has to the best of our knowledge never been described for a bread system.

In further work of this doctoral dissertation, changes in the timing and extent of phenomena associated with gelatinization and gelation were induced **by altering the bread recipe or the bread making process**. Unique wheat flours with atypical starch characteristics [Figure i.2 (b) and (c)] and α-amylase from *Bacillus stearothermophilus* (BStA) were used in bread making. The baking process of bread prepared from a control recipe was altered by *inter alia* increasing [Figure i.2 (d)] or reducing its duration.

It was found that **the timing of starch gelatinization during baking in essence is determined by the stability of AP crystals in dough**, which in turn depends on the chain length distribution and the level of AP in starch. Outer AP branch chains with a degree of polymerization (DP) of 6 to 10 are too short to form stable double helices. In dough from flour with a higher level of such short AP branch chains at the expense of longer exterior AP branch chains than in regular flour, less stable AP crystals were present. Consequently, the energy required for gelatinization decreased. Gelatinization therefore shifted to lower temperatures and, thus, occurred earlier during bread baking [Figure i.2 (b)]. While AP is the starch component

associated with starch crystallinity, AM molecules are considered as structural defects that destabilize the AP crystal structure. When using flour containing starch that had a higher AP content, gelatinization during bread baking required more energy and shifted to higher temperatures [Figure i.2 (c)].

Under all bread making conditions studied, complete AP crystal melting had occurred by the end of baking. However, **the extent to which starch polymers leached to the extragranular environment depended on their level in dough and the duration of baking**. Mainly AM leached from starch granules during baking. At higher temperatures, also some AP may have leached to the extragranular space. Evidently, in dough from flour containing starch with lower AM levels than regular starch, less AM could leach from starch granules [Figure i.2 (c)]. In contrast, when the baking phase for bread from regular wheat flour was extended, leaching of AM and also AP from the granules probably continued. By the end of prolonged baking, more AM and probably also some AP leached to the extragranular environment [Figure i.2 (d)].

The level of (leached) AM in still-warm bread crumb determined the timing and extent of gelation during cooling and, therefore, the properties of the starch network in fresh, cool bread. In bread from flour containing starch with lower AM levels than present in regular starch, less of it leached to the extragranular space during baking and was available for crystallization during cooling. As a result, cooling to lower temperatures was required for AM crystallization to become noticeable [Figure i.2 (c)]. After cooling, a less extended AM network with less crystalline junction zones was present in fresh bread crumb [Figure i.2 (c)]. The high mobility of protons in such network went hand in hand with a very soft crumb [Figure i.3 (a)]. That fresh cool bread prepared from flour with lower starch AM levels was not sliceable showed that AM has an essential structural role in such bread and determines its crumb texture.

Work on breads baked for different times showed that **not only the starch, but also the gluten network contributes to the texture of crumb of fresh, cool bread**. During baking, glutenin was the first gluten component which polymerized. Higher temperatures at the end of baking were required to covalently incorporate gliadin into the gluten network. The extent of both carbohydrate leaching and gliadin cross-linking increased with baking time. When additional amounts of AM had leached from starch granules as a result of prolonged baking, a more extended AM network with more crystalline junction zones was formed upon cooling [Figure i.2 (d)]. Crumb of the resulting fresh, cool bread was more resilient because of the presence of both more extended starch [Figure i.3 (b)] and gluten networks. However, incorporation of BStA in a standard bread recipe resulted in decreased resilience of fresh, cool bread crumb.

The mainly exoacting BStA significantly hydrolyzed starch after the onset of gelatinization and thereby primarily decreased the length of outer AP branch chains. Its slight endoaction at higher temperatures during baking resulted in AM molecules of reduced molecular weight and thus higher mobility. The increased mobility of AM molecules enhanced crystallization during cooling such that more crystalline junction zones and, thus, a more rigid AM network was formed during cooling. Accordingly, the firmness of fresh bread crumb increased while its resilience decreased [Figure i.3 (c)].

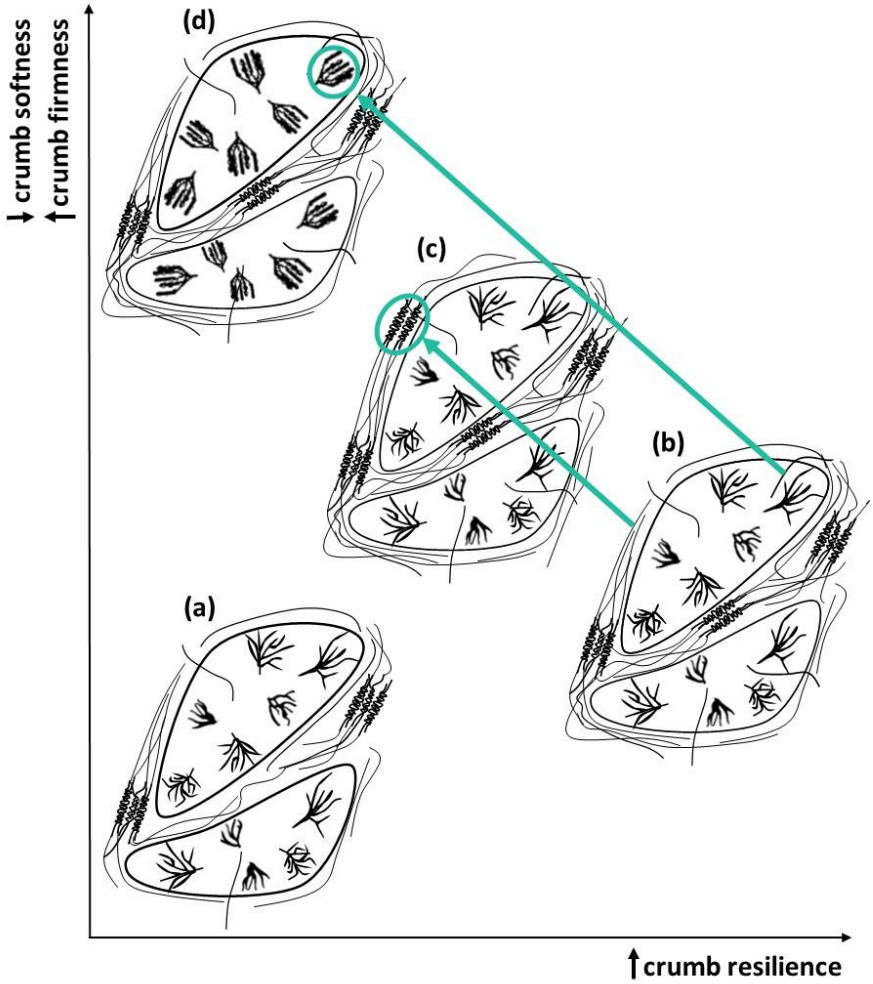

Figure i.3 The impact of starch networks on the texture of bread crumb. (a) Little extended amylose (AM) networks with few crystalline junction zones result in fresh, very soft and little resilient cool bread crumb. (b) Fresh bread with a **desired** initial crumb firmness and resilience contains an AM network that extends throughout crumb and contains sufficient crystalline junction zones. Further strengthening of the latter starch network due to (c) enhanced AM crystallization during cooling of bread or due to (d) amylopectin (AP) retrogradation during storage leads to crumb with increased firmness and decreased resilience.

During storage of bread at ambient temperature, crumb firmness increased and crumb resilience decreased due to stiffening of starch and gluten networks as a result of AP retrogradation [Figure i.3 (d)] and moisture redistribution. In breads prepared from flour containing starch with different characteristics, with addition of the same amount of water

and with or without use of BStA, the degree of AP retrogradation determined the degree of crumb firming. **The extent of AP retrogradation during storage depended on the structure and the level of (leached) AP in bread and the moisture content (MC) of bread crumb.** More specifically, AP retrogradation in bread crumb was enhanced by (i) higher concentrations of (leached) AP, (ii) higher portions of AP branch chains with DP > 10, and when (iii) AM crystals were present and served as nuclei for AP retrogradation, and (iv) bread crumb MC was about 40%.

A larger extent of AM leaching during prolonged baking resulted in higher AP concentrations in the outer zones of starch granule remnants and the formation of a more extended AM network with more crystalline junction zones during cooling. These AM crystals served as nuclei for AP retrogradation. At higher temperatures during baking, also some AP leached towards the extragranular space. Such AP molecules were close to the AM crystal nuclei and to other leached AP molecules [Figure i.2 (d)]. Prolonged baking thus resulted in a greater extent of intragranular and intergranular AP retrogradation during storage. The ability of AP to retrograde was lower when the level of short outer AP branch chains (DPs 6-10) was higher, the latter at the expense of the level of longer exterior AP branch chains. When bread was prepared from flour containing a high level of such short AP chains and BStA was simultaneously used, the level of these short AP chains further increased during baking. Consequently, AP retrogradation and crumb firming during storage were almost fully prevented.

Retrograded AP reinforced the starch network and withdrew water from the gluten network. The gluten network was further dehydrated as water migrated from the moist crumb to the dry crust during storage. **Together with the extent of AP retrogradation, the degree to which crumb MC decreased codetermined the extent of crumb firming during storage.** The extent of crumb to crust moisture migration depended on the moisture gradient between crumb and crust. The decrease of the crumb MC was more pronounced during storage after prolonged baking since longer baking times led to lower crust MCs. When the AP content of starch in flour was higher, so was the water absorption of flour such that water in both dough and bread was more strongly bound. This led to better preservation of the crumb MC and, therefore, better hydration of the crumb networks during storage. Nevertheless, crumb firming occurred to larger extent during storage of bread from flour with a higher AP content than during storage of bread made with regular flour. This was due to a higher level of AP retrogradation in the former case. When crumb networks in this bread type were even better hydrated because more water was used during dough preparation, the extent of crumb firming during storage was reduced.

Bread produced by baking for a reduced time, *i.e.* by submitting dough to partial baking, was intermediately stored at room temperature before being finished off by final baking. AP retrogradation which took place during intermediate storage was reversed by melting of AP crystals during the subsequent final baking phase. However, the moisture redistribution that had occurred during intermediate storage was not heat-reversible. The extent of moisture redistribution during intermediate storage therefore largely determined the properties of bread produced by final baking. In this context, the size of bread is of major importance. During intermediate storage, relatively more water migrated from crumb to crust when the bread size and, therefore, the crumb to crust ratio was lower. So far, the impact of bread size on crumb firming during storage at ambient temperature has never been investigated before.

MAIN CONCLUSIONS

Temperature-controlled TD ^{1}H NMR in combination with other techniques proves powerful for investigating starch and water dynamics at different length scales and *in situ* during bread baking and cooling. The use of this innovative toolbox allowed to present an **integrated view on the functionality of starch and the related water dynamics during bread making and storage**. The level and structure of AP in dough and in (the extragranular phase of) bread determine respectively the timing of gelatinization during baking and the extent to which AP recrystallizes during storage. AP retrogradation is also facilitated by the presence of AM crystal nuclei formed during cooling. The timing and extent of AM crystallization and the formation of the AM network during cooling depends on the level and structure of AM in (the extragranular phase of) bread.

The next most abundant flour constituent after starch, *i.e.* gluten, polymerizes during baking. **Together with the starch network, the gluten network in fresh bread codetermines crumb texture**. The formation of an extended AM network with sufficient AM crystals throughout the bread crumb is responsible for the initial crumb firmness and sliceability of fresh, cool bread. Together with an extended gluten network which includes sufficient gliadin, such AM network results in an optimal crumb resilience. Less extended AM and gluten networks as well as too rigid extended AM networks lead to lower resilience of the crumb of fresh bread.

Stiffening of starch and gluten networks due to AP retrogradation and water redistribution during storage dominate the undesired decrease in crumb softness and resilience. In breads with different starch characteristics but of similar water levels, the degree of AP retrogradation determines the degree of crumb firming. The redistribution of water during

storage is however of major importance in the case of small bread loaves produced by first partial and later final baking after an intermediate storage period at ambient temperature.

Based on the above, we suggest that an ideal starch in flour for bread making purposes has:

(i) an **AM to AP ratio corresponding to that of regular wheat starch, *i.e.* 25 to 75%**. Too low AM contents lead to formation of less extended starch networks which result in bread crumb which is too soft and not sliceable. Too high AM contents lead to rigid extended starch networks which lead to low crumb resilience and bring about a substantial crumb firmness even before further strengthening of crumb networks during storage takes place;

(ii) an **AM chain length distribution corresponding to that of regular wheat starch.** Shorter AM chains are more mobile such that AM crystallization during cooling is promoted and a too rigid extended starch network may be formed in fresh bread. Moreover, AM crystals can serve as nuclei that enhance AP retrogradation and, thus, further stiffening of the starch network during storage;

(iii) a **high portion of outer AP branch chains that are too short to crystallize (DP 6-10)** at the expense of the portion of longer outer branch chains such that AP retrogradation during storage is almost prevented.

Regarding the process conditions, **bread is preferably baked until its maximum crumb center temperature of 100 °C is reached**. By then, sufficient glutenin and gliadin cross-linking has occurred and adequate levels of AM have leached such that extended gluten and AM networks are present in fresh cool bread. As a result, fresh bread with a sliceable, resilient crumb is obtained. Prolonged baking may well improve the crumb resilience of the resulting fresh, cool bread, but it also results in enhanced AP retrogradation and crumb to crust moisture migration during storage.

PERSPECTIVES

This doctoral dissertation extends the knowledge of AM, AP and gluten functionality and the related water mobility during bread making and storage. The obtained results furthermore open perspectives for future research.

The temperature-controlled TD ^{1}H NMR method optimized in Chapter 3 was successfully used to study (unusual) starch and water dynamics and the impact of BStA *in situ* during bread making as shown in Chapter 4. This method can also be relevant to investigate the impact of other much used bread ingredients such as surfactants and other amylases. The resulting

insights may lead to more efficient use of bread improving agents. Based on the insights about AM and AP functionality during bread making (Chapter 4) and storage (Chapter 5) it may furthermore be possible to fine-tune wheat starch characteristics for bread making purposes by identifying and crossing wheat lines with wild-type and null genes encoding for (un)desired starch properties.

Changes in proton distributions, measured *in situ* during bread baking and cooling with temperature-controlled TD ^{1}H NMR were dominated by changes in the starch and water fraction. The timing and extent of changes in the gluten fraction could not be distinguished using this technique. The extent of gluten polymerization was only determined in fresh bread, after baking and cooling. Additional techniques that allow to study gluten transformations *in situ* during bread baking therefore would be of much added value. It would furthermore be of interest to study changes in the gluten fraction during baking of bread prepared with use of commonly used bread improving agents such as ascorbic acid.

From the work in Chapter 6 it followed that the extent of moisture redistribution during intermediate storage at ambient temperature is key to the properties of bread with a low crumb to crust ratio prepared by final baking of intermediately stored partially baked bread. It was suggested that such bread loaves do firm more rapidly than their conventionally baked counterparts produced by a single baking step. The firming mechanism at ambient temperature of bread loaves with a low crumb to crust ratio, like French bread, should therefore be further explored before and after final baking as a follow-up to the research in Chapter 6. To verify the importance of moisture redistribution to crumb firming at ambient storage in such bread types, their firming mechanism should additionally be studied during refrigerated storage. At lower temperatures, moisture redistribution occurs more slowly and the rate of AP retrogradation increases. Crumb firming is then dominated by AP retrogradation, which can be reversed during final baking.

In addition to the functionality of wheat flour biopolymers, that of biopolymers from starches and flours of different botanical origin can be explored in a bread making context. Such information is valuable in the context of improving the quality of gluten-free bread. In spite of the expanding need for gluten-free alternatives, these products in general have inferior structural and sensory properties. That the temperature-controlled NMR method allows to perform measurements *in situ* during heating and cooling processes makes it moreover suitable to investigate the role of constituents during the production process of complex bakery products other than bread, like cake and cookies. It would even be possible to create an experimental set-up to examine constituent transitions in *e.g.* doughnuts or potato crisps during frying.

References

AACC. (1999a). Method 44-15.02. Moisture - air-oven methods. In *Approved Methods of Analysis, (11th Edition*). St. Paul, MN: AACC International.

AACC. (1999b). Method 76-31.01. Determination of Damaged Starch - Spectrophotometric Method. In *Approved Methods of Analysis, (11th Edition*). St. Paul, MN: AACC International.

AACCI. (2009). Method 56-11.02. Solvent Retention Capacity Profile. In *Approved Methods of Analysis (11th Edition*). St. Paul, MN: AACC International.

AACCI. (2011). Method 54-21.02. Farinograph method for flour: constant flour weight procedure. In *Approved Methods of Analysis (11th Edition*). St. Paul, MN: AACC Internationl.

Aguirre, J. F., Osella, C. A., Carrara, C. R., Sánchez, H. D. & Buera, M. d. P. (2011). Effect of storage temperature on starch retrogradation of bread staling. *Starch/Stärke, 63*(9), 587-593.

Almeida, E. L., Steel, C. J. & Chang, Y. K. (2016). Par-baked bread technology: formulation and process studies to improve quality. *Critical Reviews in Food Science & Nutrition, 56*(1), 70-81.

Almutawah, A., Barker, S. A. & Belton, P. S. (2007). Hydration of gluten: a dielectric, calorimetric, and Fourier transform infrared study. *Biomacromolecules, 8*(5), 1601-1606.

Amigo, J. M., del Olmo Alvarez, A., Engelsen, M. M., Lundkvist, H. & Engelsen, S. B. (2016). Staling of white wheat bread crumb and effect of maltogenic α-amylases. Part 1: Spatial distribution and kinetic modeling of hardness and resilience. *Food Chemistry, 208*, 318-325.

AOAC. (1995). Protein (crude) in animal feed: combustion method (990.03). In *Official Methods of Analysis (16th Edition*). Washington, DC: Association of Official Analytical Chemists.

Assifaoui, A., Champion, D., Chiotelli, E. & Verel, A. (2006). Rheological behaviour of biscuit dough in relation to water mobility. *International Journal of Food Science & Technology, 41*(s2), 124-128.

Aston, L. M., Gambell, J. M., Lee, D. M., Bryant, S. P. & Jebb, S. A. (2008). Determination of the glycaemic index of various staple carbohydrate-rich foods in the UK diet. *European Journal of Clinical Nutrition, 62*(2), 279.

Atwell, W., Hood, L., Lineback, D., Varriano-Marston, E. & Zobel, H. (1988). The terminology and methodology associated with basic starch phenomena. *Cereal Foods World, 33*(3), 306-311.

Axford, D., Colwell, K., Cornford, S. & Elton, G. (1968). Effect of loaf specific volume on the rate and extent of staling in bread. *Journal of the Science of Food and Agriculture, 19*(2), 95-101.

Baardseth, P., Kvaal, K., Lea, P., Ellekjaer, M. & Faergestad, E. (2000). The effects of bread making process and wheat quality on French baguettes. *Journal of Cereal Science, 32*(1), 73-87.

Babin, P., Della Valle, G., Chiron, H., Cloetens, P., Hoszowska, J., Pernot, P., Réguerre, A., Salvo, L. & Dendievel, R. (2006). Fast X-ray tomography analysis of bubble growth and foam setting during breadmaking. *Journal of Cereal Science, 43*(3), 393-397.

Badenhuizen, N. & Dutton, R. (1956). Growth of 14 C-labelled starch granules in potato tubers as revealed by autoradiographs. *Protoplasma, 47*(1-2), 156-163.

Badenhuizen, N. P. (1938). Untersuchungen über die sogenannte Blöckchenstruktur der Stärkekörner. *Protoplasma, 29*(1), 246-260.

Bahnassey, Y. A. & Breene, W. M. (1994). Rapid visco-analyzer (RVA) pasting profiles of wheat, corn, waxy corn, tapioca and amaranth starches (A. hypochondriacus and A cruentus) in the

presence of konjac flour, gellan, guar, xanthan and locust bean gums. *Starch/Stärke, 46*(4), 134-141.

Bailey, C. & Von Holy, A. (1993). Bacillus spore contamination associated with commercial bread manufacture. *Food Microbiology, 10*(4), 287-294.

Baldwin, P. M. (2001). Starch granule-associated proteins and polypeptides: a review. *Starch/Stärke, 53*(10), 475-503.

Ball, S., Guan, H.-P., James, M., Myers, A., Keeling, P., Mouille, G., Buléon, A., Colonna, P. & Preiss, J. (1996). From glycogen to amylopectin: a model for the biogenesis of the plant starch granule. *Cell, 86*(3), 349-352.

Banks, W. & Greenwood, C. T. (1966). The fine structure of amylose: the action of pullulanase as evidence of branching. *Archives of Biochemistry and Biophysics, 117*, 674-675.

Bárcenas, M. E. & Rosell, C. M. (2006). Effect of frozen storage time on the bread crumb and aging of par-baked bread. *Food Chemistry, 95*(3), 438-445.

Belitz, H., Grosch, W. & Schieberle, P. (2009). *Food Chemistry (4th edition)*. Heidelberg: Springer.

Belton, P. S. (1999). On the elasticity of wheat gluten. *Journal of Cereal Science, 29*(2), 103-107.

Bijttebier, A., Goesaert, H. & Delcour, J. A. (2007). Temperature impacts the multiple attack action of amylases. *Biomacromolecules, 8*(3), 765-772.

Bijttebier, A., Goesaert, H. & Delcour, J. A. (2010). Hydrolysis of amylopectin by amylolytic enzymes: structural analysis of the residual amylopectin population. *Carbohydrate Research, 345*(2), 235-242.

Biliaderis, C., Maurice, T. & Vose, J. (1980). Starch gelatinization phenomena studied by differential scanning calorimetry. *Journal of Food Science, 45*(6), 1669-1674.

Biliaderis, C. & Seneviratne, H. (1990). On the supermolecular structure and metastability of glycerol monostearate-amylose complex. *Carbohydrate Polymers, 13*(2), 185-206.

Biliaderis, C. G., Page, C. M., Maurice, T. J. & Juliano, B. O. (1986). Thermal characterization of rice starches: A polymeric approach to phase transitions of granular starch. *Journal of Agricultural and Food Chemistry, 34*(1), 6-14.

Blanshard, J., Bates, D., Muhr, A., Worcester, D. & Higgins, J. (1984). Small-angle neutron scattering studies of starch granule structure. *Carbohydrate Polymers, 4*(6), 427-442.

Blanshard, J. M. V. (1987). Starch granule structure and function: a physicochemical approach. In T. Gaillard (Ed.), *Starch: Properties and Potential*, vol. 13 (pp. 16-54). New York: John Wiley & Sons.

Blazek, J. & Gilbert, E. P. (2011). Application of small-angle X-ray and neutron scattering techniques to the characterisation of starch structure: a review. *Carbohydrate Polymers, 85*(2), 281-293.

Blennow, A., Hansen, M., Schulz, A., Jørgensen, K., Donald, A. M. & Sanderson, J. (2003). The molecular deposition of transgenically modified starch in the starch granule as imaged by functional microscopy. *Journal of Structural Biology, 143*(3), 229-241.

Bloksma, A. (1972). Rheology of wheat flour doughs. *Journal of Texture Studies, 3*(1), 3-17.

Bloksma, A. (1990). Rheology of the breadmaking process. *Cereal Foods World*.

Bocharnikova, I., Wasserman, L., Krivandin, A., Fornal, J., Baszczak, W., Chernykh, V. Y., Schiraldi, A. & Yuryev, V. P. (2003). Structure and thermodynamic melting parameters of wheat starches with different amylose content. *Journal of Thermal Analysis and Calorimetry, 74*(3), 681-695.

Bosmans, G. (2013). *Water dynamics and biopolymer interactions in model systems and straight-dough bread as a basis for understanding the crumb firming process.* Unpublished Doctoral dissertation, KU Leuven, Leuven.

Bosmans, G. M., Lagrain, B., Deleu, L. J., Fierens, E., Hills, B. P. & Delcour, J. A. (2012). Assignments of proton populations in dough and bread using NMR relaxometry of starch, gluten, and flour model systems. *Journal of Agricultural and Food Chemistry, 60*(21), 5461-5470.

Bosmans, G. M., Lagrain, B., Fierens, E. & Delcour, J. A. (2013a). Impact of amylases on biopolymer dynamics during storage of straight-dough wheat bread. *Journal of Agricultural and Food Chemistry, 61*(26), 6525-6532.

Bosmans, G. M., Lagrain, B., Fierens, E. & Delcour, J. A. (2013b). The impact of baking time and bread storage temperature on bread crumb properties. *Food Chemistry, 141*(4), 3301-3308.

Bosmans, G. M., Lagrain, B., Ooms, N., Fierens, E. & Delcour, J. A. (2013c). Biopolymer interactions, water dynamics, and bread crumb firming. *Journal of Agricultural and Food Chemistry, 61*(19), 4646-4654.

Bosmans, G. M., Lagrain, B., Ooms, N., Fierens, E. & Delcour, J. A. (2014). Storage of parbaked bread affects shelf life of fully baked end product: a 1H NMR study. *Food Chemistry, 165*, 149-156.

Brisson, J., Chanzy, H. & Winter, W. (1991). The crystal and molecular structure of V_H amylose by electron diffraction analysis. *International Journal of Biological Macromolecules, 13*(1), 31-39.

Buléon, A., Colonna, P., Planchot, V. & Ball, S. (1998). Starch granules: structure and biosynthesis. *International Journal of Biological Macromolecules, 23*(2), 85-112.

Bushuk, W. (1966). Distribution of water in dough and bread. *Baker's Digest, 40*(5), 38-40.

Cameron, R. & Donald, A. (1992). A small-angle X-ray scattering study of the annealing and gelatinization of starch. *Polymer, 33*(12), 2628-2635.

Cameron, R. E. & Donald, A. M. (1993). A small-angle X-ray scattering study of the absorption of water into the starch granule. *Carbohydrate Research, 244*(2), 225-236.

Carlson, T.-G., Larsson, K., Dinh-Nguyen, N. & Krog, N. (1979). A study of the amylose-monoglyceride complex by raman spectroscopy. *Starch/Stärke, 31*(7), 222-224.

Carr, H. Y. & Purcell, E. M. (1954). Effects of diffusion on free precession in nuclear magnetic resonance experiments. *Physical Review, 94*(3), 630-638.

Cauvain, S. (2015). *Technology of Breadmaking (3rd edition)*. Cham: Springer International Publishing.

Chen, P., Long, Z., Ruan, R. & Labuza, T. (1997). Nuclear magnetic resonance studies of water mobility in bread during storage. *LWT-Food Science and Technology, 30*(2), 178-183.

Child, T. & Pryce, N. (1972). Steady-state and pulsed NMR studies of gelation in aqueous agarose. *Biopolymers: Original Research on Biomolecules, 11*(2), 409-429.

Christophersen, C., Otzen, D. E., Noman, B. E., Christensen, S. & Schäfer, T. (1998). Enzymatic characterisation of novamyl®, a thermostable α-amylase. *Starch/Stärke, 50*(1), 39-45.

Conde-Petit, B. & Escher, F. (1995). Complexation induced changes of rheological properties of starch systems at different moisture levels. *Journal of Rheology, 39*(6), 1497-1518.

Conde-Petit, B., Escher, F. & Nuessli, J. (2006). Structural features of starch-flavor complexation in food model systems. *Trends in Food Science & Technology, 17*(5), 227-235.

Cooke, D. & Gidley, M. J. (1992). Loss of crystalline and molecular order during starch gelatinisation: origin of the enthalpic transition. *Carbohydrate Research, 227*, 103-112.

Courtin, C. & Delcour, J. A. (2002). Arabinoxylans and endoxylanases in wheat flour bread-making. *Journal of Cereal Science, 35*(3), 225-243.

Courtin, C., Gelders, G. & Delcour, J. (2001). Use of two endoxylanases with different substrate selectivity for understanding arabinoxylan functionality in wheat flour breadmaking. *Cereal Chemistry, 78*(5), 564-571.

Courtin, C. M., Roelants, A. & Delcour, J. A. (1999). Fractionation-reconstitution experiments provide insight into the role of endoxylanases in bread-making. *Journal of Agricultural and Food Chemistry, 47*(5), 1870-1877.

Craig, J., Lloyd, J. R., Tomlinson, K., Barber, L., Edwards, A., Wang, T. L., Martin, C., Hedley, C. L. & Smith, A. M. (1998). Mutations in the gene encoding starch synthase II profoundly alter amylopectin structure in pea embryos. *The Plant Cell, 10*(3), 413-426.

Crowley, P., Schober, T. J., Clarke, C. I. & Arendt, E. K. (2002). The effect of storage time on textural and crumb grain characteristics of sourdough wheat bread. *European Food Research and Technology, 214*(6), 489-496.

Cuq, B., Abecassis, J. & Guilbert, S. (2003). State diagrams to help describe wheat bread processing. *International Journal of Food Science & Technology, 38*(7), 759-766.

Curti, E., Bubici, S., Carini, E., Baroni, S. & Vittadini, E. (2011). Water molecular dynamics during bread staling by Nuclear Magnetic Resonance. *LWT-Food Science and Technology, 44*(4), 854-859.

Dauter, Z., Dauter, M., Brzozowski, A. M., Christensen, S., Borchert, T. V., Beier, L., Wilson, K. S. & Davies, G. J. (1999). X-ray structure of Novamyl, the five-domain "maltogenic" α-amylase from Bacillus stearothermophilus: maltose and acarbose complexes at 1.7 Å resolution. *Biochemistry, 38*(26), 8385-8392.

Delcour, J., Vanhamel, S. & De Geest, C. (1989). Physico-chemical and functional properties of rye nonstarch polysaccharides. I. Colorimetric analysis of pentosans and their relative monosaccharide compositions in fractionated (milled) rye products. *Cereal Chemistry, 66*(2), 107-111.

Delcour, J. A. & Hoseney, R. C. (2010). *Principles of Cereal Science and Technology (3rd edition)*. St. Paul, MN: AACC International.

Delcour, J. A., Joye, I. J., Pareyt, B., Wilderjans, E., Brijs, K. & Lagrain, B. (2012). Wheat gluten functionality as a quality determinant in cereal-based food products. *Annual Review of Food Science and Technology, Vol 3, 3*, 469-492.

Derde, L. J. (2013). *Model system approaches to comprehend the action pattern of amylases - a focus on bread crum anti-firming enzymes.* Unpublished Doctoral dissertation, KU Leuven, Leuven.

Derde, L. J., Gomand, S. V., Courtin, C. M. & Delcour, J. A. (2012a). Characterisation of three starch degrading enzymes: thermostable B-amylase, maltotetraogenic and maltogenic a-amylases. *Food Chemistry, 135*(2), 713-721.

Derde, L. J., Gomand, S. V., Courtin, C. M. & Delcour, J. A. (2012b). Hydrolysis of B-limit dextrins by a-amylases from porcine pancreas, Bacillus subtilis, Pseudomonas saccharophila and Bacillus stearothermophilus. *Food Hydrocolloids, 26*(1), 231-239.

Derde, L. J., Gomand, S. V., Courtin, C. M. & Delcour, J. A. (2014). Moisture distribution during conventional or electrical resistance oven baking of bread dough and subsequent storage. *Journal of Agricultural and Food Chemistry, 62*(27), 6445-6453.

Dobry, A. & Boyer-Kawenoki, F. (1947). Phase separation in polymer solution. *Journal of Polymer Science, 2*(1), 90-100.

Donald, A. M., Kato, K. L., Perry, P. A. & Waigh, T. A. (2001). Scattering studies of the internal structure of starch granules. *Starch/Stärke, 53*(10), 504-512.

Donovan, J. W. (1979). Phase transitions of the starch-water system. *Biopolymers, 18*(2), 263-275.

Donovan, J. W., Mapes, C. J., Davis, J. G. & Garibaldi, J. A. (1975). A differential scanning calorimetric study of the stability of egg white to heat denaturation. *Journal of the Science of Food and Agriculture, 26*(1), 73-83.

Doona, C. J. & Baik, M.-Y. (2007). Molecular mobility in model dough systems studied by time-domain nuclear magnetic resonance spectroscopy. *Journal of Cereal Science, 45*(3), 257-262.

Doublier, J.-L. (1981). Rheological studies on starch—Flow behaviour of wheat starch pastes. *Starch/Stärke, 33*(12), 415-420.

Dries, D., Gomand, S., Delcour, J. & Goderis, B. (2016). V-type crystal formation in starch by aqueous ethanol treatment: The effect of amylose degree of polymerization. *Food Hydrocolloids, 61*, 649-661.

Dubois, M., Gilles, K. A., Hamilton, J. K., Rebers, P. t. & Smith, F. (1956). Colorimetric method for determination of sugars and related substances. *Analytical Chemistry, 28*(3), 350-356.

Eerlingen, R., Deceuninck, M. & Delcour, J. (1993). Enzyme-resistant starch. II. influence of amylose chain length on resistant starch formation. *Cereal Chemistry, 70*(3), 345-350.

Eliasson, A.-C. & Larsson, K. (1993). *Cereals in Breadmaking: a Molecular Colloidal Approach*. New York: Marcel Dekker.

Ellis, H. & Ring, S. (1985). A study of some factors influencing amylose gelation. *Carbohydrate Polymers, 5*(3), 201-213.

Engelsen, S. B., Jensen, M. K., Pedersen, H. T., Norgaard, L. & Munck, L. (2001). NMR-baking and multivariate prediction of instrumental texture parameters in bread. *Journal of Cereal Science, 33*(1), 59-69.

Englyst, H. N. & Cummings, J. H. (1984). Simplified method for the measurement of total non-starch polysaccharides by gas-liquid chromatography of constituent sugars as alditol acetates. *Analyst, 109*(7), 937-942.

Evans, I. (1986). An investigation of starch/surfactant interactions using viscosimetry and differential scanning calorimetry. *Starch/Stärke, 38*(7), 227-235.

Evers, A. (1973). The size distribution among starch granules in wheat endosperm. *Starch/Stärke, 25*(9), 303-304.

Finney, K. (1984). An optimized, straight-dough, bread-making method after 44 years. *Cereal Chemistry, 61*(1), 20-27.

FOODWIN. 2018. Factsheet bread waste. Available at https://www.foodwin.org/wp-content/uploads/2018/01/Factsheet-Bread-Waste.pdf - Retrieved on December 23 2019.

Forshult, S. E. (2004). *Quantitative analysis with pulsed NMR and the CONTIN computer program*. Department of Physical Chemistry, Karlstad University, Karlstad.

French, A. & Murphy, V. (1977). Intramolecular changes during polymorphic transformations of amylose. *Polymer, 18*(5), 489-494.

French, D. (1972). Fine structure of starch and its relationship to the organization of starch granules. *Journal of the Japanese Society of Starch Science, 19*(1), 8-25.

French, D. (1984). Organization of starch granules. In R. L. Whistler, J. N. BeMiller & E. F. Paschall (Eds.), *Starch: Chemistry and Technology (2nd edition)*, (pp. 183-247). New York: Academic Press.

Fujita, S., Yamamoto, H., Sugimoto, Y., Morita, N. & Yamamori, M. (1998). Thermal and crystalline properties of waxy wheat (Triticum aestivumL.) starch. *Journal of Cereal Science, 27*(1), 1-5.

Gabriela, C. G. & Daniela, V. (2010). The influence of different forms of backery yeast Saccharomyces cerevisie type strain on the concentration of individual sugars and their utilization during fermentation. *Romanian Biotechnological Letters, 15*(4), 5418.

Gallant, D. J., Bouchet, B. & Baldwin, P. M. (1997). Microscopy of starch: evidence of a new level of granule organization. *Carbohydrate Polymers, 32*(3), 177-191.

Gan, Z., Ellis, P. & Schofield, J. (1995). Gas cell stabilisation and gas retention in wheat bread dough. *Journal of Cereal Science, 21*(3), 215-230.

Genkina, N. K., Noda, T., Koltisheva, G. I., Wasserman, L. A., Tester, R. F. & Yuryev, V. P. (2003). Effects of growth temperature on some structural properties of crystalline lamellae in starches extracted from sweet potatoes (Sunnyred and Ayamurasaki). *Starch/Stärke, 55*(8), 350-357.

Gérard, C., Barron, C., Colonna, P. & Planchot, V. (2001). Amylose determination in genetically modified starches. *Carbohydrate Polymers, 44*(1), 19-27.

Gérard, C., Colonna, P., Buléon, A. & Planchot, V. (2002). Order in maize mutant starches revealed by mild acid hydrolysis. *Carbohydrate Polymers, 48*(2), 131-141.

Gerits, L. R., Pareyt, B. & Delcour, J. A. (2013). Single run HPLC separation coupled to evaporative light scattering detection unravels wheat flour endogenous lipid redistribution during bread dough making. *LWT-Food Science and Technology, 53*(2), 426-433.

Gernat, C., Radosta, S., Anger, H. & Damaschun, G. (1993). Crystalline parts of three different conformations detected in native and enzymatically degraded starches. *Starch/Stärke, 45*(9), 309-314.

Ghiasi, K., Hoseney, R. & Varriano-Marston, E. (1982). Gelatinization of wheat starch. III. Comparison by differential scanning calorimetry and light microscopy. *Cereal Chemistry, 59*(4), 258-262.

Ghiasi, K., Hoseney, R., Zeleznak, K. & Rogers, D. (1984). Effect of waxy barley starch and reheating on firmness of bread crumb. *Cereal Chemistry, 61*(4), 281-285.

Gibson, T., Solah, V. & McCleary, B. (1997). A procedure to measure amylose in cereal starches and flours with concanavalin A. *Journal of Cereal Science, 25*(2), 111-119.

Gidley, M. J. & Bulpin, P. V. (1987). Crystallisation of malto-oligosaccharides as models of the crystalline forms of starch: minimum chain-length requirement for the formation of double helices. *Carbohydrate Research, 161*(2), 291-300.

Giovanelli, G., Peri, C. & Borri, V. (1997). Effects of baking temperature on crumb-staling kinetics. *Cereal Chemistry, 74*(6), 710-714.

Glaring, M. A., Koch, C. B. & Blennow, A. (2006). Genotype-specific spatial distribution of starch molecules in the starch granule: a combined CLSM and SEM approach. *Biomacromolecules, 7*(8), 2310-2320.

Goderis, B., Putseys, J. A., Gommes, C. d. J., Bosmans, G. M. & Delcour, J. A. (2014). The structure and thermal stability of amylose–lipid complexes: A case study on amylose–glycerol monostearate. *Crystal Growth & Design, 14*(7), 3221-3233.

Goesaert, H., Brijs, K., Veraverbeke, W. S., Courtin, C. M., Gebruers, K. & Delcour, J. A. (2005). Wheat flour constituents: how they impact bread quality, and how to impact their functionality. *Trends in Food Science & Technology, 16*(1-3), 12-30.

Goesaert, H., Leman, P., Bijttebier, A. & Delcour, J. A. (2009a). Antifirming effects of starch degrading enzymes in bread crumb. *Journal of Agricultural and Food Chemistry, 57*(6), 2346-2355.

Goesaert, H., Leman, P. & Delcour, J. A. (2008). Model approach to starch functionality in bread making. *Journal of Agricultural and Food Chemistry, 56*(15), 6423-6431.

Goesaert, H., Slade, L., Levine, H. & Delcour, J. A. (2009b). Amylases and bread firming: an integrated view. *Journal of Cereal Science, 50*(3), 345-352.

Goldstein, I., Hollerman, C. & Merrick, J. M. (1965). Protein-carbohydrate interaction I. The interaction of polysaccharides with concanavalin A. *Biochimica Et Biophysica Acta, 97*(1), 68-76.

Gomand, S. V., Lamberts, L., Gommes, C. J., Visser, R. G., Delcour, J. A. & Goderis, B. (2012). Molecular and morphological aspects of annealing-induced stabilization of starch crystallites. *Biomacromolecules, 13*(5), 1361-1370.

Gómez, M., Del Real, S., Rosell, C. M., Ronda, F., Blanco, C. A. & Caballero, P. A. (2004). Functionality of different emulsifiers on the performance of breadmaking and wheat bread quality. *European Food Research and Technology, 219*(2), 145-150.

Gommes, C. J. & Goderis, B. (2010). CONEX, a program for angular calibration and averaging of two-dimensional powder scattering patterns. *Journal of Applied Crystallography, 43*(2), 352-355.

Graybosch, R. A. (1998). Waxy wheats: Origin, properties, and prospects. *Trends in Food Science & Technology, 9*(4), 135-142.

Graybosch, R. A., Souza, E. J., Berzonsky, W. A., Baenziger, P. S., McVey, D. J. & Chung, O. K. (2004). Registration of nineteen waxy spring wheats. *Crop Science, 44*, 1491-1492.

Guerrieri, N., Alberti, E., Lavelli, V. & Cerletti, P. (1996). Use of spectroscopic and fluorescence techniques to assess heat-induced molecular modifications of gluten. *Cereal Chemistry, 73*(3), 368-374.

Hall, R. S. & Manners, D. J. (1980). The structural analysis of some amylodextrins. *Carbohydrate Research, 83*(1), 93-101.

Hanashiro, I. & Takeda, Y. (1998). Examination of number-average degree of polymerization and molar-based distribution of amylose by fluorescent labeling with 2-aminopyridine. *Carbohydrate Research, 306*(3), 421-426.

Hanson, E. & Katz, J. (1934). Abhandlungen zur physikalischen Chemie der Stärke und der Brotbereitung. *Zeitschrift für Physikalische Chemie, 168*(1), 339-352.

Hargin, K. D. & Morrison, W. R. (1980). The distribution of acyl lipids in the germ, aleurone, starch and non-starch endosperm of four wheat varieties. *Journal of the Science of Food and Agriculture, 31*(9), 877-888.

Hayakawa, K., Tanaka, K., Nakamura, T., Endo, S. & Hoshino, T. (2004). End use quality of waxy wheat flour in various grain-based foods. *Cereal Chemistry, 81*(5), 666-672.

Hayta, M. & Schofield, J. D. (2004). Heat and additive induced biochemical transitions in gluten from good and poor breadmaking quality wheats. *Journal of Cereal Science, 40*(3), 245-256.

Hills, B., Cano, C. & Belton, P. (1991). Proton NMR relaxation studies of aqueous polysaccharide systems. *Macromolecules, 24*(10), 2944-2950.

Hills, B., Takacs, S. & Belton, P. S. (1990). A new interpretation of proton NMR relaxation time measurements of water in food. *Food Chemistry, 37*(2), 95-111.

Hills, B. P., Manning, C. E. & Ridge, Y. (1996). New theory of water activity in heterogeneous systems. *Journal of the Chemical Society, Faraday Transactions, 92*(6), 979-983.

Hizukuri, S. (1985). Relationship between the distribution of the chain length of amylopectin and the crystalline structure of starch granules. *Carbohydrate Research, 141*(2), 295-306.

Hizukuri, S. (1986). Polymodal distribution of the chain lengths of amylopectins, and its significance. *Carbohydrate Research, 147*(2), 342-347.

Hizukuri, S. (1996). Starch: analytical aspects. In A. C. Eliasson (Ed.), *Carbohydrates in Food*, (pp. 347-429). New York: Marcel Dekker.

Holz, M., Heil, S. R. & Sacco, A. (2000). Temperature-dependent self-diffusion coefficients of water and six selected molecular liquids for calibration in accurate 1H NMR PFG measurements. *Physical Chemistry Chemical Physics, 2*(20), 4740-4742.

Hoseney, R. C. & Rogers, D. E. (1990). The formation and properties of wheat flour doughs. *Critical Reviews in Food Science & Nutrition, 29*(2), 73-93.

Hug-Iten, S., Escher, F. & Conde-Petit, B. (2001). Structural properties of starch in bread and bread model systems: Influence of an antistaling α-amylase. *Cereal Chemistry, 78*(4), 421-428.

Hug-Iten, S., Handschin, S., Conde-Petit, B. a. & Escher, F. (1999). Changes in starch microstructure on baking and staling of wheat bread. *LWT-Food Science and Technology, 32*(5), 255-260.

Hukins, D. W. L. (1981). *X-ray Diffraction by Disordered and Ordered Systems (1st edition)*. Oxford: Pergamon Press.

Huschka, B., Bonomi, F., Marengo, M., Miriani, M. & Seetharaman, K. (2012). Comparison of lipid effects on structural features of hard and soft wheat flour proteins assessed by front-face fluorescence. *Food Chemistry, 133*(3), 1011-1016.

Imberty, A., Buléon, A., Tran, V. & Péerez, S. (1991). Recent advances in knowledge of starch structure. *Starch/Stärke, 43*(10), 375-384.

Imberty, A., Chanzy, H., Pérez, S., Bulèon, A. & Tran, V. (1988). The double-helical nature of the crystalline part of A-starch. *Journal of Molecular Biology, 201*(2), 365-378.

Imberty, A. & Perez, S. (1988). A revisit to the three-dimensional structure of B-type starch. *Biopolymers, 27*(8), 1205-1221.

Inokuma, T., Vrinten, P., Shimbata, T., Sunohara, A., Ito, H., Saito, M., Taniguchi, Y. & Nakamura, T. (2016). Using the hexaploid nature of wheat to create variability in starch characteristics. *Journal of Agricultural and Food Chemistry, 64*(4), 941-947.

Irvine, G. (1997). Size-exclusion high-performance liquid chromatography of peptides: a review. *Analytica Chimica Acta, 352*(1-3), 387-397.

Jane, J.-l. (2009). Structural features of starch granules II. In R. L. Whistler & J. N. BeMiller (Eds.), *Starch: Chemistry and Technology (3rd edition)*, (pp. 193-236). New York: Elsevier.

Jane, J.-L., Kasemsuwan, T., Leas, S., Zobel, H. & Robyt, J. F. (1994). Anthology of starch granule morphology by scanning electron microscopy. *Starch/Stärke, 46*(4), 121-129.

Jane, J., Xu, A., Radosavljevic, M. & Seib, P. (1992). Location of amylose in normal starch granules. I. Susceptibility of amylose and amylopectin to cross-linking reagents. *Cereal Chemistry, 69*(4), 405-409.

Jane, J. l., Chen, Y., Lee, L., McPherson, A., Wong, K., Radosavljevic, M. & Kasemsuwan, T. (1999). Effects of amylopectin branch chain length and amylose content on the gelatinization and pasting properties of starch. *Cereal Chemistry, 76*(5), 629-637.

Jenkins, P., Comerson, R., Donald, A., Bras, W., Derbyshire, G., Mant, G. & Ryan, A. (1994). In situ simultaneous small and wide angle X-ray scattering: a new technique to study starch gelatinization. *Journal of Polymer Science Part B: Polymer Physics, 32*(8), 1579-1583.

Jenkins, P. & Donald, A. (1995). The influence of amylose on starch granule structure. *International Journal of Biological Macromolecules, 17*(6), 315-321.

Jenkins, P. J. & Donald, A. M. (1997). Breakdown of crystal structure in potato starch during gelatinization. *Journal of Applied Polymer Science, 66*(2), 225-232.

Jenkins, P. J. & Donald, A. M. (1998). Gelatinisation of starch: a combined SAXS/WAXS/DSC and SANS study. *Carbohydrate Research, 308*(1), 133-147.

Jeon, J.-S., Ryoo, N., Hahn, T.-R., Walia, H. & Nakamura, Y. (2010). Starch biosynthesis in cereal endosperm. *Plant physiology and Biochemistry, 48*(6), 383-392.

Kainuma, K. & French, D. (1972). Naegeli amylodextrin and its relationship to starch granule structure. II. Role of water in crystallization of B-starch. *Biopolymers: Original Research on Biomolecules, 11*(11), 2241-2250.

Kalichevsky, M. T., Orford, P. D. & Ring, S. G. (1990). The retrogradation and gelation of amylopectins from various botanical sources. *Carbohydrate Research, 198*(1), 49-55.

Kalichevsky, M. T. & Ring, S. G. (1987). Incompatibility of amylose and amylopectin in aqueous solution. *Carbohydrate Research, 162*(2), 323-328.

Karaoglu, M. M. & Kotancilar, H. G. (2006). Effect of partial baking, storage and rebaking process on the quality of white pan bread. *International Journal of Food Science & Technology, 41*(s2), 108-114.

Karim, A. A., Norziah, M. & Seow, C. (2000). Methods for the study of starch retrogradation. *Food Chemistry, 71*(1), 9-36.

Karkalas, J., Ma, S., Morrison, W. R. & Pethrick, R. A. (1995). Some factors determining the thermal properties of amylose inclusion complexes with fatty acids. *Carbohydrate Research, 268*(2), 233-247.

Kasemsuwan, T. & Jane, J. (1994). Location of amylose in normal starch granules. II. Locations of phosphodiester cross-linking revealed by phosphorus-31 nuclear magnetic resonance. *Cereal Chemistry, 71*(3), 282-286.

Kassenbeck, P. (1975). Elektronenmikroskopischer beitrag zur kenntnis der feinstruktur der weizenstärke. *Starch/Stärke, 27*(7), 217-227.

Kassenbeck, P. (1978). Beitrag zur kenntnis der verteilung von amylose und amylopektin in stärkekörnern. *Starch/Stärke, 30*(2), 40-46.

Katz, J. (1928). The X-ray spectrography of starch. In R. P. Walton (Ed.), *A Comprehensive Survey of Starch Chemistry*, (pp. 68-76). New York: Chemical Catalog Company Inc.

Khatkar, B. S., Bell, A. E. & Schofield, J. D. (1995). The dynamic rheological properties of glutens and gluten sub-fractions from wheats of good and poor bread making quality. *Journal of Cereal Science, 22*(1), 29-44.

Kim, K.-H., Feiz, L., Martin, J. & Giroux, M. (2012). Puroindolines are associated with decreased polar lipid breakdown during wheat seed development. *Journal of Cereal Science, 56*(2), 142-146.

Kim, Y.-R. & Cornillon, P. (2001). Effects of temperature and mixing time on molecular mobility in wheat dough. *LWT-Food Science and Technology, 34*(7), 417-423.

Kim, Y.-R., Yoo, B.-S., Cornillon, P. & Lim, S.-T. (2004). Effect of sugars and sugar alcohols on freezing behavior of corn starch gel as monitored by time domain 1H NMR spectroscopy. *Carbohydrate Polymers, 55*(1), 27-36.

Knight, R. & Menlove, E. (1961). Effect of the bread-baking process on destruction of certain mould spores. *Journal of the Science of Food and Agriculture, 12*(10), 653-656.

Koehler, P. & Wieser, H. (2013). Chemistry of cereal grains. In M. Gobbetti & M. Gänzle (Eds.), *Handbook on Sourdough Biotechnology*, (pp. 11-45). New York: Springer.

Koizumi, K., Fukuda, M. & Hizukuri, S. (1991). Estimation of the distributions of chain length of amylopectins by high-performance liquid chromatography with pulsed amperometric detection. *Journal of Chromatography, 585*(2), 233-238.

Kovrlija, R. & Rondeau-Mouro, C. (2016). Hydrothermal changes of starch monitored by combined NMR and DSC methods. *Food and Bioprocess Technology, 10*(3), 445-461.

Krog, N. (1971). Amylose complexing effect of food grade emulsifiers. *Starch/Stärke, 23*(6), 206-210.

Kugimiya, M., Donovan, J. & Wong, R. (1980). Phase transitions of amylose-lipid complexes in starches: a calorimetric study. *Starch/Stärke, 32*(8), 265-270.

Kugimiya, M. & Donovan, J. W. (1981). Calorimetric determination of the amylose content of starches based on formation and melting of the amylose-lysolecithin complex. *Journal of Food Science, 46*(3), 765-770.

Kulp, K. & Ponte, J. (1981). Staling of white pan bread: fundamental causes. *Critical Reviews in Food Science & Nutrition, 15*(1), 1-48.

Lagrain, B., Brijs, K. & Delcour, J. A. (2008a). Reaction kinetics of gliadin-glutenin cross-linking in model systems and in bread making. *Journal of Agricultural and Food Chemistry, 56*(22), 10660-10666.

Lagrain, B., Brijs, K., Veraverbeke, W. S. & Delcour, J. A. (2005). The impact of heating and cooling on the physico-chemical properties of wheat gluten-water suspensions. *Journal of Cereal Science, 42*(3), 327-333.

Lagrain, B., Leman, P., Goesaert, H. & Delcour, J. A. (2008b). Impact of thermostable amylases during bread making on wheat bread crumb structure and texture. *Food Research International, 41*(8), 819-827.

Lagrain, B., Thewissen, B. G., Brijs, K. & Delcour, J. A. (2008c). Mechanism of gliadin-glutenin cross-linking during hydrothermal treatment. *Food Chemistry, 107*(2), 753-760.

Lagrain, B., Wilderjans, E., Glorieux, C. & Delcour, J. A. (2012). Importance of gluten and starch for structural and textural properties of crumb from fresh and stored bread. *Food Biophysics, 7*(2), 173-181.

Lambrecht, M. A., Rombouts, I., Van Kelst, L. & Delcour, J. A. (2015). Impact of extraction and elution media on non-size effects in size exclusion chromatography of proteins. *Journal of Chromatography A, 1415*, 100-107.

Langton, M. & Hermansson, A.-M. (1989). Microstructural changes in wheat starch dispersions during heating and cooling. *Food Structure, 8*(1), 29-39.

Larsson, H. & Eliasson, A.-C. (1996). Phase separation of wheat flour dough studied by ultracentrifugation and stress relaxation. I. Influence of water content. *Cereal Chemistry, 73*(1), 18-24.

Lavelli, V., Guerrieri, N. & Cerletti, P. (1996). Controlled reduction study of modifications induced by gradual heating in gluten proteins. *Journal of Agricultural and Food Chemistry, 44*(9), 2549-2555.

Le-Bail, A., Agrane, S. & Queveau, D. (2012). Impact of the baking duration on bread staling kinetics. *Food and Bioprocess Technology, 5*(6), 2323-2330.

Le-Bail, A., Monteau, J., Margerie, F., Lucas, T., Chargelegue, A. & Reverdy, Y. (2005). Impact of selected process parameters on crust flaking of frozen partly baked bread. *Journal of Food Engineering, 69*(4), 503-509.

Le Bail, P., Bizot, H., Ollivon, M., Keller, G., Bourgaux, C. & Buléon, A. (1999). Monitoring the crystallization of amylose–lipid complexes during maize starch melting by synchrotron x-ray diffraction. *Biopolymers: Original Research on Biomolecules, 50*(1), 99-110.

Leach, H. W., McCowen, L. & Schoch, T. J. (1959). Structure of the starch granule. I. Swelling and solubility patterns of various starches. *Cereal Chemistry, 36*(6), 534-544.

Lee, M.-R., Swanson, B. G. & Baik, B.-K. (2001). Influence of amylose content on properties of wheat starch and breadmaking quality of starch and gluten blends. *Cereal Chemistry, 78*(6), 701-706.

Lelievre, J. & Mitchell, J. (1975). A pulsed NMR study of some aspects of starch gelatinization. *Starch/Stärke, 27*(4), 113-115.

Leloup, V., Colonna, P., Ring, S. G., Roberts, K. & Wells, B. (1992). Microstructure of amylose gels. *Carbohydrate Polymers, 18*(3), 189-197.

Leman, P., Goesaert, H., Vandeputte, G. E., Lagrain, B. & Delcour, J. A. (2005). Maltogenic amylase has a non-typical impact on the molecular and rheological properties of starch. *Carbohydrate Polymers, 62*(3), 205-213.

León, A. E., Barrera, G. N., Pérez, G. T., Ribotta, P. D. & Rosell, C. M. (2006). Effect of damaged starch levels on flour-thermal behaviour and bread staling. *European Food Research and Technology, 224*(2), 187-192.

Leung, H., Magnuson, J. & Bruinsma, B. (1979). Pulsed nuclear magnetic resonance study of water mobility in flour doughs. *Journal of Food Science, 44*(5), 1408-1411.

Leuschner, R., O'Callaghan, M. & Arendt, E. (1997). Optimization of baking parameters of part-baked and rebaked Irish brown soda bread by evaluation of some quality characteristics. *International Journal of Food Science & Technology, 32*(6), 487-493.

Leuschner, R., O'Callaghan, M. & Arendt, E. (1999). Moisture distribution and microbial quality of part baked breads as related to storage and rebaking conditions. *Journal of Food Science, 64*(3), 543-546.

Li, M. & Lee, T.-C. (1998). Effect of cysteine on the molecular weight distribution and the disulfide cross-link of wheat flour proteins in extrudates. *Journal of Agricultural and Food Chemistry, 46*(3), 846-853.

Lineback, D. R. (1986). Current concepts of starch structure and its impact on properties. *Journal of the Japanese Society of Starch Science, 33*(1), 80-88.

Liu, H., Lelievre, J. & Ayoung-Chee, W. (1991). A study of starch gelatinization using differential scanning calorimetry, X-ray, and birefringence measurements. *Carbohydrate Research, 210*, 79-87.

Liu, Z. & Scanlon, M. G. (2004). Revisiting crumb texture evaluation methods: tension, compression, and indentation. *Cereal Foods World, 49*(2), 76-82.

Lucas, T., Wagner, M., Quellec, S. & Davenel, A. (2008). NMR imaging of bread and biscuit. In G. A. Webb (Ed.), *Modern Magnetic Resonance*, (pp. 1795-1799). Dordrecht: Springer Netherlands.

Maningat, C. C., Seib, P., Bassi, S., Woo, K. & Lasater, G. (2009). Wheat starch: production, properties, modification and uses. In R. L. Whistler & J. N. BeMiller (Eds.), *Starch: Chemistry and Technology (3rd edition)*, (pp. 441-510). New York: Elsevier.

Mares, D. J. & Stone, B. A. (1973). Studies on wheat endosperm II. Properties of the wall components and studies on their organization in the wall. *Australian Journal of Biological Sciences, 26*(4), 813-830.

Marsh, R. D. L. & Blanshard, J. M. V. (1988). The application of polymer crystal growth theory to the kinetics of formation of the B-amylose polymorph in a 50% wheat-starch gel. *Carbohydrate Polymers, 9*(4), 301-317.

Mason, W. R. (2009). Starch use in foods. In R. L. Whistler & J. N. BeMiller (Eds.), *Starch: Chemistry and Technology (3rd edition)*, (pp. 745-795). New York: Elsevier.

Matveev, Y. I., Elankin, N. Y., Kalistrova, E., Danilenko, A., Niemann, C. & Yuryev, V. (1998). Estimation of contributions of hydration and glass transition to heat capacity changes during melting of native starches in excess water. *Starch/Stärke, 50*(4), 141-147.

McIver, R. G., Axford, D., Colwell, K. & Elton, G. (1968). Kinetic study of the retrogradation of gelatinised starch. *Journal of the Science of Food and Agriculture, 19*(10), 560-563.

Meiboom, S. & Gill, D. (1958). Modified spin-echo method for measuring nuclear relaxation times. *Review of Scientific Instruments, 29*(8), 688-691.

Melis, S., Meza Morales, W. R. & Delcour, J. A. (2019). Lipases in wheat flour bread making: Importance of an appropriate balance between wheat endogenous lipids and their enzymatically released hydrolysis products. *Food Chemistry, 298*, 125002.

Miles, M. J., Morris, V. J., Orford, P. D. & Ring, S. G. (1985a). The roles of amylose and amylopectin in the gelation and retrogradation of starch. *Carbohydrate Research, 135*(2), 271-281.

Miles, M. J., Morris, V. J. & Ring, S. G. (1985b). Gelation of amylose. *Carbohydrate Polymers, 135*(2), 257-269.

Morell, M., Rahman, S., Regina, A., Appels, R. & Li, Z. (2001). Wheat starch biosynthesis. *Euphytica, 119*(1-2), 55-58.

Morgan, K. R., Hutt, L., Gerrard, J., Every, D., Ross, M. & Gilpin, M. (1997). Staling in starch breads: the effect of antistaling α-amylase. *Starch/Stärke, 49*(2), 54-59.

Morita, N., Maeda, T., Miyazaki, M., Yamamori, M., Miura, H. & Ohtsuka, I. (2002). Dough and baking properties of high-amylose and waxy wheat flours. *Cereal Chemistry, 79*(4), 491-495.

Morris, C. F. (2002). Puroindolines: the molecular genetic basis of wheat grain hardness. *Plant Molecular Biology, 48*(5-6), 633-647.

Morrison, W. (1978). Wheat lipid composition. *Cereal Chemistry, 55*(5), 548-558.

Morrison, W. & Gadan, H. (1987). The amylose and lipid contents of starch granules in developing wheat endosperm. *Journal of Cereal Science, 5*(3), 263-275.

Morrison, W., Tester, R. & Gidley, M. (1994). Properties of damaged starch granules. II. Crystallinity, molecular order and gelatinisation of ball-milled starches. *Journal of Cereal Science, 19*(3), 209-217.

Morrison, W. R. (1988). Lipids in cereal starches: A review. *Journal of Cereal Science, 8*(1), 1-15.

Morrison, W. R., Mann, D. L. & Coventry, W. S. A. M. (1975). Selective extraction and quantitative analysis of non-starch and starch lipids from wheat flour. *Journal of the Science of Food and Agriculture, 26*(4), 507-521.

Nagamine, T. & Komae, K. (1996). Improvement of a method for chain-length distribution analysis of wheat amylopectin. *Journal of Chromatography A, 732*(2), 255-259.

Nakamura, T., Vrinten, P., Hayakawa, K. & Ikeda, J. (1998). Characterization of a granule-bound starch synthase isoform found in the pericarp of wheat. *Plant Physiology, 118*(2), 451-459.

Nakamura, T., Yamamori, M., Hirano, H., Hidaka, S. & Nagamine, T. (1995). Production of waxy (amylose-free) wheats. *Molecular and General Genetics, 248*(3), 253-259.

Nakamura, Y. (2002). Towards a better understanding of the metabolic system for amylopectin biosynthesis in plants: rice endosperm as a model tissue. *Plant and Cell Physiology, 43*(7), 718-725.

Nivelle, M. A., Bosmans, G. M. & Delcour, J. A. (2017). The impact of parbaking on the crumb firming mechanism of fully baked tin wheat bread. *Journal of Agricultural and Food Chemistry, 65*(46), 10074-10083.

Noda, T., Takahata, Y., Sato, T., Suda, I., Morishita, T., Ishiguro, K. & Yamakawa, O. (1998). Relationships between chain length distribution of amylopectin and gelatinization properties within the same botanical origin for sweet potato and buckwheat. *Carbohydrate Polymers, 37*(2), 153-158.

Noda, T., Tohnooka, T., Taya, S. & Suda, I. (2001). Relationship between physicochemical properties of starches and white salted noodle quality in Japanese wheat flours. *Cereal Chemistry, 78*(4), 395-399.

Ong, M. H., Jumel, K., Tokarczuk, P. F., Blanshard, J. M. & Harding, S. E. (1994). Simultaneous determinations of the molecular weight distributions of amyloses and the fine structures of amylopectins of native starches. *Carbohydrate Research, 260*(1), 99-117.

Ooms, N., Vandromme, E., Brijs, K. & Delcour, J. A. (2018). Intact and damaged wheat starch and amylase functionality during multilayered fermented pastry making. *Journal of Food Science, 83*(10), 2489-2499.

Orford, P. D., Ring, S. G., Carroll, V., Miles, M. J. & Morris, V. J. (1987). The effect of concentration and botanical source on the gelation and retrogradation of starch. *Journal of the Science of Food and Agriculture, 39*(2), 169-177.

Osella, C. A., Sánchez, H. D., Carrara, C. R., de la Torre, M. A. & Pilar Buera, M. (2005). Water redistribution and structural changes of starch during storage of a gluten-free bread. *Starch/Stärke, 57*(5), 208-216.

Pareyt, B., Finnie, S. M., Putseys, J. A. & Delcour, J. A. (2011). Lipids in bread making: sources, interactions, and impact on bread quality. *Journal of Cereal Science, 54*(3), 266-279.

Pascua, Y., Koç, H. & Foegeding, E. A. (2013). Food structure: roles of mechanical properties and oral processing in determining sensory texture of soft materials. *Current Opinion in Colloid & Interface Science, 18*, 324-333.

Peat, S., Whelan, W. J. & Thomas, G. J. (1956). The enzymic synthesis and degradation of starch. Part XXII. Evidence of multiple branching in waxy-maize starch. A correction. *Journal of the Chemical Society*, 3025-3030.

Pérez, S. & Bertoft, E. (2010). The molecular structures of starch components and their contribution to the architecture of starch granules: A comprehensive review. *Starch/Stärke, 62*(8), 389-420.

Peters, G. 2018. Userfriendlyscience: quantitative analysis made accessible. R package version 0.7.2. Available at https://cran.r-project.org/web/packages/userfriendlyscience/index.html - Retrieved on December 23 2019.

Pfannemüller, B. (1987). Influence of chain length of short monodisperse amyloses on the formation of A-and B-type X-ray diffraction patterns. *International Journal of Biological Macromolecules, 9*(2), 105-108.

Pisesookbunterng, W., D'Appolonia, B. L. & Kulp, K. (1983). Bread staling studies. II. The role of refreshening. *Cereal Chemistry, 60*(4), 301-305.

Pojić, M., Musse, M., Rondeau, C., Hadnađev, M., Grenier, D., Mariette, F., Cambert, M., Diascorn, Y., Quellec, S. & Torbica, A. (2016). Overall and local bread expansion, mechanical properties, and molecular structure during bread baking: effect of emulsifying starches. *Food and Bioprocess Technology, 9*(8), 1287-1305.

Popov, D., Buléon, A., Burghammer, M., Chanzy, H., Montesanti, N., Putaux, J.-L., Potocki-Veronese, G. & Riekel, C. (2009). Crystal structure of A-amylose: A revisit from synchrotron microdiffraction analysis of single crystals. *Macromolecules, 42*(4), 1167-1174.

Provencher, S. W. (1982). CONTIN: a general purpose constrained regularization program for inverting noisy linear algebraic and integral equations. *Computer Physics Communications, 27*(3), 229-242.

Purhagen, J. K., Sjöö, M. E. & Eliasson, A.-C. (2011). Starch affecting anti-staling agents and their function in freestanding and pan-baked bread. *Food Hydrocolloids, 25*(7), 1656-1666.

Purlis, E. & Salvadori, V. O. (2009a). Bread baking as a moving boundary problem. Part 1: mathematical modelling. *Journal of Food Engineering, 91*(3), 428-433.

Purlis, E. & Salvadori, V. O. (2009b). Modelling the browning of bread during baking. *Food Research International, 42*(7), 865-870.

Putseys, J., Lamberts, L. & Delcour, J. (2010). Amylose-inclusion complexes: formation, identity and physico-chemical properties. *Journal of Cereal Science, 51*(3), 238-247.

Putseys, J. A., Derde, L. J., Lamberts, L., Goesaert, H. & Delcour, J. A. (2009). Production of tailor made short chain amylose–lipid complexes using varying reaction conditions. *Carbohydrate Polymers, 78*(4), 854-861.

Putseys, J. A., Gommes, C., Van Puyvelde, P., Delcour, J. & Goderis, B. (2011). In situ SAXS under shear unveils the gelation of aqueous starch suspensions and the impact of added amylose–lipid complexes. *Carbohydrate Polymers, 84*(3), 1141-1150.

R Core Team. 2019. R: A language and environment for statistical computing. R foundation for statistical computing. Available at http://www.R-project.org/ - Retrieved on December 23 2019.

Rappenecker, G. & Zugenmaier, P. (1981). Detailed refinement of the crystal structure of Vh-amylose. *Carbohydrate Research, 89*(1), 11-19.

Regnier, F. E. (1983). High-performance liquid chromatography of biopolymers. *Science, 222*(4621), 245-252.

Reyniers, S., De Brier, N., Matthijs, S., Brijs, K. & Delcour, J. (2018). Impact of physical and enzymatic cell wall opening on the release of pre-gelatinized starch and viscosity forming potential of potato flakes. *Carbohydrate Polymers, 194*, 401-410.

Ribotta, P. & Le Bail, A. (2007). Thermo-physical and thermo-mechanical assessment of partially baked bread during chilling and freezing process: Impact of selected enzymes on crumb contraction to prevent crust flaking. *Journal of Food Engineering, 78*(3), 913-921.

Ridout, M. J., Parker, M. L., Hedley, C. L., Bogracheva, T. Y. & Morris, V. J. (2003). Atomic force microscopy of pea starch granules: granule architecture of wild-type parent, r and rb single mutants, and the rrb double mutant. *Carbohydrate Research, 338*(20), 2135-2147.

Ring, S. G., Colonna, P., I'Anson, K. J., Kalichevsky, M. T., Miles, M. J., Morris, V. J. & Orford, P. D. (1987). The gelation and crystallisation of amylopectin. *Carbohydrate Research, 162*(2), 277-293.

Ritota, M., Gianferri, R., Bucci, R. & Brosio, E. (2008). Proton NMR relaxation study of swelling and gelatinisation process in rice starch-water samples. *Food Chemistry, 110*(1), 14-22.

Robin, J., Mercier, C., Charbonniere, R. & Guilbot, A. (1974). Lintnerized starches. Gel filtration and enzymatic studies of insoluble residues from prolonged acid treatment of potato starch. *Cereal Chemistry, 51*, 389-406.

Roels, S., Cleemput, G., Vandewalle, X., Nys, M. & Delcour, J. (1993). Bread volume potential of variable-quality flours with constant protein level as determined by factors governing mixing time and baking absorption levels. *Cereal Chemistry, 70*(3), 318-323.

Rondeau-Mouro, C., Cambert, M., Kovrlija, R., Musse, M., Lucas, T. & Mariette, F. (2015). Temperature-associated proton dynamics in wheat starch-based model systems and wheat flour dough evaluated by NMR. *Food and Bioprocess Technology, 8*(4), 777-790.

Rosell, C. M. & Santos, E. (2010). Impact of fibers on physical characteristics of fresh and staled bake off bread. *Journal of Food Engineering, 98*(2), 273-281.

Rouillé, J., Chiron, H., Colonna, P., Della Valle, G. & Lourdin, D. (2010). Dough/crumb transition during French bread baking. *Journal of Cereal Science, 52*(2), 161-169.

Ruan, R., Almaer, S., Huang, V., Perkins, P., Chen, P. & Fulcher, R. (1996). Relationship between firming and water mobility in starch-based food systems during storage. *Cereal Chemistry, 73*(3), 328-332.

Rundle, R., Daasch, L. & French, D. (1944). The structure of the "B" modification of starch from film and fiber diffraction diagrams. *Journal of the American Chemical Society, 66*(1), 130-134.

Rundle, R. & Edwards, F. C. (1943). The configuration of starch in the starch-iodine complex. IV. an X-ray diffraction investigation of butanol-precipitated amylose. *Journal of the American Chemical Society, 65*(11), 2200-2203.

Saibene, D. & Seetharaman, K. (2010). Amylose involvement in the amylopectin clusters of potato starch granules. *Carbohydrate Polymers, 82*(2), 376-383.

Salman, H., Blazek, J., Lopez-Rubio, A., Gilbert, E. P., Hanley, T. & Copeland, L. (2009). Structure–function relationships in A and B granules from wheat starches of similar amylose content. *Carbohydrate Polymers, 75*(3), 420-427.

Sargeant, J. (1982). Determination of amylose:amylopectin ratios of starches. *Starch/Stärke, 34*(3), 89-92.

Scherrer, P. (1922). Bestimmung der inneren struktur und der gröBe von kolloidteilchen mittels röntgenstrahlen. In R. Zsigmondy (Ed.), *Kolloidchemie (4th edition)*, (pp. 387-409). Leipzig: Verlag von Otto Spamer.

Schirmer, M., Höchstötter, A., Jekle, M., Arendt, E. & Becker, T. (2013). Physicochemical and morphological characterization of different starches with variable amylose/amylopectin ratio. *Food Hydrocolloids, 32*(1), 52-63.

Schmidt, S. J. (2007). Water mobility in foods. In G. V. Barbosa-Cánovas, A. J. J. Fontana, S. J. Schmidt & T. P. Labuza (Eds.), *Water Activity in Foods: Fundamentals and Applications*, (pp. 47-108). Ames, IA: Blackwell Publishing.

Schoch, T. J. & French, D. (1947). Studies on bread staling. I. The role of starch. *Cereal Chemistry, 24*(4), 231-249.

Schofield, J., Bottomley, R., Timms, M. & Booth, M. (1983). The effect of heat on wheat gluten and the involvement of sulphydryl-disulphide interchange reactions. *Journal of Cereal Science, 1*(4), 241-253.

Sciarini, L. S., Pérez, G. T., de Lamballerie, M., León, A. E. & Ribotta, P. D. (2012). Partial-baking process on gluten-free bread: impact of hydrocolloid addition. *Food and Bioprocess Technology, 5*(5), 1724-1732.

Serial, M. R., Blanco Canalis, M. S., Carpinella, M., Valentinuzzi, M. C., León, A. E., Ribotta, P. D. & Acosta, R. H. (2016). Influence of the incorporation of fibers in biscuit dough on proton mobility characterized by time domain NMR. *Food Chemistry, 192*, 950-957.

Shannon, J. C., Garwood, D. L. & Boyer, C. D. (2009). Genetics and physiology of starch development. In R. L. Whistler & J. N. BeMiller (Eds.), *Starch: Chemistry and Technology (3rd edition)*, (pp. 23-82). New York: Elsevier.

Shewry, P. R., Popineau, Y., Lafiandra, D. & Belton, P. (2001). Wheat glutenin subunits and dough elasticity: findings of the EUROWHEAT project. *Trends in Food Science & Technology, 11*(12), 433-441.

Shi, Y.-C. & Seib, P. A. (1992). The structure of four waxy starches related to gelatinization and retrogradation. *Carbohydrate Research, 227*, 131-145.

Shibanuma, K., Takeda, Y., Hizukuri, S. & Shibata, S. (1994). Molecular structures of some wheat starches. *Carbohydrate Polymers, 25*(2), 111-116.

Sievert, D. & Hoseney, R. C. (2007). Bread and other baked products. *Ullmann's Encyclopedia of Industrial Chemistry*.

Singh, H. & MacRitchie, F. (2001). Application of polymer science to properties of gluten. *Journal of Cereal Science, 33*(3), 231-243.

Singh, S., Singh, N., Isono, N. & Noda, T. (2010). Relationship of granule size distribution and amylopectin structure with pasting, thermal, and retrogradation properties in wheat starch. *Journal of Agricultural and Food Chemistry, 58*(2), 1180-1188.

Slade, L. & Levine, H. (1987). Recent advances in starch retrogradation. In S. S. Stivala, V. Crescenzi & I. C. M. Dea (Eds.), *Industrial polysaccharides*, (pp. 387-430). New York: Gordon and Breach Science Publishers.

Slade, L. & Levine, H. (1988). Non-equilibrium melting of native granular starch: part I. temperature location of the glass transition associated with gelatinization of A-type cereal starches. *Carbohydrate Polymers, 8*(3), 183-208.

Slade, L., Levine, H. & Reid, D. S. (1991). Beyond water activity: recent advances based on an alternative approach to the assessment of food quality and safety. *Critical Reviews in Food Science & Nutrition, 30*(2-3), 115-360.

Song, Y. & Zheng, Q. (2007). Dynamic rheological properties of wheat flour dough and proteins. *Trends in Food Science & Technology, 18*(3), 132-138.

Spendler, T., Nilsson, L. & Fuglsang, C. C. (2002). Preparation of dough and baked products. *International patent Application., WO 99/53769*.

Sroan, B. S., Bean, S. R. & MacRitchie, F. (2009). Mechanism of gas cell stabilization in bread making. I. The primary gluten-starch matrix. *Journal of Cereal Science, 49*(1), 32-40.

Sroan, B. S. & MacRitchie, F. (2009). Mechanism of gas cell stabilization in breadmaking. II. The secondary liquid lamellae. *Journal of Cereal Science, 49*(1), 41-46.

Swinkels, J. (1985). Composition and properties of commercial native starches. *Starch/Stärke, 37*(1), 1-5.

Szczesniak, A. S. (2002). Texture is a sensory property. *Food Quality and Preference, 13*(4), 215-225.

Takeda, Y., Hizukuri, S., Takeda, C. & Suzuki, A. (1987). Structures of branched molecules of amyloses of various origins, and molar fractions of branched and unbranched molecules. *Carbohydrate Research, 165*(1), 139-145.

Tanaka, H. (2012). Viscoelastic phase separation in soft matter and foods. *Faraday Discussions, 158*(1), 371-406.

Tananuwong, K. & Reid, D. S. (2004). DSC and NMR relaxation studies of starch-water interactions during gelatinization. *Carbohydrate Polymers, 58*(3), 345-358.

Tang, H.-R., Brun, A. & Hills, B. (2001). A proton NMR relaxation study of the gelatinisation and acid hydrolysis of native potato starch. *Carbohydrate Polymers, 46*(1), 7-18.

Tang, H., Mitsunaga, T. & Kawamura, Y. (2006). Molecular arrangement in blocklets and starch granule architecture. *Carbohydrate Polymers, 63*(4), 555-560.

Tang, H. R., Godward, J. & Hills, B. (2000). The distribution of water in native starch granules-a multinuclear NMR study. *Carbohydrate Polymers, 43*(4), 375-387.

Tester, R. F. & Karkalas, J. (1996). Swelling and gelatinization of oat starches. *Cereal Chemistry, 73*(2), 271-277.

Tester, R. F., Karkalas, J. & Qi, X. (2004). Starch-composition, fine structure and architecture. *Journal of Cereal Science, 39*(2), 151-165.

Tester, R. F. & Morrison, W. R. (1990). Swelling and gelatinization of cereal starches. I. Effects of amylopectin, amylose, and lipids. *Cereal Chemistry, 67*(6), 551-557.

Thebaudin, J.-Y., Lefebvre, A.-C. & Doublier, J.-L. (1998). Rheology of starch pastes from starches of different origins: applications to starch-based sauces. *LWT-Food Science and Technology, 31*(4), 354-360.

Tolstoguzov, V. (1997). Thermodynamic aspects of dough formation and functionality. *Food Hydrocolloids, 11*(2), 181-193.

Tolstoguzov, V. (2003). Thermodynamic considerations of starch functionality in foods. *Carbohydrate Polymers, 51*(1), 99-111.

Ubbink, J., Burbidge, A. & Mezzenga, R. (2008). Food structure and functionality: a soft matter perspective. *Soft Matter, 4*(8), 1569-1581.

Vallera, A., Cruz, M., Ring, S. & Boue, F. (1994). The structure of amylose gels. *Journal of Physics: Condensed Matter, 6*(2), 311.

van der Sman, R. & Meinders, M. (2011). Prediction of the state diagram of starch water mixtures using the Flory–Huggins free volume theory. *Soft Matter, 7*(2), 429-442.

van Duynhoven, J., Voda, A., Witek, M. & Van As, H. (2010). Time-domain NMR applied to food products. In G. A. Webb (Ed.), *Annual Reports on NMR Spectroscopy*, vol. 69 (pp. 145-197). New York: Elsevier.

Van Soest, J., De Wit, D., Tournois, H. & Vliegenthart, J. (1994). Retrogradation of potato starch as studied by Fourier transform infrared spectroscopy. *Starch/Stärke, 46*(12), 453-457.

Vandeputte, G., Vermeylen, R., Geeroms, J. & Delcour, J. (2003). Rice starches. III. Structural aspects provide insight in amylopectin retrogradation properties and gel texture. *Journal of Cereal Science, 38*(1), 61-68.

Vansteelandt, J. & Delcour, J. A. (1999). Characterisation of starch from durum wheat (Triticum durum). *Starch/Stärke, 51*(2-3), 73-80.

Varriano-Marston, E., Ke, V., Huang, G. & Ponte, J. (1980). Comparison of methods to determine starch gelatinization in bakery foods. *Cereal Chemistry, 57*(4), 242-248.

Veraverbeke, W. S., Courtin, C. M., Verbruggen, I. M. & Delcour, J. A. (1999). Factors governing levels and composition of the sodium dodecyl sulphate-unextractable glutenin polymers during straight dough breadmaking. *Journal of Cereal Science, 29*(2), 129-138.

Veraverbeke, W. S. & Delcour, J. A. (2002). Wheat protein composition and properties of wheat glutenin in relation to breadmaking functionality. *Critical Reviews in Food Science and Nutrition, 42*(3), 179-208.

Vermeylen, R., Derycke, V., Delcour, J. A., Goderis, B., Reynaers, H. & Koch, M. H. (2006). Gelatinization of starch in excess water: beyond the melting of lamellar crystallites. A combined wide-and small-angle X-ray scattering study. *Biomacromolecules, 7*(9), 2624-2630.

Vermeylen, R., Goderis, B., Reynaers, H. & Delcour, J. A. (2004). Amylopectin molecular structure reflected in macromolecular organization of granular starch. *Biomacromolecules, 5*(5), 1775-1786.

Vilaplana, F., Hasjim, J. & Gilbert, R. G. (2012). Amylose content in starches: Toward optimal definition and validating experimental methods. *Carbohydrate Polymers, 88*(1), 103-111.

Wagner, M. J., Lucas, T., Le Ray, D. & Trystram, G. (2007). Water transport in bread during baking. *Journal of Food Engineering, 78*(4), 1167-1173.

Waigh, T. A., Gidley, M. J., Komanshek, B. U. & Donald, A. M. (2000a). The phase transformations in starch during gelatinisation: a liquid crystalline approach. *Carbohydrate Research, 328*(2), 165-176.

Waigh, T. A., Kato, K. L., Donald, A. M., Gidley, M. J., Clarke, C. J. & Riekel, C. (2000b). Side-chain liquid-crystalline model for starch. *Starch/Stärke, 52*(12), 450-460.

Wang, X., Choi, S.-G. & Kerr, W. L. (2004). Water dynamics in white bread and starch gels as affected by water and gluten content. *LWT-Food Science and Technology, 37*(3), 377-384.

Ward, K., Hoseney, R. & Seib, P. (1994). Retrogradation of amylopectin from maize and wheat starches. *Cereal Chemistry, 71*(2), 150-154.

Waterschoot, J., Gomand, S. V., Fierens, E. & Delcour, J. A. (2015). Production, structure, physicochemical and functional properties of maize, cassava, wheat, potato and rice starches. *Starch/Stärke, 67*(1-2), 14-29.

Whittam, M. A., Orford, P. D., Ring, S. G., Clark, S. A., Parker, M. L., Cairns, P. & Miles, M. J. (1989). Aqueous dissolution of crystalline and amorphous amylose-alcohol complexes. *International Journal of Biological Macromolecules, 11*(6), 339-344.

Wieser, H. (2007). Chemistry of gluten proteins. *Food Microbiology, 24*(2), 115-119.

Willhoft, E. (1971a). Bread staling: I.—Experimental study. *Journal of the Science of Food and Agriculture, 22*(4), 176-180.

Willhoft, E. (1971b). Bread staling: II.-Theoretical study. *Journal of the Science of Food and Agriculture, 22*(4), 180-183.

Willhoft, E. (1973). Mechanism and theory of staling of bread and baked goods, and associated changes in textural properties. *Journal of Texture Studies, 4*(3), 292-322.

Wynne-Jones, S. & Blanshard, J. (1986). Hydration studies of wheat starch, amylopectin, amylose gels and bread by proton magnetic resonance. *Carbohydrate Polymers, 6*(4), 289-306.

Yamaguchi, M., Kainuma, K. & French, D. (1979). Electron microscopic observations of waxy maize starch. *Journal of Ultrastructure Research, 69*(2), 249-261.

Yeh, A.-I. & Li, J.-Y. (1996). A continuous measurement of swelling of rice starch during heating. *Journal of Cereal Science, 23*(3), 277-283.

Yost, D. & Hoseney, R. (1986). Annealing and glass transition of starch. *Starch/Stärke, 38*(9), 289-292.

Young, A. H. (1984). Fractionation of starch. In R. L. Whistler, J. N. BeMiller & E. F. Paschall (Eds.), *Starch: Chemistry and Technology (2nd edition)*, (pp. 249-283). New York: Academic Press.

Yuryev, V. P., Krivandin, A. V., Kiseleva, V. I., Wasserman, L. A., Genkina, N. K., Fornal, J., Blaszczak, W. & Schiraldi, A. (2004). Structural parameters of amylopectin clusters and semi-crystalline growth rings in wheat starches with different amylose content. *Carbohydrate Research, 339*(16), 2683-2691.

Zanoni, B., Peri, C. & Bruno, D. (1995). Modelling of browning kinetics of bread crust during baking. *LWT-Food Science and Technology, 28*(6), 604-609.

Zanoni, B., Peri, C. & Pierucci, S. (1993). A study of the bread-baking process. I: a phenomenological model. *Journal of Food Engineering, 19*(4), 389-398.

Zeleznak, K. & Hoseney, R. (1986). The role of water in the retrogradation of wheat starch gels and bread crumb. *Cereal Chemistry, 63*(5), 407-411.

Zeleznak, K. & Hoseney, R. (1987). The glass transition in starch. *Cereal Chemistry, 64*(2), 121-124.

Zhou, X., Wang, R., Yoo, S.-H. & Lim, S.-T. (2011). Water effect on the interaction between amylose and amylopectin during retrogradation. *Carbohydrate Polymers, 86*(4), 1671-1674.

Zobel, H. (1988). Molecules to granules: a comprehensive starch review. *Starch/Stärke, 40*(2), 44-50.

Zobel, H. & Kulp, K. (1996). The staling mechanism. In R. Hebeda & Z. HF (Eds.), *Baked Goods Freshness: Technology, Evaluation, and Inhibition of Staling*, (pp. 1-64). New York: Marcel Dekker Inc.

List of publications

PUBLICATIONS IN INTERANTIONAL PEER REVIEWED JOURNALS

Lambrecht M.A., Rombouts I., Nivelle M.A., Delcour J.A. (2017) The role of wheat and egg constituents in the formation of a covalent and non-covalent protein network in fresh and cooked egg noodles. *Journal of Food Science. 82*(1), 24-35

Lambrecht M.A., Rombouts I., Nivelle M.A., Delcour J.A. (2017) The impact of protein characteristics on the protein network in and properties of fresh and cooked wheat-based noodles. *Journal of Cereal Science. 75*, 234-242.

Nivelle, M.A., Bosmans, G.M. and Delcour, J.A. (2017) The impact of parbaking on the crumb firming mechanism of fully baked tin wheat bread. *Journal of Agricultural and Food Chemistry. 65*(46), 10074-10083.

Nivelle, M.A., Beghin, A.S., Bosmans, G.M. and Delcour, J.A. (2019) Molecular dynamics of starch and water during bread making monitored with temperature-controlled time domain ^{1}H NMR. *Food Research International*. *119*, 675-682.

Nivelle, M.A., Remmerie, E., Bosmans, G.M., Vrinten, P., Nakamura T., and Delcour, J.A. (2019) Amylose and amylopectin functionality during baking and cooling of bread prepared from flour of wheat containing unusual starches: A temperature-controlled time domain ^{1}H NMR study. *Food Chemistry*. 295, 110-119.

Nivelle, M.A., Beghin, A.S., Vrinten, P., Nakamura T., and Delcour, J.A. Amylose and amylopectin functionality during storage of bread prepared from flour of wheat containing unique starches. (Submitted for publication).

CONTRIBUTIONS AT INTERNATIONAL MEETINGS PUBLISHED AS ABSTRACT

Nivelle M.A., Bosmans G.M., Delcour J.A. (2017). Molecular dynamics of flour biopolymers and water during bread making using temperature-controlled ^{1}H NMR. 16th European Young Cereal Scientists and Technologists Workshop. April 18-21, 2017. Thessaloniki, Greece. Oral presentation.

Nivelle M.A., Bosmans G.M., Delcour J.A. (2018). The impact of parbaking on the firming mechanism of crumb of fully baked tin wheat bread. 32nd EFFoST International Conference. November 6-8, 2018. Nantes, France. Oral presentation.

Nivelle M.A., Bosmans G.M., Vrinten P., Nakamura T., Delcour J.A. (2019). The role of amylose and amylopectin during baking and cooling of bread containing unusual starch. Cereals & Grains 19. November 3-5, 2019, Denver, CO, USA. Oral presentation.